IJBM

International Journal of

BIOMEDICINE

ISSN 2158-0510

Available online at
www.ijbm.org

INTERNATIONAL JOURNAL OF BIOMEDICINE

Aims and Scope: *International Journal of Biomedicine (IJBM)* publishes peer-reviewed articles on the topics of basic, applied, and translational research on biology and medicine. Original research studies, reviews, hypotheses, editorial commentary, and special reports spanning the spectrum of human and experimental and tissue research will be considered. All research studies involving animals must have been conducted following animal welfare guidelines such as the National Institutes of Health (NIH) Guide for the Care and Use of Laboratory Animals, or equivalent documents. Studies involving human subjects or tissues must adhere to the Declaration of Helsinki and Title 45, US Code of Federal Regulations, Part 46, Protection of Human Subjects, and must have received approval of the appropriate institutional committee charged with oversight of human studies. Informed consent must be obtained.

International Journal of Biomedicine endorses and behaves in accordance with the codes of conduct and international standards established by the Committee on Publication Ethics (COPE).

International Journal of Biomedicine (ISSN 2158-0510) is published four times a year by International Medical Research and Development Corp. (IMRDC), 6308, 12 Avenue, Brooklyn, NY 11219 USA

Customer Service: International Journal of Biomedicine, 6308, 12 Avenue, Brooklyn, NY 11219 USA; Tel: 1-917-740-3053; E-mail: editor@ijbm.org

Manuscript Submission: Original works will be accepted with the understanding that they are contributed solely to the Journal, are not under review by another publication, and have not previously been published except in abstract form. Accepted manuscripts become the sole property of the Journal and may not be published elsewhere without the consent of the Journal. A form stating that the authors transfer all copyright ownership to the Journal will be sent from the Publisher when the manuscript is accepted; this form must be signed by all authors of the article. All manuscripts must be submitted through the International Journal of Biomedicine`s online submission and review website. Authors who are unable to provide an electronic version or have other circumstances that prevent online submission must contact the Editorial Office prior to submission to discuss alternate options (editor@ijbm.org).

IJBM

INTERNATIONAL JOURNAL OF BIOMEDICINE

SAVE THE DATE

5th Annual

HEART iN DIABETES

Live CME Conference

June 18-20, 2021

Grand Hyatt • New York City

www.heartindiabetes.com

IJBM

INTERNATIONAL JOURNAL OF BIOMEDICINE

www.ijbm.org

Volume 11 Issue 2 June 2021

CONTENTS

CONTENTS

CONTINUED

essfn 2021

XXIV Congress of the European Society for Stereotactic and Functional Neurosurgery

MARSEILLE

INDIVIDUAL BRAIN PREDICTION

France

PALAIS DU PHARO

www.essfncongress.org

08>11
September

mco congrès

GENERAL ORGANISATION :
MCO Congrès - Villa Gaby
285 Corniche JF. Kennedy
13007 Marseille
T. : +33(0)4 91 09 38 00
natalie.ruston@mcocongres.com

PROVENCE | alpes | CÔTE d'AZUR FRANCE

RÉGION SUD | Marseille | VILLE DE MARSEILLE

The 66th ANNUAL CONGRESS of INTERNATIONAL COLLEGE of SURGEONS JAPAN SECTION

2021.6.26[SAT]

Venue **KURUME CITY PLAZA**

Chairman **YOSHITO AKAGI**

Department of Surgery, Kurume University School of Medicine

https://www.c-linkage.co.jp/icsj66

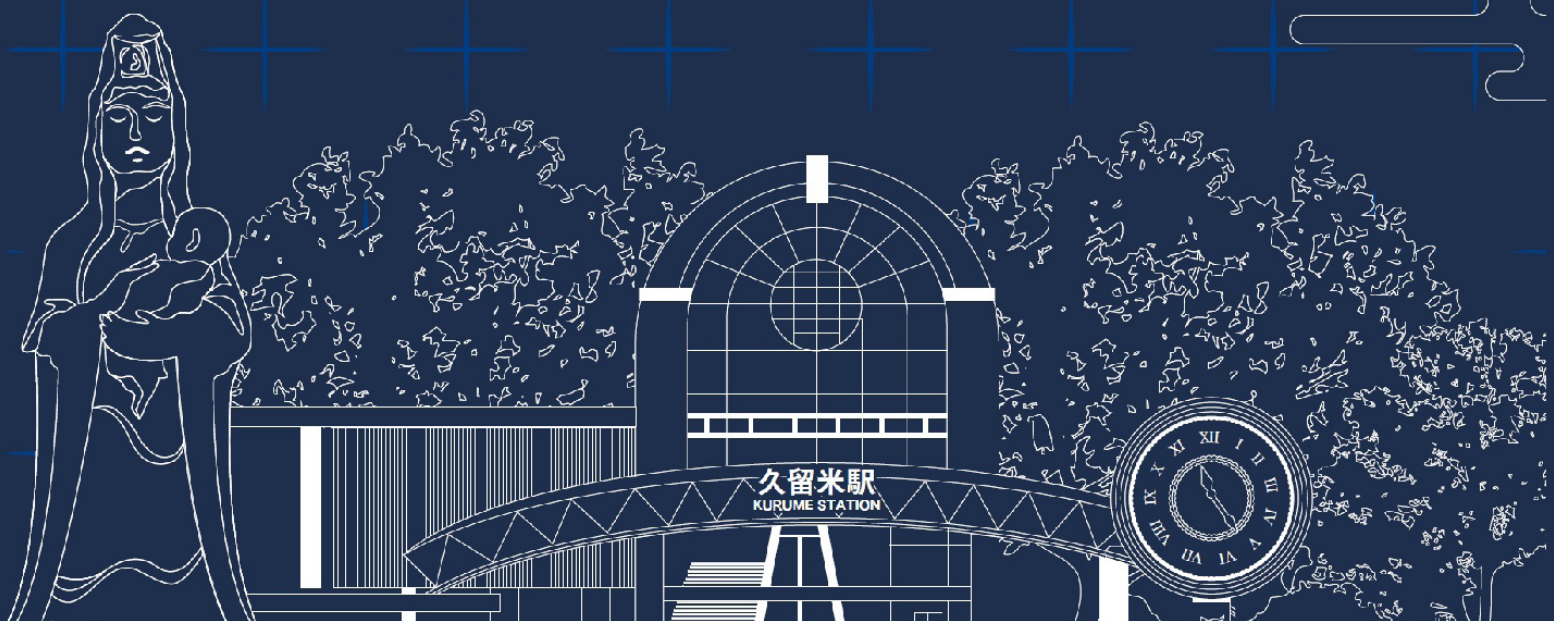

International Journal of Biomedicine 11(2) (2021) 111-122
http://dx.doi.org/10.21103/Article11(2)_RA1

REVIEW ARTICLE

INTERNATIONAL JOURNAL OF BIOMEDICINE

Twindemic of Coronavirus Disease (COVID-19) and Cardiometabolic Diseases

Gundu H. R. Rao, Emeritus Professor

Laboratory Medicine and Pathology
Director of Thrombosis Research, Lillehei Heart Institute
University of Minnesota, Minneapolis, USA

Abstract

Metabolic diseases, like hypertension, excess weight, obesity, type 2 diabetes, and vascular diseases, have rapidly increased to epidemic proportions worldwide. Metabolic risks (such as oxidative stress, chronic inflammation, insulin resistance, altered glucose and lipid metabolism, changes in hemodynamics, endothelial dysfunction, and subclinical atherosclerosis) contribute significantly to the progress of vascular disease and drive it eventually to acute vascular events like heart attacks and stroke. Although this situation has been noticed and discussed extensively by the global public health experts, and professional societies, the unprecedented SARS-CoV-2 pandemic has demonstrated for the first time the interdependency or syndemic nature of metabolic diseases and a pathogenic virus that takes advantage of the compromised metabolic function in these diseases. The most common clinical symptoms reported are fever, cough, fatigue, shortness of breath, dyspnea, chest pain, sore throat, and sputum production. The main mode of transmission is through respiratory particles containing viral virions. Both asymptomatic and symptomatic patients seem to be infectious. The spike (S) protein of SARS-CoV-2 seems to have a 10- to 20-fold higher affinity to the human ACE2 receptor than that of SARS-CoV. Since these receptors are highly expressed on a variety of cells, including vascular endothelial cells and adipose tissue, individuals with compromised function of these tissues are more vulnerable to greater infection, replication, and severity with COVID-19. In most cases, the severity of the coronavirus disease is associated with pre-existing comorbidities, which include metabolic diseases such as hypertension, obesity, diabetes, and vascular diseases. Those with such diseases, or with elevated risk factors for such diseases, will have a compromised endothelium, favoring endothelial dysfunction. The infection of the endothelium by SARS-CoV-2 and resulting endothelialitis seems to add to this problem by further damaging the endothelium, causing dysfunction, disruption of vascular integrity, and endothelial cell death. These events lead to the exposure of the thrombogenic basement membrane and result in the activation of the thrombotic and clotting cascade. Because of these observations, critical care clinicians recommend aggressive anti-thrombotic and thrombolytic therapies in the management of acute COVID-19 cases. In the absence of a cure for coronavirus disease, sensible medicine proposes the following: primary prevention by following the best public health practices, such as social distancing, use of face coverings, and quarantine of COVID-positive individuals; and a gentler, moderate, and humble view and application of available treatment options and their effectiveness in patients with COVID-19. The FDA has created a special emergency program for possible coronavirus therapies, the Coronavirus Treatment Acceleration Program (CTAP). Currently, there are 590 drug development programs in planning stages, 390 trials in review, and five authorized for emergency use. None are approved for use in COVID-19 management. Currently, there are at least 51 studies listed in the COVID-19 vaccine tracker of the Regulatory Affairs Professional Society (RAPS) site. At the time of this writing, vaccines from Pfizer-BioNTech, Moderna, Oxford-AstraZeneca, and Johnson&Johnson have emergency use authorization in the US. (**International Journal of Biomedicine. 2021;11(2):111-122.**)

Key Words: SARS-CoV-2 • COVID-19 • vaccine • metabolic diseases

For citation: Rao GHR. Twindemic of Coronavirus Disease (COVID-19) and Cardiometabolic Diseases. International Journal of Biomedicine. 2021;11(2):111-122. doi:10.21103/Article11(2)_RA1

Introduction

A novel coronavirus SARS-CoV-2, which escaped from Wuhan, China, in early January of 2019, has caused unprecedented healthcare and economic crisis worldwide.[1-9] This $16 trillion killer virus has caused havoc in all countries, and now after almost a year, has mutated into much more sophisticated 'new novel' virus variants, with a very high rate of transmission.[10,11] The spreading rate of the British and South African variants seems to be greater than 70%, compared to the normal SARS-CoV-2 virus. Variations in the UK variant seem to occur at the level of N501Y of the spike protein and involve

Contact Information: *Emeritus Professor Gundu H.R. Rao, Laboratory Medicine and Pathology, Director, Thrombosis Research, Lillehei Heart Institute, University of Minnesota. E-mail: gundurao9@gmail.com*

23 separate mutations of the spike.[11] Globally, according to Johns Hopkins University in Baltimore, Maryland, USA, over 112 million (mil) individuals are COVID-19 positive with 2.4 million deaths. The USA (28 mil), India (11.0 mil) Brazil (10.3 mil), Russia (4.16 mil), and the UK (4.15 mil) are competing for the top five ranks in terms of the number individuals COVID-positive. In COVID-related deaths, the USA, Brazil, Mexico, India, UK, and Italy are the top-ranking countries. In early April 2019, when I published my first article on this topic, the rankings were different: there were 2.9 million infected individuals worldwide with 203,670 deaths. Confirmed cases ranked as follows: USA (941,628), Spain (223,759), Italy (195,351), France (161,665), Germany (157, 026), United Kingdom (149,569), Turkey (107,773), Iran (90,481), China (83,909), Russia (80, 949), and Brazil (59,479). India with the second largest population and second-highest number of diabetics, with relatively poor healthcare infrastructure (1.2% GDP VS 17% in the USA), ranked 16th with 26,917 cases. Malaysia and Bangladesh were way far below in their rankings. If one were to rank these countries based on case fatality rates (CFRs), then the ranking was as follows; Mexico (87%), Italy (3.5%), Hungary (3.1%), Indonesia (2.9%), South Africa (2.7%). India with 1.4% CFR, ranked number 19.

COVID medicine and the public health response to this pandemic is a fast-changing field, with many controversies. The authors of CovidReference.com have been making every effort to provide updates on this topic with the mini-series; the most recent is the sixth edition of this mini-book.[6] According to the authors, in December of 2019, several patients from Wuhan developed pneumonia and respiratory failure. In early January 2020, a beta-coronavirus, later named SARS-CoV2, was isolated from the bronchoalveolar lavage of patients. From the first identification of COVID-19 in Wuhan, to the time of the first publication of this reference book (January 13, 2020), SARS-CoV-2 had spread to every corner of the world. According to Nobel laureate Joshua Lederberg, the success of the "wonder drugs" of the 1950s led to the belief that the "war on microbes" had been won, but the emergence of new infectious agents such as HIV and Ebola has shattered that illusion. In a speech in 1989, Lederberg warned against complacency in the age-old contest between mankind and microbes—viruses and bacteria. He laid out why man's "only real competitors remain viruses"; he further explained how all terrestrial life "is a dense web of mutualism and genetic interactions"; there are abundant sources of genetic variation "for viruses to learn new tricks (as proved by SARS-CoV-2), not necessarily confined to what happens routinely or even frequently." Now we have the proof of his prophecy, SARS-CoV-2, a novel and intelligent virus, if one may call it that, which has acquired multiple reading frames to delete unwanted mutations. One feels as if it has used artificial intelligence, pattern recognition, and machine learning techniques to become a highly contagious and most potent killer virus. The novel virus has improved over all the other members of this family, by acquiring the biochemical and structural features essential for rapid transmission, transfection, and replication by avoiding and deleting deleterious mutations and keeping favorable ones.

A recent comment published in the Lancet says that COVID-19 is not a pandemic, it is a syndemic.[12] Syndemics involve the clustering of two or more diseases within a population; the biological, social, and psychological interaction of those diseases; and the large-scale social forces that precipitate disease clustering in the first place.[13-15] According to the experts, a syndemic approach reveals biological and social interactions that are important for prognosis, treatment, and health policy. Therefore, limiting the harm caused by SARS-CoV-2 will demand far greater attention to non-communicable diseases (NCDs), and socioeconomic inequality than has hitherto been admitted. Disparities that exist in the rate of infection and severity of this disease in the African American community and other minority communities substantiate this observation by the experts. For argument's sake, COVID-19, for instance, is a pandemic over another pandemic—cardiometabolic diseases.[16-18] If we were to stretch our imagination further, we would have to include all the metabolic disease risk factors also as coexisting conditions. Addressing COVID-19 management, therefore, means, addressing all the metabolic risk factors as well as metabolic diseases such as hypertension, excess weight, endothelial dysfunction, inflammation, obesity, diabetes, vascular diseases, and chronic respiratory diseases. The SARS-CoV-2 pandemic is a nightmare for workers in public health and critical care. The effect of this pandemic will stay with us for a long time to come. In this overview, we will discuss coronavirus disease and its syndemic nature on cardiometabolic risks, and metabolic and vascular diseases.

SARS-CoV-2 Biochemistry

The first human coronavirus was first discovered and characterized by June Almeida a virologist in St Thomas Hospital in London in 1964. Since that time, five new human coronaviruses have been identified, including the severe acute respiratory syndrome virus, which caused significant mortality. Coronaviruses are single-stranded RNA virus genomes. The virion consists of genomic RNA embedded in phospholipid double layers and coated with two different types of nucleocapsid proteins (N). The membrane (M) protein (a type of transmembrane glycoprotein), the envelope (E) protein, and the surface (S) protein. Beta coronaviruses have a shorter spike-like surface protein called hemagglutinin esterase. The lipid bilayer envelope of the virus protects the membrane proteins and the nucleocapsid proteins when the virus survives outside the host.

Coronaviruses have positive-sense RNA genomes, consisting of six conserved proteins. The conserved proteins are the polyproteins pp1a and pp1b, which encompass multiple protein domains involved in various aspects of coronavirus genome replication. The size of this virus is between 60 nanometers (nm) to a maximum of 140 nm. Respiratory droplets are typically 5-10 micrometers, and each droplet may contain 250 virions, which means just normal talking can generate more than 750,000 virions. In the high-case fatality rate (CFR) strain, the nucleocapsid protein and the spike protein are significantly enriched. The N protein is multifunctional, contributes to viral transcription efficiency and pathogenicity. The SARS-CoV-2 spike proteins bind to the ACE2 host receptor with a 10 to 20-

fold affinity compared to SARS-CoV and contain a polybasic furin cleavage site, resulting in a unique insert to SARS-CoV-2 that enhances infectivity. Cleavage of S protein generates a polybasic Arg-Arg-Ala-Arg C-terminal sequence on S1 and S2. Furthermore, their analysis revealed a four-amino acid insertion in the long connecting region between the fusion peptide of the spike protein, in all high-CFR viruses, but not in low-CFR ones. Yet another difference they noticed was increased positive charge of the amino acids, comprising the nuclear localization signals (NLSs), a known marker of NLS strength. [19] Recent findings suggest the interaction of yet another receptor, called neuropilin-1(NRP1), and neuropilin 2 (NRP2) that facilitate the entry of this virus into cells. Key cell entry mechanism includes higher ACE2 (hACE2) binding affinity of the spike to the receptor-binding domain, reduced dependence on target cell proteases for entry, due to pre-activation by convertase furin.[20]

Transmission

The spike protein is a type 1 transmembrane protein, comprising 1255 amino acids and seems to be the key to the host cell interactions. The virus has undergone significant mutations as it has evolved worldwide. However, the S protein seems to be the key determinant of evolution, transmission, and virulence of SARS-CoV-2. Coronavirus entry into host cells is mediated by the transmembrane spike (S) glycoprotein that forms homotrimers protruding from the viral surface.[21] This protein comprises two functional subunits, responsible for binding to the host cell receptor (S1subunit), and fusion of the viral and cellular membranes (S2 subunit). For all viruses of this group, the S unit is cleaved by host proteases at the S2 site of the fusion peptide. Because of this mode of transmission, coronavirus entry into the host cell is a complex process, that requires both receptor binding and proteolytic processing of the S protein, to promote virus-cell fusion. SARS-CoV-2 entry into a cell involves the interaction of its spike protein with the cell's membrane-bound angiotensin-converting enzyme 2 (ACE2), which is cleaved by the transmembrane protease serine 2 (TMPRSS2), suggesting that co-expression of both genes is required for infection. [22]

The step between the SARS-CoV-2 spike glycoprotein and the ACE2 receptor seems to be the most critical point for the entry of the virus into the host cells. The high affinity of the S protein to the human ACE2 receptor seems to facilitate the spread of this virus in human populations. According to experts, four important enzymes are essential for the pathogenesis: the S protein that facilitates virus entry through the ACE2 to the host cell surface receptor, the major protease of CoV3Clpro, the papain-like protease (PLpro) involved in the assembly of new viruses, and RNA-dependent polymerase (RdPr) that facilitate CoV RNA genome replication. The processing and activation of coronavirus S protein are critical for the infectivity of the virus. The proprotein convertase family (PC) is composed of nine serine-secreting proteases and is widely involved in regulating various biological processes in normal and disease states. Therefore, the PC family, especially Furin, can be considered the key player that mediates the maturation of the S protein processing and recognition of membrane proteins. According to the experts, Furin can be considered a critical molecule that makes SARS-COV-2 cause adverse cardiovascular events through the ACE receptor. [23]

Clinical Manifestations

Researchers from the department of statistics, University of Dhaka, published a Meta-Analysis on clinical manifestations and comorbidities of coronavirus infection.[24] Of the total of 33 eligible studies, including 7673 infected patients, the most prevalent clinical symptoms were fever (84.49%), cough (56.39%), fatigue (33.65%), dyspnea (22.34%), sputum production (22.34%), and myalgia (16.26%). Other symptoms included shortness of breath, diarrhea, headache, chest pain, vomiting, sore throat, and poor appetite, loss of smell and taste, and chills. The most prevalent comorbidity was hypertension (20%), cardiovascular disease (11.9%), and diabetes (9.8%). Other less know comorbidities include excess weight, obesity, chronic kidney disease, chronic liver disease, chronic pulmonary disease, and cerebrovascular disease.[25-29] These viruses enter the nasal epithelial cells, using the surface spike (S) protein to bind ACE2, which serves as receptors for SARS-CoV-2, on the bronchial epithelial cells and type II pneumocytes. Researchers have analyzed the ACE2 RNA expression profile at single-cell resolution. High ACE2 (hACE2) expression has been identified in type II alveolar cells of the lung, esophagus, enterocytes of the ileum and colon, cholangiocytes, myocardial cells, kidney proximal tubule cells, bladder urothelial cells, fat cells, and vascular endothelial cells.[20-22]

Following infection and viral replication, downregulation of ACE2 enzyme occurs, resulting in dysfunction of the angiotensin system, resulting in hypokalemia, vasoconstriction, and development of acute respiratory distress syndrome (ARDS). Endothelium, comprising a monolayer of endothelial cells is the largest organ of the body, covering a large surface area, and reaching out to every tissue and organ. Based on emerging evidence from patients with COVID-19, experts postulate that endothelial cells are essential contributors to the initiation and propagation of severity of COVID-19. Because of these observations, one can further speculate that the injury to the endothelium could introduce a cascade of events, leading to platelet activation, thrombin generation, and promotion of both thrombotic and thrombolytic events (Figure 1).

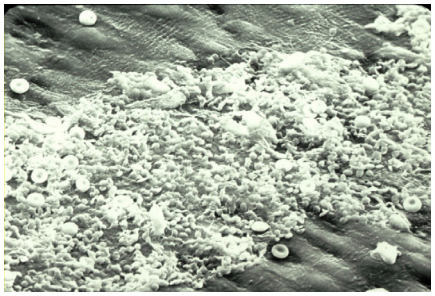

Fig. 1. *Platelet interaction with injured endothelium. (Courtesy: Prof. James G. White).*

To distinguish the term 'vascular disease' from the vascular damage and pathology observed in the severely ill

Covid-19 patients, we refer to this condition as a disease of the blood vessels.[29] In most cases, the severity of the coronavirus disease is associated with pre-existing comorbidities, which include metabolic diseases such as hypertension, obesity, diabetes, and vascular diseases. Those with such diseases, or with elevated risk factors for such diseases, will have a compromised endothelium, favoring endothelial dysfunction. The infection of endothelium by SARS-CoV-2 seems to add to this problem, by further damaging the endothelium, causing dysfunction, disruption of vascular integrity, and endothelial cell death. These events lead to the exposure of the thrombogenic basement membrane and result in the activation of the thrombotic and clotting cascade. Because of these observations, critical care clinicians recommend aggressive anti-thrombotic and thrombolytic therapies in the management of acute COVID-19 cases.

Twindemic of COVID-19 and Cardio-metabolic Diseases

The hospitalization rate for COVID-19 is 4.6% per 100,000 population, and almost 90% of the hospitalized patients have some type of underlying condition, according to the Centers for Disease Control and Prevention, USA. According to the Associated Hospitalization Surveillance Network, which includes laboratory-confirmed cases in 99 counties in 14 states, the hospitalization rate increased with patient age. Those aged 65 years and older were admitted at a rate of 13.8%, those aged 50 to 64 at 7.4%, and 18 to 49 at 2.5%. Hypertension was the most common morbidity among the oldest patients, with a prevalence of 72%, followed by cardiovascular disease (CVD) at 50.8% and obesity at 41%. Is this the common pattern of comorbidity in all geographical areas? Not necessarily. The first large study conducted in the city of New York concluded that pre-existing conditions such as hypertension and diabetes were highly prevalent, and the pattern was similar to the data reported from China.[30] In January of 2020, Huang and associates reported clinical features of 41 patients hospitalized with Covid-19 in Wuhan.[31] The median age was 49 and all were males. According to the authors, less than half had underlying diseases, including diabetes (20%), hypertension (15%), and cardiovascular disease (15%). Chen and associates from Wuhan's Jinyintan Hospital reported a study of 99 COVID-19 patients.[32,33] The average age was 55 years. Half of the patients had chronic diseases, including cardiovascular and cerebrovascular diseases. Wang and associates from Zhongnan Hospital, Wuhan, reported clinical characteristics of 138 hospitalized patients with the 2019 coronavirus.[34] Of the 138 COVID-19 patients, 64 had one or more coexisting medical conditions; hypertension (31.2%), diabetes (10.1%), and CVD (14.5%).

A meta-analysis of five studies by cardiologists of Shandong University, China, reported the presence of comorbidities in COVID-19 patients admitted to hospitals.[34] The leading comorbidities were hypertension (17.1%), cardiac-cerebrovascular disease (16.4%), and diabetes (9.7%), in that order.[34] Severity and fatality seem to increase with comorbidities such as hypertension, obesity, cardiovascular disease, diabetes, and chronic pulmonary disease.[26-28] In a large study of 72,314 patients from China, the authors reported that those who needed hospitalization had underlying conditions, especially hypertension, diabetes, and cardiovascular disease.[35,36] Early risk assessment—monitoring risk factors for hypoxia, neutrophil extracellular traps, blood vessel damage, lung injury, cardiac injury (cTn1 and proBNP), cytokine storm (IL-6, IL-7, IL-22, IL-17, etc.), and activation of the coagulation cascade cascade (fibrinogen, D-dimer, plasmin)—will help the clinicians in making a wise decision for appropriate interventions.

COVID-19: Hematological Disorders

The most common hematological findings reported include lymphocytopenia, neutrophilia, eosinopenia, mild thrombocytopenia, less frequently thrombocytosis.[37] According to a meta-analysis, leukocytosis, lymphopenia, and thrombocytopenia are associated with the severity and even fatality of COVID-19 cases.[38] During this disease, changes in hemostasis have also been reported, such as prolonged prothrombin time and activated partial thromboplastin time and increased D-dimer levels. In severe cases of this disease, D-dimer levels seem to get elevated, with the formation of microthrombi in peripheral blood vessels. Furthermore, IL-6, IL-10, and serum ferritin were also strong discriminators for the severity of the disease. Several mediators modulate the release of chemoattractant and neutrophil activity. It is believed that higher values of proinflammatory markers are related to extensive lung injury.[39] The neutrophils are known to develop a sophisticated network of extracellular fibers composed of DNA containing histones, called neutrophil extracellular traps (NETs). There is some evidence to suggest that NETosis is conditional on the production of reactive oxygen species (ROS). Whereas several stimuli trigger NETosis, including pathogen-associated molecular patterns, damage-associated molecular patterns, and inflammatory mediators.

In an earlier article on this topic, we described that neutrophilia predicts poor outcome in patients with severe COVID-19 cases, and neutrophil to lymphocyte ratio may be an independent risk factor for the severity of this disease.[27] In a recent article, Shivakumar with associates from India found that the neutrophil-to-lymphocyte-to monocyte ratio and the platelet-to-lymphocyte ratio were prognostic significant in COVID-19.[40] According to these authors, in inflammation, platelet production increases due to the increased synthesis of thrombopoietin, which is modulated by cytokines. Acute lung injury also leads to leaky blood vessels. Activated platelets enhance lymphocyte adhesion to the endothelium. These events enhance the inflammation, platelet activation, expression of tissue factor, and promote a prothrombotic condition. The elevation of D-dimer, observed in some of the studies, indicates the occurrence of a prothrombotic event, followed by thrombolysis. In a normal situation, the thrombolytic system should clear thrombus formed by endogenous thrombolytic agents. Researchers from the University of North Carolina by infecting Serpine1-knockout mice with SARS-CoV have demonstrated the increased expression of tissue factor and Serpine2 in the absence of Serpine1 and an overall dysfunction of the urokinase pathway. The results of these studies

demonstrate that a fine balance exists between host coagulation and fibrinolysis pathways regulating pathological disease outcomes, including infection by highly pathogenic viruses such as SARS-CoV-2.[41-43]

COVID-19: Hypertension

Hypertension is the leading cause of cardiovascular disease and premature death worldwide.[44] Estimates suggest that 31% of adults (1.39 billion) worldwide had hypertension in 2010. These figures just estimate and do not represent reality. Having said that, we assure readers that hypertension is one of the leading metabolic diseases, which significantly contributes to vascular dysfunction, arterial stiffness, hardening of the arteries, and progress of subclinical atherosclerosis.

In the editorial of the American Journal of Hypertension (AJH. 2020;33(5):373), Schiffrin and associates discuss hypertension as one of the most frequently reported comorbidities in patients with COVID-19. They state in their review that the frequency with which COVID-19 patients are hypertensive is not entirely surprising nor does it necessarily imply a causal relationship between hypertension and COVID-19 or its severity, since hypertension is exceedingly frequent in the elderly, and older people appear to be at particular risk of being infected with SARS-CoV-2 virus and of experiencing severe forms of and complications of this disease.

This can be said for all the known metabolic diseases. Early reports suggesting that SARS-CoV-2 binds to ACE2 in the lungs to enter the cells has raised questions about the possibilities that ACE-inhibitors or angiotensin receptor blockers (ARBs) used in the treatment of hypertension may somehow alter the severity of the otherwise of coronavirus disease.

The authors of this editorial concluded, that there is no evidence that hypertension is related to the outcomes of COVID-19, or that ACE-inhibitors or ARBs use is harmful. This editorial in AJH discussed the coronavirus disease more from the treatment of hypertension point of view and did not discuss the role of hypertension as a pre-existing condition that enhanced the severity of the coronavirus disease.

A great number of studies have shown that aging and hypertension are associated with impairments of endothelium-dependent vascular relaxation in the coronary, forearm, and renal arteries, and endothelial dysfunction.[45, 46] The normal hemodynamics is maintained by a fine balance between the vasoactive compounds generated between the vessel wall components and the circulating blood components. As an example, in Figure 2, we have shown a schematic representation of the role of vasoactive metabolites of arachidonic acid and L-arginine, generated by the endothelial cells as the mediators of vasodilation.

We also have shown that the synthesis of these endogenous vasodilators is inhibited by lipid hydroperoxides and oxidized lipoproteins formed in the circulating blood. According to Prof. Mehra of Harvard University, the virus enters the lung, destroys the lung tissue, breaks open some blood vessels, then starts to infect endothelial cells, initiates a local immune response, and inflames the endothelium. He further elaborates, "A respiratory virus infecting blood cell, and circulating through the body, is virtually never heard of." The pathophysiology of hypertension involves the complex interaction of multiple vascular effectors, including activation of the sympathetic nervous system, of the renin-angiotensin-aldosterone system, and the inflammatory mediators. Oxidative stress and endothelial dysfunction are consistently observed in hypertensive subjects. COVID-19 patients with hypertension seem to have severe pneumonia, excessive inflammation, compromised endothelium, organ and tissue damage, and severity of the disease. Patients with hypertension should be given additional attention to prevent the added disease burden posed by the pre-existing comorbidity.

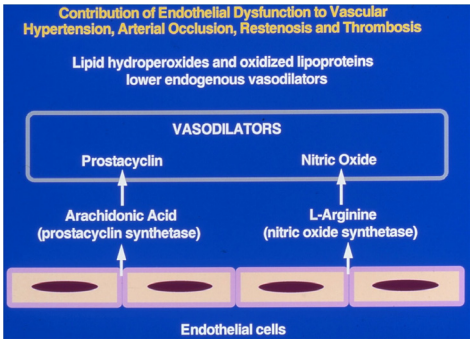

Fig. 2. *Contribution of endothelial dysfunction to altered hemodynamics*

COVID-19: Excess Weight and Obesity

According to the World Health Organization, in 2016 more than 1.9 billion adults, 18 years or older, were overweight. Of these over 650 million were obese. Over 340 million children and adolescents, aged 5-19, were overweight or obese. These obese individuals are at a higher risk for coronavirus disease. In the first meta-analysis of its kind, published on 26 August 2020, in Obesity Reviews, researchers pooled data from scores of articles capturing 399,000 patients. They found that people with obesity who contacted SARS-CoV-2 were 113% more likely than people of healthy weight to land in the hospital, 74% more likely to be admitted to an ICU, and 48% more likely to die.[47] People with obesity are prone to have the metabolic disease, with unhealthy levels of blood sugar, fat, and elevated blood pressure. They also seem to have a lower immune response than healthy individuals. Patients with metabolic syndrome, as well as those who are obese have been shown to have reduced response to the vasodilator acetylcholine after intra-arterial infusion, suggesting vascular dysfunction.[48-50]

Researchers who reviewed Data from 6916 patient records from Kaiser Permanente reported that compared to normal body mass index (BMI) of 18-24 kg/m^2, the risk of death more than doubled for patients with a BMI of 40-44 kg/m^2 and nearly doubled again, for those with a BMI of 45kg/m^2 or more.[51] In an accompanying editorial, David A Kass, a Cardiologist at the Johns Hopkins University, wrote, "that these findings are taken with prior research, should put to rest the contention that obesity is common in severe COVID-19, because it is common in the population." The pathophysiology of hypertension involves the complex interaction of multiple vascular effectors, including activation of the sympathetic nervous system, of the renin-

angiotensin-aldosterone system, and the inflammatory mediators.[52] Oxidative stress and endothelial dysfunction are consistently observed in hypertensive subjects.[53] As the body weight increases, the blood pressure also rises. Therefore, people with excess weight or obesity will have the added burden of hypertension and clinical manifestation associated with this altered blood vessel function. Each metabolic disease is syndemic in its nature, as it adds additional disease burden to the pre-existing conditions.

As we have discussed earlier, obesity has reached epidemic proportions worldwide. In the USA alone, the prevalence of obesity has increased 50% in the past three decades, with 70% of all adults being classified as either overweight or obese. Beyond an impaired response to infections, people with obesity also suffer from chronic, low-grade inflammation. Fat cells secrete inflammation triggering chemical messengers called cytokines, and more come from immune cells called macrophages, that clean up dead and dying fat cells. These, in turn, impair vascular homeostasis and lead to endothelial dysfunction.[54] Data on how to treat COVID-19 patients with obesity are scant. Dr. Scott Khan, an obesity medicine physician at the National Center for Weight and Wellness, suggests giving such patients higher doses of anticoagulants. Looks like it is left to the attending clinicians to develop and administer the best treatment protocol, based on the clinical symptoms presented at the time of admission.

COVID-19: Type-2 Diabetes

According to a recent article in the journal Science, dozens of studies have reported that many of the sickest COVID-19 patients have been people with obesity.[47] The impact extends to the 32% of people in the United States who are overweight. The largest descriptive study of hospitalized COVID-19 patients by Genentech researchers found that 77% of the nearly 17,000 patients hospitalized with CIVID-19 were overweight (29%) or obese (48%). These obese individuals also will have other compounding problems, diabetes being one. It is well known that the blood of people with diabetes has prothrombotic status, meaning, 'increased tendency to clot.' Coronavirus injures endothelial cells, which are already compromised in obese and diabetic individuals, and as such response to this insult by activation of platelet and coagulation pathways. Furthermore, immunity also weakens in people with excess weight, obesity, and diabetes. According to the authors of an article in NEJM, there seems to be a bidirectional relationship between Covid-19 and diabetes.[55] The virus binds to the ACE2 receptors, which are expressed in key metabolic organs and tissues, including pancreatic beta cells, adipose tissue, the small intestine, kidneys. The authors speculate that SARS-CoV-2 may cause pleiotropic alterations of glucose metabolism that could complicate the pathophysiology of pre-existing diabetes or its clinical manifestations.

Metabolic diseases such as hypertension, excess weight, and obesity induce vascular remodeling through various mechanisms. Under normal conditions, vascular structure, vessel wall physiology, and flow dynamics are maintained by a variety of endogenous modulators. However, metabolic stress forces the vessel to adapt and remodel depending upon the nature of the stress. Metabolic factors such as hyperglycemia, oxidative stress, and chronic inflammation play a role in diabetes. Since hypertension, excess weight, and obesity contribute significantly to the development of diabetes, major drivers of vascular remodeling are endothelial dysfunction due to altered synthesis of vasodilators and vasoconstrictors, and changes in the complex signaling pathways.[56] Irrespective of whether it is hypertension, excess weight, obesity, or diabetes, the molecular mechanisms involved in the development of altered blood flow, arterial stiffness, hardening of the arteries, and vascular dysfunction seem to be the same. However, in the case of diabetes hyperglycemic state of the blood adds one more contributor to the vascular damage and remodeling. No matter how we look at this situation, all the metabolic diseases have one thing in common, a dysfunctional vascular system, and a compromised immune system, that contributes to the severity of coronavirus disease in these patients.

To address such issues, an international group of leading diabetes researchers participating in the CoviDIAB Project have established a global registry of patients with Covid-19-related diabetes. The goal of the registry is to establish the extent and phenotype of new-onset diabetes that is defined by hyperglycemia, confirmed Covid-19, negative history of diabetes, and a history of normal glycated hemoglobin (covidiab.e-dendrite.com). Since our interest is metabolic diseases, any infectious disease that is syndemic on metabolic risks becomes an important topic of interest. In the countries with the largest number of diabetic individuals, China, India, and the USA, there are an equal number of prediabetic individuals. If we put together pre-diabetics and diabetics, the total number of people at risk for COVID-19 related risk exceeds a billion individuals. Therefore, in our opinion, individuals with hypertension, excess weight, obesity, and diabetes are at a greater risk of severe COVID-19. The question of why China and India with the largest populations of diabetics have relatively low rates of COVID-related mortality is quite puzzling. In China, the COVID-19 pandemic's epicenter, Wuhan, and its province, Hubei, Chinese Center for Disease Control-network, formed 1300 epidemic investigation teams, in addition to the 40,000 doctors and nurses. They used very cleverly tracing tools with big data support. In the first week of January the novel coronavirus infection was detected, and on 23 January 2020, they locked down the city of 11 million people and soon the rest of the Hubei-a province of nearly 60 million. The WHO-China Joint Mission on Coronavirus Disease 2019 Task Force concluded, "In the face of an unknown virus, China has rolled out perhaps the most ambitious, agile, and aggressive, disease containment effort in history." The strategy that underpinned this containment effort was initially a national approach, that promoted universal temperature monitoring, masking, and handwashing.[57] As far as India is concerned, the general population thinks that they have innate immunity, as they are exposed to a variety of Asian viruses, including several strains of coronaviruses. The second surge of COVID-19 in India has demonstrated that those individuals with comorbidities such as hypertension and type 2 diabetes are at higher risk for severe coronavirus disease and death. Yet, COVID-related deaths and case fatality rates reported are relatively low in India.

COVID-19: Cardiac Health

Novel coronavirus disease seems to affect all the vital organs of the body including the heart. Several studies have

reported that many COVID-19 survivors experience some type of heart damage, even if they do not have underlying heart disease. "Very early into the pandemic, it was clear that many patients who were hospitalized were showing evidence of cardiac injury," says Dr. Gregg Fonarow, chief of the division of cardiology at the University of California, Los Angeles. He further elaborates on this condition, "This raises concerns that there may be individuals who get through the initial infection but are left with cardiovascular damage and complications." In JAMA Cardiology, analysis of autopsies on 39 COVID-19 patients identified infections in the hearts of patients who had not been diagnosed with cardiovascular issues while they were ill.[58] The novel virus can damage the heart in several ways. For instance, the virus may directly invade the heart muscle; it may indirectly harm the heart by disrupting the balance between oxygen supply and demand. The heart injury may be measured by elevated levels of the enzyme, cardiac troponin in the blood. An elevated level of this cardiac enzyme has been reported in about one-quarter of patients hospitalized with COVID-19. Invasion of the heart muscle may induce myocarditis, which results in an enlarged or weakened heart, low blood pressure, and fluid accumulation in the lungs.

Since the virus uses the ACE2 enzyme as the preferred receptor for entry, the virus may directly invade these receptors on myocardial tissues and cause direct viral harm. It also can affect the heart muscle itself through inflammation, leading to significant heart failure. Dr. Hyung Chun a Yale Cardiologist and director of Translational Research, says one emerging belief is that the endothelial cells, which line the blood vessels, in people with cardiac issues respond differently to the body's immune response. They seem to release inflammatory cytokines that further compromise the body's inflammatory process and lead to the formation of blood clots. The 'inflamed' endothelium seems to contribute to worsening outcomes in COVID-19 and is an important factor contributing to the risk of heart attacks and stroke. As a rule, those confirmed with COVID-19 infection should be on the lookout for symptoms that may indicate damage to the heart or cardiac complications. These symptoms include shortness of breath, chest pain, or heart palpitations. These symptoms may indicate myocarditis, which is one of the potential factors for developing acute coronavirus disease 2019 cardiovascular syndrome (ACovCS). The American Heart Association Journal, Circulation, has published a 'White paper' on this topic.[59] The article reviews the best available data on acute COVID-19 Cardiovascular syndrome epidemiology, pathogenesis, diagnostic, and treatment.

COVID-19: Cardiovascular Disease

The pre-existing metabolic risks seem to cause worse outcomes and increased risk of death in patients with COVID-19, whereas this virus can also cause vascular damage, myocardial injury, arrhythmia, acute coronary syndrome, and venous thromboembolism. Dr. Nishiga and associates of the Stanford Cardiovascular Institute (CVI), Stanford University School of Medicine, summarized the current understanding of COVID-19 and the cardiovascular system in the journal Nature.[60] As we have discussed earlier, the interaction between the viral spike (S) protein and angiotensin-converting enzyme 2, which facilitates the entry of the virus into host cells, seems to be involved in the cardiovascular manifestations of COVID-19. In one of the earliest reports from Wuhan, involving 41 hospitalized covid-19 patients, the prevalence of comorbidity was greater than 30% and the most common underlying metabolic diseases were diabetes(20%), hypertension (15%), and CVD (15%).[2] In a report from Italy involving 1,591 patients with COVID-19 who needed ICU care, 49% had hypertension, 22% had CVD, and 17% had diabetes.[61] Whereas in a report from New York, USA, of the 393 COVID patients who were on ventilators, up to 50% had hypertension, 36% had obesity, 25% had diabetes and 14% had coronary artery disease.[62] Recent observations suggest that approximately 25% of people hospitalized with COVID-19 have cardiovascular complications, contributing to about 40% of all COVID-19-related deaths.

Even though acute hypoxic respiratory failure is the characteristic clinical feature of SARS-CoV-2, many diverse clinical cardiovascular (CV) manifestations have been reported, including heart failure, circulatory shock, cardiomyopathy, arrhythmia, and vascular thrombosis. Since it has been well established that CV-related manifestations portend greater mortality, they pose a great challenge to the clinicians working to develop an appropriate treatment protocol. It becomes essential for the clinicians to think through and consider all possible CV clinical manifestations, appropriate biomarkers for early diagnosis of these risks, and to develop appropriate therapies for COVID-19-positive patients.[63] According to a white paper published by the American Heart Association editors, the two take-home points are 1) Elevated levels of troponin are frequently seen in patients with COVID-19 disease and are associated with increased severity of disease and risk of death; and 2) In the absence of a specific cause, elevated levels of cardiac troponins are likely attributable to myocardial injury from inflammation or a direct effect of SARS-CoV-2 infection.[64] The paper also poses some questions that need to be addressed. 1) The role of troponin in clinical risk stratification, and as a prognostic factor of disease severity and mortality. 2) Mechanistic studies are needed to evaluate the cause of myocardial injury and determine whether there is a potential for a therapeutic option. Many studies have reported that infection with COVID-19 may predispose one to venous and arterial thromboembolism to a greater degree with worse disease severity.[65] The management of CVD in patients with COVID-19 includes general supportive treatment, circulatory support, other symptomatic treatment, and psychological assistance, as well as online consultation.

COVID-19: Cerebrovascular Disease

In one of the early studies reported from Wuhan, China, researchers conducted a retrospective study of 214 patients admitted with COVID-19 infection. Of these (mean age of 52) 78 patients (36.4%) had neurologic manifestations.[66] SARS-CoV-2 binds to ACE-2, leading to the downregulation of this receptor function and contributes to the post-ischemic inflammation cascade resulting in decreased perfusion of the ischemic areas of cerebral tissue with larger infarct volume and ischemic stroke.[67] Furthermore, ACE2 dysfunction may

cause hypertensive peaks and impairment of cerebrovascular endothelium, leading to intracerebral hemorrhage. It has also been reported that systemic hypotension may induce hypo ischemic encephalopathy and microbleeds. Researchers from Saudi Arabia report that neurological complications range from dizziness, headache, hyposmia, encephalopathy, infarcts, microhemorrhages, and stroke.[68] They also report decreased deformability of red blood cells and hypercoagulability, resulting in hypoxia and inflammation in these patients. A systematic review has analyzed data from 1,210 articles with 226 cases of ischemic stroke.[69,70] According to this report, large vessel occlusion (LVO) was observed in 105 patients, acute intracranial bleeding in 35 patients, intracerebral hemorrhage (ICH) in 24 patients, 4 patients had non-traumatic subarachnoid hemorrhage (SAH), remaining 7 patients had simultaneous presence of SAH and ICH. The authors concluded that cerebrovascular events are relatively common findings in COVID-19 infection and could have a multifactorial etiology.

Furthermore, of the total of 226 cases of ischemic stroke, 35 cases of intracranial bleeding, and 14 cases of cerebrovascular sinus thrombosis (CVST), were reported. According to these investigators, postmortem brain magnetic resonance imaging (MRI) showed extensive signs of cerebrovascular involvement, including microbleeds with subcortical and posterior predominance. Among these patients, D-dimer levels were at least four-fold higher than normal values. Inflammation is a common occurrence in Covid-19 patients. It is well known that both acute and chronic infections and inflammatory states serve as triggers of stroke. By and large, COVID-19 patients with pre-existing metabolic diseases such as hypertension, excess weight, obesity, type-2 diabetes, and CVDs have increased severity at the time of admission to the hospital. These pre-existing risks make it very difficult to develop an optimal treatment regimen.

COVID-19: Arterial and Venous Diseases

Coronavirus disease severity is associated with venous thromboembolism as well as arterial thrombosis. Thrombotic complications, as well as coagulopathy, have been reported in COVID-19 positive individuals. COVID-19 associated coagulopathy (CAC), detected by the increase in D-dimer and fibrinogen levels with minimal abnormalities in prothrombin time and platelet count has been reported in COVID-positive cases. The high mortality associated with thromboembolic diseases in COVID-19 has prompted clinicians to use D-dimer as a useful marker for assessing the severity of the disease.[71] According to a review by Harvard Medical School researchers, in critically ill patients with COVID-19, elevated levels of D-dimer were found in 100% of participants, elevated fibrinogen in 74% of the participants, and factor V11 in 100% of participants. Antiphospholipid antibodies were detected in 53% of the participants, decreased protein C, protein S, and antithrombin levels were detected in all participants.[72] Coagulation abnormalities were associated with acute vascular events such as stroke, peripheral arterial ischemia, and venous thromboembolism. Guidelines from the American College of Chest Physicians suggest prophylaxis with Low Molecular Weight Heparins (40mg) and fondaparinux 2.5 mg, in the absence of any contraindications, such as active bleeding. However, this professional society does not recommend post-discharge thromboprophylaxis. The International Society on Thrombosis and Hemostasis suggests duration of 14 to 30 days for post-discharge thromboprophylaxis. Thromboprophylaxis for patients who do not require hospitalization is not currently recommended.

Prevention

When discussing prevention strategies, we need to consider the unprecedented pandemic of SARS-CoV-2 as well as a pre-existing epidemic of metabolic risks, metabolic diseases, and vascular diseases worldwide, which increase the severity of COVID-19. Having said that, we need to remember that no country has reduced, reversed, or prevented the increase in the incidence of metabolic diseases. Metabolic diseases have increased rapidly to epidemic proportions worldwide in the last three decades. COVID-19 is not going to go away any sooner. Twindemic is going to continue to play havoc for quite some time to come and will be a public health experts' nightmare. In a large study of 72,314 patients from China, the authors reported that those who needed hospitalization had underlying conditions, especially hypertension, obesity, diabetes, and cardiovascular disease.[35,36] Early risk assessment, monitoring risk factors for hypoxia, neutrophil extracellular traps (NETs), blood vessel damage, lung injury, platelet activation, the formation of microthrombi or microbleeds, cardiac injury (cTn1 and proBNP), cytokine storm (IL-6, IL-7, IL-22, IL-17, etc.), activation of the coagulation cascade (fibrinogen, D-dimer, plasmin), will help the clinicians in making a wise decision for appropriate interventions.[73,74]

In the absence of a cure for coronavirus disease, sensible medicine proposes a gentler, moderate, and humble view of available treatment options and their effectiveness in patients with COVID-19. The approach encourages clinicians, to elevate usual care, reduce unnecessary interventionism, focus, and rely on scientific rigor. By and large, treatment options are based on clinical diagnosis-based treatments for observed symptoms. For patients with COVID-19, who are not hospitalized or who are hospitalized with moderate disease, but do not require supplemental oxygen, the National Institutes of Health (NIH, USA) panel does not recommend any specific antiviral or immunomodulatory therapy, for the treatment of coronavirus disease in these patients. For those hospitalized with severe conditions, the panel recommends Remedesivir 200 mg intravenously (IV) for 1 day followed by a 100 mg dose for four days or until hospital discharge. A combination of Remedesivir and dexamethasone 6 mg IV up to 10 days. As mentioned earlier, currently, there are no US FDA-approved therapies, for coronavirus disease treatment. FDA has created a special emergency program for possible coronavirus therapies, the Coronavirus Treatment Acceleration Program (CTAP). Currently, there are 590 drug development programs in planning stages, 390 trials in review, and five authorized for emergency use, none approved for use in COVID-19 management.

As of this writing, there are at least 51 studies listed in the COVID-19 vaccine tracker of the Regulatory Affairs Professional Society (RAPS) site. The top ten entries, which are

under phase 3 trial, include Ad5-nCoV, a recombinant vaccine by CanSino Biologics (China); AZD1222, a replication-deficient adenovirus vector vaccine (The University of Oxford, the Jenner Institute); CoronaVac by Sinovac; JNJ-78436735, a non-replicating viral vector by Johnson and Johnson; mRNA-1273, an mRNA-based vaccine by Moderna; an unnamed inactivated vaccine by Wuhan Institute of Biological Products; NVX-CoV2373, a nanoparticle vaccine by Novavax. There are several new entries in phase 2/3 trials, including the BCG vaccine by the University of Melbourne and Mass. General Hospital, Boston; BNT162, an mRNA-based vaccine by Pfizer-BioNTech; and Covaxin, an inactivated virus vaccine by Bharat Biotech, National Institute of Virology, India. According to a recent article in the New Engl. J. Med., confidence in any COVID-19 vaccine that is made available under an emergency use authorization (EUA) will depend on the rigor of the clinical criteria, including the duration of follow-up, safety, and efficacy of the vaccine.[75] With phase 3 clinical trials of COVID-19 vaccine underway, safety and efficacy data will be provided to the FDA soon after they are compiled.[76] Emergency use authorization will be made by the FDA's Center for Biologics Evaluation and Research (CBER). The decision of this branch of the FDA has been approved by the Vaccines and Related Biological Products Advisory Committee (VRBPAC).

There are twelve vaccines against SARS-CoV-2 that have been authorized for use in various locations around the world. These include mRNA vaccines, viral vector vaccines, subunit vaccines, and inactivated virus vaccines. mRNA vaccines do not contain any part of the virus. They carry a chemically synthesized piece of messenger RNA, containing the information needed for cells to make the spike proteins of the virus that is essential for infection. Like the mRNA, vector vaccines also do not contain the SARS-Cov-2 virus. They use adenovirus as the delivery system. Subunit vaccines use part (spike protein) of the SARS-Cov-2 virus. Inactivated vaccines contain the entire SARS-CoV-2 virus inactivated by beta-propiolactone. At the time of this writing, globally, the following vaccines have been given emergency use authorization against COVID-19: mRNA-1273 (Moderna, US), BNT162b2 (Pfizer-BioNTech, US), Ad26CoV2.S (Viral vector, Johnson & Johnson, US), ChAdOx1(Viral vector, AstraZeneca/Oxford, UK), NVX-CoV2373 (Novavax Inc, US), CVnCoV-mRNA (GSK, Germany), Gam-COVID-Vac (Sputnik V, Viral vector, Russia), CoronaVac (inactivated virus, China), and BBIBP-CorV (inactivated virus, China), Covaxin (inactivated virus, Bharath Biotech, India).[77]

A variety of nanobodies (nAbs) against SARS-CoV-2, which target the S protein of the virus, are in preclinical development.[78] Monoclonal antibodies are usually large and must be produced in mammalian cell expression systems. On the other hand, nanobodies are single-domain antibodies with small size, good solubility, stability and could be produced in *Escherichia coli* and yeast cell cultures. Therefore, they could be produced at relatively low cost in large quantities. National Institutes of Health researchers have isolated tiny antibodies against SARS-CoV-2. One of the advantages of the nanoantibodies is that they can be aerosolized to use in inhalers to coat the lungs and airways, the preferred route of SARS-CoV-2 entry.

Considering the contribution of comorbidities to the progression and severity of the coronavirus disease, one would expect that China, India, and the USA, with the largest populations of diabetic subjects, should have the highest CFR (Deaths per 100,000 population) for COVID-19. On the other hand, Mexico (8.5%), Peru (3.6%), Italy (3.5%), and South Africa have a lot more mortality than the USA (1.0%) and India (1.7%) (Coronavirus.jhu.edu/data/mortality; February 4, 2021). Since the three major populations with the highest number of diabetics have not shown a comparatively high case fatality rate, it is worthwhile discussing the other two comorbidities (hypertension and obesity) as the chief contributors for the Covid-19 progression and severity. Trends in the prevalence of hypertension in the USA, according to the NHANES survey of age-standardized prevalence, decreased from 48.4% in 1999-2000 to 45.4% in 2015-2016. However, the absolute burden of hypertension consistently increased, from 87.0 million in 1999-2000 to 108 million in 2015-2016.[79] Hypertension appears to be more common in Mexico, than among Mexican Immigrants in the United States. As far as obesity goes, the number of obese children and adolescents aged five to 19 years, has risen tenfold in the past four decades and if current trends continue, there will be more obese children and adolescents than those moderately.[80] Among adolescents, obesity prevalence in the USA was 16.8% in 2007 and 18.5% in 2016. Age-standardized obesity in adults increased from 33.7% in 2007 to 39.6% in 2015. Whereas 62% of the participants in Mexico reported, at least, being overweight.[81] When considering obesity data based on the BMI, we should keep in mind that South Asians have a different body fat distribution, compared to the European and Western populations. South Asians in general have central abdominal obesity.

If we carefully analyze a series of clinical events, that develop a post-SARS-CoV-2 infection, we can begin to understand, why metabolic diseases serve as independent risk factors for the progression and severity of coronavirus disease. The initial route of entry is via the nasal and oral mucosa, the preferred receptor that facilitates the transmission seems to be the ubiquitous ACE2, which is found in multiple types of cells and tissue including vascular endothelium. Recent findings, that following the injury to the lung tissue, the virus gets entry into the endothelium, opens a whole new avenue for the progress of the disease and its severity. The endothelium is the largest organ of the body, covering a large surface area and reaching out to every tissue and organ. As such, the injury to the endothelium could introduce a cascade of events, leading to platelet activation, thrombin generation, and promotion of both thrombotic and thrombolytic events.[29,41] Furthermore, people with metabolic diseases such as hypertension, excess weight, obesity, diabetes (Type 2), and vascular disease, already have a compromised endothelium, and invasion of the SARS-CoV-2 virus leads to endothelialitis and causes further injury to the vascular system, disruption of vascular integrity and endothelial cell death.[82-85] These events lead to the exposure of the subendothelial basement membrane and result in the activation of thrombotic and clotting cascade of events.

This unprecedented pandemic of SARS-CoV-2 has taught us two lessons: first, the importance of robust public

health infrastructure, and second, the need for an immediate call for action to reduce, reverse, or prevent metabolic diseases worldwide. The recent statement from the Institute for Fiscal Studies *Deaton Review on inequality* (IFS Deaton Review, Jan 5, 2021), stressed that the opportunity cost of the pandemic for young people is potentially huge, but also that it is a "once-in-a-generation opportunity to tackle the disadvantages faced by many that this pandemic has so devastatingly exposed." In a recent editorial of the Lancet Public Health, the editor concludes that adopting a broadened, equity-based approach to population health should be an essential part of building a more resilient society that is better prepared for future pandemics.[86]

References

1. Zhu N, Zhang D, Wang W, Li X, Yang B, Song J, et al.; China Novel Coronavirus Investigating and Research Team. A Novel Coronavirus from Patients with Pneumonia in China, 2019. N Engl J Med. 2020 Feb 20;382(8):727-733. doi: 10.1056/NEJMoa2001017.
2. Huang C, Wang Y, Li X, Ren L, Zhao J, Hu Y, et al. Clinical features of patients infected with 2019 novel coronavirus in Wuhan, China. Lancet. 2020 Feb 15;395(10223):497-506. doi: 10.1016/S0140-6736(20)30183-5.
3. Chen N, Zhou M, Dong X, Qu J, Gong F, Han Y, et al. Epidemiological and clinical characteristics of 99 cases of 2019 novel coronavirus pneumonia in Wuhan, China: a descriptive study. Lancet. 2020 Feb 15;395(10223):507-513. doi: 10.1016/S0140-6736(20)30211-7.
4. Wang D, Hu B, Hu C, Zhu F, Liu X, Zhang J, et al. Clinical Characteristics of 138 Hospitalized Patients With 2019 Novel Coronavirus-Infected Pneumonia in Wuhan, China. JAMA. 2020 Mar 17;323(11):1061-1069. doi: 10.1001/jama.2020.1585. Erratum in: JAMA. 2021 Mar 16;325(11):1113. PMID: 32031570; PMCID: PMC7042881.
5. Wu C, Chen X, Cai Y, Xia J, Zhou X, Xu S, et al. Risk Factors Associated With Acute Respiratory Distress Syndrome and Death in Patients With Coronavirus Disease 2019 Pneumonia in Wuhan, China. JAMA Intern Med. 2020 Jul 1;180(7):934-943. doi: 10.1001/jamainternmed.2020.0994. Erratum in: JAMA Intern Med. 2020 Jul 1;180(7):1031. PMID: 32167524; PMCID: PMC7070509.
6. Kamps BS, Hoffmann C: COVID REFERENC ENG/2021.6.covidreference.com https://amedeo.com/CovidReference06.pdf (www.CovdiRefrence.com)
7. Karabag SF: An unprecedented Global Crisis! The Global, Regional, National, Political, Economic and Commercial Impact of the Coronavirus Pandemic. J App. Econ. & Bus. Res. 10)10):1-6 (2020)
8. Shrestha N, Shad MY, Ulvi O, Khan MH, Karamehic-Muratovic A, Nguyen UDT, et al. The impact of COVID-19 on globalization. One Health. 2020 Dec 20;11:100180. doi: 10.1016/j.onehlt.2020.100180.
9. Haghani M, Bliemer MCJ. Covid-19 pandemic and the unprecedented mobilisation of scholarly efforts prompted by a health crisis: Scientometric comparisons across SARS, MERS and 2019-nCoV literature. Scientometrics. 2020 Sep 21:1-32. doi: 10.1007/s11192-020-03706-z.
10. Cutler DM, Summers LH. The COVID-19 Pandemic and the $16 Trillion Virus. JAMA. 2020 Oct 20;324(15):1495-1496. doi: 10.1001/jama.2020.19759.
11. Conti P, Caraffa A, Gallenga CE, Kritas SK, Frydas I, Younes A, et al. The British variant of the new coronavirus-19 (Sars-Cov-2) should not create a vaccine problem. J Biol Regul Homeost Agents. 2021 Jan-Feb;35(1):1-4. doi: 10.23812/21-3-E. PMID: 33377359.
12. Horton R: COVID-19 is not a pandemic. Lancet 2020; 396 (10255): 874.
13. Singer M, Bulled N, Ostrach B, Mendenhall E. Syndemics and the biosocial conception of health. Lancet. 2017 Mar 4;389(10072):941-950. doi: 10.1016/S0140-6736(17)30003-X. PMID: 28271845.
14. Mendenhall E. Beyond Comorbidity: A Critical Perspective of Syndemic Depression and Diabetes in Cross-cultural Contexts. Med Anthropol Q. 2016 Dec;30(4):462-478. doi: 10.1111/maq.12215.
15. Rao GHR: Global Syndemic of Metabolic Diseases: Editorial Comments. Journal of Diabetes & Clin. Res. 2018; I(1): 2-4.
16. Rao GHR: COVID-19 and Cardiometabolic Diseases.: Guest Editorial. EC Cardiol 2020; 7.6:08-12.
17. Rao GHR: Coronavirus (COVID-19), Comorbidities, and Acute Vascular Events; Guest Editorial. ECCMC EC Clinical Case Reports. 2020; 3.6:87-91.
18. Rao GHR: Coronavirus Disease (Covid-19), Comorbidities, and Clinical Manifestations. Guest Editorial. EC Diab, Met Res. 2020; 4.6 : 27-33.
19. Gussow AB, Auslander N, Faure G, Wolf YI, Zhang F, Koonin EV. Genomic determinants of pathogenicity in SARS-CoV-2 and other human coronaviruses. bioRxiv [Preprint]. 2020 Apr 9:2020.04.05.026450. doi: 10.1101/2020.04.05.026450. Update in: Proc Natl Acad Sci U S A. 2020 Jun 30;117(26):15193-15199.
20. Shang J, Wan Y, Luo C, Ye G, Geng Q, Auerbach A, Li F. Cell entry mechanisms of SARS-CoV-2. Proc Natl Acad Sci U S A. 2020 May 26;117(21):11727-11734. doi: 10.1073/pnas.2003138117.
21. Tortorici MA, Veesler D. Structural insights into coronavirus entry. Adv Virus Res. 2019;105:93-116. doi: 10.1016/bs.aivir.2019.08.002.
22. Hoffmann M, Kleine-Weber H, Schroeder S, Krüger N, Herrler T, Erichsen S, et al. SARS-CoV-2 Cell Entry Depends on ACE2 and TMPRSS2 and Is Blocked by a Clinically Proven Protease Inhibitor. Cell. 2020 Apr 16;181(2):271-280.e8. doi: 10.1016/j.cell.2020.02.052.
23. Ming Y, Qiang L. Involvement of Spike Protein, Furin, and ACE2 in SARS-CoV-2-Related Cardiovascular Complications. SN Compr Clin Med. 2020 Jul 11:1-6. doi: 10.1007/s42399-020-00400-2.
24. Noor FM, Islam M: Prevalence of Clinical Manifestations and Comorbidities of Coronavirus (COVID-19) Infection: A Meta-Analysis. Fortune J. Health Sci 3 (2020):55-97.
25. Rao GHR. Coronavirus Disease and Acute Vascular Events. Clin Appl Thromb Hemost. 2020 Jan-Dec;26:1076029620929091. doi: 10.1177/1076029620929091.
26. Rao GHR: COVID-19 and Cardiometabolic Diseases.: Guest Editorial. EC Cardiol 2020; 7.6:08-12.
27. Rao GHR: Coronavirus (COVID-19), Comorbidities, and Acute Vascular Events; Guest Editorial. ECCMC EC Clinical Case Reports. 2020;3.6:87-91.
28. Coronavirus Disease (Covid-19), Comorbidities, and Clinical Manifestations. Guest Editorial. EC Diab, Met Res. 2020;4.6:27-33.
29. Rao GHR: Coronavirus Disease (Covid-19): A Disease of the Vascular Endothelium. Series Cardiology Res 2020; 2(1): 23-27.

30. Richardson S, Hirsch JS, Narasimhan M, Crawford JM, McGinn T, Davidson KW; the Northwell COVID-19 Research Consortium, Barnaby DP, Becker LB, Chelico JD, Cohen SL, Cookingham J, Coppa K, et al. Presenting Characteristics, Comorbidities, and Outcomes Among 5700 Patients Hospitalized With COVID-19 in the New York City Area. JAMA. 2020 May 26;323(20):2052-2059. doi: 10.1001/jama.2020.6775. Erratum in: JAMA. 2020 May 26;323(20):2098.
31. Huang C, Wang Y, Li X, Ren L, Zhao J, Hu Y, et al. Clinical features of patients infected with 2019 novel coronavirus in Wuhan, China. Lancet. 2020 Feb 15;395(10223):497-506. doi: 10.1016/S0140-6736(20)30183-5. Epub 2020 Jan 24. Erratum in: Lancet. 2020 Jan 30;. PMID: 31986264; PMCID: PMC7159299.
32. Chen N, Zhou M, Dong X, Qu J, Gong F, Han Y,et al. Epidemiological and clinical characteristics of 99 cases of 2019 novel coronavirus pneumonia in Wuhan, China: a descriptive study. Lancet. 2020 Feb 15;395(10223):507-513. doi: 10.1016/S0140-6736(20)30211-7.
33. Wu C, Yang W, Wu X, Zhang T, Zhao Y, Ren W, Xia J. Clinical Manifestation and Laboratory Characteristics of SARS-CoV-2 Infection in Pregnant Women. Virol Sin. 2020 Jun;35(3):305-310. doi: 10.1007/s12250-020-00227-0.
34. Wang B, Li R, Lu Z, Huang Y. Does comorbidity increase the risk of patients with COVID-19: evidence from meta-analysis. Aging (Albany NY). 2020 Apr 8;12(7):6049-6057. doi: 10.18632/aging.103000.
35. Wu Z, McGoogan JM. Characteristics of and Important Lessons From the Coronavirus Disease 2019 (COVID-19) Outbreak in China: Summary of a Report of 72 314 Cases From the Chinese Center for Disease Control and Prevention. JAMA. 2020 Apr 7;323(13):1239-1242. doi: 10.1001/jama.2020.2648.
36. Adão R, Guzik TJ. Inside the heart of COVID-19. Cardiovasc Res. 2020 May 1;116(6):e59-e61. doi: 10.1093/cvr/cvaa086.
37. Letícia de Oliveira Toledo S, Sousa Nogueira L, das Graças Carvalho M, Romana Alves Rios D, de Barros Pinheiro M. COVID-19: Review and hematologic impact. Clin Chim Acta. 2020 Nov;510:170-176. doi: 10.1016/j.cca.2020.07.016.
38. Henry BM, de Oliveira MHS, Benoit S, Plebani M, Lippi G. Hematologic, biochemical and immune biomarker abnormalities associated with severe illness and mortality in coronavirus disease 2019 (COVID-19): a meta-analysis. Clin Chem Lab Med. 2020 Jun 25;58(7):1021-1028. doi: 10.1515/cclm-2020-0369.
39. Borges L, Pithon-Curi TC, Curi R, Hatanaka E. COVID-19 and Neutrophils: The Relationship between Hyperinflammation and Neutrophil Extracellular Traps. Mediators Inflamm. 2020 Dec 2;2020:8829674. doi: 10.1155/2020/8829674.
40. Bg S, Gosavi S, Ananda Rao A, Shastry S, Raj SC, Sharma A, Suresh A, Noubade R. Neutrophil-to-Lymphocyte, Lymphocyte-to-Monocyte, and Platelet-to-Lymphocyte Ratios: Prognostic Significance in COVID-19. Cureus. 2021 Jan 11;13(1):e12622. doi: 10.7759/cureus.12622.
41. Varga Z, Flammer AJ, Steiger P, Haberecker M, Andermatt R, Zinkernagel AS, et al. Endothelial cell infection and endotheliitis in COVID-19. Lancet. 2020 May 2;395(10234):1417-1418. doi: 10.1016/S0140-6736(20)30937-5.
42. Ackermann M, Verleden SE, Kuehnel M, Haverich A, Welte T, Laenger F, et al. Pulmonary Vascular Endothelialitis, Thrombosis, and Angiogenesis in Covid-19. N Engl J Med. 2020 Jul 9;383(2):120-128. doi: 10.1056/NEJMoa2015432.
43. Gralinski LE, Bankhead A 3rd, Jeng S, Menachery VD, Proll S, Belisle SE, et al. . Mechanisms of severe acute respiratory syndrome coronavirus-induced acute lung injury. mBio. 2013 Aug 6;4(4):e00271-13. doi: 10.1128/mBio.00271-13.
44. Mills KT, Stefanescu A, He J. The global epidemiology of hypertension. Nat Rev Nephrol. 2020 Apr;16(4):223-237. doi: 10.1038/s41581-019-0244-2.
45. Higashi Y, Kihara Y, Noma K. Endothelial dysfunction and hypertension in aging. Hypertens Res. 2012 Nov;35(11):1039-47. doi: 10.1038/hr.2012.138.
46. Panza JA, Quyyumi AA, Brush JE Jr, Epstein SE. Abnormal endothelium-dependent vascular relaxation in patients with essential hypertension. N Engl J Med. 1990 Jul 5;323(1):22-7. doi: 10.1056/NEJM199007053230105.
47. Wadman M: Why COVID-19 is more deadly in people with obesity-even if they are young? Science 2020; doi:10.1126/science.abe7010.
48. Ignarro LJ, Buga GM, Wood KS, Byrns RE, Chaudhuri G. Endothelium-derived relaxing factor produced and released from artery and vein is nitric oxide. Proc Natl Acad Sci U S A. 1987 Dec;84(24):9265-9. doi: 10.1073/pnas.84.24.9265.
49. Van Guilder GP, Hoetzer GL, Dengel DR, Stauffer BL, DeSouza CA. Impaired endothelium-dependent vasodilation in normotensive and normoglycemic obese adult humans. J Cardiovasc Pharmacol. 2006 Feb;47(2):310-3. doi: 10.1097/01.fjc.0000205097.29946.d3. PMID: 16495771.
50. Steinberg HO, Chaker H, Leaming R, Johnson A, Brechtel G, Baron AD. Obesity/insulin resistance is associated with endothelial dysfunction. Implications for the syndrome of insulin resistance. J Clin Invest. 1996 Jun 1;97(11):2601-10. doi: 10.1172/JCI118709.
51. Tartof SY, Qian L, Hong V, Wei R, Nadjafi RF, Fischer H, et al. Obesity and Mortality Among Patients Diagnosed With COVID-19: Results From an Integrated Health Care Organization. Ann Intern Med. 2020 Nov 17;173(10):773-781. doi: 10.7326/M20-3742.
52. Kass DA. COVID-19 and Severe Obesity: A Big Problem? Ann Intern Med. 2020 Nov 17;173(10):840-841. doi: 10.7326/M20-5677.
53. Schulz E, Gori T, Münzel T. Oxidative stress and endothelial dysfunction in hypertension. Hypertens Res. 2011 Jun;34(6):665-73. doi: 10.1038/hr.2011.39.
54. Iantorno M, Campia U, Di Daniele N, Nistico S, Forleo GB, Cardillo C, Tesauro M. Obesity, inflammation and endothelial dysfunction. J Biol Regul Homeost Agents. 2014 Apr-Jun;28(2):169-76.
55. Rubino F, Amiel SA, Zimmet P, Alberti G, Bornstein S, Eckel RH, et al. New-Onset Diabetes in Covid-19. N Engl J Med. 2020 Aug 20;383(8):789-790. doi: 10.1056/NEJMc2018688.
56. Gerrard JM, Stuart MJ, Rao GH, Steffes MW, Mauer SM, Brown DM, White JG. Alteration in the balance of prostaglandin and thromboxane synthesis in diabetic rats. J Lab Clin Med. 1980 Jun;95(6):950-8. PMID: 6445927.
57. Report of the WHO-China Joint Mission on Coronavirus Disease 2019 (COVID-19). 16-14 February 2020. The joint Mission consisted of 25 national and international experts from China, Germany, Japan, Korea, Russia, Singapore and the United States of America, and the World Health Organization (WHO).
58. Lindner D, Fitzek A, Bräuninger H, Aleshcheva G, Edler C, Meissner K, et al. Association of Cardiac Infection With SARS-CoV-2 in Confirmed COVID-19 Autopsy Cases. JAMA Cardiol. 2020 Nov 1;5(11):1281-1285. doi: 10.1001/jamacardio.2020.3551.

59. Hendren NS, Drazner MH, Bozkurt B, Cooper LT Jr. Description and Proposed Management of the Acute COVID-19 Cardiovascular Syndrome. Circulation. 2020 Jun 9;141(23):1903-1914. doi: 10.1161/CIRCULATIONAHA.120.047349.
60. Nishiga M, Wang DW, Han Y, Lewis DB, Wu JC. COVID-19 and cardiovascular disease: from basic mechanisms to clinical perspectives. Nat Rev Cardiol. 2020 Sep;17(9):543-558. doi: 10.1038/s41569-020-0413-9.
61. Grasselli G, Zangrillo A, Zanella A, Antonelli M, Cabrini L, Castelli A, et al.; COVID-19 Lombardy ICU Network. Baseline Characteristics and Outcomes of 1591 Patients Infected With SARS-CoV-2 Admitted to ICUs of the Lombardy Region, Italy. JAMA. 2020 Apr 28;323(16):1574-1581. doi: 10.1001/jama.2020.5394.
62. Goyal P, Choi JJ, Pinheiro LC, Schenck EJ, Chen R, Jabri A, et al. Clinical Characteristics of Covid-19 in New York City. N Engl J Med. 2020 Jun 11;382(24):2372-2374. doi: 10.1056/NEJMc2010419.
63. Mahenthiran AK, Mahenthiran AK, Mahenthiran J. Cardiovascular system and COVID-19: manifestations and therapeutics. Rev Cardiovasc Med. 2020 Sep 30;21(3):399-409. doi: 10.31083/j.rcm.2020.03.124.
64. Gupta AK, Jneid H, Addison D, Ardehali H, Boehme AK, Borgaonkar S, et al. Current Perspectives on Coronavirus Disease 2019 and Cardiovascular Disease: A White Paper by the JAHA Editors. J Am Heart Assoc. 2020 Jun 16;9(12):e017013. doi: 10.1161/JAHA.120.017013.
65. Klok FA, Kruip MJHA, van der Meer NJM, Arbous MS, Gommers DAMPJ, Kant KM, et al. Incidence of thrombotic complications in critically ill ICU patients with COVID-19. Thromb Res. 2020 Jul;191:145-147. doi: 10.1016/j.thromres.2020.04.013.
66. Mao L, Jin H, Wang M, Hu Y, Chen S, He Q, et al. Neurologic Manifestations of Hospitalized Patients With Coronavirus Disease 2019 in Wuhan, China. JAMA Neurol. 2020 Jun 1;77(6):683-690. doi: 10.1001/jamaneurol.2020.1127.
67. Tsivgoulis G, Palaiodimou L, Zand R, Lioutas VA, Krogias C, Katsanos AH, et al. COVID-19 and cerebrovascular diseases: a comprehensive overview. Ther Adv Neurol Disord. 2020 Dec 8;13:1756286420978004. doi: 10.1177/1756286420978004.
68. Akhter N, Ahmad S, Alzahrani FA, Dar SA, Wahid M, Haque S, et al. Impact of COVID-19 on the cerebrovascular system and the prevention of RBC lysis. Eur Rev Med Pharmacol Sci. 2020 Oct;24(19):10267-10278. doi: 10.26355/eurrev_202010_23251.
69. Fraiman P, Godeiro Junior C, Moro E, Cavallieri F, Zedde M. COVID-19 and Cerebrovascular Diseases: A Systematic Review and Perspectives for Stroke Management. Front Neurol. 2020 Nov 5;11:574694. doi: 10.3389/fneur.2020.574694.
70. Lee MH, Perl DP, Nair G, Li W, Maric D, Murray H, et al. Microvascular Injury in the Brains of Patients with Covid-19. N Engl J Med. 2021 Feb 4;384(5):481-483. doi: 10.1056/NEJMc2033369.
71. Guan WJ, Ni ZY, Hu Y, Liang WH, Ou CQ, He JX, et al.; China Medical Treatment Expert Group for Covid-19. Clinical Characteristics of Coronavirus Disease 2019 in China. N Engl J Med. 2020 Apr 30;382(18):1708-1720. doi: 10.1056/NEJMoa2002032.
72. Piazza G, Morrow DA. Diagnosis, Management, and Pathophysiology of Arterial and Venous Thrombosis in COVID-19. JAMA. 2020 Dec 22;324(24):2548-2549. doi: 10.1001/jama.2020.23422.
73. Bikdeli B, Madhavan MV, Jimenez D, Chuich T, Dreyfus I, Driggin E, et al.; Global COVID-19 Thrombosis Collaborative Group, Endorsed by the ISTH, NATF, ESVM, and the IUA, Supported by the ESC Working Group on Pulmonary Circulation and Right Ventricular Function. COVID-19 and Thrombotic or Thromboembolic Disease: Implications for Prevention, Antithrombotic Therapy, and Follow-Up: JACC State-of-the-Art Review. J Am Coll Cardiol. 2020 Jun 16;75(23):2950-2973. doi: 10.1016/j.jacc.2020.04.031.
74. Rao GHR: SARS-CoV-2 biochemistry, Transmission, Clinical Manifestations, and Prevention. Int J. Biomed. 2020;10(4):303-311.
75. Krause PR, Gruber MF. Emergency Use Authorization of Covid Vaccines - Safety and Efficacy Follow-up Considerations. N Engl J Med. 2020 Nov 5;383(19):e107. doi: 10.1056/NEJMp2031373.
76. Schwartz JL. Evaluating and Deploying Covid-19 Vaccines - The Importance of Transparency, Scientific Integrity, and Public Trust. N Engl J Med. 2020 Oct 29;383(18):1703-1705. doi: 10.1056/NEJMp2026393.
77. Creech CB, Walker SC, Samuels RJ. SARS-CoV-2 Vaccines. JAMA. 2021 Apr 6;325(13):1318-1320. doi: 10.1001/jama.2021.3199. PMID: 33635317.
78. Jiang S, Zhang X, Yang Y, Hotez PJ, Du L. Neutralizing antibodies for the treatment of COVID-19. Nat Biomed Eng. 2020 Dec;4(12):1134-1139. doi: 10.1038/s41551-020-00660-2.
79. Dorans KS, Mills KT, Liu Y, He J. Trends in Prevalence and Control of Hypertension According to the 2017 American College of Cardiology/American Heart Association (ACC/AHA) Guideline. J Am Heart Assoc. 2018 Jun 1;7(11):e008888. doi: 10.1161/JAHA.118.008888.
80. NCD Risk Factor Collaboration (NCD-RisC). Worldwide trends in body-mass index, underweight, overweight, and obesity from 1975 to 2016: a pooled analysis of 2416 population-based measurement studies in 128·9 million children, adolescents, and adults. Lancet. 2017 Dec 16;390(10113):2627-2642. doi: 10.1016/S0140-6736(17)32129-3.
81. DiBonaventura MD, Meincke H, Le Lay A, Fournier J, Bakker E, Ehrenreich A. Obesity in Mexico: prevalence, comorbidities, associations with patient outcomes, and treatment experiences. Diabetes Metab Syndr Obes. 2017 Dec 22;11:1-10. doi: 10.2147/DMSO.S129247.
82. Vrints CJM, Krychtiuk KA, Van Craenenbroeck EM, Segers VF, Price S, Heidbuchel H. Endothelialitis plays a central role in the pathophysiology of severe COVID-19 and its cardiovascular complications. Acta Cardiol. 2020 Nov 19:1-16. doi: 10.1080/00015385.2020.1846921.
83. Teuwen LA, Geldhof V, Pasut A, Carmeliet P. COVID-19: the vasculature unleashed. Nat Rev Immunol. 2020 Jul;20(7):389-391. doi: 10.1038/s41577-020-0343-0. Erratum in: Nat Rev Immunol. 2020 Jun 4.
84. Evans PC, Rainger GE, Mason JC, Guzik TJ, Osto E, Stamataki Z, et al. Endothelial dysfunction in COVID-19: a position paper of the ESC Working Group for Atherosclerosis and Vascular Biology, and the ESC Council of Basic Cardiovascular Science. Cardiovasc Res. 2020 Dec 1;116(14):2177-2184. doi: 10.1093/cvr/cvaa230.
85. Nägele MP, Haubner B, Tanner FC, Ruschitzka F, Flammer AJ. Endothelial dysfunction in COVID-19: Current findings and therapeutic implications. Atherosclerosis. 2020 Dec;314:58-62. doi: 10.1016/j.atherosclerosis.2020.10.014.
86. The Lancet Public Health. COVID-19-break the cycle of inequality. Lancet Public Health. 2021 Feb;6(2):e82. doi: 10.1016/S2468-2667(21)00011-6.

International Journal of Biomedicine 11(2) (2021) 123-130
http://dx.doi.org/10.21103/Article11(2)_RA2

REVIEW ARTICLE

INTERNATIONAL JOURNAL OF BIOMEDICINE

Bone Marrow Adipocytes and Hematology: A Literature Review

Nataliia A. Kriventsova*; Alexander V. Shestopalov; Galina V. Tereshchenko

Dmitry Rogachev National Medical Research Center of Pediatric Hematology, Oncology and Immunology
Moscow, Russia

Abstract

This review focuses on the impact of bone marrow adipocytes on hematopoiesis and the development of hematological diseases. Bone marrow fat is a metabolically active organ capable of accumulating energy required for active hematopoiesis as well as of performing endocrine functions and participating in bone formation. Adipocytes can interact with the surrounding cells both directly and indirectly via cytokines and chemokines. Apart from their active involvement in the normal hematopoiesis, BMA have also been shown to play an important role in such diseases as leukemia, multiple myeloma and aplastic anemia. The role of fat cells in hematopoiesis is still unclear and not well studied, yet it is undoubtedly important, as demonstrated by the ever increasing number of publications supporting this conclusion. (**International Journal of Biomedicine. 2021;11(2):123-130.**)

Key Words: fat cells • hematopoiesis • leukemia • multiple myeloma • aplastic anemia

For citation: Kriventsova NA, Shestopalov AV, Tereshchenko GV. Bone Marrow Adipocytes and Hematology: A Literature Review. International Journal of Biomedicine. 2021;11(2):123-130. doi:10.21103/Article11(2)_RA2

Abbreviations

AA, aplastic anemia; **ALL**, acute lymphoblastic leukemia; **APL**, acute promyelocytic leukemia; **AML**, acute myeloid leukemia; **BM**, bone marrow; **BMA**, bone marrow adipocytes; **BMAT**, bone marrow adipose tissue; **cBMA**, constitutive bone marrow adipocytes; **rBMA**, regulated bone marrow adipocytes; **CLL**, chronic lymphocytic leukemia; **CML**, chronic myeloid leukemia; **3DEM**, three-dimensional electron microscopy; **DECT**, dual-energy computed tomography; **HSC**, hematopoietic stem cells; **MRI**, magnetic resonance imaging; **MM**, multiple myeloma; **MSC**, mesenchymal stem cells; **PTH**, parathyroid hormone; **RBM**, red bone marrow; **YBM**, yellow bone marrow.

Introduction

Bone marrow (BM) is one of the largest and most widely distributed organs in the human body. BM contains not only hematopoietic stem cells (HSC) but also the cells of the microenvironment, such as macrophages, endothelial cells, osteoclasts, osteoblasts and adipocytes. In the late 19th and early 20th centuries, two types of bone marrow were distinguished: "red" bone marrow (RBM) and "yellow" bone marrow (YBM).[1] Since that time, research has been conducted on BM and its components, including fat cells. The 1970s became the golden years for the studies on bone marrow adipose tissue (BMAT), or bone marrow adipocytes (BMA) as it is referred to in modern literature. These years were marked by the discovery of differences in the histogenesis of RBM and YBM, which were described by M. Tavassoli,[2] who also described the origin of BMA from unique progenitor cells, different from those of regular white fat. Furthermore, the author made an assumption that epigenetic factors could influence the differentiation and development of adipocytes, which is the subject of research carried out by many scientists at the present time.[2,3]

At the next stage in the study of bone marrow fat, fat cells were distinguished by their functions into regulated bone marrow adipocytes (rBMAs) and constitutive bone marrow adipocytes (cBMAs), which resulted in the separation of the functions of these cells and their influence on the microenvironment.[4] rBMAs are diffusely distributed in the RBM, while cBMAs

***Corresponding author**: Nataliia A. Kriventsova. Dmitry Rogachev National Medical Research Center of Pediatric Hematology, Oncology and Immunology. Moscow, Russia. E-mail: nataliya.krivencova@fccho-moscow.ru*

are one of the main components of the YBM.[5] After BMAT had been classified as a separate type within the entire adipose tissue, active research on the relationship between BM and fat began. As a result, it has been shown that fat cells play an important role in the development of osteoporosis.[6]

Adipocytes originate from mesenchymal stem cells (MSC) and are an important component of the BM microenvironment.[7] Currently, many study groups are investigating the relationship between BMAT and bone metabolism. Interest in the function of fat cells has also increased among those scientists who carry out research on the pathology of BM hematopoiesis. It has been shown that adipocytes are involved in the regulation of hematopoiesis and interact with HSC via direct cell contact, affecting the secretion of growth factors and cytokines.[8,9]

BMAT is an active cellular element of the BM that stores free fatty acids and produces adipokines.[10]

Researchers delineate an important role for fat cells in oncology and oncohematology. Several studies show that fat cells contribute to the development and the continued growth of tumors, the metastasis of tumors to the BM and the development of resistance to chemotherapy through interaction with other stromal cells.[10] The increased interest in BMAT has contributed to the development of noninvasive diagnosis of BMA using modern high-tech methods. Densitometry, MRI, dual-energy computed tomography (DECT), and positron emission tomography (PETCT) open up new possibilities in the assessment of BMAT.[11]

This article is devoted to a review of the literature describing the normal development of adipose tissue in the BM, and the influence of adipose tissue on hematopoietic cells during normal BM evolution. We will elucidate the contribution of adipocytes to diseases involving the BM.

I. Normal BMA

The development of adipocytes in the BM

Bone modeling occurs during prenatal development. Bones grow not only in length, but also in diameter, and a BM cavity enlarges along with the growth of a bone itself. During fetal development, this cavity is gradually filled with RBM, and by the end of the first trimester of pregnancy, it is completely filled.[12] It has been shown that the replacement of RBM by YBM in some bones, for example, in phalanges, begins shortly before the birth of a child.[13] After birth, fatty involution of the BM occurs in different bones in different ways: in the femur and tibia, it begins at the age of 7 and ends at the age of 18; however, in the ribs and vertebrae, microscopic fat is not found until adulthood.[14] In addition, several studies have revealed some regularities in the development of adipose tissue in the BM: from the periphery to the axial skeleton, from diaphyses to metaphyses.

Regulation

Adipocytes originate from MSC of the BM. MSC also give rise to other types of cells: osteoblasts (cells forming bone tissue) and chondrocytes (cells forming cartilage). Regarding the differentiation of cells, adipocytes and osteoblasts are closely related to each other; these cells have common stages of development. A number of factors are activated during the emergence of preosteoblasts (runt-related transcription factor 2 (RUNX2), homeobox protein 1 (Prx1) and osterix (Osx, Sp7)) and during the differentiation of preadipocytes (platelet-derived growth factor receptor beta (PDGFRb), CCAAT/enhancer binding protein alpha (C/EBP alpha), zinc finger proteins (Zfp) 423 and 467, and Prx 1). During a certain period of time, progenitor cells of adipocytes and osteoblasts can exhibit plasticity; they can mutually transform between phenotypes, a process that is regulated by microenvironmental molecules and cytokines. Type I collagen (COL1a1), osteocalcin (OCN) and RANKL stimulate osteoblast differentiation. Peroxisome proliferator-activated receptor gamma (PPARG), fatty acid-binding protein (FABP4), perilipin 2 (PLN2), and fatty acid synthase (FASN) promote adipocyte differentiation [12,15] (Fig. 1).

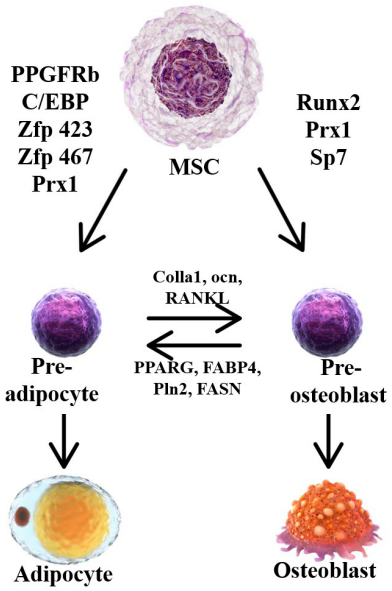

Fig. 1. *The origin and interaction between adipocytes and osteoblasts derived from mesenchymal stromal cells (MSC).*

There are also other factors that affect the amount of fat in the BM. These factors include hormones such as estrogen and parathyroid hormone (PTH). Several studies have shown that an increase in estrogen raises the number of osteoblasts and suppresses the differentiation of adipocytes in the BM.[16,17] Studies on PTH have shown that PTH can influence MSC, thereby increasing or reducing the development of adipocytes (Fig. 2).

Fig. 2*. Interaction between adipocytes and MSC: a schematic illustration.*

In those studies, the loss of PTH receptor expression in MSC increased the amount of BMA, while PTH receptor overexpression suppressed the formation of fat cells.[18]

The influence of age and gender

In healthy young adults, bone mass peaks at the age of 15 to 30. Then the amount of fat in the BM inevitably increases with age. This finding has been confirmed by numerous multiparametric studies, mainly based on new methods of quantitative MRI assessment. MRI spectroscopy has revealed that in groups of healthy controls aged 11-61, distributed by age with a 10-year interval, the amount of fat in the bones increases from 23% to 60%. During almost their entire lives, men have a higher BM fat content; however, in women, the amount of BMAT sharply increases in the postmenopausal period (over 55 years of age).[19]

Functions of adipocytes

Recently, not only the regulation of adipocyte formation in the BM has been under study, but active research has also been carried out on the functions of adipocytes and their interaction with other surrounding cells. An important function of BMA is the secretion of mediators, for example, adipokines, which can act as both paracrine and endocrine mediators. Adiponectin is the most extensively studied adipokine in the BM. Adiponectin is involved in the regulation of insulin sensitivity and energy metabolism. Adiponectin is mostly secreted by BMA, which has been shown in animal models when comparing the expression and secretion of adiponectin by BMA and by adipocytes from other peripheral fat depots.[9]

Adiponectin facilitates osteoblast differentiation *in vitro*. As evidenced by a number of clinical studies, an increase in circulating adiponectin levels is associated with the loss of bone mass. This parameter can potentially be used as a marker of increased BMAT.[20]

Furthermore, it has been demonstrated that increased adiponectin production by BMA after myeloablative chemotherapy promotes hematopoietic recovery in mice.[21] Another study showed that stem cell factors secreted by adipocytes following chemotherapy also facilitate hematopoietic recovery. The study was performed in murine models with impaired adipogenesis (A-ZIP/F1 mice) that was also accompanied by impaired hematopoiesis [22] (Figure 3).

Fig. 3. *A schematic representation of the adipocyte-secreted factors promoting hematopoietic recovery.*

D. Mattiucci et al.[23] showed *in vitro* that human BMA secrete CXCL12, which is important for hematopoietic stem cell maintenance in the BM. The co-culture of human BMA with HSC supported the survival of hematopoietic cells.

A comparison of cytokines secreted by subcutaneous adipocytes and those secreted by BMA led to the identification of 53 proteins secreted by the latter. These proteins became activated with age and affected osteoblasts by reducing bone mass.[24]This group of researchers also identified palmitate, a saturated fatty acid produced by BMA that inhibits osteoblast function.[25]

Another important function of BMA is the secretion of fatty acids that act as an additional source of energy for the surrounding cells. One of the first discovered adipokines involved in the regulation of energy metabolism was leptin.[26] In recent years, there have been a number of studies suggesting that adipocytes supply energy to osteoblasts and HSC through lipolysis. This is most evident when bone cells and hematopoietic cells are under stress; as well as in cases of trauma, diets, other forms of energy restriction, and aging. It has been shown that fatty acid oxidation in BMA may play an important role in the growth and survival of prostate cancer bone metastases.[27]

Thus, the results of many studies indicate that BMA are functionally heterogeneous. It is clear that BMA secrete factors that influence processes in the BM as well as bone remodeling and hematopoiesis. They also secrete factors that are released into the bloodstream and act outside the BM. Bone remodeling and hematopoiesis are energy-demanding processes that are tightly regulated to maintain bone mass and blood cell counts, and BMA appear to also be involved in this important process.

The role in hematopoiesis

The microenvironment of BM hematopoietic cells, also known as the "hematopoietic niche," comprises cytokines (produced by HSC themselves), BM stroma, capillaries and nerves.[28] Three-dimensional electron microscopy (3DEM) of the BM allows one to study BMA as well as their relationship with the surrounding tissues. 3DEM has revealed that BMA display features of metabolically active cells, including lipid accumulation, dense mitochondrial networks and areas of endoplasmic reticulum. It has been shown that triacylglycerol droplets containing fatty acids are absorbed and/or released in three areas: at the endothelial border, in the hematopoietic environment, and on the bone surface.[29] A group of researchers led by H. Robles [29] demonstrated that, in the hematopoietic environment of the proximal tibia, BMA interact extensively with mature cells of the myeloid lineage and are closely associated with erythroblastic islands. At the microstructural level, this directly indicates that BMAT is actively involved in many processes in the bone, and is not just some "inert filler." BMAT, as a part of the hematopoietic niche, influences the proliferation and differentiation of HSC by secreting adiponectin, leptin, prostaglandins, IL-6, and other adipocyte-related factors.[30-33] Leptin, independently or synergetically, promotes HSC proliferation,[31,32] prostaglandins inhibit HSC through the induction of apoptosis,[34] and IL-6 facilitates HSC differentiation.[33]

In vitro, BMA secrete factors that inhibit B cell lymphopoiesis, especially at the stage where lymphoid progenitor cells differentiate into pre-B cells, and at the same

time, promote the differentiation and subsequent proliferation of HSC into the myeloid lineage. BMA were also shown to negatively affect early stages of B-lymphocyte proliferation in the BM of elderly people.[35]

Kennedy et al.[36] discovered that adipocytes induce generation of myeloid suppressor cells that inhibit B cell lymphopoiesis by producing IL-1. At the same time, BMA induce inflammation via NLRP3 (NOD-like receptor 3) activation and directly inhibit B cell lymphopoiesis.[37] The activation of inflammation may also promote degeneration of the thymus,[38,39] which in turn negatively affects T-lymphocyte proliferation.[40] NLRP3 blockade enhanced B cell lymphopoiesis and prevent thymic atrophy and a decrease in T lymphocytes.[40]

Naveiras et al.[41] demonstrated that the removal of adipocytes from the BM of mice enhances hematopoiesis, including B cell lymphopoiesis. Other researchers showed that adipogenesis stimulation with the tributyltin toxicant leads to PPARγ activation in the BM, resulting in a decrease in peripheral B lymphocytes.[42]

Leptin, another mediator mentioned above, has the opposite effect on lymphopoiesis.[43] Leptin promotes differentiation and proliferation of cells of the lymphoid lineage and stimulates myelopoiesis.[26] In leptin-deficient mice, the levels of peripheral blood B cells and CD4+-expressing T cells are significantly reduced.[26,32] It has also been shown that high plasma leptin levels promote the differentiation of pluripotent CD34+ cells into granulocytes[44] (Figure 4).

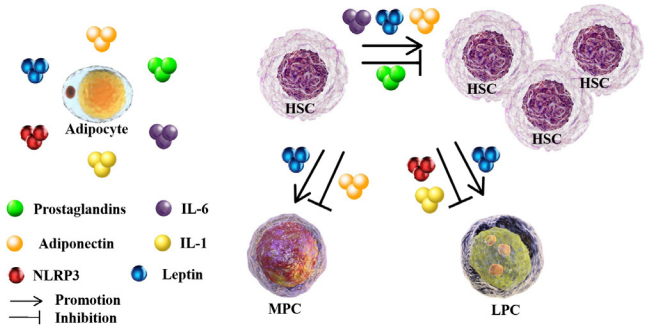

Fig. 4. *The influence of adipocyte-derived factors (adiponectin, leptin, prostaglandins, IL-6, IL-1, and NLRP3) on normal hematopoiesis in the BM, including the proliferation of HSC as well as their differentiation into myeloid (MPC) and lymphoid progenitor cells (LPC).*

As mentioned above, electron microscopy studies have shown that BMA interact closely with erythroblastic islands.[29] It has been estimated that a single adipocyte can interact with more than 100 erythropoietic cells, both directly, via cell-cell contact, and indirectly, using macrophages of erythroblastic islands.[45] Adipocytes deliver energy to maturing erythroid progenitor cells. This has been confirmed by a number of researchers in animal experiments. It has been shown that the amount of fat and the size of BMA decrease rapidly during active erythropoiesis in response to massive blood loss.[46] A recent study in mice published in the Blood journal demonstrated that stimulation with erythropoietin, which promotes differentiation of erythrocytes, leads to a decrease in BMAT.[47]

Currently, the role of BMA in hematopoiesis is controversial and yet significant. Many mechanisms of interaction between hematopoietic cells of the BM and adipocytes have not been investigated yet, so further research is needed to identify their signaling pathways.

II. BMA and Hematologic Diseases

Leukemia

There are many research groups in different countries that investigate the interaction of adipocytes, not only with normal hematopoietic cells, but also with transformed cell clones. They study these interaction effects in ALL, acute promyelocytic leukemia (APL), acute myeloid leukemia (AML), chronic lymphocytic leukemia (CLL), chronic myeloid leukemia (CML), multiple myeloma (MM), and aplastic anemia (AA).[48] On experimental murine models, using human ALL and AML clones, Battula et al.[49] demonstrated that leptin secreted by BMA into the microenvironment of tumor cells facilitated their engraftment, growth, and development in the BM of mice. The authors also suggested that adipocytes may play an important role in the setting of AA or hypoplastic myelodysplastic syndromes.[49]

BMA protect lymphoblasts in ALL; however, this mechanism has not been studied well. A study on a large cohort of ALL patients over age 10 revealed that, regardless of sex and age, obesity at diagnosis increases the risk of relapse by ~50% and reduces the effectiveness of treatment.[50] In murine models, it was repeatedly demonstrated that general obesity leads to an increase in the number of adipocytes in the BM.[51-53] When in the tumor environment, leptin secreted by BMAs influences cell proliferation, survival, and apoptosis. During chemotherapy, leptin protects ALL cells from drug-induced apoptosis.[54] Recent studies have shown that under treatment with daunorubicin, an antileukemic cytostatic drug, ALL cells induce oxidative stress in adipocytes. In response to oxidative stress, adipocytes secrete soluble factors, which protect ALL cells from daunorubicin.[55] BMA were also shown to confer protection against vincristine and nilotinib.[56] In APL, blast cells have a lot of leptin receptors.[54] In AML, cytokines and chemokines secreted by BMA can induce the proliferation of AML cells.[57,58] A possible mechanism of these interactions may involve the induction of lipolysis and the formation of fatty acids, which are then transported into the tumor microenvironment and serve as a good metabolic substrate for the survival and proliferation of AML cells.[59] In AML patients, leptin stimulates blast cell growth by promoting angiogenesis. It has been shown that the use of leptin receptor inhibitors in animal models leads to a reduction in angiogenesis.[60] When investigating AML cell lines and blast cells obtained from patients with AML, researchers also detected a high level of leptin isomer expression, which promotes their active proliferation.[61] A study by Yokota et al.[62] aimed at investigating the interaction between adiponectin and hematopoietic cells demonstrated that adiponectin inhibits the proliferation of myeloid cell lines and induces apoptosis in myelomonocytic leukemia lines.

Diaz-Blanco et al.[63] showed that the expression of leptin receptors is reduced in patients with CML. At the onset of the disease, BMA partially inhibit the expression of CML clones. Cytokines produced by CML cells induce the lipolysis of BMA. Then polyunsaturated fatty acids released

from the adipocytes impair CML proliferation and survival by inhibiting the PI3K pathway. However, this effect is soon inhibited by leptin released from adipocytes, which increases the lipolysis of adipocytes and protects CML cells from apoptosis by activating the PI3K pathway.[64]

In CLL, the expression of lipoprotein lipase, which is also expressed in adipocytes and prompts the hydrolysis of triglycerides into free fatty acids, is increased.[65] CLL cells accumulate these fatty acids in vacuoles and then utilize them to produce energy via oxidative phosphorylation by binding free fatty acids with receptors PPARα.[66] PPARα overexpression was demonstrated in CLL cells, and the level of the expression correlated with the disease progression.[67] Moreover, fatty acids were shown to mediate the resistance of CLL cells to treatment.[58]

Multiple myeloma

J. Caers et al. [68] showed that adipocytes in the BM microenvironment affect MM cell proliferation, apoptosis, and migration. However, fat cells were found in the BM only at the initial stages of MM. These results suggest that BMA play a significant role at the initial stages of the disease. Other researchers have found that one of the enzymes that protect MM cells against chemotherapy is resistin. Its main effect is the inhibition of chemotherapy-induced caspase cleavage.[70,71] However, resistin is expressed not only by adipocytes but also by other cells of the BM environment, so further studies are needed.[69,71]

Aplastic anemia

Aplastic anemia (AA) is the opposite of the above-mentioned BM disorders. It is characterized by a significant decrease in BM cellularity and peripheral blood pancytopenia. The BM microenvironment is one of the key pathogenetic factors in AA.[72] Normally, adipogenesis and osteogenesis are well-balanced; but in patients with pathological changes in BM, the balance between them may be seriously disrupted, resulting in the BM hypo- and hypercellularity.[73-75] In the BM of patients with AA, adipocytes are much more numerous than osteoblasts.[75] *In vitro* studies showed that MSC in patients with AA tend to differentiate into adipocytes rather than into osteoblasts.[76] Signaling pathways continue to be explored in order to improve treatment outcomes for AA patients.[77-79]

Conclusion

Over the recent years, the number of relevant studies has increased tremendously. Today, the interactions between BMA and HSC, MSC, osteoblasts, and other cells of the BM environment are being actively investigated. Apart from the exploration of processes occurring in healthy BM, many researchers have focused on the relationship between BMA and abnormal cells in the BM.

It is not always possible to determine the role of BMA in some known mechanisms of interaction between stromal and hematopoietic cells, due to the close interaction between all cells in the BM microenvironment. There is no doubt that BMA actively participate in the hematopoietic microenvironment. Adipokines, chemokines, and cytokines secreted by adipocytes are actively involved in lipolysis and thus ensure the normal functioning of hematopoietic stem cells. However, they may also play a negative role in the abnormal transformation of the BM. In malignant hematologic diseases, adipocytes often promote the proliferation of malignant cells, provide these cells with energy, protect them against chemotherapy agents, and cause drug resistance. Active research on fat cells, adipocyte-derived mediators, and signaling pathways in the BM microenvironment, as well as their role in hematopoiesis and the development of BM disorders, may facilitate the discovery of new methods of diagnosis and treatment of hematological diseases.

Competing Interests

The authors declare that they have no competing interests.

References

1. Piney A. The anatomy of the bone marrow: with special reference to the distribution of the red marrow. Br Med J. 1922:792-795.
2. Tavassoli M, Crosby WH. Bone marrow histogenesis: a comparison of fatty and red marrow. Science. 1970 Jul 17;169(3942):291-3. doi: 10.1126/science.169.3942.291.
3. Tavassoli M. Ultrastructural development of bone marrow adipose cell. Acta Anat (Basel). 1976;94(1):65-77. doi: 10.1159/000144545.
4. Tavassoli M. Marrow adipose cells. Histochemical identification of labile and stable components. Arch Pathol Lab Med. 1976 Jan;100(1):16-8.
5. Li Y, Meng Y, Yu X. The Unique Metabolic Characteristics of Bone Marrow Adipose Tissue. Front Endocrinol (Lausanne). 2019 Feb 8;10:69. doi: 10.3389/fendo.2019.00069.
6. Burkhardt R, Kettner G, Böhm W, Schmidmeier M, Schlag R, Frisch B, et al. Changes in trabecular bone, hematopoiesis and bone marrow vessels in aplastic anemia, primary osteoporosis, and old age: a comparative histomorphometric study. Bone. 1987;8(3):157-64. doi: 10.1016/8756-3282(87)90015-9.
7. Wöhrer S, Rabitsch W, Shehata M, Kondo R, Esterbauer H, Streubel B, et al. Mesenchymal stem cells in patients with chronic myelogenous leukaemia or bi-phenotypic Ph+ acute leukaemia are not related to the leukaemic clone. Anticancer Res. 2007 Nov-Dec;27(6B):3837-41.
8. Askmyr M, Quach J, Purton LE. Effects of the bone marrow microenvironment on hematopoietic malignancy. Bone. 2011 Jan;48(1):115-20. doi: 10.1016/j.bone.2010.06.003.
9. Cawthorn WP, Scheller EL, Learman BS, Parlee SD, Simon BR, Mori H, et al. Bone marrow adipose tissue is an endocrine organ that contributes to increased circulating adiponectin during caloric restriction. Cell Metab. 2014 Aug 5;20(2):368-375. doi: 10.1016/j.cmet.2014.06.003.
10. Hardaway AL, Herroon MK, Rajagurubandara E, Podgorski I. Bone marrow fat: linking adipocyte-induced inflammation with skeletal metastases. Cancer Metastasis Rev. 2014 Sep;33(2-3):527-43. doi: 10.1007/s10555-013-9484-y.
11. Karampinos DC, Ruschke S, Dieckmeyer M, Diefenbach M, Franz D, Gersing AS, et al. Quantitative MRI and spectroscopy of bone marrow. J Magn Reson Imaging. 2018 Feb;47(2):332-353. doi: 10.1002/jmri.25769.
12. Veldhuis-Vlug AG, Rosen CJ. Clinical implications of bone marrow adiposity. J Intern Med. 2018 Feb;283(2):121-139. doi: 10.1111/joim.12718.

13. Emery JL, Follett GF. Regression of bone-marrow haemopoiesis from the terminal digits in the foetus and infant. Br J Haematol. 1964 Oct;10:485-9. doi: 10.1111/j.1365-2141.1964.tb00725.x.
14. Custer RP, Ahlfeldt FE. Studies on the structure and function of bone marrow: II. Variations in cellularity in various bones with advancing years of life and their relative response to stimuli. J Lab Clin Med. 1932;17(10):960-962.
15. Ono N, Kronenberg HM. Mesenchymal progenitor cells for the osteogenic lineage. Curr Mol Biol Rep. 2015 Sep;1(3):95-100. doi: 10.1007/s40610-015-0017-z.
16. Wend K, Wend P, Drew BG, Hevener AL, Miranda-Carboni GA, Krum SA. ERα regulates lipid metabolism in bone through ATGL and perilipin. J Cell Biochem. 2013 Jun;114(6):1306-14. doi: 10.1002/jcb.24470.
17. Okazaki R, Inoue D, Shibata M, Saika M, Kido S, Ooka H, et al. Estrogen promotes early osteoblast differentiation and inhibits adipocyte differentiation in mouse bone marrow stromal cell lines that express estrogen receptor (ER) alpha or beta. Endocrinology. 2002 Jun;143(6):2349-56. doi: 10.1210/endo.143.6.8854.
18. Fan Y, Hanai JI, Le PT, Bi R, Maridas D, DeMambro V, et al. Parathyroid Hormone Directs Bone Marrow Mesenchymal Cell Fate. Cell Metab. 2017 Mar 7;25(3):661-672. doi: 10.1016/j.cmet.2017.01.001.
19. Griffith JF, Yeung DK, Ma HT, Leung JC, Kwok TC, Leung PC. Bone marrow fat content in the elderly: a reversal of sex difference seen in younger subjects. J Magn Reson Imaging. 2012 Jul;36(1):225-30. doi: 10.1002/jmri.23619.
20. Naot D, Musson DS, Cornish J. The Activity of Adiponectin in Bone. Calcif Tissue Int. 2017 May;100(5):486-499. doi: 10.1007/s00223-016-0216-5.
21. Masamoto Y, Arai S, Sato T, Kubota N, Takamoto I, Kadowaki T, Kurokawa M. Adiponectin Enhances Quiescence Exit of Murine Hematopoietic Stem Cells and Hematopoietic Recovery Through mTORC1 Potentiation. Stem Cells. 2017 Jul;35(7):1835-1848. doi: 10.1002/stem.2640.
22. Zhou BO, Yu H, Yue R, Zhao Z, Rios JJ, Naveiras O, Morrison SJ. Bone marrow adipocytes promote the regeneration of stem cells and haematopoiesis by secreting SCF. Nat Cell Biol. 2017 Aug;19(8):891-903. doi: 10.1038/ncb3570.
23. Mattiucci D, Maurizi G, Izzi V, Cenci L, Ciarlantini M, Mancini S, et al. Bone marrow adipocytes support hematopoietic stem cell survival. J Cell Physiol. 2018 Feb;233(2):1500-1511. doi: 10.1002/jcp.26037.
24. Gasparrini M, Rivas D, Elbaz A, Duque G. Differential expression of cytokines in subcutaneous and marrow fat of aging C57BL/6J mice. Exp Gerontol. 2009 Sep;44(9):613-8. doi: 10.1016/j.exger.2009.05.009.
25. Elbaz A, Wu X, Rivas D, Gimble JM, Duque G. Inhibition of fatty acid biosynthesis prevents adipocyte lipotoxicity on human osteoblasts in vitro. J Cell Mol Med. 2010 Apr;14(4):982-91. doi: 10.1111/j.1582-4934.2009.00751.x.
26. Bennett BD, Solar GP, Yuan JQ, Mathias J, Thomas GR, Matthews W. A role for leptin and its cognate receptor in hematopoiesis. Curr Biol. 1996 Sep 1;6(9):1170-80. doi: 10.1016/s0960-9822(02)70684-2.
27. Diedrich JD, Rajagurubandara E, Herroon MK, Mahapatra G, Hüttemann M, Podgorski I. Bone marrow adipocytes promote the Warburg phenotype in metastatic prostate tumors via HIF-1α activation. Oncotarget. 2016 Oct 4;7(40):64854-64877. doi: 10.18632/oncotarget.11712.
28. Lassailly F, Foster K, Lopez-Onieva L, Currie E, Bonnet D. Multimodal imaging reveals structural and functional heterogeneity in different bone marrow compartments: functional implications on hematopoietic stem cells. Blood. 2013 Sep 5;122(10):1730-40. doi: 10.1182/blood-2012-11-467498.
29. Robles H, Park S, Joens MS, Fitzpatrick JAJ, Craft CS, Scheller EL. Characterization of the bone marrow adipocyte niche with three-dimensional electron microscopy. Bone. 2019 Jan;118:89-98. doi: 10.1016/j.bone.2018.01.020.
30. DiMascio L, Voermans C, Uqoezwa M, Duncan A, Lu D, Wu J, Sankar U, Reya T. Identification of adiponectin as a novel hemopoietic stem cell growth factor. J Immunol. 2007 Mar 15;178(6):3511-20. doi: 10.4049/jimmunol.178.6.3511.
31. Dias CC, Nogueira-Pedro A, Tokuyama PY, Martins MN, Segreto HR, Buri MV, Miranda A, Paredes-Gamero EJ. A synthetic fragment of leptin increase hematopoietic stem cell population and improve its engraftment ability. J Cell Biochem. 2015 Jul;116(7):1334-40. doi: 10.1002/jcb.25090.
32. Claycombe K, King LE, Fraker PJ. A role for leptin in sustaining lymphopoiesis and myelopoiesis. Proc Natl Acad Sci U S A. 2008 Feb 12;105(6):2017-21. doi: 10.1073/pnas.0712053105.
33. Poloni A, Maurizi G, Serrani F, Mancini S, Zingaretti MC, Frontini A, et al. Molecular and functional characterization of human bone marrow adipocytes. Exp Hematol. 2013 Jun;41(6):558-566.e2. doi: 10.1016/j.exphem.2013.02.005.
34. Shimozato T, Kincade PW. Prostaglandin E(2) and stem cell factor can deliver opposing signals to B lymphocyte precursors. Cell Immunol. 1999 Nov 25;198(1):21-9. doi: 10.1006/cimm.1999.1575.
35. Bilwani FA, Knight KL. Adipocyte-derived soluble factor(s) inhibits early stages of B lymphopoiesis. J Immunol. 2012 Nov 1;189(9):4379-86. doi: 10.4049/jimmunol.1201176.
36. Kennedy DE, Knight KL. Inhibition of B Lymphopoiesis by Adipocytes and IL-1-Producing Myeloid-Derived Suppressor Cells. J Immunol. 2015 Sep 15;195(6):2666-74. doi: 10.4049/jimmunol.1500957.
37. Kennedy DE, Knight KL. Inflammatory Changes in Bone Marrow Microenvironment Associated with Declining B Lymphopoiesis. J Immunol. 2017 May 1;198(9):3471-3479. doi: 10.4049/jimmunol.1601643.
38. Vandanmagsar B, Youm YH, Ravussin A, Galgani JE, Stadler K, Mynatt RL, et al. The NLRP3 inflammasome instigates obesity-induced inflammation and insulin resistance. Nat Med. 2011 Feb;17(2):179-88. doi: 10.1038/nm.2279.
39. Salminen A, Kaarniranta K, Kauppinen A. Inflammaging: disturbed interplay between autophagy and inflammasomes. Aging (Albany NY). 2012 Mar;4(3):166-75. doi: 10.18632/aging.100444.
40. Youm YH, Kanneganti TD, Vandanmagsar B, Zhu X, Ravussin A, Adijiang A, et al. The Nlrp3 inflammasome promotes age-related thymic demise and immunosenescence. Cell Rep. 2012 Jan 26;1(1):56-68. doi: 10.1016/j.celrep.2011.11.005.
41. Naveiras O, Nardi V, Wenzel PL, Hauschka PV, Fahey F, Daley GQ. Bone-marrow adipocytes as negative regulators of the haematopoietic microenvironment. Nature. 2009 Jul 9;460(7252):259-63. doi: 10.1038/nature08099.
42. Baker AH, Wu TH, Bolt AM, Gerstenfeld LC, Mann KK, Schlezinger JJ. From the Cover: Tributyltin Alters the Bone Marrow Microenvironment and Suppresses B Cell Development. Toxicol Sci. 2017 Jul 1;158(1):63-75. doi:

10.1093/toxsci/kfx067.
43. Umemoto Y, Tsuji K, Yang FC, Ebihara Y, Kaneko A, Furukawa S, Nakahata T. Leptin stimulates the proliferation of murine myelocytic and primitive hematopoietic progenitor cells. Blood. 1997 Nov 1;90(9):3438-43.
44. Laharrague P, Oppert JM, Brousset P, Charlet JP, Campfield A, Fontanilles AM, et al. High concentration of leptin stimulates myeloid differentiation from human bone marrow CD34+ progenitors: potential involvement in leukocytosis of obese subjects. Int J Obes Relat Metab Disord. 2000 Sep;24(9):1212-6. doi: 10.1038/sj.ijo.0801377.
45. Manwani D, Bieker JJ. The erythroblastic island. Curr Top Dev Biol. 2008;82:23-53. doi: 10.1016/S0070-2153(07)00002-6.
46. Bathija A, Davis S, Trubowitz S. Marrow adipose tissue: response to erythropoiesis. Am J Hematol. 1978;5(4):315-21. doi: 10.1002/ajh.2830050406.
47. Suresh S, Alvarez JC, Noguchi CT. Erythropoietin eliminates increased bone marrow adiposity and alters bone features in obese mice. Blood. 2017;130 (Suppl 1):3778-3778.
48. Wang H, Leng Y, Gong Y. Bone Marrow Fat and Hematopoiesis. Front Endocrinol (Lausanne). 2018 Nov 28;9:694. doi: 10.3389/fendo.2018.00694.
49. Battula VL, Chen Y, Cabreira Mda G, Ruvolo V, Wang Z, Ma W, et al. Connective tissue growth factor regulates adipocyte differentiation of mesenchymal stromal cells and facilitates leukemia bone marrow engraftment. Blood. 2013 Jul 18;122(3):357-66. doi: 10.1182/blood-2012-06-437988.
50. Butturini AM, Dorey FJ, Lange BJ, Henry DW, Gaynon PS, Fu C, et al. Obesity and outcome in pediatric acute lymphoblastic leukemia. J Clin Oncol. 2007 May 20;25(15):2063-9. doi: 10.1200/JCO.2006.07.7792.
51. Styner M, Thompson WR, Galior K, Uzer G, Wu X, Kadari S, et al. Bone marrow fat accumulation accelerated by high fat diet is suppressed by exercise. Bone. 2014 Jul;64:39-46. doi: 10.1016/j.bone.2014.03.044.
52. Scheller EL, Khoury B, Moller KL, Wee NK, Khandaker S, Kozloff KM, et al. Changes in Skeletal Integrity and Marrow Adiposity during High-Fat Diet and after Weight Loss. Front Endocrinol (Lausanne). 2016 Jul 27;7:102. doi: 10.3389/fendo.2016.00102.
53. Doucette CR, Horowitz MC, Berry R, MacDougald OA, Anunciado-Koza R, Koza RA, Rosen CJ. A High Fat Diet Increases Bone Marrow Adipose Tissue (MAT) But Does Not Alter Trabecular or Cortical Bone Mass in C57BL/6J Mice. J Cell Physiol. 2015 Sep;230(9):2032-7. doi: 10.1002/jcp.24954.
54. Tabe Y, Konopleva M, Munsell MF, Marini FC, Zompetta C, McQueen T, et al. PML-RARalpha is associated with leptin-receptor induction: the role of mesenchymal stem cell-derived adipocytes in APL cell survival. Blood. 2004 Mar 1;103(5):1815-22. doi: 10.1182/blood-2003-03-0802.
55. Sheng X, Tucci J, Parmentier JH, Ji L, Behan JW, Heisterkamp N, Mittelman SD. Adipocytes cause leukemia cell resistance to daunorubicin via oxidative stress response. Oncotarget. 2016 Nov 8;7(45):73147-73159. doi: 10.18632/oncotarget.12246.
56. Behan JW, Yun JP, Proektor MP, Ehsanipour EA, Arutyunyan A, Moses AS, et al. Adipocytes impair leukemia treatment in mice. Cancer Res. 2009 Oct 1;69(19):7867-74. doi: 10.1158/0008-5472.CAN-09-0800.
57. Frączak E, Olbromski M, Piotrowska A, Glatzel-Plucińska N, Dzięgiel P, Dybko J, et al. Bone marrow adipocytes in haematological malignancies. Acta Histochem. 2018 Jan;120(1):22-27. doi: 10.1016/j.acthis.2017.10.010.
58. Tung S, Shi Y, Wong K, Zhu F, Gorczynski R, Laister RC, et al. PPARα and fatty acid oxidation mediate glucocorticoid resistance in chronic lymphocytic leukemia. Blood. 2013 Aug 8;122(6):969-80. doi: 10.1182/blood-2013-03-489468.
59. Shafat MS, Oellerich T, Mohr S, Robinson SD, Edwards DR, Marlein CR, et al. Leukemic blasts program bone marrow adipocytes to generate a protumoral microenvironment. Blood. 2017 Mar 9;129(10):1320-1332. doi: 10.1182/blood-2016-08-734798.
60. Han TJ, Wang X. Leptin and its receptor in hematologic malignancies. Int J Clin Exp Med. 2015 Nov 15;8(11):19840-9.
61. Gorska E, Popko K, Wasik M. Leptin receptor in childhood acute leukemias. Adv Exp Med Biol. 2013;756:155-61. doi: 10.1007/978-94-007-4549-0_20.
62. Yokota T, Oritani K, Takahashi I, Ishikawa J, Matsuyama A, Ouchi N, et al. Adiponectin, a new member of the family of soluble defense collagens, negatively regulates the growth of myelomonocytic progenitors and the functions of macrophages. Blood. 2000 Sep 1;96(5):1723-32.
63. Diaz-Blanco E, Bruns I, Neumann F, Fischer JC, Graef T, Rosskopf M, et al. Molecular signature of CD34(+) hematopoietic stem and progenitor cells of patients with CML in chronic phase. Leukemia. 2007 Mar;21(3):494-504. doi: 10.1038/sj.leu.2404549.
64. Beaulieu A, Poncin G, Belaid-Choucair Z, Humblet C, Bogdanovic G, Lognay G, et al. Leptin reverts pro-apoptotic and antiproliferative effects of α-linolenic acids in BCR-ABL positive leukemic cells: involvement of PI3K pathway. PLoS One. 2011;6(10):e25651. doi: 10.1371/journal.pone.0025651. E
65. Rozovski U, Hazan-Halevy I, Barzilai M, Keating MJ, Estrov Z. Metabolism pathways in chronic lymphocytic leukemia. Leuk Lymphoma. 2016;57(4):758-65. doi: 10.3109/10428194.2015.1106533.
66. Rozovski U, Grgurevic S, Bueso-Ramos C, Harris DM, Li P, Liu Z, et al. Aberrant LPL Expression, Driven by STAT3, Mediates Free Fatty Acid Metabolism in CLL Cells. Mol Cancer Res. 2015 May;13(5):944-53. doi: 10.1158/1541-7786.MCR-14-0412.
67. Ruby MA, Goldenson B, Orasanu G, Johnston TP, Plutzky J, Krauss RM. VLDL hydrolysis by LPL activates PPAR-alpha through generation of unbound fatty acids. J Lipid Res. 2010 Aug;51(8):2275-81. doi: 10.1194/jlr.M005561.
68. Caers J, Deleu S, Belaid Z, De Raeve H, Van Valckenborgh E, De Bruyne E, et al. Neighboring adipocytes participate in the bone marrow microenvironment of multiple myeloma cells. Leukemia. 2007 Jul;21(7):1580-4. doi: 10.1038/sj.leu.2404658.
69. Pang J, Shi Q, Liu Z, He J, Liu H, Lin P, et al. Resistin induces multidrug resistance in myeloma by inhibiting cell death and upregulating ABC transporter expression. Haematologica. 2017 Jul;102(7):1273-1280. doi: 10.3324/haematol.2016.154062.
70. Liu Z, Xu J, He J, Liu H, Lin P, Wan X, et al. Mature adipocytes in bone marrow protect myeloma cells against chemotherapy through autophagy activation. Oncotarget. 2015 Oct 27;6(33):34329-41. doi: 10.18632/oncotarget.6020.
71. Fain JN, Cheema PS, Bahouth SW, Lloyd Hiler M. Resistin release by human adipose tissue explants in primary culture. Biochem Biophys Res Commun. 2003 Jan 17;300(3):674-8. doi: 10.1016/s0006-291x(02)02864-4. Erratum in: Biochem Biophys Res Commun. 2003 Mar 21;302(4):917-8.

72. Shipounova IN, Petrova TV, Svinareva DA, Momotuk KS, Mikhailova EA, Drize NI. Alterations in hematopoietic microenvironment in patients with aplastic anemia. Clin Transl Sci. 2009 Feb;2(1):67-74. doi: 10.1111/j.1752-8062.2008.00074.x.
73. Chen YH, Yeh FL, Yeh SP, Ma HT, Hung SC, Hung MC, Li LY. Myocyte enhancer factor-2 interacting transcriptional repressor (MITR) is a switch that promotes osteogenesis and inhibits adipogenesis of mesenchymal stem cells by inactivating peroxisome proliferator-activated receptor gamma-2. J Biol Chem. 2011 Mar 25;286(12):10671-80. doi: 10.1074/jbc.M110.199612.
74. Hoshiba T, Kawazoe N, Chen G. The balance of osteogenic and adipogenic differentiation in human mesenchymal stem cells by matrices that mimic stepwise tissue development. Biomaterials. 2012 Mar;33(7):2025-31. doi: 10.1016/j.biomaterials.2011.11.061.
75. Tripathy NK, Singh SP, Nityanand S. Enhanced adipogenicity of bone marrow mesenchymal stem cells in aplastic anemia. Stem Cells Int. 2014;2014:276862. doi: 10.1155/2014/276862.
76. Zhao J, Wang C, Song Y, Fang B. Arsenic trioxide and microRNA-204 display contrary effects on regulating adipogenic and osteogenic differentiation of mesenchymal stem cells in aplastic anemia. Acta Biochim Biophys Sin (Shanghai). 2014 Oct;46(10):885-93. doi: 10.1093/abbs/gmu082.
77. Fujimaki S, Harigae H, Sugawara T, Takasawa N, Sasaki T, Kaku M. Decreased expression of transcription factor GATA-2 in haematopoietic stem cells in patients with aplastic anaemia. Br J Haematol. 2001 Apr;113(1):52-7. doi: 10.1046/j.1365-2141.2001.02736.x.
78. Zeng W, Chen G, Kajigaya S, Nunez O, Charrow A, Billings EM, Young NS. Gene expression profiling in CD34 cells to identify differences between aplastic anemia patients and healthy volunteers. Blood. 2004 Jan 1;103(1):325-32. doi: 10.1182/blood-2003-02-0490.
79. Tong Q, Tsai J, Hotamisligil GS. GATA transcription factors and fat cell formation. Drug News Perspect. 2003 Nov;16(9):585-8. doi: 10.1358/dnp.2003.16.9.829340.

International Journal of Biomedicine 11(2) (2021) 131-136
http://dx.doi.org/10.21103/Article11(2)_OA1

ORIGINAL ARTICLE

Cardiology

INTERNATIONAL JOURNAL OF BIOMEDICINE

Relationship between the Deformation Properties of the Left Ventricle and the Severity of Coronary Atherosclerosis in Patients with Coronary Artery Disease

F. M. Bekmetova*; Kh. G. Fozilov; Sh. N. Doniyorov; R. B. Alieva; M. G. Mukhamedova; L. T. I'lkhomova; Sh. U. Khoshimov; S. I. Bekmetova

Republican Specialized Centre of Cardiology
Tashkent, Uzbekistan

Abstract

The purpose of this study was to assess the properties of left ventricular myocardial deformation in patients with coronary artery disease (CAD) with various degrees of coronary lesions.

***Methods and Results*:** The study included 74 patients with stable angina pectoris Class II-IV aged between 40 and 70 years. All patients underwent the following examinations: assessment of traditional risk factors, physical examination, general clinical and laboratory blood tests, 12-lead ECG, 24-hour ABPM, transthoracic echocardiography, two-dimensional speckle tracking echocardiography (STE), and coronary angiography (CAG). The SYNTAX score was calculated retrospectively according to the SYNTAX score algorithm. All patients were divided into 3 groups: Group 1 included 21 patients with a low SYNTAX score (0–22), for whom standard drug therapy was recommended; Group 2 included 28 patients with an intermediate SYNTAX score (23–32), to whom PCI was recommended; Group 3 included 25 patients with a high SYNTAX score (≥33), to whom CABG was recommended.

Left ventricular ejection fraction (LVEF) obtained using the modified biplane Simpson's method was significantly lower in Group 3 than in Groups 1 and 2 (P=0.001); it should be noted that this indicator was within the normative values in Groups 1 and 2, and belonged to the gradation "mild dysfunction." A more objective quantitative assessment of the contractile function of the LV myocardium was obtained by assessing the GLS and SR. The comparative analysis of the LV myocardial deformation properties in the three studied groups showed that in Group 3 the GLS and SR indicators were significantly lower than in Group 1 (P=0.000 and P=0.0020). Moreover, GLS (global longitudinal strain) and SR (strain rate) were significantly higher in Group 1 than in Group 2 (P=0.0001 and P=0.0133, respectively). GLS significantly correlated with LVEF (r=0.57; P<0.05), E/A (r=0.22; P<0.05), and SYNTAX score (r=-0.63; P<0.05). SR significantly correlated with LVEF (r=0.49; P<0.05) and SYNTAX score (r=-0.37; P<0.05)

***Conclusion*:** The results obtained indicate the diagnostic value of STE with the determination of GLS and SR in a comprehensive assessment of the severity of CAD. GLS and SR significantly correlate with the clinical course of the disease, as well as indicators of LV remodeling and LV diastolic dysfunction. STE analysis of GLS and SR has incremental diagnostic value over transthoracic echocardiography in predicting significant CAD.(**International Journal of Biomedicine. 2021;11(2):131-136.**)

Key Words: coronary artery disease • speckle tracking echocardiography • global longitudinal strain

For citation: Bekmetova FM, Fozilov KhG, Doniyorov ShN, Alieva RB, Mukhamedova MG, I'lkhomova LT, Khoshimov ShU, Bekmetova SI, Relationship between the Deformation Properties of the Left Ventricle and the Severity of Coronary Atherosclerosis in Patients with Coronary Artery Disease. International Journal of Biomedicine. 2021;11(2):131-136. doi:10.21103/Article11(2)_OA1

Abbreviations

CAD, coronary artery disease; **CABG**, coronary artery bypass grafting; **CAG**, coronary angiography: **GLS**, global longitudinal strain; **IVST**, interventricular septal thickness; **LV**, left ventricle; **LVEF**, left ventricular ejection fraction; **LVDD**, left ventricular diastolic dysfunction; **LVEDD**, left ventricular end-diastolic dimension; **LVESD**, left ventricular end-systolic dimension; **LVEDV**, left ventricular end-diastolic volume; **LVESV**, left ventricular end-systolic volume; **LVPWT**, left ventricular posterior wall thickness; **PCI**, percutaneous coronary intervention; **STE**, speckle tracking echocardiography; **SR**, strain rate.

Introduction

Coronary artery disease (CAD), being the main clinical manifestation of atherosclerosis, for many years has remained one of the main causes of death in economically developed countries. According to the WHO, about 17 million people die from heart disease every year, 7.2 million of them from CAD.

The study of the functional capacity of the myocardium in CAD is an important task from a prognostic point of view, and echocardiography has become the leading method of its study. Conventional echocardiography is a reliable method for analyzing regional contractility and global heart function. However, it has a number of limitations. The most common measure of LV systolic function, the left ventricular ejection fraction (LVEF), evaluates changes in LV chamber volume during the cardiac cycle without directly measuring myocardial muscle contraction, and thus cannot detect early contractile dysfunction. In addition, the reliability of LVEF depends on image quality and in particular the ability to visualize the endocardial border. In contrast, speckle tracking echocardiography (STE) is a promising modern technique for assessing structural and functional changes in the myocardium.

A common standard for STE is provided by a consensus document of the EACVI/ASE/Industry Task Force.[1] LV peak global longitudinal strain (GLS), a measure of myocardial deformation, directly measures the amount of myocardial longitudinal shortening and can detect subclinical myocardial dysfunction.[2] LV peak global longitudinal strain rate (SR), which assesses rate of change in strain, is another robust measure of LV systolic function.[2,3]

The reported normal mean values of GLS among the studies varied from -15.80% to -23.40% (mean -19.05%; 95% CI: -18.18% to -19.93%; I^2 = 99.0%)[4]; normal mean values of SR varied from -1.30 to -2.40 sec(-1) (mean, -1.88 sec(-1); 95% CI: -2.10 to -1.59 sec(-1))[5]. Recent studies have reported that LV GLS is a more sensitive measure of myocardial dysfunction and is more reproducible than LVEF. Additionally, it is a more powerful predictor of outcomes in patients with heart failure with a reduced LVEF.[6,7] Previous studies have shown that GLS may both diagnose and exclude acute CAD better than LVEF. In addition, GLS has better intra- and inter-observer reproducibility in post hoc analysis than LVEF.[8,11-13]

Lacalzada et al.[14] found that GLS measured immediately after primary percutaneous coronary intervention is an excellent predictor of adverse LV remodeling and cardiac events in patients with acute myocardial infarction. Geyer et al.[15] summarized the recent developments in STE, a relatively new technique that can be used in conjunction with two-dimensional or three-dimensional echocardiography for resolving the multidirectional components of LV deformation.

The purpose of this study was to assess the properties of LV myocardial deformation in patients with CAD with various degrees of coronary lesions.

Material and Methods

The study included 74 patients with stable angina pectoris Class II-IV (Canadian Cardiovascular Society Classification) aged between 40 and 70 years. The study protocol was reviewed and approved by the Ethics Committee of the Republican Specialized Centre of Cardiology. All participants provided the written informed consent.

Diagnosis of stable angina pectoris was performed according to the European Guidelines on the management of stable angina pectoris.[16] Exclusion criteria were history of myocardial infarction within previous 3 months, hypertension Grades 2-3 (ESC/ESH,2018), valvular heart disease, acute coronary syndrome, chronic heart failure (NYHA FC>III), cardiac arrhythmia, renal impairment, severe co-morbidities, orthostatic hypotension.

Pharmacological therapy included aspirin 75 mg daily in all patients without specific contraindications, clopidogrel as an alternative antiplatelet agent in patients who cannot take aspirin, statin therapy, ACE-inhibitor, beta-blockers.

All patients underwent the following examinations: assessment of traditional risk factors, physical examination, general clinical and laboratory blood tests, 12-lead ECG, 24-hour ABPM, echocardiography, and CAG.

Transthoracic echocardiography (TTE)

Conventional 2D echocardiography was carried out according to the recommendations of the American Society of Echocardiography and the European Association of Cardiovascular Imaging[17] in M- and B-modes using an ACUSON X700 ultrasound machine equipped with a 1.0-4.0 MHz transducer (SIEMENS, Germany). The LV volumes and LVEF were measured by 2 methods. LVEDV, LVESV and LVEF were calculated using 1) the area–length method (using the apical 4-chamber and apical 2-chamber views) and 2) the modified Simpson's method (biplane method of disks) by tracing the endocardial border of LV cavity in both the apical four-chamber and two-chamber views in end-systole and end-diastole.

LV diastolic function was analyzed by measuring peak early diastolic filling (*E*) and late diastolic filling (*A*) velocities, *E*/*A* ratio. All parameters were obtained as the average value of 5 consecutive cardiac cycles.

The values of LVEF (modified Simpson's method) were as follows:

Normal: >55%
Mild dysfunction: 45-54%
Moderate dysfunction: 30%-44%
Severe dysfunction: <30%

Two-dimensional speckle tracking echocardiography (STE)

Two-dimensional images of 4-chamber, 3-chamber and 2-chamber apical views, as well as an LV parasternal short-axis view (at the root of papillary muscle), were recorded with the same ultrasound machine. Three consecutive cardiac cycle loops were recorded at end expiration. To ensure acceptable image quality, the frame rate was between 50 and 80 frames per second. A well-defined cardiac cycle was acquired for each view and stored digitally for offline analysis. All images were stored digitally and analyzed with offline software (Syngo Dynamics 9.0 software, Siemens Medical Solutions). Speckle tracking for myocardial strain was performed using Velocity Vector Imaging (VVI) software (*T*omTec-Arena TTA2 , Germany). GLS and SR were automatically calculated as the

average of 6 myocardial segments from 3 echocardiographic views.

Coronary angiography

CAG was performed via the Judkins technique through the femoral or radial artery access using Phillip Allura CV20 (Phillips Medical Systems, The Netherlands). The angiographical severity of coronary stenosis was assessed in the position with the most luminal narrowing, and the percentage of luminal narrowing was recorded according to the American Heart Association reporting system.[18] The SYNTAX score, an anatomical scoring system to grade the complexity of CAD, was calculated for each patient accordingly. All coronary lesions resulting in luminal narrowing of ≥50% in diameter for vessels ≥1.5 mm in diameter were considered significant stenosis. The SYNTAX score was calculated retrospectively according to the SYNTAX score algorithm.[19] All patients were divided into 3 groups: low SYNTAX score (0–22), intermediate score (23–32) and high score (≥33).

Statistical analysis was performed using the statistical software «Statistica» (v6.0, StatSoft, USA). Baseline characteristics were summarized as frequencies and percentages for categorical variables and as mean±standard deviation (SD) for continuous variables. Multiple comparisons were performed with one-way ANOVA with Tukey's *pairwise comparisons*. Group comparisons with respect to categorical variables were performed using chi-square tests. Pearson's correlation coefficient (r) was used to determine the strength of the relationship between the two continuous variables. A probability value of $P<0.05$ was considered statistically significant.

Results

The patients were further divided into 3 groups based on the results of CAG and the SYNTAX score: Group 1 included 21 patients with a low SYNTAX score, for whom standard drug therapy was recommended; Group 2 included 28 patients with an intermediate SYNTAX score, to whom PCI was recommended; Group 3 included 25 patients with a high SYNTAX score, to whom CABG was recommended. The baseline clinical characteristics of the patients included in the study are presented in Table 1.

*Tab**le 1.***

***Clinical characteristics of the CAD patient**s*

Variable	Group 1 (n=21)	Group 2 (n=28)	Group 3 (n=25)	Statistics
Average age, yrs	59.3±9.4	60.0±8.1	61.6±6.2	$P>0.05$
Gender (M/F)	8/13 (38.1%/61.9%)	18/10 (64.3%/35.7%)	23/2 (92%/8%)	$\chi^2=14.9$ $P=0.000$
Hypertension, n (%)	12 (57.1%)	23 (82.1%)	21 (84%)	$\chi^2=5.496$ $P=0.064$
History of MI, n (%)	1 (4.8%)	11 (39.3%)	23 (92%)	$\chi^2=36.05$ $P=0.000$
T2D, n (%)	1 (4.8%)	7 (25%)	4 (16%)	$\chi^2=3.619$ $P=0.164$

MI - myocardial infarction; T2D - Type 2 diabetes

The average age of the patients in the 3 groups was comparable. Analysis of gender differences showed a significant predominance of men in Group 3, compared to Groups 1 and 2 ($P=0.000$). In Group 3, there were more patients with a history of myocardial infarction than in Groups 1 and 2 ($P=0.000$). The number of patients with hypertension and diabetes was slightly predominant in Groups 2 and 3, compared with Group 1.

Comparative analysis of the parameters of central hemodynamics revealed significant differences in contractility of the LV myocardium in the studied groups of patients (Table 2). Thus, LVEF (area–length method) was significantly lower in Group 3 than in Groups 1 and 2 ($P=0.001$). At the same time, the LV dimensions (LVESD and LVEDD) in Group 3 were significantly larger than in Groups 1 and 2 ($P=0.000$ and $P=0.001$, respectively).

Table 2.

Echo-based parameters of central hemodynamics

Variable	Group 1 (n=21)	Group 2 (n=28)	Group 3 (n=25)	Statistics
Aorta, mm	28.5±6.4	27.3±6.1	31.7±7.8	F=2.8887 $P=0.0622$
Left atrium, mm	34.8±3.7	33.1±3.4	35.3±5.7	F=1.8332 $P=0.1674$
IVST, mm	11.0±1.6	11.8±1.6	11.4±1.9	F=1.3266 $P=0.2719$
LVPWT, mm	10.4±1.5	10.5±1.3	10.3±1.2	F=0.1499 $P=0.8610$
LVEDD, mm	47.0±4.8	48.1±5.0	54.0±9.6	F=7.2803 $P=0.0013$ $P_{1-2}=0.8443$ $P_{1-3}=0.0027$ $P_{2-3}=0.0072$
LVESD, mm	31.3±4.5	32.3±5.2	40.3±10.6	F=11.0067 $P=0.0001$ $P_{1-2}=0.8849$ $P_{1-3}=0.0003$ $P_{2-3}=0.0005$
LVEF (area–length), %	61.1±9.9	56.1±11.0	48.0±12.5	F=8.0544 $P=0.0007$ $P_{1-2}=0.2785$ $P_{1-3}=0.0006$ $P_{2-3}=0.0288$
Biplane Simpson's LVEDV, ml	107.4±26.3	111.3±29.6	141.1±75.1	F=3.4049 $P=0.0387$ $P_{1-2}=0.9595$ $P_{1-3}=0.0612$ $P_{2-3}=0.0790$
Biplane Simpson's LVESV, ml	42.1±18.1	50.4±21.4	78.0±58.0	F=6.0193 $P=0.0038$ $P_{1-2}=0.7241$ $P_{1-3}=0.0052$ $P_{2-3}=0.0247$
Biplane Simpson's LVEF, %	61.3±9.1	55.9±9.9	48.4±12.2	F=8.7657 $P=0.0004$ $P_{1-2}=0.1849$ $P_{1-3}=0.0003$ $P_{2-3}=0.0310$

LVESV obtained by the modified biplane Simpson's method was significantly higher in Group 3 than in Groups 1 and 2 ($P=0.038$) and exceeded the standard values (>70 ml). LVEF obtained using the modified biplane Simpson's method

was significantly lower in Group 3 than in Groups 1 and 2 (P=0.000); it should be noted that this indicator was within the normative values in Groups 1 and 2, and belonged to the gradation "mild dysfunction."

A more objective quantitative assessment of the contractile function of the LV myocardium was obtained by assessing the GLS and SR (Table 3). The comparative analysis of the LV myocardial deformation properties in the three studied groups showed that in Group 3 the GLS and SR indicators were significantly lower than in Group 1 (P=0.000 and P=0.002). Moreover, GLS and SR were significantly higher in Group 1 than in Group 2 (P=0.0001 and P=0.0133, respectively). GLS significantly correlated with LVESD (r=-0.38; P<0.05), LVEDD (r=-0.34, P<0.05), LVEF (r=0.57; P<0.05), E/A (r=0.22; P<0.05), and SYNTAX score (r=-0.63; P<0.05). SR significantly correlated with LVEF (r=0.49; P<0.05) and SYNTAX score (r=-0.37; P<0.05).

Table 3.

Quantitative assessment of the contractile function of the LV myocardium obtained by VVI

Variable	Group 1 (n=21)	Group 2 (n=28)	Group 3 (n=25)	Statistics
GLS, %	-18.1±4.4	-11.8±5.9	-10.3±3.6	F=16.6499 P=0.0000 P_{1-2}=0.0001 P_{1-3}=0.0000 P_{2-3}=0.4960
SR, c^{-1}	-1.5±0.6	-1.1±0.5	-1.0±0.3	F=6.9184 P=0.0018 P_{1-2}=0.0133 P_{1-3}=0.0020 P_{2-3}=0.7268

Table 4.

Relationship between LV deformation properties and structural-functional and clinical parameters in CAD patients

Variable	GLS	SR
IVST	-0.18	-0.33
LVPWT	-0.06	-0.01
LVEDD	-0.34*	-0.24
LVESD	-0.38*	-0.29
E/A	0.22*	0.18
LVEF	0.57*	0.49*
SYNTAX Score	-0.63*	-0.37*

*$P<0.05$

Discussion

The most commonly used strain-based measure of LV global systolic function is GLS. It is usually assessed by STE.[1,20] According to AES/EACVI, to provide some guidance, a peak GLS in the range of 20% can be expected in a healthy person, and the lower the absolute value of strain is below this value, the more likely it is to be abnormal.[17] There is evidence that women have slightly higher absolute values of GLS than men and that strain values decrease with age.[21,22]

The HUNT study in Norway, in which longitudinal strain and SR were determined in 1266 healthy individuals from 3 standard apical views, showed that mean (SD) overall GLS and SR were -17.4% (2.3) and -1.05 s(-1) (0.13) in women, and -15.9% (2.3) and -1.01 s(-1) (0.13) in men. Deformation indices decreased with increasing age.[20]

A study performed by Smedrsrud et al.[23] showed that global systolic strain was significantly lower in patients with significant CAD than in patients without significant coronary artery stenoses (-17.7 ± 3.0% vs. -19.5 ± 2.6%, P=0.003).

The results obtained in studies performed by Bochenek et al.[24] and Cong et al.[25] showed the clinical value of GLS measured by STE in the prediction of LV remodeling after STEMI treated by PCI. D'Andrea et al.[26] found that in patients with recent NSTEMI, longitudinal LV global and regional speckle-tracking strain measurements are powerful independent predictors of LV remodeling after reperfusion therapy.

A study performed by Abdelrazek et al.[27] showed that GLS decreased incrementally with increasing SYNTAX score, which indicates increasing severity of CAD. Vrettos et al.[28] showed similar results when they studied 71 patients and reported that GLS values were inversely correlated to SYNTAX score values.

Abdelrazek et al.[27] found a significant correlation between left ventricle EF and GLS (r=0.25; P=0.04), and Benyounes et al.[29] reported similar results when they demonstrated that two-dimensional GLS can predict LVEF (r=−0.53; P<0.001). Lima et al.[30] concluded that LVEF and GLS showed a powerful correlation (r=0.95; r^2=0.89; P<0.001), especially in patients with LV systolic dysfunction, compared to those with normal LVEF.

In conclusion, the results obtained indicate the diagnostic value of STE with the determination of GLS and SR in a comprehensive assessment of the severity of CAD. GLS and SR significantly correlate with the clinical course of the disease, as well as indicators of LV remodeling and LV diastolic dysfunction. STE analysis of GLS and SR has incremental diagnostic value over TTE in predicting significant CAD.

Competing Interests

The authors declare that they have no competing interests.

References

1. Voigt JU, Pedrizzetti G, Lysyansky P, Marwick TH, Houle H, Baumann R, Pedri S, Ito Y, Abe Y, Metz S, Song JH, Hamilton J, Sengupta PP, Kolias TJ, d'Hooge J, Aurigemma GP, Thomas JD, Badano LP. Definitions for a

***Corresponding author**: Feruza M. Bekmetova, PhD, ScD. The Republican Specialized Center of Cardiology, Tashkent, Uzbekistan. E-mail: bekmetova@rambler.ru*

common standard for 2D speckle tracking echocardiography: consensus document of the EACVI/ASE/Industry Task Force to standardize deformation imaging. Eur Heart J Cardiovasc Imaging. 2015 Jan;16(1):1-11. doi: 10.1093/ehjci/jeu184.
2. Duncan AE, Alfirevic A, Sessler DI, Popovic ZB, Thomas JD. Perioperative assessment of myocardial deformation. Anesth Analg. 2014 Mar;118(3):525-44. doi: 10.1213/ANE.0000000000000088.
3. Weidemann F, Jamal F, Sutherland GR, Claus P, Kowalski M, Hatle L, De Scheerder I, Bijnens B, Rademakers FE. Myocardial function defined by strain rate and strain during alterations in inotropic states and heart rate. Am J Physiol Heart Circ Physiol. 2002 Aug;283(2):H792-9. doi: 10.1152/ajpheart.00025.2002.
4. Truong VT, Phan HT, Pham KNP, Duong HNH, Ngo TNM, Palmer C, Nguyen TTH, Truong BH, Vo MA, Tretter JT, Nagueh SF, Chung ES, Mazur W. Normal Ranges of Left Ventricular Strain by Three-Dimensional Speckle-Tracking Echocardiography in Adults: A Systematic Review and Meta-Analysis. J Am Soc Echocardiogr. 2019 Dec;32(12):1586-1597.e5. doi: 10.1016/j.echo.2019.07.012.
5. Levy PT, Sanchez Mejia AA, Machefsky A, Fowler S, Holland MR, Singh GK. Normal ranges of right ventricular systolic and diastolic strain measures in children: a systematic review and meta-analysis. J Am Soc Echocardiogr. 2014 May;27(5):549-60, e3. doi: 10.1016/j.echo.2014.01.015.
6. Smiseth OA, Torp H, Opdahl A, Haugaa KH, Urheim S. Myocardial strain imaging: how useful is it in clinical decision making? Eur Heart J. 2016 Apr 14;37(15):1196-207. doi: 10.1093/eurheartj/ehv529.
7. Adamo L, Perry A, Novak E, Makan M, Lindman BR, Mann DL. Abnormal Global Longitudinal Strain Predicts Future Deterioration of Left Ventricular Function in Heart Failure Patients With a Recovered Left Ventricular Ejection Fraction. Circ Heart Fail. 2017 Jun;10(6):e003788. doi: 10.1161/CIRCHEARTFAILURE.116.003788.
8. Stanton T, Leano R, Marwick TH. Prediction of all-cause mortality from global longitudinal speckle strain: comparison with ejection fraction and wall motion scoring. Circ Cardiovasc Imaging. 2009 Sep;2(5):356-64. doi: 10.1161/CIRCIMAGING.109.862334.
9. Grenne B, Eek C, Sjøli B, Dahlslett T, Uchto M, Hol PK, Skulstad H, Smiseth OA, Edvardsen T, Brunvand H. Acute coronary occlusion in non-ST-elevation acute coronary syndrome: outcome and early identification by strain echocardiography. Heart. 2010 Oct;96(19):1550-6. doi: 10.1136/hrt.2009.188391.
10. Dahlslett T, Karlsen S, Grenne B, Eek C, Sjøli B, Skulstad H, Smiseth OA, Edvardsen T, Brunvand H. Early assessment of strain echocardiography can accurately exclude significant coronary artery stenosis in suspected non-ST-segment elevation acute coronary syndrome. J Am Soc Echocardiogr. 2014 May;27(5):512-9. doi: 10.1016/j.echo.2014.01.019.
11. Kalam K, Otahal P, Marwick TH. Prognostic implications of global LV dysfunction: a systematic review and meta-analysis of global longitudinal strain and ejection fraction. Heart. 2014 Nov;100(21):1673-80. doi: 10.1136/heartjnl-2014-305538.
12. Negishi T, Negishi K, Thavendiranathan P, Cho GY, Popescu BA, Vinereanu D, Kurosawa K, Penicka M, Marwick TH; SUCCOUR Investigators. Effect of Experience and Training on the Concordance and Precision of Strain Measurements. JACC Cardiovasc Imaging. 2017 May;10(5):518-522. doi: 10.1016/j.jcmg.2016.06.012.
13. Karlsen S, Dahlslett T, Grenne B, Sjøli B, Smiseth O, Edvardsen T, Brunvand H. Global longitudinal strain is a more reproducible measure of left ventricular function than ejection fraction regardless of echocardiographic training. Cardiovasc Ultrasound. 2019 Sep 2;17(1):18. doi: 10.1186/s12947-019-0168-9.
14. Lacalzada J, de la Rosa A, Izquierdo MM, Jiménez JJ, Iribarren JL, García-González MJ, López BM, Duque MA, Barragán A, Hernández C, Carrillo-Pérez M, Laynez I. Left ventricular global longitudinal systolic strain predicts adverse remodeling and subsequent cardiac events in patients with acute myocardial infarction treated with primary percutaneous coronary intervention. Int J Cardiovasc Imaging. 2015 Mar;31(3):575-84. doi: 10.1007/s10554-015-0593-2.
15. Geyer H, Caracciolo G, Abe H, Wilansky S, Carerj S, Gentile F, Nesser HJ, Khandheria B, Narula J, Sengupta PP. Assessment of myocardial mechanics using speckle tracking echocardiography: fundamentals and clinical applications. J Am Soc Echocardiogr. 2010 Apr;23(4):351-69; quiz 453-5. doi: 10.1016/j.echo.2010.02.015. Erratum in: J Am Soc Echocardiogr. 2010 Jul;23(7):734.
16. Fox K, Garcia MA, Ardissino D, Buszman P, Camici PG, Crea F, et al.; Task Force on the Management of Stable Angina Pectoris of the European Society of Cardiology; ESC Committee for Practice Guidelines (CPG). Guidelines on the management of stable angina pectoris: executive summary: The Task Force on the Management of Stable Angina Pectoris of the European Society of Cardiology. Eur Heart J. 2006 Jun;27(11):1341-81. doi: 10.1093/eurheartj/ehl001.
17. Lang RM, Badano LP, Mor-Avi V, Afilalo J, Armstrong A, Ernande L, Flachskampf FA, Foster E, Goldstein SA, Kuznetsova T, Lancellotti P, Muraru D, Picard MH, Rietzschel ER, Rudski L, Spencer KT, Tsang W, Voigt JU. Recommendations for cardiac chamber quantification by echocardiography in adults: an update from the American Society of Echocardiography and the European Association of Cardiovascular Imaging. J Am Soc Echocardiogr. 2015 Jan;28(1):1-39.e14.
18. Austen WG, Edwards JE, Frye RL, Gensini GG, Gott VL, Griffith LS, McGoon DC, Murphy ML, Roe BB. A reporting system on patients evaluated for coronary artery disease. Report of the Ad Hoc Committee for Grading of Coronary Artery Disease, Council on Cardiovascular Surgery, American Heart Association. Circulation. 1975 Apr;51(4 Suppl):5-40. doi: 10.1161/01.cir.51.4.5.
19. Sianos G, Morel MA, Kappetein AP, Morice MC, Colombo A, Dawkins K, van den Brand M, Van Dyck N, Russell ME, Mohr FW, Serruys PW. The SYNTAX Score: an angiographic tool grading the complexity of coronary artery disease. EuroIntervention. 2005 Aug;1(2):219-27.
20. Dalen H, Thorstensen A, Aase SA, Ingul CB, Torp H, Vatten LJ, Stoylen A. Segmental and global longitudinal strain and strain rate based on echocardiography of 1266 healthy individuals: the HUNT study in Norway. Eur J Echocardiogr. 2010 Mar;11(2):176-83. doi: 10.1093/ejechocard/jep194.
21. Kocabay G, Muraru D, Peluso D, Cucchini U, Mihaila S, Padayattil-Jose S, Gentian D, Iliceto S, Vinereanu D, Badano LP. Normal left ventricular mechanics by two-dimensional speckle-tracking echocardiography. Reference values in healthy adults. Rev Esp Cardiol (Engl Ed). 2014 Aug;67(8):651-8. doi: 10.1016/j.rec.2013.12.009.
22. Kuznetsova T, Herbots L, Richart T, D'hooge J, Thijs L, Fagard RH, Herregods MC, Staessen JA. Left ventricular

strain and strain rate in a general population. Eur Heart J. 2008 Aug;29(16):2014-23. doi: 10.1093/eurheartj/ehn280.
23. Smedsrud MK, Sarvari S, Haugaa KH, Gjesdal O, Ørn S, Aaberge L, Smiseth OA, Edvardsen T. Duration of myocardial early systolic lengthening predicts the presence of significant coronary artery disease. J Am Coll Cardiol. 2012 Sep 18;60(12):1086-93. doi: 10.1016/j.jacc.2012.06.022.
24. Bochenek T, Wita K, Tabor Z, Grabka M, Krzych Ł, Wróbel W, Berger-Kucza A, Elżbieciak M, Doruchowska A, Gluza MT. Value of speckle-tracking echocardiography for prediction of left ventricular remodeling in patients with ST-elevation myocardial infarction treated by primary percutaneous intervention. J Am Soc Echocardiogr. 2011 Dec;24(12):1342-8. doi: 10.1016/j.echo.2011.09.003.
25. Cong T, Sun Y, Shang Z, Wang K, Su D, Zhong L, Zhang S, Yang Y. Prognostic Value of Speckle Tracking Echocardiography in Patients with ST-Elevation Myocardial Infarction Treated with Late Percutaneous Intervention. Echocardiography. 2015 Sep;32(9):1384-91. doi: 10.1111/echo.12864.
26. D'Andrea A, Cocchia R, Caso P, Riegler L, Scarafile R, Salerno G, Golia E, Di Salvo G, Calabrò P, Bigazzi MC, Liccardo B, Esposito N, Cuomo S, Bossone E, Russo MG, Calabrò R. Global longitudinal speckle-tracking strain is predictive of left ventricular remodeling after coronary angioplasty in patients with recent non-ST elevation myocardial infarction. Int J Cardiol. 2011 Dec 1;153(2):185-91. doi: 10.1016/j.ijcard.2010.08.025.
27. Abdelrazek G, Yassin A, Elkhashab K. Correlation between global longitudinal strain and SYNTAX score in coronary artery disease evaluation. Egypt Heart J. 2020 May 15;72(1):22. doi: 10.1186/s43044-020-00064-2.
28. Vrettos A, Dawson D, Grigoratos C, Nihoyannopoulos P. Correlation between global longitudinal peak systolic strain and coronary artery disease severity as assessed by the angiographically derived SYNTAX score. Echo Res Pract. 2016 Jun;3(2):29-34. doi: 10.1530/ERP-16-0005.
29. Benyounes N, Lang S, Soulat-Dufour L, Obadia M, Gout O, Chevalier G, Cohen A. Can global longitudinal strain predict reduced left ventricular ejection fraction in daily echocardiographic practice? Arch Cardiovasc Dis. 2015 Jan;108(1):50-6. doi: 10.1016/j.acvd.2014.08.003.
30. Lima MSM, Villarraga HR, Abduch MCD, Lima MF, Cruz CBBV, Sbano JCN, Voos MC, Mathias W Junior, Tsutsui JM. Global Longitudinal Strain or Left Ventricular Twist and Torsion? Which Correlates Best with Ejection Fraction? Arq Bras Cardiol. 2017 Jul;109(1):23-29. doi: 10.5935/abc.20170085.

International Journal of Biomedicine 11(2) (2021) 137-140
http://dx.doi.org/10.21103/Article11(2)_OA2

ORIGINAL ARTICLE

Internal Medicine

INTERNATIONAL JOURNAL OF BIOMEDICINE

Life Quality and Cytokines Profile in Patients with Asthma and Osteoarthritis

Yuliya S. Ivanchuk, PGS; Ludmila V. Tribuntceva, PhD; Andrey V. Budnevsky, PhD, ScD; Yanina S. Shkatova, PGS; Evgeniy S. Ovsyannikov, PhD, ScD*; Roman E. Tokmachev, PhD

Voronezh State Medical University named after N. N. Burdenko
Voronezh, the Russian Federation

Abstract

The objective of this study was to evaluate levels of leptin, adiponectin, IL-4, IL-6, TNF-α, oxidative damage, and antioxidant status in patients with bronchial asthma (BA), compared to patients who suffer from both BA and **o**steoarthritis (OA), and analyze the quality of life in such patients.

Methods and Results: The study included 103 patients (34 men and 69 women) diagnosed with moderate asthma aged from 30 to 70 years (mean age of 58.52±7.14 years). The levels of IL-4, IL-6, TNF-α, adiponectin, leptin, total antioxidant status (TAS), and total oxidative damage (TOD) were measured. Two questionnaires were used in this study: Asthma Quality of Life Questionnaire (AQLQ) and Asthma Control Test (ACT).

The levels of leptin, TNF-α, and Il-6 were significantly higher in Group 2 than in Group 1. On the contrary, the IL-4 level was higher in Group 1 than in Group 2. The TAS value was significantly higher in Group 1 than in Group 2 (P=0.0001). The TOD value was significantly higher in Group 2 than in Group 1 (P=0.0000). The domains of AQLQ(S) activity, symptoms, and emotions were decreased in patients of Group 2. The values of the ACT test were 18.0±2.61 points and 16.78±1.92 points in Group 1 and Group 2, respectively (P=0.0077).

Conclusion: In patients with both asthma and osteoarthritis, levels of inflammatory cytokines, such as leptin, IL-6, and TNF-α, are significantly elevated as well as values of total oxidative status, which correlate with poorer asthma control and quality of life.(**International Journal of Biomedicine. 2021;11(2):137-140.**)

Key Words: asthma • osteoarthritis • IL-6 • TNF-α • quality of life

For citation: Ivanchuk YuS, Tribuntceva LV, Budnevsky AV, Shkatova YaS, Ovsyannikov ES, Tokmachev RE. Life Quality and Cytokines Profile in Patients with Asthma and Osteoarthritis. International Journal of Biomedicine. 2021;11(2):137-140. doi:10.21103/Article11(2)_OA2

Abbreviations

OA, osteoarthritis; **BMI**, body mass index; **BA**, bronchial asthma; **IL**, interleukin; **TNF-α**, tumor necrosis factor alpha; **TAS**, total antioxidant status; **TOD**, total oxidative damage.

Introduction

Among respiratory diseases, bronchial asthma (BA) is one of the most common; almost 250,000 patients die from BA every year as a result of severe exacerbation.[1] Asthma affects more than 300 million people in the world and costs over $80 billion annually in the United States.[2] It has been shown that asthmatic patients often have comorbidities, which influence their overall health, life quality, and clinical course of asthma.[3,4] The most researched comorbidities of asthma include cardiovascular diseases, cerebrovascular diseases, mental diseases, diabetes mellitus, and obesity.[5-8] Osteoarthritis (OA) is a less studied comorbidity; however, according to a German telephone interview health survey, German Health Update (GEDA) 2009 and 2010, OA was noted in 18.4% of all patients with no current asthma and in 29.4% of patients with current asthma, making this comorbidity one of the most common ones, following closely after cardiovascular diseases.[9] Nevertheless, the data is

limited on the association between BA and OA, as well as on the influence these diseases might have on each other.

The objective of this study was to evaluate levels of leptin, adiponectin, IL-4, IL-6, TNF-α, oxidative damage, and antioxidant status in patients with BA, compared to patients who suffer from both BA and OA, and analyze the quality of life in such patients.

Materials and Methods

The study included 103 patients (34 men and 69 women) diagnosed with moderate asthma aged from 30 to 70 years (mean age of 58.52±7.14 years). Excluded criteria were mental illness, rheumatic diseases, fibromyalgia, tuberculosis, severe and decompensated diseases of liver and kidneys, severe and decompensated cardiovascular diseases, cancer, pregnancy and lactation, severe infectious diseases, and previous joint surgery.

The study was approved by the Ethics Committee of Voronezh State Medical University named after N.N. Burdenko. Written informed consent was obtained from each patient.

The diagnosis of asthma was made according to GINA. We analyzed complaints, anamnesis data, objective status data, and laboratory and instrumental data (spirometry with a 400-mg salbutamol test). All patients received standard asthma therapy.

Two questionnaires were used in this study: Asthma Quality of Life Questionnaire (AQLQ) and Asthma Control Test (ACT).

The levels of IL-4, IL-6, TNF-α, adiponectin, leptin, TAS, and TOD were measured. The levels of leptin and adiponectin were measured using the appropriate reagent kits for quantitative determination of leptin and adiponectin in serum. The determination of TOD was carried out with use of a reagent kit to determine the degree of TOD to biological molecules (PerOx (TOS) (Oxidative Capacity)). We determined the overall antioxidant status by using reagents for determining TAS (ImAnOx (TAS) (Antioxidative Capacity)). The IL-4 level was determined by using a set of reagents for the EIA test; the IL-6 level was determined by using a set of reagents for the ELISA test.

All data was evaluated with STATGRAPHICS Plus 5.1. Baseline characteristics were summarized as frequencies and percentages for categorical variables and as mean±SD for continuous variables. Group comparisons with respect to categorical variables are performed using the Chi-square test. Comparisons of quantitative parameters was performed using one-way ANOVA. A probability value of $P<0.05$ was considered statistically significant.

Results

During the study, all asthma patients were divided into 2 groups. Group 1 included 38 patients with BA; Group 2 included 65 patients with BA and OA. The formed groups did not differ by age, gender, marriage status, or level of education ($P<0.05$).

BMI values were 26.76±2.09 kg/m^2 in Group 1 and 27.46±1.33 kg/m^2 in Group 2 ($P=0.04$). There was no statistically significant difference in spirometry parameters between the groups. Laboratory test results are presented in the Table 1. The levels of leptin, TNF-α, and Il-6 were significantly higher in Group 2 than in Group 1. On the contrary, the IL-4 level was higher in Group 1 than in Group 2. The TAS value was significantly higher in Group 1 than in Group 2 ($P=0.0001$). The TOD value was significantly higher in Group 2 than in Group 1 ($P=0.0000$).

Table 1.
Biochemical parameters in the study groups

Variable	Group 1	Group 2	*P*-value
Leptin, ng/ml	25.11±5.44	27.83±4.77	0.0093
Adiponectin, μg/ml	11.22±4.85	9.82±2.30	0.0502
IL-6, pg/ml	16.79±5.61	19.77±4.89	0.0057
IL-4, pg/ml	6.83±3.81	5.05±2.41	0.0045
TNF-α, pg/ml	2.14±0.60	2.63±0.61	0.0000
TAS, μmol/l	304.62±80.48	248.30±55.58	0.0001
TOS, μmol/l	1443.16±691.74	2146.99±537.40	0.0000

AQLQ(S) questionnaire results are presented in the Table 2. The domains of AQLQ(S) activity, symptoms, and emotions were decreased in patients of Group 2. The AQLQ(S) environment domain was also decreased in patients of Group 2: 3.67±1.13 points compared with 4.04±1.53 points in Group 1; however, the difference was not statistically significant.

The values of the ACT test were 18.0±2.61 points and 16.78±1.92 points in Group 1 and Group 2, respectively ($P=0.0077$). AQLQ(S) total score positively correlated with the ACT score (r=0,77; $P<0,05$), IL-4 level (r=0,53; $P<0,05$), and TAS level (r=0,53; $P<0,05$), and had an inverse correlation with the levels of IL-6(r=-0,67; $P<0,05$), TOS (r=-0,68; $P<0,05$), and TNF-α (r=-0,47; $P<0,05$). The Il-6 level had a positive correlation with BMI (r=0,82; $P<0,05$), leptin level (r=0,83; $P<0,05$), TNF-α level (r=0,70; P<0,05), and TOS (r=0,80; $P<0,05$), and an inverse correlation with adiponectin level (r=-0,79; $P<0,05$) and TAS (r=-0,80; $P<0,05$).

Table 2.
AQLQ(S) questionnaire results

Domain	Group 1	Group 2	*P*-value
Activity, points	4.70±1.08	3.46±0.56	0.0000
Symptoms, points	4.38±0.85	3.34±0.53	0.0000
Environment, points	4.04±1.53	3.67±1.13	0.1635
Emotions, points	4.68±1.10	3.50±0.61	0.0000
Total score, points	4.69±1.11	3.49±0.59	0.0000

Discussion

There is very limited data on the association between asthma and osteoarthritis. Koo et al.[10] analyzed 9344 people,

among whom the percentage of patients with asthma was 4.6%±0.3%. The prevalence of OA in the asthma group was 31.9±2.8%, which was significantly higher than in the COPD group (17.8%±1.5%) or control group (16.2%±0.6%). OA was predominant in asthma patients after adjusting for age, sex, BMI, and smoking status (OR=1.65; 95% CI: 1.27–2.13). After further adjusting this model for an OA drug, OA still remained independently associated with asthma(OR 1.56; 95% CI 1.10–2.20). Moreover, radiographic severity of knee OA was correlated with asthma (OR=1.10; 95% CI: 1.0–1.21. In another study on the association between BA and OA by Mahmood et al.,[11] the authors examined 56 patients with BA and OA over the age of 40. They found that asthma patients suffered from more severe knee pain than the general population (control group) (P=0.001). On the other hand, these asthmatic patients had the same frequency and severity of hip pain as the general population (P=0.162). One of the most important findings was that functional impairment, as measured by the WOMAC scale, was very high among asthma patients with osteoarthritis. They also found that the rate of emergency hospitalization for asthmatic patients, which reflects the severity and uncontrollability of asthma, was associated with a higher risk of developing OA (P=0.044). In our study, we had similar results – asthmatic patients with OA had worse asthma control than patients without OA.

Both BA and OA are associated with the IL-6 level. In asthmatic patients, serum levels of IL-6 were higher in allergic and non-allergic asthma than in healthy controls, and those levels increased in exacerbations; the IL-6 level also negatively correlated with ACT score, indicating an association with poor asthma control.[12,13] Serum IL-6 is a significant predictor of radiographic OA.[14] High IL-6 serum levels were also found in patients with symptomatic OA.[15]

In our study, patients with both BA and OA had higher levels of IL-6 than asthmatic patients without OA. The IL-6 level also had a negative correlation with ACT score and a positive correlation with leptin level. Leptin is a proinflammatory cytokine, which induces release of IL-6 and TNF-α.[16,17] High leptin levels are associated not only with knee and hip OA, but also with hand OA.[18] Studies have shown that high leptin levels can also be found in synovial fluid, and synovial fibroblasts showed a dose-dependent increase in the expression of IL-6 when treated with leptin.[19,20] This suggests that leptin can promote the progression of OA through IL-6. At the same time, leptin also affects lung cells, promoting allergic airway inflammation as it influences protein response factor XBP1s in an mTOR- and MAPK-dependent manner in pro-allergic TH2 cells.[21] TNF-α is known to play an important role in OA pathogenesis. One of the reasons for that could be that chondrocytes in human OA cartilage have a high expression of the p55 TNF-α receptor, which could make OA cartilage particularly susceptible to TNF-α degradative stimuli.[22] TNF-α also has been studied in asthma: high serum levels of TNF-α were found in asthmatic patients.[23] In our study TNF-α levels were higher in patients with BA and OA.

Several studies showed that OA progression is related to oxidative stress.[24] The most likely initial pathological syndrome in OA is the activation of the mitotic division of cartilage cells, with their production of proteoglycans, collagen II, and hypertrophy. The reason for these phenomena may be the predominance of oxidative damage over the antioxidant system. Oxidative stress has also been implicated in the pathology of asthma due to its induction of different proinflammatory mediators, enhancing bronchial hyperresponsiveness, stimulating bronchospasm, and increasing mucin secretion.[25] In our study, oxidative stress was much more prominent in patients with BA and OA than in asthmatic patients without OA.

In conclusion, to our current knowledge there are no studies that concentrate on cytokine profile or quality of life in patients with asthma and osteoarthritis. Our study showed that in patients with both asthma and osteoarthritis, levels of inflammatory cytokines, such as leptin, IL-6, and TNF-α, are significantly elevated as well as values of total oxidative status, which correlate with poorer asthma control and quality of life. Osteoarthritis is a severe co-morbid pathology in asthmatic patients. Further research on the association between asthma and osteoarthritis and its underlying mechanisms is required.

Sources of Funding

This work was supported by the Council on Grants of the President of the Russian Federation (NSh 4994.2018.7.).

Competing Interests

The authors declare that they have no competing interests.

References

1. Rehman A, Amin F, Sadeeqa S. Prevalence of asthma and its management: A review. J Pak Med Assoc. 2018 Dec;68(12):1823-1827.
2. McGeachie MJ, Wang AL, Lutz SM, Sordillo JE, Weiss ST, Tantisira KG, Iribarren C, Lu MX, Wu AC. Real-Life Patterns of Exacerbations While on Inhaled Corticosteroids and Long-Acting Beta Agonists for Asthma over 15 Years. J Clin Med. 2020 Mar 18;9(3):819. doi: 10.3390/jcm9030819.
3. Tsvetikova LN, Budnevsky AV, Ovsyannikov ES, Kudashova EA. Melatonin: Possibilities for use in the treatment of asthma. Ter Arkh. 2017;89(3):112–5. Russian. doi: 10.17116/terarkh2017893112-115.
4. Brussino L, Solidoro P, Rolla G. Is it severe asthma or asthma with severe comorbidities? J Asthma Allergy. 2017 Nov 29;10:303-305. doi: 10.2147/JAA.S150462.
5. Budnevsky A, Tribuntceva L, Kozhevnikova S, Ovsyannikov E. Impact of Metabolic Syndrome Components on Asthma Control and Life Quality of Patients. International Journal of Biomedicine. 2018;8(1):33–6. doi: 10.21103/article8(1)_oa4.

***Corresponding author**: Evgeniy S. Ovsyannikov, PhD, ScD. Department of Faculty Therapy, Voronezh State Medical University named after N.N. Burdenko. Voronezh, Russia. E-mail: ovses@yandex.ru*

6. Budnevsky AV, Isaeva YV, Malysh EY, Kozhevnikova SA. [Pulmonary rehabilitation as an effective method for optimizing therapeutic and preventive measures in patients with chronic obstructive pulmonary disease concurrent with metabolic syndrome]. Ter Arkh. 2016;88(8):25-29. Russian. doi: 10.17116/terarkh201688825-29.
7. Budnevsky AV, Malysh EY, Ovsyannikov ES, Drobysheva ES. [Asthma and metabolic syndrome: Clinical and pathogenetic relationships]. Ter Arkh. 2015;87(10):110-114. doi: 10.17116/terarkh20158710110-114. [Article in Russian].
8. Ermolova AV, Budnevsky AV, Yu ME, Ovsyannikov ES, Drobysheva ES. [BRONCHIAL ASTHMA AND METABOLIC SYNDROME]. Klin Med (Mosk). 2015;93(6):44-9. [Article in Russian].
9. Steppuhn H, Langen U, Keil T, Scheidt-Nave C. Chronic disease co-morbidity of asthma and unscheduled asthma care among adults: results of the national telephone health interview survey German Health Update (GEDA) 2009 and 2010. Prim Care Respir J. 2014 Mar;23(1):22-9. doi: 10.4104/pcrj.2013.00107.
10. Koo HK, Song P, Lee JH. Novel association between asthma and osteoarthritis: a nationwide health and nutrition examination survey. BMC Pulm Med. 2021 Feb 16;21(1):59. doi: 10.1186/s12890-021-01425-6.
11. Mahmood ZA, Malghooth ZT. Relationship of Hips and Knees Osteoarthritis with Bronchial Asthma. Res J Pharm Biol Chem Sci. 2019; 10(2):64-70.
12. Ghebre MA, Pang PH, Desai D, Hargadon B, Newby C, Woods J, et al. Severe exacerbations in moderate-to-severe asthmatics are associated with increased pro-inflammatory and type 1 mediators in sputum and serum. BMC Pulm Med. 2019 Aug 8;19(1):144. doi: 10.1186/s12890-019-0906-7.
13. Dimitrova D, Youroukova V, Ivanova-Todorova E, Tumangelova-Yuzeir K, Velikova T. Serum levels of IL-5, IL-6, IL-8, IL-13 and IL-17A in pre-defined groups of adult patients with moderate and severe bronchial asthma. Respir Med. 2019 Jul-Aug;154:144-154. doi: 10.1016/j.rmed.2019.06.024.
14. Livshits G, Zhai G, Hart DJ, Kato BS, Wang H, Williams FM, Spector TD. Interleukin-6 is a significant predictor of radiographic knee osteoarthritis: The Chingford Study. Arthritis Rheum. 2009 Jul;60(7):2037-45. doi: 10.1002/art.24598.
15. Imamura M, Ezquerro F, Marcon Alfieri F, Vilas Boas L, Tozetto-Mendoza TR, Chen J, Özçakar L, Arendt-Nielsen L, Rizzo Battistella L. Serum levels of proinflammatory cytokines in painful knee osteoarthritis and sensitization. Int J Inflam. 2015;2015:329792. doi: 10.1155/2015/329792.
16. Matsusaka M, Fukunaga K, Kabata H, Izuhara K, Asano K, Betsuyaku T. Subphenotypes of type 2 severe asthma in adults. J Allergy Clin Immunol Pract. 2018 Jan-Feb;6(1):274-276.e2. doi: 10.1016/j.jaip.2017.06.015.
17. Provotorov VM, Budnevskiĭ AV, Semenkova GG, Shishkina ES. [PROINFLAMMATORY CYTOKINES IN COMBINATION OF CORONARY HEART DISEASE AND CHRONIC OBSTRUCTIVE PULMONARY DISEASE]. Klin Med (Mosk). 2015;93(2):5-9. [Article in Russian].
18. Morales Abaunza RA, Rojas ÁP, Rojas C, Motta O, Atuesta J, Alzate JP, et al. Levels of serum leptin in patients with primary hand osteoarthritis. Rev Colomb Reumatol. 2020;27:20–25. doi: 10.1016/j.rcreue.2019.12.005.
19. Yan M, Zhang J, Yang H, Sun Y. The role of leptin in osteoarthritis. Medicine (Baltimore). 2018 Apr;97(14):e0257. doi: 10.1097/MD.0000000000010257.
20. Budnevsky AV, Ovsyannikov ES, Labzhania NB. [Chronic obstructive pulmonary disease concurrent with metabolic syndrome: Pathophysiological and clinical features]. Ter Arkh. 2017;89(1):123-127. doi: 10.17116/terarkh2017891123-127. [Article in Russian].
21. Zheng H, Wu D, Wu X, Zhang X, Zhou Q, Luo Y, Yang X, Chock CJ, Liu M, Yang XO. Leptin Promotes Allergic Airway Inflammation through Targeting the Unfolded Protein Response Pathway. Sci Rep. 2018 Jun 11;8(1):8905. doi: 10.1038/s41598-018-27278-4.
22. Fernandes JC, Martel-Pelletier J, Pelletier JP. The role of cytokines in osteoarthritis pathophysiology. Biorheology. 2002;39(1-2):237-46.
23. Ren J, Sun Y, Li G, Zhu XJ, Cui JG. Tumor necrosis factor-α, interleukin-8 and eosinophil cationic protein as serum markers of glucocorticoid efficacy in the treatment of bronchial asthma. Respir Physiol Neurobiol. 2018 Dec;258:86-90. doi: 10.1016/j.resp.2018.06.004.
24. Zahan OM, Serban O, Gherman C, Fodor D. The evaluation of oxidative stress in osteoarthritis. Med Pharm Rep. 2020 Jan;93(1):12-22. doi: 10.15386/mpr-1422.
25. Provotorov VM, Budnevsky AV, Filatova YI, Perfil'eva MV. [ANTIOXIDANT THERAPY OF BRONCHIAL ASTHMA]. Klin Med (Mosk). 2015;93(8):19-22. [Article in Russian].

International Journal of Biomedicine 11(2) (2021) 141-145
http://dx.doi.org/10.21103/Article11(2)_OA3

ORIGINAL ARTICLE

Hematology

INTERNATIONAL JOURNAL OF BIOMEDICINE

Quantitative Bone Marrow MRI in Children with Acute Lymphoblastic Leukemia

Galina V. Tereshchenko[1]; Nataliia A. Kriventsova[1*]; Dmitry A. Kupriyanov[1,2]; Peter E. Menshchikov[1,2]; Dmitry V. Litvinov[1]; Galina A. Novichkova[1]

[1]Dmitry Rogachev National Medical Research Center of Pediatric Hematology, Oncology and Immunology, Moscow, Russia
[2]Philips Healthcare, Moscow, Russia

Abstract

The aim of this study was to evaluate, using MRI, the changes in bone marrow fat fraction (BMFF) of patients with acute lymphoblastic leukemia (ALL), in comparison with children without hematological disorders.

***Methods and Results*:** The cohort of the study subjects included 20 patients aged between 5 and 17 years (mean age of 11.2±3.6 years; 10 boys and 10 girls) with clinically and morphologically confirmed diagnosis of ALL All patients underwent MRI scanning in the acute phase of the disease before the start of specific therapy. Then, the study was repeated in 10 patients (mean age of 12.2±2.3 years; 8 boys and 2 girls) during treatment, according to the ALL-MB 2015 protocol for patients with primary ALL and according to the ALL-REZ-MB 2016 protocol for patients with relapsed ALL. The control group consisted of 24 healthy controls of the same age group (mean age of 12±2.8 years; 17 boys and 7 girls) with no prior hematologic diseases. MRI scanning was carried out using a Philips Achieva dStream 3T scanner with a 32-channel FlexCoverage abdominal receiving coil. The MRI protocol included images obtained with the mDIXON Quant technique in the coronal plane, completely covering the pelvic bones and lumbar spine. Fat fraction maps were generated automatically on the MRI console using the 7-peak fat model and were corrected for T2* effects. Regions of interest (ROI) measuring 150 mm^2 were placed in the bodies of the left and right iliac bones (Ilium L, Ilium R) as well as in the L4 and L5 vertebral bodies, taking care to avoid blood vessels, cortical bones and areas that could potentially contain artifacts.

In the group of healthy controls, BMFF value was 51±11% in the bodies of the iliac bones and 32±10% in the lumbar vertebrae. In the group of patients with the acute phase of the disease, BMFF was as low as 3.1±2.6% in all the bone structures. In patients who had undergone chemotherapy, the mean BMFF increased up to 77±7% in the iliac bones and up to 65±13% in the vertebrae. Student's t-test for dependent samples revealed a statistically significant increase in the mean BMFF values in all the bone structures after chemotherapy (P<0.01). After schemotherapy, BMFF was also significantly higher than under normal conditions (P<0.01).

Conclusion: This study provides important diagnostic information for various phases of ALL treatment, especially in suspected cases of resistant or recurrent disease. (**International Journal of Biomedicine. 2021;11(2):141-145.**)

Key Words: bone marrow • quantitative magnetic resonance imaging • pediatrics • hematology • fat fraction • fat cells

For citation: Tereshchenko GV, Kriventsova NA, Kupriyanov DA, Menshchikov PE, Litvinov DV, Novichkova GA. Quantitative Bone Marrow MRI in Children with Acute Lymphoblastic Leukemia. International Journal of Biomedicine. 2021;11(2):141-145. doi:10.21103/Article11(2)_OA3

Abbreviations

ALL, acute lymphoblastic leukemia; **BM**, bone marrow; **BMFF**, bone marrow fat fraction; **FF**, fat fraction.

Introduction

Acute lymphoblastic leukemia (ALL) is a cancer of the red bone marrow (BM).[(1)] As of 2017, the incidence rate of leukemia was 4.5 per 100,000 children (4.98 among boys, 4.18 among girls) aged between 0 and 14 years. According to an analysis of the data from 2007 to 2017, the incidence rate of leukemia in this age group increased by 20.28% (the average annual growth rate - 1.82%).[(2)] Modern treatment protocols allow us to achieve a cure in up to 95% of young patients; however the treatment is long and expensive. Due to the slow but still steady growth in the number of new cases year by

year, there is a clear need for a multimodal approach to the primary prevention and diagnosis of malignant hematological disorders in children.[3]

Historically, two types of BM have been distinguished: "red" (hematopoietic) and "yellow" (fatty). Cancer researchers delineate an important role of BM adipocytes in oncohematology. Adipocytes contribute to the development and the continued growth of tumors, the metastasis to the BM and the development of resistance to chemotherapy.[4,5] Adipocytes can be studied using not only laboratory methods, but also MRI, which allows us to assess the total number of adipocytes in the BM.[6,7] It has been shown that all the sequences have high sensitivity to neoplastic and inflammatory changes in the BM of children.[8]

At different stages of ALL treatment approaches, the assessment of "red"(hematopoietic)-to-"yellow"(fat) ratio in the BM, using MRI, can provide additional information about the condition of the BM during the conducted polychemotherapy.[9]

The aim of this study was to evaluate, using MRI, the changes in BMFF of patients with ALL, in comparison with children without hematological disorders.

Materials and Methods

This study was approved by the Independent Ethics Committee of the D. Rogachev NMRCPHOI, supported by the Scientific Council of the D. Rogachev NMRCPHOI of the Ministry of Healthcare of the Russian Federation and complies with the World Medical Association Code of Ethics for medical research involving human subjects. Written informed consent was obtained from patients and their parents.

The cohort of the study subjects included 20 patients aged between 5 and 17 years (mean age of 11.2±3.6 years; 10 boys and 10 girls) with clinically and morphologically confirmed diagnosis of ALL, who underwent treatment at the D. Rogachev NMRCPHOI from October 2017 to March 2020. All patients underwent MRI scanning in the acute phase of the disease before the start of specific therapy (Table 1). Then, the study was repeated in 10 patients (mean age of 12.2±2.3 years, 8 boys and 2 girls) during treatment, according to the ALL-MB 2015 protocol for patients with primary ALL and according to the ALL-REZ-MB 2016 protocol for patients with relapsed ALL (Table 2).

Table 1.

The number of patients in the acute phase of ALL before the start of chemotherapy. The first acute period is the acute phase of the disease in a patient with newly diagnosed ALL; the second acute period is the acute phase of the disease in a patient with relapsed ALL.

	White blood cells ($\times 10^9$/L)			
	Number of patients	<6.05	6.05 - 9.8	>9.8
First acute period	11	4	2	5
Second acute period	9	2	1	6

The control group consisted of 24 healthy controls of the same age group (mean age of 12±2.8; 17 boys and 7 girls) with no prior hematologic diseases.

Table 2.

The number of patients with an indication of the treatment stage and the protocol according to which they received treatment.

Treatment protocol	Number of patients	Treatment stage
ALL-MB 2015	5	After cycle F1, F2
ALL REZ MB 2016	5	After cycle F1,2 R1,2

MRI protocol

MRI scanning was carried out using a Philips Achieva dStream 3T scanner (Philips Healthcare, Best, the Netherlands) with a 32-channel FlexCoverage abdominal receiving coil. The MRI protocol included images obtained with the mDIXON Quant technique in the coronal plane, completely covering the pelvic bones and lumbar spine. mDIXON images were registered with the following parameters of a gradient multi-echo sequence: repetition time (TR) = 11 ms, 6 times to echo (TE) – minimal TE (TE1) = 1.2 ms, with an interval (ΔTE) = 0.8 ms; flip angle (FA) – 3º to minimize the influence of T1 weighting; the number of slices – 35, slice thickness– 4 mm, with a gap – -2 mm; field of view (FOV) = 360×360 mm^2, voxel size - 3.5×3.5×4.0 mm for registration and 2.5×2.5×2.0 mm for reconstruction; the frequency-encoding direction - A/P (to minimize respiratory motion artifacts); the SENSE acceleration factor – 2. The scan time was 1 min.

The fat fraction (FF) was calculated as the ratio between fat signal intensity (S_{fat}) and water signal intensity (S_{H2O}) using the following formula:

$$Fat\ fraction\ (FF) = \frac{S(fat)}{S(fat) + S(H2O)}$$

FF maps were generated automatically on the MRI console using the 7-peak fat model and were corrected for T2* effects.[10]

Regions of interest (ROI) measuring 150 mm^2 were placed in the bodies of the left and right iliac bones (Ilium L, Ilium R) as well as in the L4 and L5 vertebral bodies, taking care to avoid blood vessels, cortical bones and areas that could potentially contain artifacts (Fig.1).

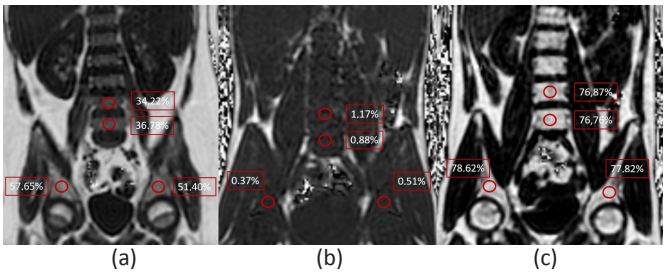

Fig. 1. *FF maps with regions of interest and mean values measured in these regions. (a) A healthy control. (b) A patient diagnosed with ALA, before the start of chemotherapy. (c) The same patient after the first chemotherapy cycle.*

Statistical analysis was performed using Jamovi 1.1.9.0.25. The Shapiro-Wilk W test was used in testing for normality. For data with normal distribution, inter-group comparisons were performed using Student's t-test. The Mann-Whitney U Test was used to compare the differences between the two independent groups (for nonparametric data).

The Wilcoxon criterion was used to compare the differences between the paired samples. A probability value of $P<0.05$ was considered statistically significant.

Results

The Mann-Whitney U test did not show any significant differences between the groups of patients with respect to age ($P=0.854$). The BMFF values during the first and the second acute periods were compared within the "before specific therapy" group of patients (n=20) Student's t-test did not reveal any significant differences between the values ($P=0.962$). In the "after chemotherapy" group (n=10), the data were compared in patients who had been treated in accordance with the ALL-MB 2015 protocol and those who had received treatment under the ALL-REZ-MB 2016 protocol. The Mann-Whitney U test did not show any significant differences between the values ($P=0.753$).

In the group of healthy controls, BMFF value was 51±11% in the bodies of the iliac bones and 32±10% in the lumbar vertebrae. All patients in the acute phase of the disease were included in one group. In these patients, BMFF was as low as 3.1±2.6% in all the bone structures. All patients who had undergone treatment were included in another group. In this group, the mean BMFF increased up to 77±7% in the iliac bones and up to 65±13% in the vertebrae. The BMFF values measured at several sites in the three groups of patients are summarized in Table 3.

Table 3.

Fat fraction in the three groups of study patients in the ROI

Group		Fat fraction (mean ±SD, %)			
		Ilium L	Ilium R	L4	L5
Healthy controls (n=24)		52±11	50±12	31±9	32±12
Patients with ALL	The acute phase of the disease (n=20)	3.2±2.7	3.7±3.3	2.6±1.9*	2.9±2.5
	P-value	*P*<0.01*	*P*<0.01*	*P*<0.01*	*P*<0.01*
	After chemotherapy (n=10)	78±9	78±7	64±13	66±13
	P-value	*P*<0.01^	*P*<0.01^	*P*<0.01^	*P*<0.01^

**- between healthy controls and acute phase of ALL*

^- between healthy controls and after chemotherapy; between acute phase of ALL and after chemotherapy

Under normal conditions, the mean fat content in the iliac bones was statistically significantly higher than in the L4 and L5 vertebrae ($P<0.01$). In the acute phase of the disease, BMFF values were statistically significantly lower than under normal conditions ($P<0.01$). Student's t-test for dependent samples revealed a statistically significant increase in the mean BMFF values in all the bone structures after chemotherapy ($P<0.01$). After specific therapy, BMFF was also significantly higher than under normal conditions ($P<0.01$) (Fig.2).

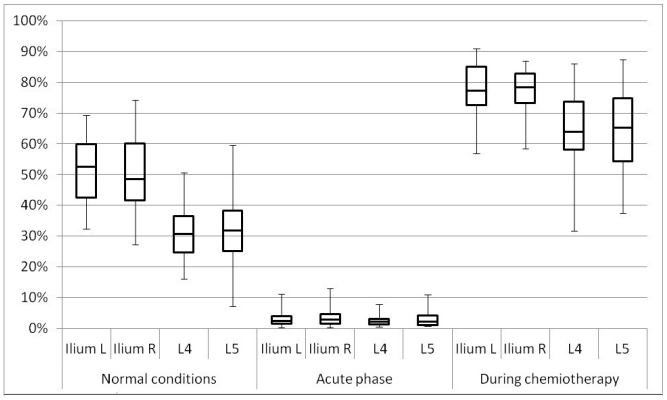

Fig. 2. *A chart showing the range of fat fraction values (%) in the three groups of patients in the four regions of interest.*

Discussion

Malignant leukemic processes in the BM affect the cellularity and composition of the BM, which inevitably leads to changes in signal intensity of bone structures on MRI.[11] In healthy adolescents, bones have a moderately hyperintense signal on T1-weighted (T1WI) and T2-weighted (T2WI) images, as compared to the surrounding muscles. In case of malignant transformation of the BM, signal intensity on T1WI and T2WI is similar to that of the surrounding muscles. After chemotherapy, the signal intensity of the BM on T1WI and T2WI becomes significantly higher than the signal intensity of the muscles, and is then comparable to that of the subcutaneous fat (Fig.3). Although visual assessment is more applicable in a clinical setting, it is not objective and cannot provide us with any quantitative data, so it may not be sufficient to evaluate BM involvement at the time of investigation.

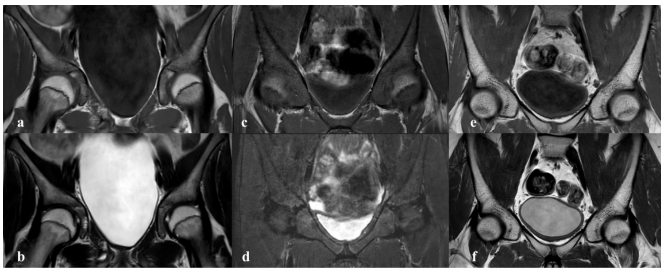

Fig. 3. *Pelvic bone MRI in the coronal plane. (a-b) A healthy control without any hematologic diseases, T1WI and T2WI; (c-d) A female patient in the acute phase of ALA before treatment, T1WI and T2WI/STIR; (e-f) A male patient undergoing chemotherapy, T1WI and T2WI.*

The signal intensity (SI) of BM is different on T1W images for the patients with hematological disorders and for the healthy control group.[12] Assessment of the BMFF, defined as a ratio of the fat content to the water content within a chosen area, can be used as a biomarker of changes in the BM.[7]

In this study, we used a multiple echo DIXON FFE sequence (mDIXON Quant) for the quantification of fat and water. There are several factors influencing the accuracy of tissue fat quantification, such as fast T2* signal decay, field inhomogeneities, the complexity of the spectral model of fat,

and T1 effects. The mDIXON-Quant sequence with multiple echoes helps us to avoid these confounding factors by using a low flip angle to minimize influence of T1 effects and by taking into account spectral complexity of the fat signal model and T2* correction.[13,14]

According to the international guidelines, the preferred site for BM aspiration in children is the iliac crest. For this reason, we used a large field of view (FOV), which covered both iliac bones.[15] Since in a number of articles on BM examination vertebrae were chosen as a region of interest, we also included the lumbar spine in the FOV.[16]

BM that changes drastically during a person's life is very susceptible to pathological processes occurring in the body. Starting from prenatal development and up to the age of 30, red BM is gradually being replaced by yellow BM.[16] In order to avoid unreliable results, the healthy controls and the patients included in the study were of the same age.

In the group of controls, the fat content in the vertebrae was, on average, 20% lower than in the iliac bones. This may be associated with a higher BM cellularity in the vertebrae and fatty bone marrow conversion in children and adolescents, which occurs in the vertebrae and ribs much later than in other bones.[17]

MRI for the measurement of BMFF is applied in a number of hematologic and bone disorders: to assess focal changes in bones,[18] in osteoporosis,[19] in Gaucher disease,[20] and to evaluate treatment response in patients with myelofibrosis.[21] The majority of studies include only adult patients; therefore, there is a lack of data on children. In the literature, there is only one pilot study, which included four patients with ALL before the initiation of a specific therapy.[22] Samet et al.[22] showed that BMFF in children with ALL was below 10%, which correlates with our results. Our study included more subjects and the BM assessment was performed not just before the initiation of treatment but also during chemotherapy.

This study demonstrated that the BM water-fat ratios in children with ALL vary depending on clinical status and significantly differ from normal values. A decrease in BMFF below 10% in patients in the acute phase of the disease may be associated with the total infiltration of the BM by abnormal cells, and the displacement of adipocytes.[23] Cytoreductive chemotherapy significantly reduces the number of both abnormal and normal cells in the BM, resulting in "exhaustion" of BM. Hematopoietic cells are replaced by adipocytes, and at that time, the BMFF increases to over 70%.[5]

In conclusion, quantitative MRI assessment of BMFF is a promising technique, allowing for the assessment of BM cellularity as a longitudinal study. This study provides important diagnostic information for various phases of ALL treatment, especially in suspected cases of resistant or recurrent disease.

Competing Interests

The authors declare that they have no competing interests.

***Corresponding author**: Nataliia A. Kriventsova. Dmitry Rogachev National Medical Research Center of Pediatric Hematology, Oncology and Immunology. Moscow, Russia. E-mail: nataliya.krivencova@fccho-moscow.ru*

References

1. Davis AS, Viera AJ, Mead MD. Leukemia: an overview for primary care. Am Fam Physician. 2014 May 1;89(9):731-8.
2. Kaprin AD, Starinsky VV, Petrova G V. Malignant neoplasms in Russia in 2017. Moscow; 2018. Available from: https://glavonco.ru/upload/pages/cancer-register/statistika_zabol_2017.pdf
3. Whitehead TP, Metayer C, Wiemels JL, Singer AW, Miller MD. Childhood Leukemia and Primary Prevention. Curr Probl Pediatr Adolesc Health Care. 2016 Oct;46(10):317-352. doi: 10.1016/j.cppeds.2016.08.004.
4. Veldhuis-Vlug AG, Rosen CJ. Clinical implications of bone marrow adiposity. J Intern Med. 2018 Feb;283(2):121-139. doi: 10.1111/joim.12718.
5. Wang H, Leng Y, Gong Y. Bone Marrow Fat and Hematopoiesis. Front Endocrinol (Lausanne). 2018 Nov 28;9:694. doi: 10.3389/fendo.2018.00694.
6. Karampinos DC, Ruschke S, Dieckmeyer M, Diefenbach M, Franz D, Gersing AS, Krug R, Baum T. Quantitative MRI and spectroscopy of bone marrow. J Magn Reson Imaging. 2018 Feb;47(2):332-353. doi: 10.1002/jmri.25769
7. Kriventsova NA, Kupriyanov DA, Menchshikov PE, and Terechshenko GV. MR-biomarker of bone marrow in children with acute lymphoblast leukemia. RJER. 2020;10(4):159-168. doi:10.21569/2222-7415-2020-10-4-159-168
8. Chan BY, Gill KG, Rebsamen SL, Nguyen JC. MR Imaging of Pediatric Bone Marrow. Radiographics. 2016 Oct;36(6):1911-1930. doi: 10.1148/rg.2016160056.
9. Foster K, Chapman S, Johnson K. MRI of the marrow in the paediatric skeleton. Clin Radiol. 2004 Aug;59(8):651-73. doi: 10.1016/j.crad.2004.02.001.
10. Lee SH, Yoo HJ, Yu SM, Hong SH, Choi JY, Chae HD. Fat Quantification in the Vertebral Body: Comparison of Modified Dixon Technique with Single-Voxel Magnetic Resonance Spectroscopy. Korean J Radiol. 2019 Jan;20(1):126-133. doi: 10.3348/kjr.2018.0174.
11. Chan BY, Gill KG, Rebsamen SL, Nguyen JC. MR Imaging of Pediatric Bone Marrow. Radiographics. 2016 Oct;36(6):1911-1930. doi: 10.1148/rg.2016160056.
12. Koyama H, Yoshihara H, Kotera M, Tamura T, Sugimura K. The quantitative diagnostic capability of routine MR imaging and diffusion-weighted imaging in osteoporosis patients. Clin Imaging. 2013 Sep-Oct;37(5):925-9. doi: 10.1016/j.clinimag.2013.05.001.
13. Ma J. Dixon techniques for water and fat imaging. J Magn Reson Imaging. 2008 Sep;28(3):543-58. doi: 10.1002/jmri.21492.
14. Karampinos DC, Melkus G, Baum T, Bauer JS, Rummeny EJ, Krug R. Bone marrow fat quantification in the presence of trabecular bone: initial comparison between water-fat imaging and single-voxel MRS. Magn Reson Med. 2014 Mar;71(3):1158-65. doi: 10.1002/mrm.24775.
15. Abla O, Friedman J, Doyle J. Performing bone marrow aspiration and biopsy in children: Recommended guidelines. Paediatr Child Health. 2008 Jul;13(6):499-501. doi: 10.1093/pch/13.6.499.
16. Baum T, Rohrmeier A, Syväri J, Diefenbach MN, Franz D, Dieckmeyer M, et al. Anatomical Variation of Age-Related Changes in Vertebral Bone Marrow Composition Using Chemical Shift Encoding-Based Water-Fat Magnetic Resonance Imaging. Front Endocrinol (Lausanne). 2018 Apr 4;9:141. doi: 10.3389/fendo.2018.00141.

17. Custer RP and Ahlfeldt FE. Studies on the structure and function of bone marrow: II. Variations in cellularity in various bones with advancing years of life and their relative response to stimuli. J Lab Clin Med. 1932;17(10):960-962.
18.Yoo HJ, Hong SH, Kim DH, Choi JY, Chae HD, Jeong BM, Ahn JM, Kang HS. Measurement of fat content in vertebral marrow using a modified dixon sequence to differentiate benign from malignant processes. J Magn Reson Imaging. 2017 May;45(5):1534-1544. doi: 10.1002/jmri.25496.
19. Chang R, Ma X, Jiang Y, Huang D, Chen X, Zhang M, Hao D. Percentage fat fraction in magnetic resonance imaging: upgrading the osteoporosis-detecting parameter. BMC Med Imaging. 2020 Mar 17;20(1):30. doi: 10.1186/s12880-020-00423-0.
20. Maas M, van Kuijk C, Stoker J, Hollak CE, Akkerman EM, Aerts JF, den Heeten GJ. Quantification of bone involvement in Gaucher disease: MR imaging bone marrow burden score as an alternative to Dixon quantitative chemical shift MR imaging--initial experience. Radiology. 2003 Nov;229(2):554-61. doi: 10.1148/radiol.2292020296.
21. Luker GD, Nguyen HM, Hoff BA, Galbán CJ, Hernando D, Chenevert TL, et al. A Pilot Study of Quantitative MRI Parametric Response Mapping of Bone Marrow Fat for Treatment Assessment in Myelofibrosis. Tomography. 2016 Mar;2(1):67-78. doi: 10.18383/j.tom.2016.00115.
22. Samet JD, Deng J, Schafernak K, Arva NC, Lin X, Peevey J, Fayad LM. Quantitative magnetic resonance imaging for determining bone marrow fat fraction at 1.5 T and 3.0 T: a technique to noninvasively assess cellularity and potential malignancy of the bone marrow. Pediatr Radiol. 2021 Jan;51(1):94-102. doi: 10.1007/s00247-020-04809-8.
23. Samimi A, Ghanavat M, Shahrabi S, Azizidoost S, Saki N. Role of bone marrow adipocytes in leukemia and chemotherapy challenges. Cell Mol Life Sci. 2019 Jul;76(13):2489-2497. doi: 10.1007/s00018-019-03031-6.

International Journal of Biomedicine 11(2) (2021) 146-150
http://dx.doi.org/10.21103/Article11(2)_OA4

ORIGINAL ARTICLE

Pediatrics

INTERNATIONAL JOURNAL OF BIOMEDICINE

Molecular Diagnosis of Human Metapneumovirus in Hospitalized Children with Acute Respiratory Tract Infections using RT-LAMP: A Population-Based Prospective Study

Ahmed Osman Gasim Attar[1]; Khalid Enan[2]; Sara Abdelghani[3]; Lienda Bashier Eltayeb[4*]

[1]*Department of Medical Microbiology, Faculty of Medical Laboratory Sciences, Al-Neelain University, Khartoum, Sudan*
[2]*Department of Virology, Central Laboratory of the Ministry of Higher Education and Scientific Research, Khartoum, Sudan*
[3]*Department of Parasitology, Faculty of Medical Laboratory Sciences, Al-Neelain University, Khartoum, Sudan*
[4]*Department of Medical Laboratory Science, College of Applied Medical Science, Prince Sattam bin Abdulaziz University, Al-Kharj, Saudi Arabia*

Abstract

Background: Human metapneumovirus (hMPV) is a major novel cause of acute respiratory infections ranging from wheezing to bronchiolitis and pneumonia in children worldwide. The aim of this study was to detect hMPV in hospitalized children with acute respiratory tract infections (ARTIs) by using reverse transcription-loop mediated isothermal amplification (RT-LAMP) assay.

Methods and Results: A total of 68 children with ARTIs who were clinically suspected of acquiring hMPV were included in the study in the period between January 2019 and February 2020. Posterior-pharyngeal (throat) swabs were obtained from each patient. hMPV RNA was revealed in 18(26.5%) cases. The age range was from <1 year to 10 years (mean age of 5.25±2.62). Sixteen (23.5%) of the participants were in the age group of <1 year, where the majority of hMPV-positive subjects (n=11) were found (16.2% of the total number of infected children) (*P*=0.0025). The majority of hMPV-negative subjects (n=15) were found in the age group of 5-10 years (22% of the total number of infected children) (*P*=0.0025). Cough, fever, and shortness of breath were common symptoms in hMPV-positive children: 15(83.3%), 13(72.2%), and 12(66.7%), respectively. There was a statistically significant correlation between common clinical symptoms and the age group of hMPV-positive children: symptoms were common in the age group of <1 year.

Conclusion: Our study represents the first report in Khartoum, Sudan, on the detection of hMPV using RT-LAMP. RT-LAMP is a valuable, quick diagnostic technique for hMPV detection. (**International Journal of Biomedicine. 2021;11(2):146-150.**)

Key Words: human metapneumovirus • acute respiratory tract infections • RT-LAMP

For citation: Attar AOG, Enan Kh, Abdelghani S, Eltayeb, LB. Molecular Diagnosis of Human Metapneumovirus in Hospitalized Children with Acute Respiratory Tract Infections using RT-LAMP: A Population-Based Prospective Study. International Journal of Biomedicine. 2021;11(2):146-150. doi:10.21103/Article11(2)_OA4

Introduction

Human metapneumovirus (hMPV) is a major novel cause of acute respiratory infections ranging from wheezing to bronchiolitis and pneumonia in children worldwide. hMPV is a member of the Paramyxoviridae family of viruses. The hMPV genome is a negative-sense, single-stranded RNA molecule, 13.3Kb long, encoding eight proteins.[1] Three surface proteins (F-fusion, G-attachment glycoprotein, and SH-small hydrophobic) are encoded within the hMPV genome.[2] The F- and G-nucleotide sequences have been largely used to study hMPV genetic variation.[3] The *hMPV G* gene shows higher

sequence and amino acid diversity.[4,5] The highly conserved F protein constitutes an antigenic determinant that mediates cross-lineage neutralization and protection.[1,6]

hMPV was first identified in the Netherlands by Hoogen et al.[7] hMPV has currently been detected in Europe, America, Australia, Asia, and Africa.[8-10] hMPV was first isolated from stored nasopharyngeal aspirates of infected children collected over a 20-year period. hMPV appears to have respiratory epithelium tropism.[11] The symptoms of both upper and lower respiratory tract disease have been associated with hMPV infections in infants, young children, the elderly, and immunocompromized patients. However, at the age of five years, virtually every individual has experienced at least one hMPV infection.[12,13] Different studies have noted that temperate regions are more prevalent for hMPV, which circulates mainly during the winter.[14-17] Clinical symptoms of hMPV infection resemble those caused by respiratory syncytial virus and range from mild upper respiratory tract infections to wheezing and severe lower respiratory tract illnesses that require hospitalization.[18-20] Although hMPV infections have been diagnosed in all age groups, the virus likely has its greatest effect on children.[21] Several studies have demonstrated that hMPV accounts for a major proportion of hospitalizations for lower respiratory tract infections in infants and young children. The most frequent diagnoses in hospitalized children are bronchiolitis and pneumonia, but occasionally hMPV may also cause severe illnesses that require treatment at intensive care units.[24,25]

The aim of this study was to detect hMPV in hospitalized children with acute respiratory tract infections (ARTIs) by using reverse transcription-loop mediated isothermal amplification (RT-LAMP) assay.

Materials and Methods

This descriptive cross-sectional study was carried out in Mohammed El Amin Hamid Hospital for Children (MEHHC) in Omdurman (Khartoum State, Sudan), in the period between January 2019 and February 2020.

The study was conducted in accordance with ethical principles of the WMA Declaration of Helsinki (1964, ed. 2013) and approved by the Ethics Committee of Faculty of Medical Laboratory Sciences, Al-Neelain University.. Informed consent was obtained from the children's parents or guardians.

A total of 68 children with ARTIs who were clinically suspected of acquiring hMPV were included in the study. Participants were enrolled in the study according to the following inclusion criteria: children between <1 to 10 years, of both sexes, hospitalized and suffering from ARTIs. All subjects with other respiratory diseases were excluded.

Collection of Posterior-Pharyngeal (throat) Swabs

Samples were obtained from each patient as described in the CDC's specimen collection guidelines.[26] Using a tongue depressor, the investigator swabbed both the posterior pharynx and the tonsillar areas with a sterile nylon swab (Regular Flocked swabs, Copan Diagnostics Inc., Murrieta, California, USA), in the clockwise direction, and the swabs were withdrawn (without touching the tongue). The swabs were immediately placed in the virus transport medium. The collected samples were transported in an ice bag to the laboratory and stored at -80°C until used.

RT-LAMP reaction

Throat samples in VTM were vortexed for 10 seconds, the obtained solution was used for RNA extraction, and the viral RNA was eluted in 30ul of elution buffer. Then RT-PCR was used to produce cDNA, which was finally eluted in 30µl of elution buffer and stored at -20°C.

For RT-LAMP, viral RNA was extracted from throat specimens with QIAamp Viral RNA Mini Kit (Qiagen, Germany) according to the manufacturer's instructions. Six primers, including two outer primers (F3 and B3), two inner primers (FIP [F1c +F2], BIP [B1c +B2]) and two loop primers (LF and LB), were used for hMPV N gene.[27] The sequences of each primer are shown in Table 1. RT-LAMP reaction was performed according to Wang et al.[.27]

Table 1.

Primer sets to detect hMPV N gene by RT-LAMP

F3	ACAGGAGTCTATTCATTGAGT
B3	ACCAAATCATAAACCTCTGTG
FIP(F1c+F2)	C G G C T C C A T A A G C T T G C A T A A A T A T - GGGAAAGCTTTAGGCTCA
BIP(B1c+B2)	A C A A T G C T A A G G T G G G G T G T C - CTTCAATTCAGCTTGCACAG
LF	CAAACAAACTTTCTGCTTTGCTTCC
LB	CATCTAACAACATAATGCTAGGGCA

Statistical analysis was performed using the IBM SPSS Statistics for Windows, Version 20.0. Armonk, NY: IBM Corp.). Baseline characteristics were summarized as frequencies and percentages for categorical variables. Group comparisons were performed using chi-square tests with Yates correction. A probability value of $P<0.05$ was considered statistically significant.

Results

The results of RT-LAMP for the diagnosis of hMPV in 68 throat swab samples collected from hospitalized children with ARTIs in Khartoum State are shown in Table 2. hMPV RNA was revealed in 18(26.5%) cases (Table 2).

Table 2.

The results of RT-LAMP for the diagnosis of hMPV

RT-LAMP	Positive	Negative	Total
hMPB RNA	18 (26.5)%	50 (73.5)%	68 (100%)

The age range was from <1 year to 10 years (mean age of 5.25±2.62). Sixteen (23.5%) of the participants were in the age group of <1 year old, where the majority of hMPV-positive subjects (n=11) were found (16.2% of the total

number of infected children) (P=0.0025). The majority of hMPV-negative subjects (n=15) were found in the age group of 5-10 years (22% of the total number of infected children) (P=0.0025) (Table 3).

Table 3.

Frequency of hMPV among Hospitalized Children with ARTIs regarding their gender, fever , cough and SOB.

Parameters	Positive n=18	Negative n=50	Total n=68	Statistics
Gender				
Male	9 (13.2%)	23 (33.8%)	32 (47%)	Chi-square: 0.085 *P*-value: 0.771
Female	9 (13.2%)	27 (39.7%)	36 (53%)	
Age group				
< 1	11 (16.2%)	5 (7.3%)	16 (23.5%)	Yates' chi-square: 16.449 Yates' *P*-value: 0.0025
1 - 2.5	2 (3%)	10 (14.7%)	12 (17.6%)	
2.5 - 3.5	1 (1.5%)	11 (16.2%)	12 (17.6%)	
3.5 -5	3 (4.4%)	9 (13.2%)	12 (17.6%)	
5 – 10	1 (1.5%)	15 (22%)	16 (23.5%)	

Cough, fever, and shortness of breath (SOB) were common symptoms in hMPV-positive children: 15(83.3%), 13(72.2%), and 12(66.7%), respectively (Table 4). There was a statistically significant correlation between common clinical symptoms and the age group of hMPV-positive children: symptoms were common in the age group of <1 year (Table 4).

Table 4.

Common clinical symptoms in the age groups of hMPV-positive subjects

Age group (yrs)	Fever (n=15)	Cough (n=13)	SOB (n=12)
<1 (n=16)	9 (60.0)	9 (69.2%)	9 (75.0%)
1 – <2.5 (n=12)	2 (13.3%)	1 (7.7%)	1 (8.3%)
2.5 – < 3.5 (n=12)	1 (6.7%)	1 (7.7%)	0
3.5 – <5 (n=12)	2 (13.3%)	1 (7.7%)	1 (8.3%)
5 – 10 (n=16)	1 (6.7%)	1 (7.7%)	1 (8.3%)
Statistics	Yates' chi-square: 11.137 Yates' *P*-value: 0.0251	Yates' chi-square: 13.969 Yates' *P*-value: 0.0074	Yates' chi-square: 16.549 Yates' *P*-value: 0.0024

Discussion

The latest characterization of a new family member, which belongs to Paramyxoviridae, subfamily Pneumovirus, has provided a chance to assess the severity of the disease triggered by this previously unrecognized human pathogen.[28] To the best of our knowledge, this is the first report on the detection of hMPV infection in Sudan using the RT-LAMP technique. In this study, hMPV has been shown to be responsible for a significant number of ARTIs in early infancy and childhood (26.5%).

Regardless of the techniques used, different studies have concluded that hMPV infection occurs frequently early in childhood.[19,29,30]

The frequency of hMPV infections found in this study showed similarity and some variations with those that have emerged from previously published studies in different countries.[31,32]

These variations in incidence among studies might reflect different epidemiological patterns of hMPV infection in different countries, which in turn might be related to environmental factors, geographical factors, differences in host genetic susceptibility, sampling techniques, detection methods, and/or different viral strains circulating in different geographical areas. The use of RT-LAMP was particularly advantageous for hMPV because the virus is fastidious and difficult to grow in most cell lines. The newly established visual RT-LAMP assay is simple, efficient, cost-effective and convenient to use as a diagnostic tool in clinical practice.[27]

In our study, fever, cough, and dyspnea were the most significantly frequent clinical features among hMPV-positive children, while Wang et al.[33] noted that fever, cough, and rhinorrhea were the main clinical manifestations; Papenburg et al.[34] reported fever, dyspnea, wheezing, abnormal breathing sounds, and added that sounds were the most frequent clinical features among hMPV-positive children. This might reflect the broad spectrum of clinical diseases with different manifestations in hMPV infections, but all authors agreed that fever and cough are the most common clinical manifestations.

The study showed that hMPV infections were higher among age group <1 year (16%) than among older children. This result was comparable to that of Zhang et al.[35] and Wei et al.[36] The higher incidence of hMPV infections among age group <1 year might signify the importance of this age group as a risk factor for infection.

Our findings are consistent with the results of Heikkinen et al.,[37] who revealed that the occurrence of hMPV infection in children <2 years of age was probably twice that in children 2–5 years of age and 10 times greater than in children >9 years of age. However, Papenburg reported comparable results that children <6 months are at risk of hMPV infection.[34] These findings may be attributed to the immature immune system among pediatrics.

The results of our study showed that among hMPV-positive children, the male-to-female ratio was 1:1. Zuo et al.[38] recorded results similar to the current study. Rein et al. found that of the 32 patients in whom hMPV was detected, 17(53.2%) were female and 15(46.8%) male.[39] Most published studies reported no significant gender predominance.

<u>Limitations of the Study and Prospective</u>

The current study consisted of a total of only 68 participants (representativeness not achieved), so further investigation in different parts of the country with a larger sample size and cohort study design is indicated to highlight

the severity of the problem. Moreover, it is necessary to include other variables, such as oxygen level and the existence of co-morbidities, as well as laboratory investigations, such as C-reactive protein level and complete blood count, which will help better management of the ARTIs caused by hMPV.

In conclusion, the study performed demonstrates that hMPV infection is significantly more severe in the age group of <1 year. Our study represents the first report in Khartoum, Sudan, on the detection of hMPV using RT-LAMP. RT-LAMP is a valuable, quick diagnostic technique for hMPV detection.

Acknowledgments

This study was supported by the Deanship of Scientific Research at Prince Sattam bin Abdulaziz University, Al-Kharj, Saudi Arabia. We would like to express our gratitude to the Faculty of Medical Laboratory Sciences at Al-Neelain University, Khartoum, Sudan.

Competing Interests

The authors declare that they have no competing interests.

References

1. van den Hoogen BG, Bestebroer TM, Osterhaus AD, Fouchier RA. Analysis of the genomic sequence of a human metapneumovirus. Virology. 2002 Mar 30;295(1):119-32. doi: 10.1006/viro.2001.1355.
2. Skiadopoulos MH, Biacchesi S, Buchholz UJ, Amaro-Carambot E, Surman SR, Collins PL, Murphy BR. Individual contributions of the human metapneumovirus F, G, and SH surface glycoproteins to the induction of neutralizing antibodies and protective immunity. Virology. 2006 Feb 20;345(2):492-501. doi: 10.1016/j.virol.2005.10.016.
3. Banerjee S, Sullender WM, Choudekar A, John C, Tyagi V, Fowler K, Lefkowitz EJ, Broor S. Detection and genetic diversity of human metapneumovirus in hospitalized children with acute respiratory infections in India. J Med Virol. 2011 Oct;83(10):1799-810. doi: 10.1002/jmv.22176.
4. van den Hoogen BG, Herfst S, Sprong L, Cane PA, Forleo-Neto E, de Swart RL, Osterhaus AD, Fouchier RA. Antigenic and genetic variability of human metapneumoviruses. Emerg Infect Dis. 2004 Apr;10(4):658-66. doi: 10.3201/eid1004.030393.
5. Ishiguro N, Ebihara T, Endo R, Ma X, Kikuta H, Ishiko H, Kobayashi K. High genetic diversity of the attachment (G) protein of human metapneumovirus. J Clin Microbiol. 2004 Aug;42(8):3406-14. doi: 10.1128/JCM.42.8.3406-3414.2004.
6. Schildgen V, van den Hoogen B, Fouchier R, Tripp RA, Alvarez R, Manoha C, et al. Human Metapneumovirus: lessons learned over the first decade. Clin Microbiol Rev. 2011 Oct;24(4):734-54. doi: 10.1128/CMR.00015-11.
7. van den Hoogen BG, de Jong JC, Groen J, Kuiken T, de Groot R, Fouchier RA, Osterhaus AD. A newly discovered human pneumovirus isolated from young children with respiratory tract disease. Nat Med. 2001 Jun;7(6):719-24. doi: 10.1038/89098.
8. Howe M. Australian find suggests worldwide reach for metapneumovirus. Lancet Infect Dis. 2002 Apr;2(4):202. doi: 10.1016/s1473-3099(02)00257-8.
9. Peret TC, Boivin G, Li Y, Couillard M, Humphrey C, Osterhaus AD, Erdman DD, Anderson LJ. Characterization of human metapneumoviruses isolated from patients in North America. J Infect Dis. 2002 Jun 1;185(11):1660-3. doi: 10.1086/340518.
10. Zhu RN, Qian Y, Deng J, Wang F, Hu AZ, Lu J, Cao L, Yuan Y, Cheng HZ. [Human metapneumovirus may associate with acute respiratory infections in hospitalized pediatric patients in Beijing, China]. Zhonghua Er Ke Za Zhi. 2003 Jun;41(6):441-4. [Article in Chinese].
11. Darniot M, Petrella T, Aho S, Pothier P, Manoha C. Immune response and alteration of pulmonary function after primary human metapneumovirus (hMPV) infection of BALB/c mice. Vaccine. 2005 Aug 22;23(36):4473-80. doi: 10.1016/j.vaccine.2005.04.027.
12. Tarig AGA, Salmo N, Bayati AH. Seroprevalence of Anti-Human Metapneumovirus Antibodies in Hospitalized Children in Sulaimani City/Iraq. Microbiology Research Journal International.2014;4(12):1325-34. https://doi.org/10.9734/BMRJ/2014/11658.
13. Brook I, Windle ML, Barton LL, Rauch D, Steele R. Human Metapneumovirus. Pediatr Infect Dis. 2002;10:15-18
14. Maggi F, Pifferi M, Vatteroni M, Fornai C, Tempestini E, Anzilotti S, Lanini L, Andreoli E, Ragazzo V, Pistello M, Specter S, Bendinelli M. Human metapneumovirus associated with respiratory tract infections in a 3-year study of nasal swabs from infants in Italy. J Clin Microbiol. 2003 Jul;41(7):2987-91. doi: 10.1128/jcm.41.7.2987-2991.2003.
15. Peiris JS, Tang WH, Chan KH, Khong PL, Guan Y, Lau YL, Chiu SS. Children with respiratory disease associated with metapneumovirus in Hong Kong. Emerg Infect Dis. 2003 Jun;9(6):628-33. doi: 10.3201/eid0906.030009.
16. van den Hoogen BG, van Doornum GJ, Fockens JC, Cornelissen JJ, Beyer WE, de Groot R, Osterhaus AD, Fouchier RA. Prevalence and clinical symptoms of human metapneumovirus infection in hospitalized patients. J Infect Dis. 2003 Nov 15;188(10):1571-7. doi: 10.1086/379200.
17. Williams JV, Wang CK, Yang CF, Tollefson SJ, House FS, Heck JM, Chu M, Brown JB, Lintao LD, Quinto JD, Chu D, Spaete RR, Edwards KM, Wright PF, Crowe JE Jr. The role of human metapneumovirus in upper respiratory tract infections in children: a 20-year experience. J Infect Dis. 2006 Feb 1;193(3):387-95. doi: 10.1086/499274.
18. Jartti T, van den Hoogen B, Garofalo RP, Osterhaus AD, Ruuskanen O. Metapneumovirus and acute wheezing in children. Lancet. 2002 Nov 2;360(9343):1393-4. doi: 10.1016/S0140-6736(02)11391-2.
19. Esper F, Boucher D, Weibel C, Martinello RA, Kahn JS. Human metapneumovirus infection in the United States: clinical manifestations associated with a newly emerging respiratory infection in children. Pediatrics. 2003 Jun;111(6 Pt 1):1407-10. doi: 10.1542/peds.111.6.1407.
20. van den Hoogen BG, Osterhaus DM, Fouchier RA. Clinical impact and diagnosis of human metapneumovirus infection. Pediatr Infect Dis J. 2004 Jan;23(1 Suppl):S25-32.

***Corresponding author**: Dr. Lienda Bashier Eltayeb. Department of Medical Laboratory Science, College of Applied Medical Science, Prince Sattam bin Abdulaziz University, Al-Kharj, Saudi Arabia. E-mail: lindarose009@hotmail.com*

doi: 10.1097/01.inf.0000108190.09824.e8.
21. Williams JV, Harris PA, Tollefson SJ, Halburnt-Rush LL, Pingsterhaus JM, Edwards KM, Wright PF, Crowe JE Jr. Human metapneumovirus and lower respiratory tract disease in otherwise healthy infants and children. N Engl J Med. 2004 Jan 29;350(5):443-50. doi: 10.1056/NEJMoa025472.
22. Boivin G, De Serres G, Côté S, Gilca R, Abed Y, Rochette L, Bergeron MG, Déry P. Human metapneumovirus infections in hospitalized children. Emerg Infect Dis. 2003 Jun;9(6):634-40. doi: 10.3201/eid0906.030017.
23. Mullins JA, Erdman DD, Weinberg GA, Edwards K, Hall CB, Walker FJ, Iwane M, Anderson LJ. Human metapneumovirus infection among children hospitalized with acute respiratory illness. Emerg Infect Dis. 2004 Apr;10(4):700-5. doi: 10.3201/eid1004.030555.
24. Ulloa-Gutierrez R, Skippen P, Synnes A, Seear M, Bastien N, Li Y, Forbes JC. Life-threatening human metapneumovirus pneumonia requiring extracorporeal membrane oxygenation in a preterm infant. Pediatrics. 2004 Oct;114(4):e517-9. doi: 10.1542/peds.2004-0345.
25. Schildgen O, Glatzel T, Geikowski T, Scheibner B, Matz B, Bindl L, Born M, Viazov S, Wilkesmann A, Knöpfle G, Roggendorf M, Simon A. Human metapneumovirus RNA in encephalitis patient. Emerg Infect Dis. 2005 Mar;11(3):467-70. doi: 10.3201/eid1103.040676.
26. Centers for Disease Control [CDC]. Specimen collection guidelines. https://www.cdc.gov/urdo/downloads/speccollectionguidelines.pdf
27. Wang X, Zhang Q, Zhang F, Ma F, Zheng W, Zhao Z, Bai Y, Zheng L. Visual detection of the human metapneumovirus using reverse transcription loop-mediated isothermal amplification with hydroxynaphthol blue dye. Virol J. 2012 Jul 27;9:138. doi: 10.1186/1743-422X-9-138.
28. Mackay IM, Jacob KC, Woolhouse D, Waller K, Syrmis MW, Whiley DM, Siebert DJ, Nissen M, Sloots TP. Molecular assays for detection of human metapneumovirus. J Clin Microbiol. 2003 Jan;41(1):100-5. doi: 10.1128/jcm.41.1.100-105.2003.
29. Døllner H, Risnes K, Radtke A, Nordbø SA. Outbreak of human metapneumovirus infection in Norwegian children. Pediatr Infect Dis J. 2004 May;23(5):436-40. doi: 10.1097/01.inf.0000126401.21779.74.
30. McAdam AJ, Hasenbein ME, Feldman HA, Cole SE, Offermann JT, Riley AM, Lieu TA. Human metapneumovirus in children tested at a tertiary-care hospital. J Infect Dis. 2004 Jul 1;190(1):20-6. doi: 10.1086/421120.
31. Yi L, Zou L, Peng J, Yu J, Song Y, Liang L, Guo Q, Kang M, Ke C, Song T, Lu J, Wu J. Epidemiology, evolution and transmission of human metapneumovirus in Guangzhou China, 2013-2017. Sci Rep. 2019 Oct 1;9(1):14022. doi: 10.1038/s41598-019-50340-8.
32. Yahia S, Kandeel AY, Hammad E, El-Gilany AH. Human metapneumovirus (hMPV) in acute respiratory infection: a clinic-based study in Egypt. Indian J Pediatr. 2012 Oct;79(10):1323-7. doi: 10.1007/s12098-011-0677-5.
33. Ji W, Wang Y, Chen Z, Shao X, Ji Z, Xu J. Human metapneumovirus in children with acute respiratory tract infections in Suzhou, China 2005-2006. Scand J Infect Dis. 2009;41(10):735-44. doi: 10.1080/00365540903148264.
34. Papenburg J, Hamelin MÈ, Ouhoummane N, Carbonneau J, Ouakki M, Raymond F, Robitaille L, Corbeil J, Caouette G, Frenette L, De Serres G, Boivin G. Comparison of risk factors for human metapneumovirus and respiratory syncytial virus disease severity in young children. J Infect Dis. 2012 Jul 15;206(2):178-89.
35. Zhang C, Du LN, Zhang ZY, Qin X, Yang X, Liu P, Chen X, Zhao Y, Liu EM, Zhao XD. Detection and genetic diversity of human metapneumovirus in hospitalized children with acute respiratory infections in Southwest China. J Clin Microbiol. 2012 Aug;50(8):2714-9. doi: 10.1128/JCM.00809-12.
36. Wei HY, Tsao KC, Huang CG, Huang YC, Lin TY. Clinical features of different genotypes/genogroups of human metapneumovirus in hospitalized children. J Microbiol Immunol Infect. 2013 Oct;46(5):352-7. doi: 10.1016/j.jmii.2012.07.007.
37. Heikkinen T, Osterback R, Peltola V, Jartti T, Vainionpää R. Human metapneumovirus infections in children. Emerg Infect Dis. 2008 Jan;14(1):101-6. doi: 10.3201/eid1401.070251.
38. Zou LR, Mo YL, Wu D, Fang L, Li H, Chen QX, Huang P, Deng XL, Ke CW. [Investigation of human metapneumovirus in children with acute respiratory tract infections in Guangzhou areas]. Zhonghua Yu Fang Yi Xue Za Zhi. 2009 Apr;43(4):314-8. [Article in Chinese].
39. Reina J, Ferrés F, Mena A, Figuerola J, Alcoceba E. Características clínicas y epidemiológicas de las infecciones respiratorias causadas por el metapneumovirus humano en pacientes pediátricos [Clinical and epidemiological characteristics of respiratory infections caused by human metapneumovirus in pediatric patients]. Enferm Infecc Microbiol Clin. 2008 Feb;26(2):72-6. doi: 10.1157/13115540. [Article in Spanish].

International Journal of Biomedicine 11(2) (2021) 151-155
http://dx.doi.org/10.21103/Article11(2)_OA5

ORIGINAL ARTICLE

Parasitic Diseases

INTERNATIONAL JOURNAL OF BIOMEDICINE

Hematological Alterations Induced by Visceral Leishmaniasis

Twasol Elsheikh Musa Altayeb[1]; Nasreldeen Ali Mohammed[1]; Sara Abdelghani[2]; Lienda Bashier Eltayeb[3*]

[1]Department of Hematology, Faculty of Medical Laboratory Sciences, Al-Neelain University, Khartoum, Sudan
[2]Department of Parasitology, Faculty of Medical Laboratory Sciences, Al-Neelain University, Khartoum, Sudan
[3]Department of Medical Laboratory Science, College of Applied Medical Science, Prince Sattam bin Abdulaziz University, Al-Kharj, Saudi Arabia

Abstract

The aim of this study was to assess visceral leishmaniasis (VL) among infected Sudanese patients in Al–Gedaref state.

***Methods and Results*:** A case-control study was conducted among patients with VL attending Al–Gaderif Teaching Hospital. A total of 80 subjects were included in the study: 40 patients with VL (the main group [MG]) and 40 apparently healthy individuals (the control group [CG]). The complete blood count (CBC) was determined using the Sysmex KX-21 N hematological analyzer. The platelet-poor plasma was used to determine prothrombin time (PT), thrombin time (TT), and activated partial thromboplastin time (aPTT).

The age group of 12-21 years was the most frequent (40%) among VL patients. Male patients were significantly more frequent (72.5%) than females ($P<0.05$). In MG, the Hb level was 8.71±1.73 g/dL, compared to 14.25±4.11 g/dL in CG, which reflected the severity of the disease. WBCs and neutrophils decreased significantly, compared to CG, but lymphocytes increased significantly. Thrombocytopenia was observed among pediatric patients, indicating bleeding tendency as one of the VL complications. The platelet and coagulation profile of patients was also altered. PT and aPTT were prolonged significantly, compared to CG.(**International Journal of Biomedicine. 2021;11(2):151-155.**)

Key Words: visceral leishmaniasis • anemia • leukopenia • thrombocytopenia • coagulopathy

For citation: Altayeb TEM, Mohammed NA, Abdelghani S, Eltayeb LB. Hematological Alterations Induced by Visceral Leishmaniasis. International Journal of Biomedicine. 2021;11(2):151-155. doi:10.21103/Article11(2)_OA5

Abbreviations

aPTT, activated partial thromboplastin time; **CBC**, complete blood count; **Hb**, hemoglobin; **Hct**, hematocrit; **MPS**, mononuclear phagocyte system; **MCV**; mean corpuscular volume; **MCH**, mean corpuscular hemoglobin; **MCHC**, mean corpuscular hemoglobin concentration; **PPP**, platelet-poor plasma; **PT**, prothrombin time; **RBC**, red blood cells; **TT**, thrombin time; **VL**, visceral leishmaniasis; **WBC**, white blood cells.

Introduction

Visceral leishmaniasis (VL), also known as Kala-Azar, is fatal if left untreated in over 95% of cases.[(1)] Al–Gedaref state in Sudan is a major endemic region for VL, with the prevalence rates varying greatly between villages, based on average rainfall and altitude. *Leishmania donovani* bodies have been identified as parasitic etiological agents causing VL, which are transmitted by the sandfly *Phlebotomus orientalis* in Eastern Sudan.[(2)] *P. orientalis* sandfly populations increase in the rainy season [(2,3)] and are concentrated in an environment with heavy abundances of Acacia seyal (locally

known as "Taleh") and Balanites aegyptica trees (locally known as "Lalob" or "Higleeg") that grow on vertisols (black cotton soil); these account for the high prevalence rate of VL in Gedaref state in Sudan.[3,4]

The L. donovani parasite persists in the spleen and bone marrow, and its expansion in these sites is associated with an increase in local hematopoietic changes.[5] Various hematologic manifestations are found in visceral forms. VL may present with splenomegaly, hepatomegaly, and fever. VL is endemic in more than 60 countries worldwide, including Southern Europe, North Africa, and the Middle East. VL is a systemic infection of the reticuloendothelial system caused by the protozoa Leishmania donovani of the genus Leishmania. The British medical doctor Ronald Ross published a paper in November 1903 commenting on the discovery of the ovoid bodies found by Leishman and Donovan in spleen pulp of patients with chronic pyrexia and splenomegaly. [6] He concluded that the ovoid bodies were not degenerated trypanosomes but a novel protozoan organism and that the clinical picture of the cases resembled that of kala-azar. [7] In a follow-up paper, Ross concluded that these ovoid bodies belonged to a new genus and proposed to name them Leishmania donovani.[8] Leishmania parasites are dimorphic organisms that live and replicate in the gut of sandflies as flagellated forms (promastigote) or as aflagellated forms (amastigotes) in mammalian cells. Amastigotes exist and proliferate in the MPS, especially the spleen, liver, and marrow; this leads to hyperplasia of the MPS with resultant disturbances in phagocytic-bearing organs, producing hematological manifestations.[2] Leishamnia spp. is endemic in tropical and sub- tropical regions, and human disease mainly occurs in parts of Africa, Asia, and the Middle East.[4,5] Poverty, war, conflicts, and migration have significantly aggravated leishmaniasis in East Africa.

Al–Gedaref state is an endemic area for VL, which affects individuals of different age groups, particularly children and young adults. Most of the patients presented to clinics with irregular bouts of fever, weight loss, enlargement of the spleen and liver, anemia, leukopenia, and thrombocytopenia. Thrombocytopenia is detected after a long duration of illness; splenic sequestration is a possible contributing factor. Liver dysfunction with jaundice, ascites, and deranged coagulation may occur in the late stages. Liver dysfunction may be caused by the protozoa itself or indirectly by an effect related to the immune response of the parasite.

The disease is more frequent among rural populations and domains. Around 95% of patients are under 5 years of age, the male-to-female ratio is 1.3:1.6. The appearance of the parasite in the human body stimulates the humeral immune system resulting in antibody production. The principal involved organs are the reticuloendothelial system; other organs such as kidneys, digestive system, and mucosa may be filled with macrophages. Bacterial infection is one of the major complications leading to death in VL patients.[9,10]

VL is characterized by a chronic course of hepatomegaly, which leads to anemia and pancytopenia. The parasite migrates to the internal organs, such as liver, spleen, and bone marrow, and if left untreated will almost always result in the death of the host. Anemia is the most common hematological manifestation of VL; the disease may be associated with leukopenia, thrombocytopenia, hemophagocytosis, and disseminated intravenous coagulation.[11-13] Normochromic normocytic anemia is a frequent and clinically significant feature of VL, and hemoglobin levels of 7–10 g/dl are commonly found. It is more severe in pediatric patients. The cause of anemia in these patients is multifactorial: sequestration and destruction of RBCs in the enlarged spleen; immune mechanisms and alterations in RBC membrane permeability have been implicated; hemolysis is the major cause of anemia; and plasma volume expansion associated with a massively enlarged spleen.

The aim of this study was to assess the VL among infected Sudanese patients in Al–Gedaref state.

Materials and Methods

A case-control study was conducted among patients with VL attending Al–Gaderif Teaching Hospital. Written informed consent was obtained from each research participant (or the participant's parent/guardian).

A total of 80 subjects were included in the study: 40 patients with VL (the main group [MG]) and 40 apparently healthy individuals (the control group [CG]). Subjects were enrolled according to the following inclusion criteria: VL patients (both sexes) under treatment. Excluded were patients newly diagnosed with VL and patients with associated diseases that may affect hemostatic profile, as well as patients taking medications affecting blood coagulation. The questionnaire was used to collect demographic and clinical data.

A total of 5ml venous blood was collected from each subject: 2.5ml in EDTA container, and 2.5ml in TSC container. PPP was used to determine PT, TT, and aPTT. The CBC was determined using the Sysmex KX-21 N hematological analyzer.

Statistical analysis was performed using the IBM SPSS Statistics for Windows, Version 22.0. Armonk, NY: IBM Corp.). Baseline characteristics were summarized as frequencies and percentages for categorical variables and as mean±standard deviation (SD) for continuous variables. Spearman's rank correlation coefficient was calculated to measure the strength and direction of the relationship between two variables. A probability value of $P<0.05$ was considered statistically significant.

Results

Table 1 presents the age distribution among VL patients and control subjects. The age group of 12-21 years was the most frequent (40%) among VL patients. Male patients were significantly more frequent (72.5%) than females ($P<0.05$); males often work as farmers, which makes them more vulnerable to sandfly bites. Tables 2 and 3 displayed all hematological and coagulation parameters: MG was significantly different than CG. Although all patients received treatment, Hb, RBC count, and RBC indices significantly decreased, compared to control subjects. In MG, the Hb level was 8.71±1.73g/dL, compared to 14.25±4.11g/dL in CG, which reflected the severity of

the disease. WBCs and neutrophils decreased significantly, compared to CG, but lymphocytes increased significantly. Thrombocytopenia was observed among pediatric patients, indicating bleeding tendency as one of the VL complications, as reported by many previous investigators. The platelet and coagulation profile of patients was also altered. PT and APTT were prolonged significantly, compared to CG.

Table 1.

The age distribution among VL patients and control subjects

Age group, years	MG (n=40)		CG (n=40)		*P*-value
	n	%	No	%	
≤11	8	20.0	1	2.5	>0.05
12-21	16	40.0	22	55.0	
22-31	8	20.0	10	25.0	
32-41	5	12.5	4	10.0	
>41	3	7.5	3	7.5	
Total	40	100.0	40	100.0	
Male	29	72.5	20	50	<0.05
Female	11	27.5	20	50	
Total	40	100.0	40	100.0	

Table 2.

Hematological parameters in VL patients and control subjects

Parameter	MG	CG	*P*-value
Neutrophils, %	51.49±12.93	60.16±16.19	0.010
Lymphocytes, %	40.40±12.32	30.66±14.78	0.002
MCHC, g/dL	31.61±2.44	34.05±1.00	0.000
MCH, pg	25.11±3.19	28.08±1.91	0.000
MCV, fL	79.78±8.68	80.19±11.32	0.856
Hct, %	28.04±6.21	41.13±7.34	0.000
Hb, g/dL	8.71±1.73	14.25±4.11	0.000
RBC, $\times10^{12}$/L	3.49±0.81	5.06±1.29	0.000
WBC, $\times10^{9}$/L	2.97±1.21	6.36±1.89	0.000

Table 3.

Blood platelets, PT, and aPTT in VL patients and control subjects

Parameter	MG	CG	*P*-value
PT, sec	16.42±4.06	14.22±0.98	0.001
aPTT, sec	47.63±10.72	27.03±2.15	0.000
Platelets, $\times10^{9}$/L	111.0±58.15	285.2±76.38	0.000

Tables 4 and 5 show a comparison of hematological and coagulation parameters across gender and age. There was no significant correlation between genders or age groups.

Table 4.

A comparison of hematological and coagulation parameters across gender in VL patients

Parameter	Male (n=29)	Female (n=11)	*P*-value
PT, sec	16.27±3.25	16.71±5.40	>0.05
aPTT, sec	46.52±9.73	49.71±12.49	>0.05
Neutrophils, %	53.13±13.43	48.42±11.80	>0.05
Lymphocytes, %	39.18±11.66	42.68±13.40	>0.05
Platelets, $\times10^{9}$/L	116.6±58.20	100.7±58.76	>0.05
MCHC, g/dL	31.65±2.73	31.53±1.89	>0.05
MCH, pg	25.18±3.57	24.97±2.46	>0.05
MCV, fL	80.50±9.53	78.45±7.00	>0.05
Hct, %	29.38±6.70	25.55±4.38	>0.05
Hb, g/dL	8.99±1.80	8.17±1.53	>0.05
RBC, $\times10^{12}$/L	3.60±0.90	3.29±0.59	>0.05
WBC, $\times10^{9}$/L	2.99±1.90	2.94±1.77	>0.05

Table 5.

Correlations between hematological/coagulation parameters and age

Parameter	R-value	P-value
PT	0.045	0.782
aPTT	0.078	0.634
Neutrophils	0.254	0.114
Lymphocytes	-0.313*	0.044
Platelets	0.061	0.710
MCHC	-0.225	0.162
MCH	0.114	0.483
MCV	0.229	0.155
HCT	-0.127	0.433
Hb	-0.235	0.144
RBC	-0.090	0.582
WBC	0.071	0.665

Discussion

Hematological disorders in VL determine the leading role of hematologists in the diagnosis of this disease. Hematologists must ensure a high standard of suspicion for VL and include it in the differential diagnosis of patients who expressed fever, hepatosplenomegaly, anemia, leukopenia, thrombocytopenia, pancytopenia, and DIC, especially in endemic areas.

The current study noted that VL affects individuals in different age groups, but the age group of 12-21 years occurs most frequently. A study, performed in Yemen, revealed that VL predominated among five-year-old patients

(mainly 1-3 years).[14] Our results were in conflict with a study, performed in Iraq,[9] which showed that both genders were equally infected, with mean age ranging between 7 months and 12 years. An Iranian study showed that 91.5% of VL cases were in the age group ≤5 years, 57.1% of which were females.[15] The discrepancy could be attributed to different factors, such as sample size, occupation of participants, the season when samples were collected, as well as the immune status of participants.

Gamal Hamid et al.[14] concluded that children under 10 years old are the main victims of VL, as in Sudan where the risk factors for death among pediatric VL were highest for those less than 2 years old. Among adult patients, the most affected age ranged between 21 and 30 years. The significant hematological changes observed among VL patients were similar to findings reported by many investigators.[14,16-18] A study in Yemen revealed that pancytopenia and hepatosplenomegaly are the most common clinical manifestations in Yemeni children. The reason for the higher frequency of pancytopenia is probably the longer duration of symptoms and splenomegaly before presentation to the hospital and increased peripheral destruction, rather than bone marrow failure.[14]

Laboratory findings of VL patients in the current study revealed a significant decrease in Hb, RBC, and RBC indices. Similar results have been reported by many authors.[14-16,19] Multiple factors could be the leading causes of anemia among patients with VL. Reduced plasma iron level in the presence of greatly increased iron stores suggests that the reticuloendothelial hyperplasia is accompanied by abnormal iron retention by macrophages, typical of anemia of chronic diseases.[16] This may limit the marrow response to hemolysis. Hypersplenism is another primary pathogenetic mechanism of anemia, although nutritional deficiencies of iron, folate and vitamin B12 may play a further contributory role.[16,19] Malaria infection could further complicate the situation and may co-exist in the same patients since Al–Gedaref state is characterized by heavy rains, which provide suitable habitat for both sandfly and mosquito vector activities.

The WBC count and percentage of neutrophils in VL patients significantly decreased while the percentage of lymphocytes significantly increased, compared to control. Many studies showed similar results and concluded that leukopenia and neutropenia were common among pediatric patients.[11,16,17] The main cause for their development has been attributed to hypersplenism. In addition, suppression of the immune system is expected in patients with VL, as previously reported,[11] since the parasite actively secretes proteases and other factors that affect immune cells and cytokines.(9) Furthermore, the humoral and cell-mediated immune response of the host depends on the severity of VL and parasite burden.[20]

Thrombocytopenia, along with anemia, is a common clinical finding in patients with VL. Thrombocytopenia is exhibited in 40% to 65% of patients.[5] Helmi et al. in Iraq[21] and Rahim et al.[22] in Pakistan found thrombocytopenia in 80%-90% of the patients. It is postulated that the thrombocytopenia observed in the peripheral blood may have been due to hypersplenism, and partly due to poor platelet formation.[23,24]

In our study, in VL patients PT and APTT were significantly prolonged, compared to healthy control subjects. These findings were confirmed by previous studies. [12,16,25] Accordingly, the bleeding tendency existed among patients with VL in the current study. This may be due to liver dysfunction, coagulopathy, and exhaustion of plasma proteins. Previous authors concluded that bleeding is one of the main causes of death in VL patients.[2,12,,13,19]

In conclusion, VL is common in Al–Gedaref state, and it is more frequent among children. The disease affects primary hemostasis, coagulation, and fibrinolysis, and these alterations are related to the severity of clinical symptoms. Anemia and thrombocytopenia are observed in the majority of patients, and splenic sequestration is possibly the main contributing factor. A significant increase in the levels of aPTT, PT, and TT is common for VL. Liver dysfunction may be caused directly by the protozoa themselves or indirectly by an effect related to the host's immune response to the parasite.

Competing Interests

The authors declare that they have no competing interests.

Acknowledgments

This publication was supported by the Deanship of Scientific Research at Prince Sattam Bin Abdulaziz University.

References

1. WHO. Leishmaniasis. Key facts. 2 March 2020. Available from: https://www.who.int/news-room/fact-sheets/detail/leishmaniasis#:~:text=Visceral%20leishmaniasis%20(VL)%2C%20also,East%20Africa%20and%20in%20India.
2. Oskam L, Pratlong F, Zijlstra EE, Kroon CC, Dedet IP, Kager PA, Schönian G, Ghalib HW, el-Hassan AM, Meredith SE. Biochemical and molecular characterization of Leishmania parasites isolated from an endemic focus in eastern Sudan. Trans R Soc Trop Med Hyg. 1998 Jan-Feb;92(1):120-2. doi: 10.1016/s0035-9203(98)90982-8.
3. Elnaiem DA, Hassan HK, Ward RD. Phlebotomine sandflies in a focus of visceral leishmaniasis in a border area of eastern Sudan. Ann Trop Med Parasitol. 1997 Apr;91(3):307-18. doi: 10.1080/00034989761157.
4. Ngure P, Kimutai A, Tonui W, Nganga Z. A Review of Leishmaniasis in Eastern Africa. Original Article. The Internet Journal of Parasitic Diseases. 2008;4(1).
5. Cotterell SE, Engwerda CR, Kaye PM. Leishmania donovani infection of bone marrow stromal macrophages selectively enhances myelopoiesis, by a mechanism involving GM-CSF and TNF-alpha. Blood. 2000 Mar 1;95(5):1642-51.
6. 5Ross R. Note on the bodies recently described by Leishman and Donovan. Br Med J. 1903;2:1261–2. doi: 10.1136/bmj.2.2237.1261.

***Corresponding author**: Dr. Lienda Bashier Eltayeb. Department of Medical Laboratory Science, College of Applied Medical Science, Prince Sattam bin Abdulaziz University, Al-Kharj, Saudi Arabia. E-mail: lindarose009@hotmail.com*

7. Steverding D. The history of leishmaniasis. Parasit Vectors. 2017 Feb 15;10(1):82. doi: 10.1186/s13071-017-2028-5.
8. Ross R. Further notes of Leishman's bodies. Br Med J. 1903;2:1401. doi: 10.1136/bmj.2.2239.1401.
9. Alborzi A, Pouladfar GR, Aelami MH. Visceral Leishmaniasis; Literature review and Iranian experience. Iranian Journal of Clinical Infectious Diseases 2007; 2(2): 99-108.
10. Varma N, Naseem S. Hematologic changes in visceral leishmaniasis/kala azar. Indian J Hematol Blood Transfus. 2010 Sep;26(3):78-82. doi: 10.1007/s12288-010-0027-1.
11. Bafghi AF, Shahcheraghi SH, Nematollahi S. Comparison of hematological aspects: Visceral leishmaniasis and healthy children. Trop Parasitol. 2015 Jul-Dec;5(2):133-5. doi: 10.4103/2229-5070.145597.
12. Middib MM, Al-Mouktar FA. Hematological Changes Including the Immune system in Patients with Visceral Leishmaniasis at Al-Muthanna Governorate. Journal of Babylon University (Pure and Applied Sciences). 2014;(4):22.
13. Costa CH, Werneck GL, Costa DL, Holanda TA, Aguiar GB, Carvalho AS, Cavalcanti JC, Santos LS. Is severe visceral leishmaniasis a systemic inflammatory response syndrome? A case control study. Rev Soc Bras Med Trop. 2010 Jul-Aug;43(4):386-92. doi: 10.1590/s0037-86822010000400010.
14. Hamid GA, Gobah GA. Clinical and hematological manifestations of visceral leishmaniasis in Yemeni children. Turk J Haematol. 2009 Mar 5;26(1):25-8.
15. Sarkari B, Naraki T, Ghatee MA, Abdolahi Khabisi S, Davami MH. Visceral Leishmaniasis in Southwestern Iran: A Retrospective Clinico-Hematological Analysis of 380 Consecutive Hospitalized Cases (1999-2014). PLoS One. 2016 Mar 4;11(3):e0150406. doi: 10.1371/journal.pone.0150406.
16. Pippard MJ, Moir D, Weatherall DJ, Lenicker HM. Mechanism of anaemia in resistant visceral leishmaniasis. Ann Trop Med Parasitol. 1986 Jun;80(3):317-23. doi: 10.1080/00034983.1986.11812022.
17. Jain K, Jain NK. Vaccines for visceral leishmaniasis: A review. J Immunol Methods. 2015 Jul;422:1-12. doi: 10.1016/j.jim.2015.03.017.
18. Pahwa R, Gupta SK, Singh T, Nigam S. Acute fulminant visceral leishmaniasis in children--a report of two cases. Indian J Pathol Microbiol. 2004 Jul;47(3):428-30.
19. Al-Muhammadi MO, Al-Shujiri GSH, Noor. MH Hematological changes in children suffering from Visceral Leishmaniasis (Kalaz-Aazar). Medical Journal of Babylon. 2014;1:4. doi: 1812-156X1-4.
20. Kafetzis DA. An overview of paediatric leishmaniasis. J Postgrad Med. 2003 Jan-Mar;49(1):31-8. doi: 10.4103/0022-3859.930.
21. Helmi FI, Al-Allawi NAS, Al-Attar AM. Hematological changes in kala azar: a study of 82 Iraqi patients. J Community Med 1993;69:85-90.
22. Rahim F, Rehman F, Ahmad S, Zada B. Visceral leishmaniasis in District Dir, NWFP. J Pak Med Assoc. 1998 Jun;48(6):161-2.
23. Dameshek W, Miller EB. The megakaryocytes in idiopathic thrombocytopenia purpura, a form of hypersplenism. Opera Omnia 1975;27-48.
24. Rani GF, Preham O, Ashwin H, Brown N, Hitchcock IS, Kaye PM. Dissecting pathways to thrombocytopenia in a mouse model of visceral leishmaniasis. Blood Adv. 2021 Mar 23;5(6):1627-1637. doi: 10.1182/bloodadvances.2020004082.
25. Gulati S, Paljor HP, Panadit S, et al. Kala-Azar without Splenomegaly. Annals of Tropical Medicine and Public Health. 2009;2(2):57-60.

International Journal of Biomedicine 11(2) (2021) 156-159
http://dx.doi.org/10.21103/Article11(2)_OA6

ORIGINAL ARTICLE

Obstetrics and Gynecology

INTERNATIONAL JOURNAL OF BIOMEDICINE

Programmed Labor in Gestational Diabetes Mellitus as a Reserve for Reducing the Frequency of Cesarean Section

Agamurad A. Orazmuradov[1], PhD, ScD; Marina B. Khamoshina[1], PhD, ScD; Anastasiya N. Akhmatova[1], PhD; Irina V. Bekbaeva[1*]; Gayane A. Arakelyan[1]; Zh. Z. Suleymanova[1]; Khalid Haddad[1]; Sergey I. Kyrtikov[1]; Alina A. Sazhina[1]; Aleksey A. Lukaev[2], PhD

[1]*Peoples' Friendship University of Russia (RUDN University), Moscow Russia*
[2]*Mytishchi City Clinical Hospital Mytishchi, Moscow Region, Russia*

Abstract

The aim of this study was to investigate the perinatal outcomes of delivery by various methods in patients with gestational diabetes mellitus (GDM).

Methods and Results: The study included 403 pregnant women (gestational age of 37.0–41.0 weeks) with GDM and 68 without disorders of carbohydrate metabolism, who gave birth from the second quarter of 2018 to the third quarter of 2020 in the maternity ward of the City Clinical Hospital No. 29 named after N.E. Bauman. All patients with GDM were divided into 2 groups. Group 1 included 187 patients receiving insulin therapy; Group 2 included 216 patients receiving a well-balanced diet. The main indicators of the health status of newborns in the early neonatal period were assessed taking into account the methods of delivery: programmed labor (PL), planned cesarean section (PCS), and spontaneous delivery.

The 1-minute Apgar score in newborns from mothers of Groups 1 and 2 was higher at the PL, compared with PCS. The 5-minute Apgar score in newborns from mothers of Group 2 was also statistically significantly higher at the PL, compared with planned CS. The incidence of hypoglycemia in newborns from mothers of all groups was minimal at the PL, including a statistically significant low rate in newborns from mothers of Group 1. Symptoms of neonatal CNS depression were significantly more common in newborns born by abdominal delivery from mothers with GDM.

Conclusion: PL in women with GDM reduces the incidence of the main complications of the early neonatal period: hypoglycemia and symptoms of neonatal CNS depression. PL may be considered more acceptable than abdominal delivery for women with GDM.**(International Journal of Biomedicine. 2021;11(2):156-159.)**

Key Words: gestational diabetes mellitus • programmed labor • cesarean section

For citation: Orazmuradov AA, Khamoshina MB, Akhmatova AN, Bekbaeva IV, Arakelyan GA, Suleymanova ZhZ, Haddad Kh, Kyrtikov SI, Sazhina AA, Lukaev AA. Programmed Labor in Gestational Diabetes Mellitus as a Reserve for Reducing the Frequency of Cesarean Section. International Journal of Biomedicine. 2021;11(2):156-159. doi:10.21103/Article11(2)_OA6

Abbreviations

CNS, central nervous system; **CS**, cesarean section: **ECS**, emergency cesarean section; **GDM**, gestational diabetes mellitus; **PL**, programmed labor; **PCS**, planned cesarean section; **RDS**, respiratory distress syndrome.

Introduction

Gestational diabetes mellitus (GDM) is associated with various maternal and neonatal complications. Women with GDM have a higher risk of cesarean delivery than women with normal glucose tolerance. Delivery in GDM, as a rule, is associated with a large number of interventions in the process of childbirth: preparation of the cervix, induction of labor, and instrumental delivery (both vaginal and cesarean sections). An increased rate of cesarean section in women with GDM has been mentioned in many studies.[1-5] The frequency of both planned and emergency abdominal delivery, according to the literature,

is influenced by the following factors as parity: obesity, scar on the uterus after the previous CS, fetal macrosomia.[5-8]

In primiparous women, the risk of CS increases 3.9-4.6 times; with a combination of obesity and GDM - at least 2.25 times; with a combination of a scar on the uterus and GDM - almost 5 times.[5,6,9-11] CS in GDM is considered as a method of preventing fetal injury. Modern measures for the prevention of fetal injury in GDM include planned abdominal delivery if the weight of the fetus exceeds 4500g, as well as induction of labor if the gestational age is more than 39 weeks and the weight of the fetus is more than the 95th percentile.[7]

According to Radzinsky et al.[12] and Savicheva et al.,[13] PL accounts for an increasing share in the structure of delivery methods. Among GDM patients, in whom the PL protocol was applied, fetal macrosomia was 1.4 times more frequent; diabetic fetopathy - 1.5 times; obesity - 1.3 times, compared with patients with spontaneous onset of labor. However, the overall frequency of abdominal delivery was lower in the group with PL.[6,12,13]

Thus, the literature data demonstrate the high significance of the PL method with a clear selection of indications as the optimal method of delivery of pregnant women with GDM in the absence of absolute indications for CS.

The aim of this study was to investigate the perinatal outcomes of delivery by various methods in patients with GDM.

Material and Methods

The study included 403 pregnant women (gestational age of 37.0–41.0 weeks) with GDM and 68 without disorders of carbohydrate metabolism, who gave birth from the second quarter of 2018 to the third quarter of 2020 in the maternity ward of the City Clinical Hospital No. 29 named after N.E. Bauman. This was a prospective case-control study.

All patients with GDM were divided into 2 groups. Group 1 included 187 patients receiving insulin therapy; Group 2 included 216 patients receiving a well-balanced diet. A third group, Group 3, consisted of 68 pregnant women without disorders of carbohydrate metabolism.

The study was conducted in accordance with the ethical principles of the WMA Declaration of Helsinki (1964, ed. 2013) and was approved by the Ethics Committee of the RUDN University. Written informed consent was obtained from all participants.

Inclusion criteria were full-term pregnancy, cephalic presentation, and singleton pregnancy. Exclusion criteria were multiple pregnancy, premature birth, and breech presentation of the fetus. The diagnosis of GDM was based on the clinical recommendations of the MH of RF.[14] The women were questioned with the aim of assessing 1) family history of disorders of carbohydrate metabolism and obesity; 2) chronic somatic and gynecological diseases; 3) reproductive history; and 4) complications of current pregnancy, the timing of GDM detection.

The condition of newborns was assessed in the first minutes of life, in the first day of life and in the early neonatal period. The assessment of the newborns' condition included: 1) measurement of anthropometric parameters (weight, height, head circumference, chest circumference); 2) the presence or absence of phenotypic signs of diabetic fetopathy, such as macrosomia, disproportionate physique, morpho-functional immaturity, moonlike face, cardiomegaly, splenomegaly, hepatomegaly, hypertrichosis, hyperbilirubinemia, hypoglycemia, neonatal CNS depression; 3) assessment of the Apgar score (at 1 minute and 5 minutes after birth); 4) the need for respiratory support and its duration, the duration of hospital stay, transfer to the second stage of nursing; 6) birth trauma; and 7) perinatal brain damage.

Macrosomia was defined as a birth weight greater than or equal to 4000 g. The blood glucose concentration in newborns was measured 1 or more times a day, depending on the condition of the newborn, using a Glucometer "Accu-Chek Active New"(Switzerland) and visual test strips "Accu-Chek." Hypoglycemia was defined as blood glucose concentration <2.6 mmol/L at any time after birth.

The level of total bilirubin in the blood serum of newborns was determined on a BF-TsN-01Bilirubinometer (Belarus) by the method of reagentless two-wave photometry. Hyperbilirubinemia was defined as serum concentration of total bilirubin >256 μmol/L.

Statistical analysis was performed using the Statistica 8.0 software package (StatSoft Inc, USA). Baseline characteristics were summarized as frequencies and percentages for categorical variables and as means and standard error of the mean (SEM) for continuous variables. Differences of continuous variables were tested by the Mann-Whitney U-test. Group comparisons with respect to categorical variables are performed using using the chi-square test or, alternatively, Fisher's exact test. A value of $P<0.05$ was considered statistically significant.

Results and Discussion

In Group 1, the methods of delivery were as follows: spontaneous delivery (n=68), PL(n=98), PCS(n=17), and the emergency CS (n=4) (Figure 1). In Group 2, the methods of delivery were as follows: spontaneous delivery (114), PL (n=83), and PCS (n=19) (Figure 2).

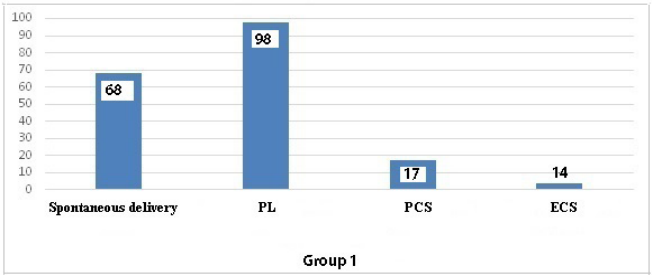

Fig.1. *The methods of delivery in Group 1*

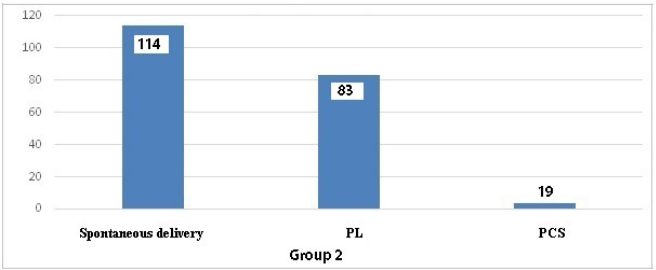

Fig.2. *The methods of delivery in Group 2*

The main indicators of the health status of newborns in the early neonatal period were assessed taking into account the methods of delivery (PL, CS, spontaneous delivery).

The 1-minute Apgar score in newborns from mothers of Groups 1 and 2 was higher at the PL, compared with PCS. The 5-minute Apgar score in newborns from mothers of Group 2 was also statistically significantly higher at the PL, compared with PCS (Table 1). The data obtained indicate a better adaptation of children from mothers with GDM in the first minutes after birth at the PL, compared with abdominal delivery.

Table 1.

The Apgar score in newborns depending on the methods of delivery

	Spontaneous delivery	PL	PCS	ECS
The 1-minute Apgar score				
Group 1	8.3±0.6 (n=68)	8.2±0.7* (n=98)	7.9±0.5* (n=17)	8.0±0.8 (n=4)
Group 2	8.5±0.5 (n=114)	8.3±0.7* (n=83)	7.8±0.6* (n=19)	-
Group 3	8.7±0.4	8.8±0.6	0	-
The 5-minute Apgar score				
Group 1	8.9±0.7	8.8±0.7	8.6±0.7	8.7±0.5
Group 2	9.1±0.6	9.0±1.2*	8.6±0.4*	-
Group 3	9.4±0.5	9.2±0.7	0	-

The incidence of hypoglycemia in newborns from mothers of all groups was minimal at the PL, including a statistically significant low rate in newborns from mothers of Group 1 (Table 2). Consequently, PL reduces the incidence of hypoglycemia in newborns, contributing to the formation of better adaptive mechanisms.

Table 2.

The incidence of hypoglycemia in newborns depending on the methods of delivery

	Spontaneous delivery	PL	PGS	ECS
The incidence of hypoglycemia (n,%)				
Group 1	14 (20.5%)	17 (17.3%)*	7 (41.1%)*	1 (25,0%)
Group 2	24 (21.0%)	16 (19.2%)	4 (21.0%)	-
Group 3	1(14.2%)	2 (3.3%)	-	-

Symptoms of neonatal CNS depression were significantly more common in newborns born by abdominal delivery from mothers with GDM (Table 3). Thus, in newborns from mothers of Group 1, this complication was found in 24.4% of the cases with PL and in 52.9% of the cases with PCS (P=0.02). In newborns from mothers of Group 2, this complication was found in 20.4% of the cases with PL and in 47.3% of the cases with PCS (P=0.01).

Table 3.

Symptoms of neonatal CNS depression in newborns depending on the methods of delivery

	Spontaneous delivery	PL	PCS	ECS
Symptoms of neonatal CNS depression (n,%)				
Group 1	20 (29.4%)	24 (24.4%)*	9 (52.9%)*	1 (25.0%)
Group 2	18 (15.7%)	17 (20.4%)*	9 (47.3%)*	-
Group 3	3(5.0%)	-	-	-

Thus, when the 2 methods of delivery (PL and PCS) were compared, the health level of newborns was higher in PL. The data obtained are consistent with the opinion of P. Rozenberg that programmed labor is the optimal method for women with GDM.[15] This technique reduces the level of neonatal morbidity and mortality in GDM. A similar opinion is shared by Biesty et al., who noted the comparability of perinatal outcomes in PL in women with GDM and without disorders of carbohydrate metabolism.[16]

In conclusion, PL in women with GDM reduces the incidence of the main complications of the early neonatal period: hypoglycemia and symptoms of neonatal CNS depression. Given the prevalence of favorable perinatal outcomes, PL may be considered more acceptable than abdominal delivery for women with GDM. By reducing the incidence of perinatal complications, PL may be a reserve for reducing the frequency of CS in GDM in the absence of absolute indications for abdominal delivery.

Competing Interest

The authors declare that they have no competing interests.

Sources of Funding

This paper has been supported by the RUDN University Strategic Academic Leadership Program,

References

1. Goldman M, Kitzmiller JL, Abrams B, Cowan RM, Laros RK Jr. Obstetric complications with GDM. Effects of maternal weight. Diabetes. 1991 Dec;40 Suppl 2:79-82. doi: 10.2337/diab.40.2.s79.

*__Corresponding author:__ *Irina V. Bekbaeva. Peoples' Friendship University of Russia (RUDN University, Moscow, Russia. E-mail: iridescentgirl@yandex.ru*

2. Naylor CD, Sermer M, Chen E, Sykora K. Cesarean delivery in relation to birth weight and gestational glucose tolerance: pathophysiology or practice style? Toronto Trihospital Gestational Diabetes Investigators. JAMA. 1996 Apr 17;275(15):1165-70. PMID: 8609683.
3. Gorgal R, Gonçalves E, Barros M, Namora G, Magalhães A, Rodrigues T, Montenegro N. Gestational diabetes mellitus: a risk factor for non-elective cesarean section. J Obstet Gynaecol Res. 2012 Jan;38(1):154-9. doi: 10.1111/j.1447-0756.2011.01659.x.
4. Boriboonhirunsarn D, Waiyanikorn R. Emergency cesarean section rate between women with gestational diabetes and normal pregnant women. Taiwan J Obstet Gynecol. 2016 Feb;55(1):64-7. doi: 10.1016/j.tjog.2015.08.024.
5. Zeki R, Oats JJN, Wang AY, Li Z, Homer CSE, Sullivan EA. Cesarean section and diabetes during pregnancy: An NSW population study using the Robson classification. J Obstet Gynaecol Res. 2018 May;44(5):890-898. doi: 10.1111/jog.13605.
6. Radzinsky VE, Botasheva TL, Papysheva OV. Obesity. Diabetes. Pregnancy. Versions and contraversions. Clinical practices. Perspectives. M: GEOTAR-Media, 2020.
7. Zeki R, Wang AY, Lui K, Li Z, Oats JJN, Homer CSE, Sullivan EA. Neonatal outcomes of live-born term singletons in vertex presentation born to mothers with diabetes during pregnancy by mode of birth: a New South Wales population-based retrospective cohort study. BMJ Paediatr Open. 2018 Jan 30;2(1):e000224. doi: 10.1136/bmjpo-2017-000224.
8. Zhou X, Chen R, Zhong C, Wu J, Li X, Li Q, et al, Maternal dietary pattern characterised by high protein and low carbohydrate intake in pregnancy is associated with a higher risk of gestational diabetes mellitus in Chinese women: a prospective cohort study. Br J Nutr. 2018 Nov;120(9):1045-1055. doi: 10.1017/S0007114518002453.
9. Orazmuradov AA, Papysheva OV, Soyunov MA, Bekbaeva IV, Arakelyan GA, Haddad Kh, Lopatin AM, Kyrtikov SI, Zokirova NM, Mukovnikova EV. Peculiar Properties of Pregnancy and Childbirth in Women with Gestational Diabetes Mellitus Depending on Body Weight. Systematic Reviews in Pharmacy. 2020;11(11):1338-1340.
10. Orazmuradov AA, Savenkova IV, Arakelyan GA, Loginova EV, Lukanovskaya OB, Kotaysh GA. Modern Notions of Health of Newborns from Mothers with Gestational Diabetes Mellitus. Systematic Reviews in Pharmacy. 2020;11(3):526-531.
11. Orazmuradov AA, Savenkova IV, Arakelyan GA, Damirova SF, Papysheva OV, Lukanovskaya OB. Peculiar Properties of Metabolism Women with Gestational Diabetes Mellitus. Systematic Reviews in Pharmacy. 2020;11(2):237-241.
12. Radzinsky VE., Papysheva OV, Esipova LN, Startseva NM, Kotaysh GA, Lukanovskaya OB. The effectiveness of programmed labor in gestational diabetes mellitus in reducing the frequency of caesarean section. Akusherstvo i Ginekologiia: Novosti, Mneniia, Obuchenie. 2019;(3(25)):25–31. doi: 10.24411/2303-9698-2019-13004.
13. Savicheva AM, Papysheva OV, Startseva NM, Ordiyants IM. Programmed labor and metabolic homeostasis in gestational diabetes mellitus. Akusherstvo i Ginekologiia: Novosti, Mneniia, Obuchenie. 2018;6(3, Suppl):46–50. doi: 10.24411/2303-9698-2018-13907.
14. Gestational diabetes mellitus. Diagnostics, treatment, obstetric tactics, postpartum follow-up. Clinical guidelines. Russian Association of Endocrinologists. Russian Society of Obstetricians and Gynecologists. Moscow, 2020.
15. Rozenberg P. [In case of fetal macrosomia, the best strategy is the induction of labor at 38 weeks of gestation]. J Gynecol Obstet Biol Reprod (Paris). 2016 Nov;45(9):1037-1044. doi: 10.1016/j.jgyn.2016.09.001. [Article in French].
16. Biesty LM, Egan AM, Dunne F, Dempsey E, Meskell P, Smith V, Ni Bhuinneain GM, Devane D. Planned birth at or near term for improving health outcomes for pregnant women with gestational diabetes and their infants. Cochrane Database Syst Rev. 2018 Jan 5;1(1):CD012910. doi: 10.1002/14651858.CD012910.

International Journal of Biomedicine 11(2) (2021) 160-163
http://dx.doi.org/10.21103/Article11(2)_OA7

ORIGINAL ARTICLE

General Surgery

INTERNATIONAL JOURNAL OF BIOMEDICINE

The Use of the Hemostatic Agent Zhelplastan in Combination with a Granulated Sorbent in the Treatment of Patients with Mallory-Weiss Syndrome

Evgeniy F. Cherednikov[1*], PhD, ScD; Igor S. Yuzefovich[1], PhD; Yuri V. Maleev[2], PhD, ScD; Sergey V. Barannikov[1], PhD; Tatyana E. Litovkina[3], PhD; Galina V. Polubkova[1], PhD; Evgeniy S. Ovsyannikov[1], PhD, ScD

[1]Voronezh State Medical University named after N. N. Burdenko
[2]Voronezh Basic Medical College
[3]Voronezh City Clinical Emergency Hospital №1
Voronezh, the Russian Federation

Abstract

***Background*:** Mallory-Weiss syndrome (MWS) is one of the common causes of acute upper gastrointestinal bleeding. The aim of our research was to develop a method for the treatment of MWS, which would improve the efficiency of local hemostasis, reduce the risk of re-bleeding and shorten the treatment time.

***Methods and Results*:** The study involved 102 patients with MWS. All patients were divided by random sampling into two groups: the main group (MG) and control group (CG). Patients of both groups were comparable in age, gender, concomitant diseases, type of bleeding, size of bleeding defect, and duration of observations.

The MG included 52 patients, who were given the developed method of MWS treatment. Patients with ongoing bleeding were treated with a combined method of endoscopic hemostasis: active bleeding was initially stopped by infiltration or coagulation (argon-plasma coagulation was preferred), and then to increase the reliability of hemostasis and prevent the resumption of bleeding, powdered Zhelplastan 0.2 g was applied to the rupture area with an insufflator, followed by Sephadex G-25 0.3 g (Patent RF №2633925). In patients with signs of unstable hemostasis, the developed method of cytoprotective action on a clot or thrombosed vessel was used by applying a local hemostatic, Zhelplastan 0.2 g, to the defect area in combination with a granular sorbent, Sephadex G-25 0.3 g, during therapeutic endoscopy to prevent the resumption of bleeding. In patients with stable stopped bleeding, a hemostatic powdered Zhelplastan was applied to the defect area using an endoscope in combination with Sephadex G-25, according to the developed method.

In the CG (n=50), well-known methods of arresting endoscopic bleeding (pricking with aminocaproic acid, vasoconstrictors, argon-plasma coagulation, etc.) were used without local hemostatics and granular sorbents.

Summing up the results of patients with Mallory-Weiss syndrome in the compared groups, in the MG final hemostasis was performed in 51(98.1%) patients. In the MG, bleeding resumed in 1(1.9%) patient. There were no emergency operations or deaths. In the CG, the bleeding was finally stopped in 43(86%) patients, and it resumed in 7(14%) patients. Emergency surgery was required for 1(2%) patient. In the CG, the mortality rate was 4%.

Conclusion: In MWS, the use of the developed method of endoscopic treatment, including pneumoinsufflation of a powdered hemostatic agent in combination with a granular sorbent, against the background of conservative therapy, improved the results of treatment, increased the reliability of local hemostasis, reduced the number of recurrent bleedings, and excluded emergency operations.(**International Journal of Biomedicine. 2021;11(2):160-163.**)

Key Words: Mallory-Weiss syndrome • endoscopic treatment • pneumoinsufflation • Zhelplastan • Sephadex G-25

For citation: Cherednikov EF, Yuzefovich IS, Maleev YuV, Barannikov SV, Litovkina TE, Polubkova GV, Ovsyannikov ES.The Use of the Hemostatic Agent Zhelplastan in Combination with a Granulated Sorbent in the Treatment of Patients with Mallory-Weiss Syndrome.International Journal of Biomedicine. 2021;11(2):160-163. doi:10.21103/Article11(2)_OA7

Abbreviations: **APC**, argon-plasma coagulation; **GEJ**, gastroesophageal junction; **MWS**, Mallory-Weiss syndrome.

Introduction

The problem of treating patients with gastroduodenal bleeding remains one of the most acute in emergency surgery. The number of patients with MWS does not decrease and even tends to increase. The leading role in the treatment of patients with MWS belongs to therapeutic endoscopy.[1-8]

The number of relapses of bleeding in MWS reaches 42%, and postoperative mortality is 10%-17%. At the same time, MWS patients are of working age, which indicates the high social and economic significance of this disease. These circumstances demonstrate the need to develop new highly effective treatments for MWS patients.[9-12] The use of local hemostatic agents in combination with a granular sorbent seems to be promising.[13-19]

The aim of our research was to develop a method for the treatment of MWS, which would improve the efficiency of local hemostasis, reduce the risk of re-bleeding and shorten the treatment time.

Materials and Methods

A clinical study was conducted in the Voronezh City Specialized Center for the treatment of patients with gastrointestinal bleeding. The study involved 102 patients (82[80.4%] men and 20[19.6%] women) with MWS. The peak incidence in men was at the age of 32-52 years. In women, the peak incidence was at 33-53 years and at 60-75 years.

Upon admission, all patients underwent emergency esophagogastroduodenoscopy. Bleeding defects in MWS were distributed according to their localization as follows: GEJ - 88(86.3%), stomach - 3(2.9%), esophagus - 11(10.8%). Defects in the GEJ were located on the right wall in 39(38.2%) patients, on the posterior wall - in 35(34.3%) patients, on the anterior wall - in 16(15.7%), and on the left wall - in 12(11.8%).

The length of the defects varied in the range of 0.4-2.7 cm. We classified the defects into 3 categories, according to size: small (< 1 cm), medium (1.0-2.5 cm), and large (>2.5 cm). Small defects were found in 77(75.5%) patients, medium - in 23(22.5%), and large defects were rarely observed - in only 2(2%) patients.

Regarding depth, defects were within the mucous layer (Stage I) in 40(39.2%) patients, mucous-submucosal layer (Stage II) - in 57(55.9%), and defects with damage to the muscle base (Stage III) - in only 5(4.9%) patients.

Defects were single in 72/70.6% of cases. Multiple defects were less common - in 30/29.4% of patients. In patients with a sliding hiatal hernia, multiple ruptures were more common. The number of breaks and their length did not affect the volume of blood loss.

According to the endoscopic picture, patients with MWS were divided as follows: ongoing bleeding (10/9.8%); a thrombosed vessel or clot (signs of unstable hemostasis) (57/55.9%); visible hematin spots (signs of stopped bleeding) (35/34.3%).

The severity of blood loss was evaluated according to the classification of A.I. Gorbashko (1982)[20]: mild degree was observed in 54(52.9%) patients, moderate degree - in 34(33.4%) and severe degree - in 14(13.7%) patients.

All patients were divided by random sampling into two groups: the main group (MG) and control group (CG).

The MG included 52 patients, who were given the developed method of MWS treatment. Patients with ongoing bleeding (6 people) were treated with a combined method of endoscopic hemostasis: active bleeding was initially stopped by infiltration or coagulation (APG was preferred), and then to increase the reliability of hemostasis and prevent the resumption of bleeding, powdered Zhelplastan 0.2 g was applied to the rupture area with an insufflator, followed by Sephadex G-25 0.3g (Patent RF №2633925).

In patients with signs of unstable hemostasis (n=28), the developed method of cytoprotective action on a clot or thrombosed vessel was used by applying a local hemostatic, Zhelplastan 0.2g, to the defect area in combination with a granular sorbent, Sephadex G-25 0.3 g, during therapeutic endoscopy to prevent the resumption of bleeding. At the same time, patients with localized ruptures along the right wall of the GEJ were identified and assigned to the group with a high risk of recurrent bleeding. These patients first underwent APC of the thrombosed vessel, and then also pneumoinsufflation of Zhelplastan and Sephadex G-25 to prevent recurrence of bleeding.

In patients with stable stopped bleeding (n=18), a hemostatic powdered Zhelplastan was applied to the defect area using an endoscope in combination with Sephadex G-25, according to the developed method. Repeated therapeutic endoscopy in the MG patients was performed after 4-5 days.

Patients of both groups were comparable in etiology of bleeding, age, gender, concomitant diseases, type of bleeding, size of bleeding defect, and duration of observations (Table 1),

Table 1.

Clinical characteristics of the study groups

Variable	MG (n=52)	CG (n=50)	*P*	Total (n=102)
Age	43.0 (32.0;57.0)	42.5 (33.0;53.0)	>0.05	43.0(32.5;56.0)
Men	43 (82.7%)	39 (78.0%)	>0.05	82 (80.4%)
Women	9 (17.3%)	11 (22.0%)	>0.05	20 (19.6%)
Type of bleeding				
Ongoing bleeding	6 (11.5%)	4 (8.0%)	>0.05	10 (9.8%)
Unstable hemostasis (clot or trombosed vessel).	28 (53.9%)	29 (58.0%)	>0.05	57 (55.9%)
Stable stopped bleeding (hematin on the defect base)	18 (34.6%)	17 (34.0%)	>0.05	35 (34.3%)
Depth of defects				
Stage I	19 (36.5%)	21 (42.0%)	>0.05	40 (39.2%)
Stage II	30 (57.7%)	27 (54.0%)	>0.05	57 (55.9%)
Stage III	3 (5.8%)	2 (4.0%)	>0.05	5 (4.9%)
The severity of blood loss (A. I. Gorbashko, 1982)				
Mild	25 (48.1%)	29 (58.0%)	>0.05	54 (52.9%)
Moderate	19 (36.5%)	15 (30.0%)	>0.05	34 (33.4%)
Severe	8 (15.4%)	6 (12.0%)	>0.05	14 (13.7%)

In the CG (n=50), well-known methods of arresting endoscopic bleeding (pricking with aminocaproic acid, vasoconstrictors, coagulation, APC, etc.) were used without local hemostatics and granular sorbents.

The complex therapy of patients of both groups included antacids, proton pump inhibitors, infusion-transfusion, general hemostatic and symptomatic therapy.

The main criteria in assessing the results of treatment were both clinical and endoscopic indicators: the timing of final hemostasis, the frequency of rebleeding, dynamic monitoring of the size of bleeding defects, the quality of healing of defects, the presence of urgent surgical interventions, the mortality rate, and the length of hospital stay.

Statistical analysis was performed using Microsoft Excel software package. For descriptive analysis, results are presented as mean±standard deviation (SD), median (Me), interquartile range (IQR), minimum and maximum values. For data with normal distribution, inter-group comparisons were performed using Student's t-test. Wilcoxon rank sum test was used to test for difference in medians. Group comparisons with respect to categorical variables were performed using Fisher's exact test. A probability value of $P<0.05$ was considered statistically significant.

Results

Of the total number of MWS patients, active bleeding was observed in 10 of them. In patients of the MG with ongoing bleeding (n=6), the effectiveness of primary endoscopic hemostasis was 100%. After the immediate bleeding was stopped, all patients in the MG were prevented from re-bleeding by the developed method. It should be noted that none of the patients resumed bleeding, and their primary endoscopic hemostasis was reliable and final. In MG, there were no fatal outcomes or operations in patients with ongoing bleeding.

In the CG of patients with ongoing bleeding (n=4), primary endoscopic hemostasis was also effective in all patients, but recurrent bleeding was observed in 2 patients: one patient with bleeding from a rupture of the GEJ along the right wall underwent emergency surgery-stitching of the bleeding defect. The patient was discharged with improvement. In another patient, recurrent bleeding was stopped endoscopically. There were no fatal outcomes in patients with ongoing bleeding in the CG.

Signs of unstable hemostasis (clot or thrombosed vessel) were detected in 57 patients. In the MG, 28 patients underwent preventive endoscopic treatment for recurrent bleeding using the developed technique. Resumption of bleeding was observed in 1 patient with a deep rupture (Stage III) located on the right wall of the GEJ. Repeated endoscopic hemostasis in this patient was performed by a developed combined method: first, APC of the thrombosed vessel, and then application of Zhelplastan and sorbent. There were no emergency operations or deaths in this group.

When monitoring 29 patients of the CG with signs of unstable hemostasis, a recurrence of bleeding was observed in 5 patients, which was stopped by traditional methods of endoscopic hemostasis. No surgical treatment was required. In the CG, 2 patients died: 1. Patient K., 51 years old, suffering from chronic alcoholism; death occurred as a result of acute blood loss on the background of alcoholic illness. 2. Patient T., 85 years old; the fatal outcome was associated with the progression of the underlying disease against the background of anemia.

In the patients with stable stopped bleeding (MG and CG), a recurrence of bleeding was not detected; there were no deaths or operations in both groups.

Summing up the results of patients with Mallory-Weiss syndrome in the compared groups, in the MG final hemostasis was performed in 51(98.1%) patients. In the MG, bleeding resumed in 1(1.9%) patient. There were no emergency operations or deaths. In the CG, the bleeding was finally stopped in 43(86%) patients, and it resumed in 7(14%) patients. Emergency surgery was required for 1(2%) patient. In the CG, the mortality rate was 4%.

Analysis of the causes of recurrent bleeding in patients with MWS showed that the depth of the bleeding defect and its localization are important for endoscopic hemostasis. In all patients, relapses of bleeding occurred with deep ruptures penetrating through the entire muco-submucosal base and having an esophageal-gastric localization with a predominant location on the right wall, where large vessels pass. This arrangement of bleeding defects presents certain technical difficulties during therapeutic endoscopy, which affects the quality of hemostasis.

During clinical studies, it was noted that in all patients of the MG, after pneumoinsufflation of powdered Zhelplastan and Sephadex G-25, a protective, insoluble, hydrogel layer with hemostatic and cytoprotective properties was formed on the surface of bleeding defects. This hydrogel hemostatic composition, due to its adhesive properties, lay tightly on the bleeding defect and protected it from the effects of aggressive gastric juice, while creating conditions for the active course of reparative processes.

During repeated examinations during esophago-gastroduodenoscopy, we found that the hydrogel composition was retained on the surface of the defect for up to 4-5 days. At the same time, the reparative process in the MG with such local treatment was faster and better than in the CG. Thus, the healing time of defects in the MG was 4.7±0.25 days. In the CG, the healing time of defects was 9.7±0.55 days (Table 2).

Table 2.

Results of treatment of patients with MWS in the study groups

Variable	MG (n=52)	CG (n=50)	*P*-value
Final hemostasis	51 (98.1%)	43 (86.0%)	0.0296
Recurrent bleedings	1 (1.9%)	7 (14.0%)	0.0296
Emergency surgery	–	1 (2.0%)	
Mortality rate	–	2 (4.0%)	
Healing time of defects, days	4.7±0.25	9.7±0.55	0.0000
Epithelialization of defects	49 (94.2%)	32 (64.0%)	0.0002
Length of hospital stay, days	5.0±0.5	8.0±1.2	0.0000

It is important to note that in the case of ruptures of the mucosa and submucosal layer), the healing of defects in the treatment with Zhelplastan and Sephadex G-25 occurred by

epithelialization without scar formation. The use of Zhelplastan in combination with Sephadex G-25 allowed achieving a final termination of bleeding in the MG in 98.1% of cases (compared to 86.0% of patients in the CG; *P*=0.0296), and also led to a decrease in the frequency of recurrent bleeding from 14.0% to 1.9% (*P*=0.0296) (Table 2).

In conclusion, in MWS, the use of the developed method of endoscopic treatment, including pneumoinsufflation of a powdered hemostatic agent in combination with a granular sorbent, against the background of conservative therapy, improved the results of treatment, increased the reliability of local hemostasis, reduced the number of recurrent bleedings, and excluded emergency operations.

Sources of Funding

This work was partially supported by the Council on Grants of the President of the Russian Federation for State Support of Young Scientists and Leading Scientific Schools (Grant MK-1069.2020.7).

References

1. Budnevsky AV, Cherednikov EF, Popov AV, Ovsyannikov ES, Kravchenko AY, Fursov KO. A Complex Multidisciplinary Approach to Prevention Gastro-duodenal Bleeding in Patients of General Hospital. International Journal of Biomedicine. 2017;7(3):204-207. doi: 10.21103/Article7(3)_OA8
2. Cherednikov EF, Budnevsky AV, Popov AV, Fursov KO. A new opinion on gastroduodenal bleeding preventon in patients with somatic pathology. The EPMA Journal. 2017;8(S1):46.
3. Cherednikov E F, Chernyh AV, Maleev YuV, Popov AV, Stekolnikov VV. [Topographical and anatomical prerequisites for the development of Mallory-Weiss syndrome]. Bulletin of the Russian Military Medical Academy. 2015;(S2):153-154. [Article in Russian].
4. Cherednikov EF, Deryaeva OG, Adianov VV, Ovchinnikov IF, Popov AV. [Modern directions of prevention and treatment of patients with gastrointestinal bleeding in the center]. System Analysis and Management in Biomedical Systems. 2014;13(2):426-433. [Article in Russian].
5. Cherednikov EF, Maleev YuV, Chernyh AV, Litovkina TE, Bondarenko AA, Cherednikov EE, Popov AV. [Current views on the diagnosis, treatment, and prevention of ruptured hemorrhagic syndrome (Mallory-Weiss syndrome)]. Journal of New Medical Technologies. 2016;23(4):161-172. [Article in Russian].
6. Baev VE, Kravets BB, Cherednikov EF. [Diagnostics of ulcerative forms of stomach cancer]. Voronezh. 2003:112. [In Russian].
7. Cherednikov EF, Barannikov SV, Maleev YuV, Fursov KO, Litovkina TE, Zakurdaev EI. [Experimental justification of the use of biologically active draining sorbent and plasma enriched by thrombocytes in treatment of bleeding defects of the stomach]. Journal of New Medical Technologies. 2017;24(2):114-118. [Article in Russian].
8. Cherednikov EF, Batkaev AR, Baev VE. The Reparative regeneration of erosive-ulcerative lesions of the stomach and duodenum in the local treatment of hydrophilic granular sorbents. System Analysis and Management in Biomedical Systems. 2005;4(2):224-225. [Article in Russian].
9. Cherednikov EF, Maleev YuV, Chernyh AV, Litovkina TE, Cherednikov EE, Shevtsov AN. [Modern views on the etiology and pathogenesis of ruptured hemorrhagic syndrome (Mallory-Weiss syndrome)]. Journal of anatomy and Histopathology. 2016;5(1):86-98. [Article in Russian].
10. Adianov VV, Cherednikov EF. [Optimizing treatment of gastroduodenal bleeding in patients with high surgical risk]. System Analysis and Management in Biomedical Systems. 2014;13(4):841-846. [Article in Russian].
11. Deryaeva OG, Cherednikov EF. [Multimodality therapy of erosiveulcer gastroduodenal bleeding by patients in a multidisciplinary hospital]. System Analysis and Management in Biomedical Systems. 2014; 13(3):725-730. [Article in Russian].
12. Cherednikov EF, Barannikov SV, Fursov KO, Polubkova GV, Danilenko VI, Stepanov DS. [Healing of bleeding experimental defects of the stomach with topical anilovin and platelet-rich plasma]. Journal of Volgograd State Medical University. 2017;2(62):130-133. [Article in Russian].
13. Cherednikov EF, Barannikov SV, Yuzefovich IS, Polubkova GV, Maleev YuV, Volkova IV, et al. Innovative Endoscopic Technologies in the Complex Treatment of Patients with Unstable Stopped Gastroduodenal Bleeding. International Journal of Biomedicine. 2021;11(1):24-28. doi:10.21103/Article11(1)_OA4
14. Cherednikov EF, Barannikov SV, Maleev YuV, Fursov KO, Litovkina TE, Zakurdaev EI, Ovsyannikov ES. Experimental justification of using Aseptisorb-A and platelet-rich plasma in endoscopic treatment of mold bleeding stomach defects. International Journal of Biomedicine. 2017;7(4):298-301. doi: 10.21103/Article7(4)_OA5
15. Cherednikov EF, Barannikov SV, Romantsov MN, Popov AV. New aspects of preventive endoscopic hemostasis in the treatment of peptic ulcer bleeding in the experimental condition. The EPMA Journal. 2017; 8(S1):45.
16. Cherednikov EF, Barannikov SV, Zhdanov AI, Moshurov IP, Polubkova GV, Maleev YuV, et al. Combimed Use of Biologically Active Hemostatic and Granulated Sorbent in Endoscopic Cytoprotective Hemostasis in Patients with Bleeding Gastroduodenal Ulcers. International Journal of Biomedicine. 2020;10(2):129-132. doi: 10.21103/Article10(2)_OA8
17. Cherednikov EF, Glukhov AA, Romantsov MN, Maleev YuV, Barannikov SV, Shkurina IA, et al. Hemostatic Agents in Combination with Diovine for Local Treatment of Simulated Bleeding Gastric Ulcers. International Journal of Biomedicine. 2020;10(2):138-141. doi: 10.21103/Article10(2)_OA10
18. Cherednikov EF, Kashurnikova MA, Romantsov MN, Barannikov SV, Bolkhovitinov AE, Gaponenkov DG, Lyubimov PYu. [Experimental study of new means of local hemostasis in the treatment of ulcerative bleeding]. Scientific and Medical Bulletin of the Central Chernozem Region. 2016;(65):27-33. [Article in Russian].
19. Romantsov MN, Cherednikov EF, Danilenko VI, Stepanov DS, Fursov K O, Deryaeva AG. [Morphological Characteristics of Processes of Simulated Bleeding Gastric Defects Reparation in Treatment with Gelplastan and Diovin]. Journal of Anatomy and Histopathology. 2017;6(1):81-86. [Article in Russian].
20. Gorbashko AI. Diagnostics and treatment of blood loss. Moscow: Meditsina. 1982:224. [In Russian].

***Corresponding author**: Evgeniy S. Ovsyannikov, PhD, ScD. Department of faculty therapy, Voronezh State Medical University named after N.N. Burdenko. Voronezh, Russia. E-mail: ovses@yandex.ru*

International Journal of Biomedicine 11(2) (2021) 164-168
http://dx.doi.org/10.21103/Article11(2)_OA8

ORIGINAL ARTICLE

Dentistry

INTERNATIONAL JOURNAL OF BIOMEDICINE

A New Perspective on a Morphological Confirmation of the Tissue Repair Process in the Experimental Simulation of a Surgical Dental Extraction in Rats

Arpine B. Antonyan; Dmitriy Yu. Kharitonov, PhD, ScD; Anna V. Podoprigora, PhD, ScD*; Iliya V. Stepanov, PhD, ScD; Oleg Yu.Shalaev, PhD, ScD; Irina A. Belenova, PhD, ScD; Elena A. Lecsheva, PhD, ScD; Alik E. Petrosyan

Voronezh State Medical University named after N.N. Burdenko
Voronezh, the Russian Federation

Abstract

All stages of a surgical dental extraction are accompanied by risks of various complications. Many ways and methods have been created in order to prevent the development of complications of different genesis. However, this issue still remains relevant since dental surgeons face the challenge of inflammation problems during the post-extraction period. The use of male Wistar rats as a model organism for a surgical extraction of a lower incisor allows us to conduct visual, histological and immunohistochemical evaluations of the wound healing process.

The main objective of this study was to compare the effect of ionic silver solution and hydrogen water in high concentration when irrigating the operational field of a surgical dental extraction on the lower jaw.

The results obtained showed that the use of water with an increased content of molecular hydrogen during the treatment is able to stimulate the recovery of the EM of the connective periodontal tissue to a greater extent than the ionic silver solution, connected to the participation of MCs and their secretome.(**International Journal of Biomedicine. 2021;11(2):164-168.**)

Key Words: dental extraction • ionic silver solution • inflammatory complications • hydrogen water • mast cell

For citation: Antonyan AB, Kharitonov DYu, Podoprigora AV, Stepanov IV, Shalaev OYu, Belenova IA, Lecsheva EA, Petrosyan AE. A New Perspective on a Morphological Confirmation of the Tissue Repair Process in the Experimental Simulation of a Surgical Dental Extraction in Rats. International Journal of Biomedicine. 2021;11(2):164-168. doi:10.21103/Article11(2)_OA8

Abbreviations

MC, mast cell; **CT**, connective tissue; **EM**, extracellular matrix; **RF**, reticular fiber

Introduction

Annually, a large number of ways and methods are proposed in order to prevent the development of inflammatory complications. Nevertheless, according to statistics, the number of complications does not decrease. This indicates that the proposed drugs are ineffective and the technique imperfect, both of which require adjustments and modifications.

To date, the solution to prevention and treatment of complications after a surgical dental extraction on the lower jaw is considered a pressing issue.[1-5]

The main objective of this study was to compare the effect of ionic silver solution and hydrogen water in high concentration when irrigating the operational field of a surgical dental extraction on the lower jaw.

***Corresponding author**: Prof. Anna V. Podoprigora, PhD, ScD. Department of Maxillofacial Surgery, Voronezh State Medical University named after N.N. Burdenko. Voronezh, Russia. E-mail: ovses@yandex.ru*

Material and Methods

The study was performed on male Vistar rats, weighing 180±25 g. The experiment was conducted on the basis of a certified vivarium of the Research Institute of Experimental Biology and Medicine at the Voronezh State Medical University.

The surgical dental extraction of the lower incisor was performed in laboratory rats in three study groups. In Group 1 (n=10), the operating field was irrigated with saline solution, and in Group 2 (n=10) - with ionic silver solution in a concentration of 20 mg/l, using utility model No.183521, and in Group 3 (n=10) - with high-concentration (8 ppm) of hydrogen water. In the control group of intact animals (n=10), the periodontal tissues of their lower incisors were examined without a tooth extraction procedure.

We conducted histochemical and immunomorphological studies of the periodontium of the lower incisors of the rats (gum, periodontal fibers) and soft tissues in the area of the CT of the alveolar processes in the intact animals and after removal of one of the incisors.

The sections were studied using a ZEISS Axio Imager A2 microscope. The total number of MCs was calculated with a ×40 lens. Using the ImageJ program, microphotographs of the tissue specimen were utilized to measure the periodontal area of the lower incisors of the rats and soft tissues of the CT of the alveolar processes. Next, visually, depending on the technique used, we calculated the number of MCs (mastocytes), their colocalization with RFs, fibroblasts, MCs, and the number of myofibroblasts. The data obtained as a result of measuring all microphotographs of the tissue specimen were summed up and the amount of the above criteria per 1mm^2 area of CT was calculated.

Statistical analysis was performed using the Statistica 6.1 software package (Stat-Soft Inc., USA). The normality of distribution of continuous variables was tested by the Kolmogorov-Smirnov test. The mean (M) and standard deviation (SD) were calculated. Means of 2 continuous normally distributed variables were compared by independent samples Student's t test. Mann-Whitney U test was used to compare means of 2 groups of variables not normally distributed. For multiple comparisons, the Bonferroni correction was used.

Results and Discussion

The estimation of the MC population for periodontal and interalveolar CT of rats showed a significant increase after tooth extraction (Table 1). On Day 3 of the experiment, the increase in the MC number exceeded similar indicators in the control group, reaching the maximum in Group 2. On Day 7 of the experiment, in Group 1 the amount of MCs decreased slightly, compared to the previous observation period. At the same time, in Group 2, there was a further noticeable increase, in comparison with the parameters of Day 3 of the experiment. We observed a similar increase in the number of MCs in Group 3. On Day 14 of the experiment, an increase in the MC population was observed only in Group 3. Despite the decrease in the number of MCs by Day 14 of the experiment in Group 2, the MC population exceeded this indicator in Group 1. It should be noted that the size of the MCs in the studied tissues increased as the experiment continued.

Table 1.

The number of MCs (per mm^2) in the rats periodontal membrane (May–Grünwald stain)

Observation period	Group 1	Group 2	Group 3
Control group 4.6±0.3			
Day 3	10.4±1.1*	11,1±1,8*	8.4±0.6*
Day 7	7.2±0.5*	16.8±1.1*	13.2±1.3*
Day 14	11.3±1.5*	14.2±0.9*	20.3±1.7*

** - P<0.017 compared to the control group*

Thus, each group has its own characteristics in the dynamics of the number of MCs in the periodontal region near the wound. In general, the main changes were associated with an increase in the number of MCs, which began to accumulate to a greater extent in the CT of the periodontal region adjacent to the location of the removed tooth. With an increasing duration of the post-extraction period, mastocytes increased in size and acquired a more pronounced metachromasia.

When assessing the secretory activity of the MCs, certain patterns were revealed, along with the general tendency to increase during different treatment protocols for laboratory animals. In particular, on Day 3 of the experiment, the maximum secretory activity was observed in Group 2 (Table 2, Fig. 1). By Day 7, the activity of MC degranulation decreased slightly, but by Day 14, we detected its increase again, with the highest intensity in Group 1. In accordance with the increased removal of the secretome into the EM of periodontal CT, the number of non-degranulated forms in the MC population decreased (Table 2).

Table 2.

Degranulation activity (%) of the mastocydes in rats periodontium (May–Grünwald stain)

Observation period	Control group		Group 1		Group 2		Group 3	
	D	nD	D	nD	D	nD	D	nD
	53.7	46.3						
Day 3			75.4	24.6	84.2	15.8	70.3	29.7
Day 7			72.3	27.7	78.2	21.8	68.4	31.6
Day 14			85.6	14.4	77.2	22.8	76.8	23.2

D - degranulated MCs, nD - non-degranulated MCs

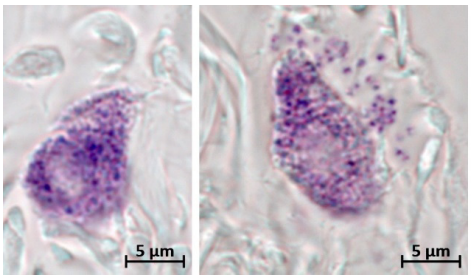

Fig. 1. *MCs of the periodontium in the area of the anterior incisors of the rat. Fixative: 10% neutral buffered formalin. Staining technique: Giemsa stain solution. A – the control group. Mast cell without signs of degranulation. B – Group 2, Day 3 of the experiment. Signs of active degranulation towards the incisor resection area.*

When assessing the level of tryptase expression in the MCs, we found that after incisor resection, there was a significant increase in the content of specific protease in all experimental groups, with the highest degree in Group 2. In Group 3, the content of tryptase-positive MCs was the lowest, despite exceeding the control parameters by more than two times (Table 3). A week after dental extraction, the number of tryptase-positive MCs continued to increase in Groups 2 and 3, while in Group 1 it decreased.

After two weeks of the experiment, we could note the preservation of an increased population of tryptase-positive MCs in the CT of the periodontium and the interalveolar region. At the same time, the highest expression of tryptase was observed in Group 3 using water enriched with molecular hydrogen (Table 3, Fig. 2), while in Group 2 the number of protease decreased slightly, compared to the previous follow-up period. The lowest number of tryptase-positive MCs by Day 14 was found in Group 1, compared to other experimental animals (Table 3).

Table 3.

The number of tryptase-positive MCs in periodontium of the rats (per mm²)

Observation period	Group 1	Group 2	Group 3
Control group 2.2±0.1			
Day 3	8.6±0.7	10.1±0.8*	5.5±0.8*
Day 7	6.1±0.5	14.2±1.2*	10.7±1.4*
Day 14	9.3±1.1	12.7±1.1*	15.4±1.3*

** - P<0.017 compared to the control group*

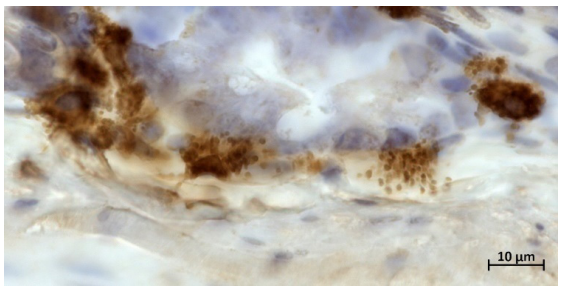

Fig. 2. *Mast cells in the periodontium after resection of the rat incisor. Group 3, Day 14 of the experiment. Fixative: 10% neutral buffered formalin. Method: immunohistochemical staining for tryptase.*

The study of colocalization of the MCs with RFs showed low numbers in general (Table 4). The MCs were mainly colocalized with mature collagen fibers forming multidirectional bundles, and much less often with thin RFs. However, by Day 3 of the post-resection period, an increase in the frequency of MC colocalization with RFs was revealed several times (Table 4). The highest numbers were achieved in Group 3 (Table 4, Fig. 3). More than half of the MCs were in close contact with RFs. The colocalization of RFs and MCs in Groups 1 and 2 was approximately equal and more than three times more frequent than in the control animals.

Table 4.

Colocalization of the mast cells and reticular fibers (in %) in the connective tissue of the rat periodontium

Observation period	Group 1	Group 2	Group 3
Control group 12.2			
Day 3	45.2	42.5	57.4
Day 7	58.2	53.4	83.2
Day 14	60.5	68.2	65.2

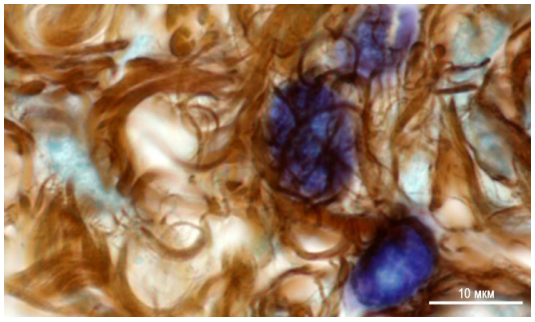

Fig. 3. *The periodontium after resection of the rat incisor. Method: combined staining of Toluidine blue and silver impregnation. Group3, Day 14 of the experiment. There is a close colocalization of the mast cells and reticular fibers.*

Seven days after dental extraction, the process of fibrillogenesis remained active, which was manifested by more frequent colocalization of MCs and RFs, compared to the control animals (Table 4). At the same time, the use of hydrogen water in the treatment protocol led to the highest frequency of detection of colocalization of the MCs and RFs in the CT of the Periodontium (Table 4).. In this experimental group,, the vast majority of MCs took part in fibrillogenesis (Table 4). Smaller and approximately equal numbers of the MCs and RFs were found in Groups 1 and 2, showing small effects of the solution in Group 2 from untreated animals on the fibrillogenesis involving MCs. By Day 14 of the post-resection period, in all experimental groups the fibrillogenesis involving MCs was approximately equalized, but remained much higher than in control animals. Thus, we can assume an increase in the fiber formation of the EM of the connective periodontal tissue with the participation of MCs. This process reaches maximum activity when using water enriched with molecular hydrogen after 7 days of the post-resection period.

From the point of view of intra-population, intercellular communication of MCs, it is necessary to note rather low indicators in the group of intact animals. However, after dental extraction, the intensity of intercellular communication of MCs with each other significantly increases, to the greatest extent in Group 2 (Table 5). The highest level in the aspect of intercellular signaling of MCs appears after 7 days in Group 3 (Table 5). At the same time, the indicators are almost 6 times higher than the levels in the control group. However, after 14 days, this effect is leveled, and the maximum frequency of attachment of MCs to each other is preserved in Group 2.

Table 5.

The frequency of intra-population intercellular communication of MCs (%) in the connective tissue of the periodontium

Observation period	Group 1	Group 2	Group 3
Control group 2.2			
Day 3	3.4	5.2	4.4
Day 7	5.5	8.8	12.7
Day 14	4.8	6.3	5.4

Therefore, the removal of the incisor is accompanied by an increase in the intensity of intercellular exchange in the MC population. This obviously affects the functional activity of the mastocytes, including the remodeling of the EM. In particular, this increase in intensity can be evidenced by the results of combined staining of MCs with Giemsa solution and impregnation with silver.

Judging by the frequency of colocalization of the MCs with fibroblasts, 3 days after tooth resection the highest parameter of this indicator was observed in the group using hydrogen water (Group 3) as an irrigation agent. At the same time, in the remaining groups, despite the lower parameters of this indicator, there was a significant increase, in comparison with the control level (Table 6, Fig.4). It should be noted that this indicator remains at the maximum level, in comparison with the other groups of the experiment, on both Days 7 and 14. At the same time, the adherence of the MCs to fibroblasts was the lowest in Group 2 by Day 7 (Table 6).

Table 6.

The frequency of adherence of mast cells to fibroblastic differon cells in the periodontium of the lower incisors of rats (%)

Observation period	Group 1	Group 2	Group 3
Control group 8.6			
Day 3	16.7	15.2	25.3
Day 7	18.4	13.4	22.2
Day 14	15.6	17.2	20.4

The number of the RFs in the group of intact animals was insignificant (Table 7). However, on Day 3 of the experiment, this indicator significantly increased with the highest parameters in Group 3 and continued to increase significantly, reaching a maximum by Day 14 (Table 7).

Table 7.

The number of the reticular fibers in the periodontium of the lower incisors of rats (c.u.)

Observation period	Group 1	Group 2	Group 3
Control group 1.9			
Day 3	7.7	6.2	9.7
Day 7	8.9	8.7	12.5
Day 14	8.7	7.1	17.4

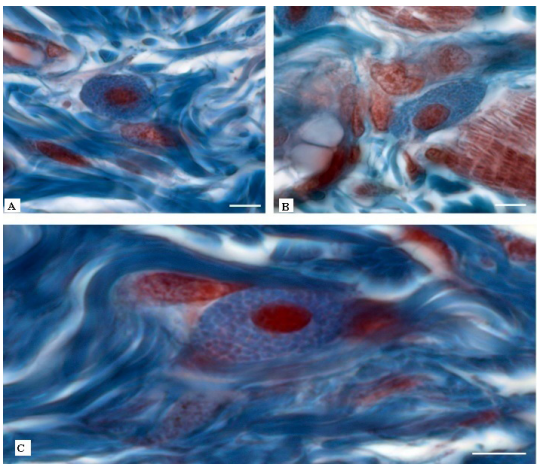

Fig. 4. *Colocalization of the mast cells with fibroblasts after dental extraction of the incisor. Fixative: 10% neutral buffered formalin. Method: staining with Picro-Mallory solution. A – Group 1, Day 3. B – Group 2, Day 7. C – Group 3, Day 14.*

The number of fibroblasts in the periodontal CT is also consistent with these data. In particular, this indicator reached the maximum by Day 14 of the experiment in Group 3 (Fig. 5, Table 8). At the same time, this indicator showed high parameters in the first periods of observation in all groups, with the greatest level in Group 2. However, on Days 7 and 14, the highest number of myofibroblasts was found in Group 3.

Table 8.

The number (c.u.) of myofibroblasts in the periodontium of the lower incisors of rats (staining with Picro-Mallory solution)

Observation period	Group 1	Group 2	Group 3
Control group 1.3			
Day 3	5.5	12.3	8.4
Day 7	7.5	8.6	14.4
Day 14	12.3	7.7	17.3

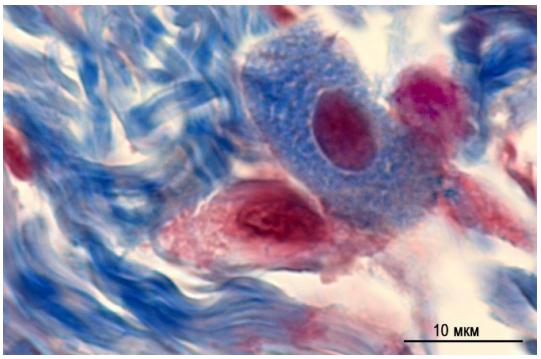

Fig. 5. *The periodontium of the rat after removal of the incisor. Fixative: 10% neutral buffered formalin. Method: staining with Picro-Mallory solution. Colocalization of a mast cell with myofibroblast.*

To explain the improvement in the regeneration of damaged tissues, we should consider the condition of CT, both fibrous and amorphous components. Among the criteria that can

reflect the intensity of recovery of the intercellular matrix we noted the number of newly formed thin collagen fibers, as well as the participation of MCs in the issues of fibrillogenesis.[6] It should be pointed out that the number of MCs in the CT of the periodontium increased significantly after resection, which is due to both the immunomodulatory effects of MCs and their regulatory properties in relation to the structures of the EM. It is obvious that the number of RFs in CT had certain differences depending on the treatment. It also should be noted that the highest numbers of RFs were found in the second, and especially in the third period of the experiment while using hydrogen water. The biological effects of molecular hydrogen on the enhancement of fibrillogenesis can be closely related to the activity of MCs, which are connected to the processes of the EM remodeling.

As a result of the analysis, it was revealed that different treatment protocols may have different effects on the state of collagen fibrillogenesis, which is the basis for the restoration of the CT framework. In particular, different treatments result in different levels of intercellular signaling of MCs, as well as MCs and fibroblasts within a specific periodontal tissue microenvironment. The adhesion of MCs to fibroblasts is a morphological confirmation of fibrillogenesis. This initiates the assembly of collagen fibrils and subsequently a full-fledged collagen fiber. It is also necessary to take into account the importance of the secretory activity of the MCs, which can change the physico-chemical properties of the integrative buffer medium. As a result of that, collagen molecules polymerize into supramolecular structures, fibrils and other stages of the organization of the collagen fiber.

Another important inductive signal for fibroblasts in terms of stimulating the biogenesis of collagen proteins is an increase in tryptase expression in MCs and secretion into EM.[6] In addition, tryptase has important properties for initiating fibroblast differentiation into myofibroblasts, and the latter are known to have a much higher capacity for collagen biosynthesis.[6] Also, an increase in the level of tryptase in the EM can stimulate the division of myofibroblasts with their accumulation in a certain locus of CT.[7]

Furthermore, the interaction of MCs with fibroblasts is one of the mechanisms of EM remodeling, in which intercellular signaling is accompanied by the changes in the expression profiles of various EM proteins in fibroblasts. In addition, an inductive effect of the MCs on the mitotic activity of fibroblasts may increase their number per unit volume of tissue, as well as possible transformation into myofibroblastic cells.

Therefore, the use of water with an increased content of molecular hydrogen during the treatment is able to stimulate the recovery of the EM of the connective periodontal tissue to a greater extent than the ionic silver solution, connected to the participation of MCs and their secretome.

Competing Interests

The authors declare that they have no competing interests.

References

1. Dallaserra M, Poblete F, Vergara C, Cortés R, Araya I, Yanine N, Villanueva J. Infectious postoperative complications in oral surgery. An observational study. J Clin Exp Dent. 2020 Jan 1;12(1):e65-e70. doi: 10.4317/medoral.55982.
2. Malkawi Z, Al-Omiri MK, Khraisat A. Risk indicators of postoperative complications following surgical extraction of lower third molars. Med Princ Pract. 2011;20(4):321-5. doi: 10.1159/000324550.
3. Shigeishi H, Ohta K, Takechi M. Risk factors for postoperative complications following oral surgery. J Appl Oral Sci. 2015 Jul-Aug;23(4):419-23. doi: 10.1590/1678-775720150130.
4. Sato J, Goto J, Harahashi A, Murata T, Hata H, Yamazaki Y, Satoh A, Notani K, Kitagawa Y. Oral health care reduces the risk of postoperative surgical site infection in inpatients with oral squamous cell carcinoma. Support Care Cancer. 2011 Mar;19(3):409-16. doi: 10.1007/s00520-010-0853-6.
5. Lodi G, Azzi L, Varoni EM, Pentenero M, Del Fabbro M, Carrassi A, Sardella A, Manfredi M. Antibiotics to prevent complications following tooth extractions. Cochrane Database Syst Rev. 2021 Feb 24;2:CD003811. doi: 10.1002/14651858.CD003811.pub3.
6. Atiakshin D, Buchwalow I, Tiemann M. Mast cells and collagen fibrillogenesis. Histochem Cell Biol. 2020 Jul;154(1):21-40. doi: 10.1007/s00418-020-01875-9.
7. Atiakshin D, Buchwalow I, Samoilova V, Tiemann M. Tryptase as a polyfunctional component of mast cells. Histochem Cell Biol. 2018 May;149(5):461-477. doi: 10.1007/s00418-018-1659-8.

International Journal of Biomedicine 11(2) (2021) 169-172
http://dx.doi.org/10.21103/Article11(2)_OA9

ORIGINAL ARTICLE

Sports Medicine

INTERNATIONAL JOURNAL OF BIOMEDICINE

The Peculiarities of Heart Rate Variability in Student Athletes

Andrew K. Martusevich[1,2*], PhD, ScD; Ivan V. Bocharin[1,2]; Natalia A. Ronzhina[1]; Solomon A. Apoyan[1]; Levon R. Dilenyan, PhD[1]; Maxim S. Gurjanov, PhD, ScD[1]

[1]Privolzhsky Research Medical University
[2]Nizhny Novgorod State Agricultural Academy
Nizhny Novgorod, Russia

Abstract

Background: Currently, the assessment of heart rate variability (HRV) is one of the most common indicators of the condition of the cardiovascular system. The aim of this research was to study the peculiarities of heart rate variability (HRV) and microcirculation in students, depending on their sport specialization.

Methods and Results: Our study included the results of a survey of 96 students from 18 to 21 years of age who were the members of the national teams of their universities in athletics (n=49) and floorball (n=47). For ECG registration and analysis of hemodynamic findings, including those characterizing the HRV, we used the "Medical Soft" sports testing system ("MS FIT Pro"). For monitoring, we used the standard hemodynamic patterns (blood pressure, HR, stroke volume, cardiac output, and others), statistical and spectral indicators of the HRV, as well as an integral criterion of the state of microcirculation. The studied HRV parameters in most students generally were within the age range. At the same time, track and field athletes have large adaptive resources and, consequently, a more optimal level of myocardial fitness, in comparison with floorball players.

Conclusion: The orientation of sports training among students affects heart condition.(**International Journal of Biomedicine. 2021;11(2):169-172.**)

Key Words: heart rate • heart rate variability • athletes • students • hemodynamics

For citation: Martusevich AK, Bocharin IV, Ronzhina RA, Apoyan SA, Dilenyan LR, Gurjanov MS. The Peculiarities of Heart Rate Variability in Student Athletes. International Journal of Biomedicine. 2021;11(2):169-172. doi:10.21103/Article11(2)_OA9

Abbreviations

HR, heart rate; **HRV**, heart rate variability; **SBP**, systolic blood pressure; **DBP**, diastolic blood pressure.

Introduction

Currently, the assessment of heart rate variability (HRV) is one of the most common indicators of the condition of the cardiovascular system.[1-3] It has been shown that HRV analysis is able to verify both the intracardiac mechanisms of hemodynamic regulation and the nature of external (neurohumoral, metabolic and other) influences on the heart rate (HR).[1,2,4,5] On this basis, an integrated study of HRV has demonstrated its informative value in various diseases and pathological conditions, including directly cardiological (for example, hypertension[6]) and extracardiac pathology (in particular, severe burns [7] and alcohol withdrawal [8]).

A separate aspect of the use of the HRV examination is to monitor the state of various social groups, including the youth, who a priori should be classified as "practically healthy persons." [9,10] However, this group showed various disorders of the cardiovascular system,[3,9,10] and from the standpoint of diagnosing premorbid pathology, this problem has not been studied in depth. Another poorly covered problem is the analysis of cardiovascular reserves in most students who are actively involved in sports.[3,11,12] In this regard, there is certain information on load tolerance[12,13] and stressful situations.[11,14]

***Corresponding author**: Prof. Andrew K. Matrusevich, PhD, ScD. Privolzhsky Research Medical University, Nizhny Novgorod, Russia. E-mail: cryst-mart@yandex.ru*

Furthermore, there is indication of a connection between the progress of students in study and the level of their physical activity, according to HRV parameters.[11,14,15] At the same time, there exists only indirect evidence of the unequal state of the HR depending on the sports orientation of the student.[16,17] It is essential to mention that taking this fact into consideration can affect the degree to which negative cardiovascular incidents are detected.[18-20] This determines the necessity for more detailed examination of HRV condition in various groups of students.[21]

The aim of this research was to study the peculiarities of HRV and microcirculation in students, depending on their sport specialization.

Material and Methods

Our study included the results of a survey of 96 students from 18 to 21 years of age who were the members of the national teams of their universities in athletics (n=49) and floorball (n=47). The study was carried out in the middle of the day, in a calm condition (in the intersessional period, the days free from tests or seminars) according to the standard rules of procedure for taking an ECG.[1,2,5,6] For ECG registration and analysis of hemodynamic findings, including those characterizing the HRV, we used the "Medical Soft" sports testing system ("MS FIT Pro", Russia). For monitoring, we used the standard hemodynamic patterns (blood pressure, HR, stroke volume, cardiac output, and others), statistical and spectral indicators of the HRV, as well as an integral criterion of the state of microcirculation.[1-5] All the values of these indicators were calculated automatically, taking into account the system software.

Statistical analysis was performed using the Statistica 6.1 software package (StatSoft Inc, USA). A probability value of $P<0.05$ was considered statistically significant.

Results

We assessed statistical indicators characterizing the HRV of students included in the formed groups (Figures 1-4). It was found that representatives of both groups do not deviate from the age standard for blood pressure.(Fig.1) At the same time, the SBP level in floorball players exceeded that in runners ($P<0.05$). On the contrary, no differences were found in the DBP level.

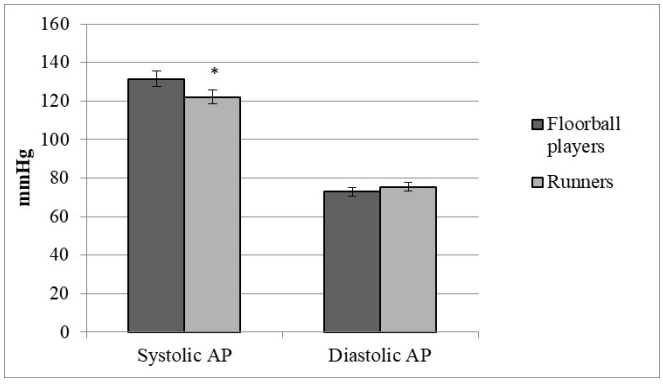

Fig. 1. *The level of SBP and DBP in students, depending on their sports specialization. * - P<0.05*

Also, the peculiarities of the HR in floorball players were relative tachycardia, compared to the group of runners (Fig.2); however, in almost all representatives of both groups, the values of the measurements were in the physiological range.[1,3,4,10] It should be noted that the visible tendency may indicate better physical fitness of runners, as it creates a reserve to increase the HR.[4,15] The same is evidenced by the patterns associated with the HR—stroke volume (Fig.2) and cardiac output (Fig.3)—which were found in runners at a lower level than in floorball players due to the adaptive restructuring of cardiohemodynamics.[11-14]

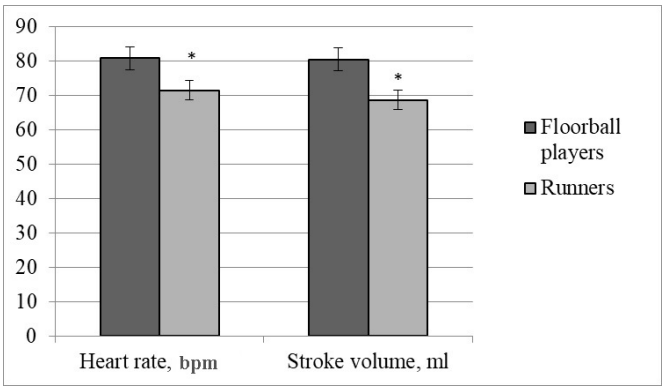

Fig. 2. *The HR and stroke volume in the students, depending on their sports specialization * - P<0.05*

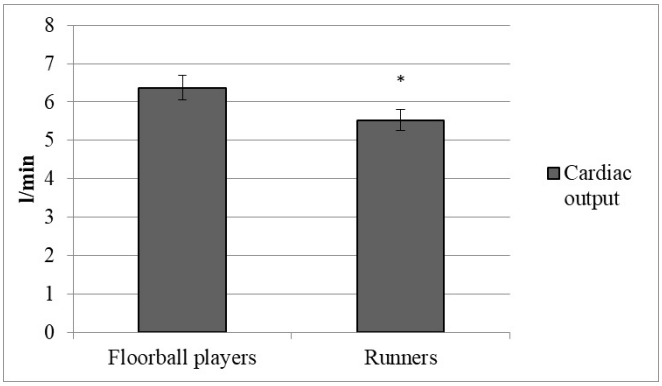

Fig 3*. The level of cardiac output in students, depending on their sports specialization.* * - P<0.05*

With regard to the pNN50 indicator (the percentage of adjacent NN [normal-to-normal] intervals that differ from each other by more than 50 ms), floorball players significantly outperform runners, showing a level of about 35%, which may indicate an increased risk of arrhythmogenic incidents in students of this group (Fig.4).

The study of the spectral analysis of the HR (Fig.5) showed that the ratio of the spectrum powers in the low and high frequency ranges (LF/HF), observed as the main spectral indicator of the autonomic support of cardiac rhythm, indicates its shift in floorball players towards sympathetic stimulation of the myocardium.[2,4,6,17] This is also proved by the level of the stress index in the representatives of the study groups.

Finally, the diagnostic measures we used allowed us to make a point assessment of microcirculation in student-

sportsmen (Fig.6). It was revealed that the activity of microcirculation is significantly higher in runners than in floorball players. At the same time, in the representatives of both groups, this parameter was within the physiological limits.

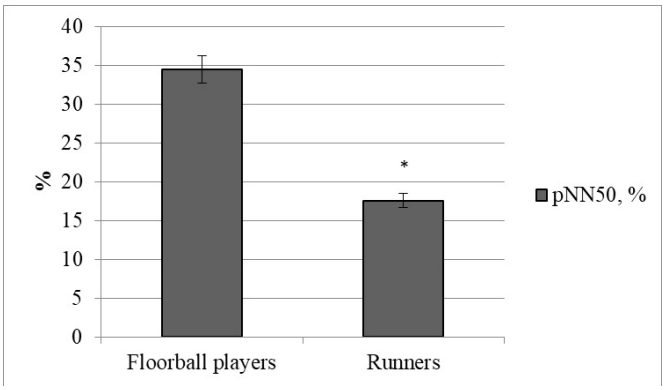

Fig. 4. *The pNN50 indicator in students, depending on sports specialization. * - P<0.05*

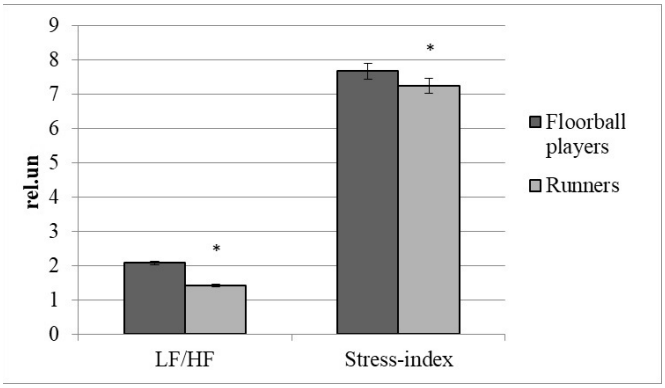

Fig. 5. *The LF/HF index and stress-index in students, depending on sports orientation. * - P<0.05*

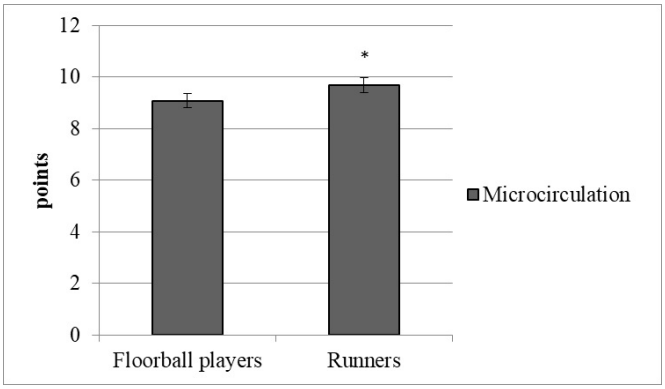

Fig. 6. *The level of microcirculation in students, depending on sports orientation. * - P<0.05*

Discussion

On the one hand, the health of the youth has been researched in a significant number of studies,[3,10,11] but, on the other hand, it continues to deteriorate due to a lifestyle that is not always correct, an increasing academic load and a decrease in physical activity.[3,5,16] This is especially true for students studying at a medical university, who experience a high level of psychoemotional stress associated with a large volume of assimilated material and extensive practical training.[5,10] It has been shown that the decline in health does not stay the same but progresses during the academic year.[10,14,15] In this regard, the program "Sport is the second profession of a doctor," which is currently being implemented, seems to be timely. At the same time, strict medical monitoring of the basic functional systems of students while they are playing sports is obligatory.[11-16,18-21] From the indicated positions, the evaluation of systemic hemodynamics was monitored by assessing the HRV,[10,11,13-16,19] which serves as an informative indicator of the direction of the influence of sports activity on the organism of students.

Currently, the study of HRV is the common way to test the functional reserves of the cardiovascular system of athletes;[12-20] however, in relation to students who systematically go in for sports, such data are few. Therefore, within the framework of our research, hemodynamic evaluation was assessed using the "Medical Soft" sports testing system, on the basis of which not only the HRV features in the student-sportsmen were established, but it was also demonstrated that the chosen sport affects the features of cardiovascular adaptation to loads. So, under conditions of physiological rest, in runners relative to floorball players, a lower level of SBP, HR, and, as a consequence, decreased values of stroke volume and cardiac output were recorded. Moreover, runners had a higher level of the indicator characterizing microcirculation. Such data indicate that although all measurements are within the age range for representatives of both groups, runners have larger resource for adapting the cardiovascular system to intensive activities.

In conclusion, the studied HRV parameters in most students generally are within the age range. At the same time, track and field athletes have large adaptive resources and, consequently, a more optimal level of myocardial fitness, in comparison with floorball players. Thus, the orientation of sports training among students affects heart condition.

Competing Interests

The authors declare that they have no competing interests.

References

1. Baevskiĭ RM. Analiz variabel'nosti serdechnogo ritma v kosmicheskoĭ meditsine [Analysis of variability of cardiac rhythm in space medicine]. Fiziol Cheloveka. 2002 Mar-Apr;28(2):70-82. [Article in Russian].
2. Nozdrachev AD, Shcherbatykh IuV. Sovremennye sposoby otsenki funktsional'nogo sostoianiia avtnomnoĭ (vegetativnoĭ) nervnoĭ sistemy [Current methods of evaluation of functional status of the autonomic nervous system]. Fiziol Cheloveka. 2001 Nov-Dec;27(6):95-101. [Article in Russian].
3. Pichon A, Nuissier F, Chapelot D. Heart rate variability and depressed mood in physical education students: a longitudinal study. Auton Neurosci. 2010 Aug 25;156(1-2):117-23. doi: 10.1016/j.autneu.2010.03.019.

4. Kotel'nikov SA, Nozdrachev AD, Odinak MM, Shustov EB, Kovalenko IIu, Davydenko VIu. Variabel'nosti ritma serdtsa: predstavleniia o mekhanizmakh [Variability in heart rhythm: approaches to mechanisms]. Fiziol Cheloveka. 2002 Jan-Feb;28(1):130-43. [Article in Russian].
5. Sztajzel J. Heart rate variability: a noninvasive electrocardiographic method to measure the autonomic nervous system. Swiss Med Wkly. 2004 Sep 4;134(35-36):514-22.
6. Ostroumova OD, Mamayev VI, Nesterova MV, Kuzmichev IA, Martynov AI. [SPECTRAL ANALYSIS OF HEART RATE FLUCTUATIONS IN PATIENTS WITH ESSENTIAL HYPERTENSION]. Russian Journal of Cardiology. 2000;(6):60-64. [Article in Russian].
7. Peretyagin SP, Martusevich AK, Borisov VI. [Investigation of heart rate variability in patients with burns]. Vestnik Anesteziologii i Reanimatologii. 2011;8(4):10-14. [Article in Russian].
8. Martusevich AK, Zhukova NE. [Heart rate variability in the dynamics of the alcohol abstinence syndrome reduction]. Voprosy Nakrologii. 2011;4:11-16. [Article in Russian].
9. Bocharin IV, Martusevich AK, Guryanov MS, Kiseliv YaV, Kanatyev KN, Polebentsev SN. [Results of screening examination of the cardiovascular system of students of Nizhny Novgorod]. International Journal of Medicine and Psychology 2020; 3(1):118-121. [Article in Russian].
10. Pershina TA, Spitsin AP. [Peculiarities of hemodynamics in junior students with a hereditary history of arterial hypertension during examination stresses]. Gig Sanit. 2013 May-Jun;(3):80-5.[Article in Russian].
11. Britton DM, Kavanagh EJ, Polman RCJ. Validating a Self-Report Measure of Student Athletes' Perceived Stress Reactivity: Associations With Heart-Rate Variability and Stress Appraisals. Front Psychol. 2019 May 9;10:1083. doi: 10.3389/fpsyg.2019.01083.
12. Misigoj-Durakovic M, Durakovic Z, Prskalo I. Heart Rate-Corrected QT and JT Intervals in Electrocardiograms in Physically Fit Students and Student Athletes. Ann Noninvasive Electrocardiol. 2016 Nov;21(6):595-603. doi: 10.1111/anec.12374.
13. Boettger S, Puta C, Yeragani VK, Donath L, Müller HJ, Gabriel HH, Bär KJ. Heart rate variability, QT variability, and electrodermal activity during exercise. Med Sci Sports Exerc. 2010 Mar;42(3):443-8. doi: 10.1249/MSS.0b013e3181b64db1.
14. Deschodt-Arsac V, Lalanne R, Spiluttini B, Bertin C, Arsac LM. Effects of heart rate variability biofeedback training in athletes exposed to stress of university examinations. PLoS One. 2018 Jul 26;13(7):e0201388. doi: 10.1371/journal.pone.0201388.
15. Hulka OV. [DYNAMICS OF SPECTRAL INDEXES OF HEART VARIABILITY RATE OF THE STUDENTS WITH DIFFERENT CHARACTER OF THE EDUCATIONAL LOADING]. Fiziol Zh. 2015;61(4):98-104. doi: 10.15407/fz61.04.098. [Article in Ukrainian].
16. Redondo B, Vera J, Luque-Casado A, García-Ramos A, Jiménez R. Associations between accommodative dynamics, heart rate variability and behavioural performance during sustained attention: A test-retest study. Vision Res. 2019 Oct;163:24-32. doi: 10.1016/j.visres.2019.07.001.
17. Wang X, Yan C, Shi B, Liu C, Karmakar C, Li P. Does the Temporal Asymmetry of Short-Term Heart Rate Variability Change during Regular Walking? A Pilot Study of Healthy Young Subjects. Comput Math Methods Med. 2018 Apr 30;2018:3543048. doi: 10.1155/2018/3543048.
18. Drezner JA, Peterson DF, Siebert DM, Thomas LC, Lopez-Anderson M, Suchsland MZ, Harmon KG, Kucera KL. Survival After Exercise-Related Sudden Cardiac Arrest in Young Athletes: Can We Do Better? Sports Health. 2019 Jan/Feb;11(1):91-98. doi: 10.1177/1941738118799084.
19. Perkins SE, Jelinek HF, Al-Aubaidy HA, de Jong B. Immediate and long term effects of endurance and high intensity interval exercise on linear and nonlinear heart rate variability. J Sci Med Sport. 2017 Mar;20(3):312-316. doi: 10.1016/j.jsams.2016.08.009.
20. Sharashdze NS, Pagava ZT, Saatashvili GA, Agladze RA. [Heart rhythm abnormalities in middle-aged veteran elite athletes]. Georgian Med News. 2008 Jun;(159):31-4. [Article in Russian].
21. Adams JA, Patel S, Lopez JR, Sackner MA. The Effects of Passive Simulated Jogging on Short-Term Heart Rate Variability in a Heterogeneous Group of Human Subjects. J Sports Med (Hindawi Publ Corp). 2018 Oct 1;2018:4340925. doi: 10.1155/2018/4340925.

International Journal of Biomedicine 11(2) (2021) 173-176
http://dx.doi.org/10.21103/Article11(2)_OA10

ORIGINAL ARTICLE

Biotechnology

INTERNATIONAL JOURNAL OF BIOMEDICINE

Production, Properties and Swelling of Composite Pectic-Gel Particles in an Artificial Gastric Environment

Anatoly A. Shubakov, PhD; Elena A. Mikhailova*

Institute of Physiology of Komi Science Centre of the Ural Branch of the RAS, FRC Komi SC UB RAS
Syktyvkar, Komi Republic, the Russian Federation

Abstract

The purpose of the present work was to obtain and study the properties of composite calcium-pectic gel particles (CaPGPs) obtained from aqueous solutions of apple pectin (AP) in the concentration of 2% and pectin heracleuman (HS) in the concentration of 3% in the presence of Ca^{2+} ions (0.34 M). The swelling of the obtained CaPGPs in an artificial gastric environment was also investigated.

***Methods and Results*:** We used commercial AP AU701 (AP, Herbstreith & Fox KG, Germany) and HS isolated from the aerial part of the Sosnovskyi hogweed *Heracleum sosnowskyi* Manden. Composite CaPGPs were obtained from aqueous solutions of AP (2%) and HS (3%) in the presence of Ca^{2+} ions (0.34 M) by the method of ionotropic gelation. The diameter and density of CaPGPs were determined. Dry gel particles from 2% AP were larger (1.18±0.19 mm) than dry gel particles from 3% HS (1.04±0.07 mm) and dry composite gel particles (1.01±0.06 mm). However, dry composite gel particles and dry gel particles from HS were approximately 3 times denser than dry gel particles from AP. Composite CaPGPs swelled by 74.2% in simulated gastric fluid (SGF). The degree of swelling in SGF of CaPGPs formed from HS was 15.6% lower, and CaPGPs formed from AP –52.2%. **(International Journal of Biomedicine. 2021;11(2):173-176.)**

Key Words: apple pectin • heracleuman • calcium ions • gel particles • artificial gastric environment

For citation: Shubakov AA, Mikhailova EA. Production, Properties and Swelling of Composite Pectic-Gel Particles in an Artificial Gastric Environment. International Journal of Biomedicine. 2021;11(2):173-176. doi:10.21103/Article11(2)_OA10

Abbreviations

AP, apple pectin; **CaPGPs**, calcium-pectic gel particles; **HS**, heracleuman; **SGF**, simulated gastric fluid.

Introduction

Pectin is a methylated ester of polygalacturonic acid.[1] Pectins are soluble dietary fibers, unique in their ability to hydrate (swell and retain water) and to form gels. As a source of nutrition for the intestinal microflora, pectins have a prebiotic effect, contributing to an increase in the number and activity of the obligate bacteria populations of the gastrointestinal tract of humans and animals.[2]

The properties of pectic-gel particles largely depend on the chemical composition and macromolecular structure of pectin polysaccharides.[3] Swelling and degradation of pectic-gel particles in the gastrointestinal tract depend on the structural and mechanical characteristics of pectin, the concentration of pectin and the type of metal ion as a cross-linking agent in the composition of pectic-gel particles, concentration of pectinases in the large intestine, pH, and temperature.[1,4,5]

Prolongation of the gastric transit time provides therapeutic benefits for orally delivered drugs by reducing the waste of the drug and the improving the bioavailability and solubility of drugs that are less soluble in high pH environments. Viscous and gel-forming dietary fibers are considered to delay gastric emptying, thus prolonging gastric

***Corresponding author:** Elena A. Mikhailova. Institute of Physiology of Komi Science Centre of the Ural Branch of the RAS, FRC Komi SC UB RAS. Syktyvkar, the Russian Federation. E-mail: elkina@physiol.komisc.ru*

transit time. However, even viscous meals undergo rapid dilution in the stomach, leading to a reduction of the initial viscosity. An alternative approach for the enhancement of gastric digesta viscosity would be to use a solution that forms a gel in the acidic media of the stomach, as pectin was found to do in the acidic conditions of the rat stomach; therefore, the use of pectin as a biopolymer gelling in the stomach appears reasonable. The rheological properties of gastric digesta after the consumption of gel-forming pectin appeared to determine the gastric transit time.[6]

Composite gels based on natural polymers allow the development of new biomaterials with new physicochemical properties that will improve their functionality. Different physicochemical characteristics of composite gel particles based on different pectins can influence their stability and swelling properties in the simulated gastric environment, the environment of the small and large intestines. Composite gel particles based on the different pectins exhibit potential applications as carrier materials in controlled release systems and particularly serve as promising systems for colon-targeted drug delivery.[7]

Previously, the properties of composite gel particles based on pectin and chitosan,[8] pectin and alginate,[7] pectin, and k-carrageenan[9] were obtained and studied. However, there is practically no data on the preparation and properties of composite gel particles formed from 2 different pectins.

The purpose of the present work was to obtain and study the properties of composite CaPGPs obtained from aqueous solutions of AP in the concentration of 2% and heracleuman pectin (HS) in the concentration of 3% in the presence of Ca^{2+} ions (0.34 M). The swelling of the obtained CaPGPs in an artificial gastric environment was also investigated.

Materials and Methods

We used commercial AP AU701 (AP, Herbstreith & Fox KG, Germany) and HS isolated from the aerial part of the Sosnovskyi hogweed *Heracleum sosnowskyi* Manden.[10]

Gel particles were obtained from aqueous solutions of pectins by the method of ionotropic gelation.[11] Composite pectin gels (2% AP+3% HS) were obtained by slowly stirring a mixture of AP (20 mg) and HS (30 mg) in distilled water (1 ml) with a magnetic stirrer MM-5 at heating (45°C) for 4 hours until complete dissolution. Composite CaPGPs were obtained from aqueous solutions of AP (2%) and HS (3%) in the presence of Ca^{2+} ions (0.34 M) by the method of ionotropic gelation.

For comparison, pectin gels were prepared from 2% AP and from 3% HS by dissolving 20 mg of AP or 30 mg of HS on a heated magnetic stirrer (45°C) for 2 or 3.5 hours, respectively, until complete dissolution.

Gel particles of spherical form were prepared by drop-by-drop injection of corresponding pectin solutions from a syringe through a needle with a hole diameter of 0.6 mm on the distance of 4-5 cm in the slowly stirred calcium chloride solution (0.34 M) and further stirring for 30 min at room temperature. The resulting gel particles were then washed three times in distilled water with stirring for 5 minutes and dried for 10-14 h at 37°C.

The diameter and density of CaPGPs were determined using an optical microscope (Altami, Russia) with a camera and an image analysis program (ImageJ 1.46r program, National Institutes of Health, USA). For calibration, a linear scale was used; one pixel corresponded to 0.024 mm.

To determine swelling, dry CaPGPs (1–2 mg) were placed in Petri dishes (diameter 3.5 cm) and incubated in 3 ml of SGF (2 h) with shaking in a shaker (Titramax 1000, Heidolph, Germany) at 100 rpm and at 37°C. SGF was prepared as described previously.[1,12] After 2h, the diameter and density of 100 randomly selected gel particles were measured as described above. The experiments were performed in triplicate. The degree of gel swelling (SD,%) was determined by the formula[8]: $SD = (D_1\text{-}D_0)/D_0 \times 100\%$, where D_1 – diameter of the particles (mm) after 2 h incubation in the medium, D_0 – initial particle diameter of the particles (mm).

The statistical analysis was performed using the statistical software BioStat (version 4.03) and Microsoft Office Excel 2007.

Results and Discussion

The morphological (size, shape) and structural-mechanical (density) characteristics of the obtained wet and dry CaPGPs were investigated.

Table 1 shows the morphological and structural-mechanical characteristics of wet CaPGPs. Wet, spherical, composite gel particles (2% AP+3% HS) have a diameter of 2.62±0.12 mm, which is less than the diameter of wet gel particles from 3% HS (2.81±0.10 mm), but larger than the diameter of wet gel particles from 2% AP (2.50±0.17 mm). The density of wet composite gel particles (0.92±0.13 mg/mm^3) and gel particles from 3% HS (0.93±0.13 mg/mm^3) is practically the same, and higher than the density of wet gel particles from 2% AP (0.76±0.16 mg/mm^3).

Table 1.

Morphological and structural-mechanical characteristics of wet CaPGPs

Gel particles	Diameter, mm	Density, mg/mm^3
2% AP	2.50±0.17	0.76±0.16
3% HS	2.81±0.10	0.93±0.10
2% AP+3% HS	2.62±0.12	0.92±0.13

Table 2 shows the morphological and structural-mechanical characteristics of dry CaPGPs. Dry gel particles from 2% AP were larger (1.18±0.19 mm) than dry gel particles from 3% HS (1.04±0.07 mm) and dry composite gel particles (1.01±0.06 mm). However, dry composite gel particles and dry gel particles from HP were approximately 3 times denser than dry gel particles from AP.

The swelling of the obtained gel particles in an SGF was studied (Fig. 1).

Table 2.

Morphological and structural-mechanical characteristics of dry CaPGPs

Gel particles	Diameter, mm	Density, mg/mm^3
2% AP	1.18±0.19	0.21±0.11
3% HS	1.04±0.07	0.64±0.14
2% AP+3% HS	1.01±0.06	0.62±0.12

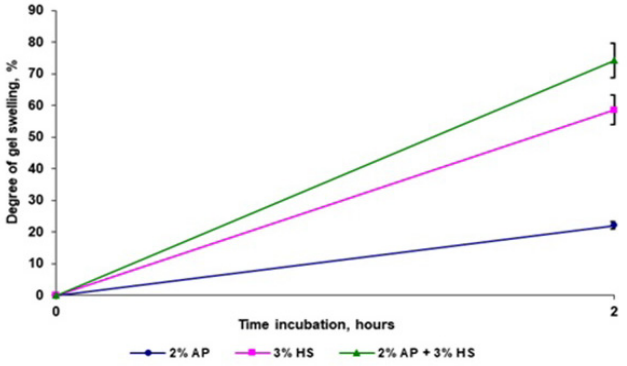

Fig.1. *Swelling of composite CaPGPs formed from AP (2%) and HS (3%) in an SGF.*

Composite CaPGPs swelled by 74.2% in SGF. Gel particles from HS swelled less strongly (by 58.6%), and the degree of swelling of gel particles from AP (by 22.0%) was more than 3 times lower.

Figure 2 shows the density of gel particles swollen in the gastric fluid, compared to the original density of dry gel particles.

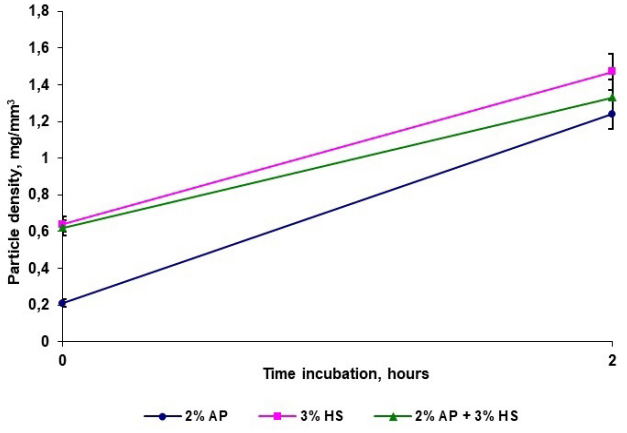

Fig. 2. *Density of composite CaPGPs formed from AP (2%) and HS (3%) in an SGF.*

The density of gel particles from 2% AP after 2h of incubation in SGF increased most strongly, by 1.03 mg/mm^3, in comparison with the density of the original dry particles of AP. To a lesser extent, in an acidic gastric fluid, the density of gel particles from HS and composite gel particles increased by 0.83 mg/mm^3 and 0.71 mg/mm^3, respectively.

Thus, dry composite CaPGPs formed from 2% AP and 3% HS and CaPGPs formed from 3% HS had a comparable diameter and density. The diameter of dry CaPGPs formed from 2% AP was 1.1-1.2 times larger, but their density was 3 times lower than the density of particles in the 2 above-mentioned variants of CaPGPs. Composite CaPGPs swelled by 74.2% in SGF. The degree of swelling in an acidic gastric fluid of CaPGPs formed from HS was 15.6% lower, and CaPGPs formed from AP –52.2%.

Thus, composite CaPGPs swelled in an SGF to a greater extent than CaPGPs formed from AP or CaPGPs formed from HS.

Competing interests

The authors declare that they have no competing interests.

Sources of Funding

The work was performed on the theme of research work (State registration number AAAA-A17-117012310147-8).

References

1. Shubakov AA, Mikhailova EA, Prosheva VI, Belyy VA. Swelling and degradation of calcium-pectic gel particles made of pectins of Silene vulgaris and Lemna minor callus cultures at different concentrations of pectinase in an artificial colon environment. International Journal of Biomedicine. 2018;8(1):60-64. doi: 10.21103/Article8(1)_OA10.
2. Efimtseva EA, Chelpanova TI. [Apples as a sources of soluble and insoluble dietary fibres. The influence of apple fibres on appetite]. Human Physiology. 2020;46(2):121-132. doi: 10.31857/S0131164620020058. [Article in Russian].
3. Volkova MV, Khasanshina ZR, Popov SV, Markov PA. [Gel granules from pectin callus Lupinus angustifolius prevent the premature release of mesalazine]. Biotechnology. 2020;36(1):53-60. doi: 10.21519/0234-2758-2020-36-1-53-60. [Article in Russian].
4. Shubakov AA, Mikhailova EA. Production, properties and transit of copper-pectic gel particles through an artificial gastroenteric environment. International Journal of Biomedicine. 2020;10(4):421-423.doi: 10.21103/Article10(4)_OA18.
5. Shubakov AA, Mikhailova EA. Production, properties and swelling of copper-pectic gel particles in an artificial gastroenteric environment. International Journal of Biomedicine. 2021;11(1):50-52. doi: 10.21103/Article11(1)_OA10.
6. Khramova DS, Vityazev FV, Saveliev NY, Burkov AA, Beloserov VS, Martinson EA, Litvinets SG, Popov SV. Pectin gelling in acidic gastric condition increases rheological properties of gastric digesta and reduces glycaemic response in mice. Carbohydr Polym. 2019;205:456-464. doi: 10.1016/j.carbpol.2018.10.053.

7. Günter EA, Popeyko OV, Belozerov VS, Martinson EA, Litvinets SG. Physicochemical and swelling properties of composite gel microparticles based on alginate and callus cultures pectins with low and high degrees of methylesterification. Int J Biol Macromol. 2020;164:863-870. doi: 10.1016/j.ijbiomac.2020.07.189.
8. Oliveira GF, Ferrari PC, Carvalho LQ, Evangelista RC. Chitosan-pectin multiparticulate systems associated with enteric polymers for colonic drug delivery. Carbohydr Polym. 2010;82(3):1004-1009. doi: 10.1016/j.carbpol.2010.06.041.
9. Günter EA, Martynov VV, Belozerov VS, Martinson EA, Litvinets SG. Characterization and swelling properties of composite gel microparticles based on the pectin and κ-carrageenan. Int J Biol Macromol. 2020;164:2232-2239. doi: 10.1016/j.ijbiomac.2020.08.024.
10. Patova OA, Golovchenko VV, Vityazev FV, Burkov AA, Litvinets SG, Martinson EA, Belyi VA, Kuznetsov SN. Physicochemical and rheological properties of gelling pectin from Sosnowskyi's hogweed (Heracleum sosnowskyi) obtained using different pretreatment conditions. Food Hydrocolloids. 2017;65:77-86. doi: 10.1016/j.foodhyd.2016.10.042.
11. Sriamornsak P. Effect of calcium concentration, hardening agent and drying condition on release characteristics of oral proteins from calcium pectinate gel beads. Eur J Pharm Sci. 1999;8(3):221-227. doi: 10.1016/s0928-0987(99)00010-x.
12. Gebara C, Chaves KS, Ribeiro MCE, Souza FN, Grosso CRF, Gigante ML. Viability of Lactobacillus acidophilus La5 in pectin-whey protein microparticles during exposure to simulated gastrointestinal conditions. Food Res Int. 2013;51:872-878. doi: 10.1016/j.foodres.2013.02.008.

International Journal of Biomedicine 11(2) (2021) 177-180
http://dx.doi.org/10.21103/Article11(2)_CR1

CASE REPORT

INTERNATIONAL JOURNAL OF BIOMEDICINE

The Experience of Surfactant Therapy in Severe COVID-19 Pneumonia: A Case Report

Igor N. Banin[1], PhD; Andrey V. Budnevsky[2], PhD, ScD; Vyacheslav I. Grechkin[2], PhD; Evgeniy S. Ovsyannikov[2], PhD, ScD[*]; Roman E. Tokmachev[2], PhD; Oleg D. Neznamov[1], PhD; Inessa A. Savushkina[1], PGS

[1]Voronezh City Clinical Emergency Hospital №1
[2]Voronezh State Medical University named after N. N. Burdenko
Voronezh, the Russian Federation

Abstract

The COVID-19 pandemic has presented challenges to finding effective treatment for lung damage. Medical researchers from different countries recognize the deficiency of pulmonary surfactant (PS) as a significant cause of the alveolar collapse, followed by microatelectasis and severe disturbances in the ventilation-perfusion relationship. Due to the pathophysiological rationale, experimental confirmations, and accumulated clinical experience, the PS preparations can be used to treat patients with severe COVID-19. The article provides a description of a case when surfactant therapy was successfully used in a patient with severe COVID-19 pneumonia.(**International Journal of Biomedicine. 2021;11(2):177-180.**)

Key Words: COVID-19 • pneumonia • pulmonary surfactant

For citation: Banin IN, Budnevsky AV, Grechkin VI, Ovsyannikov ES, Tokmachev RE, Neznamov OD, Savushkina IA. The Experience of Surfactant Therapy in Severe COVID-19 Pneumonia: A Case Report. International Journal of Biomedicine. 2021;11(2):177-180. doi:10.21103/Article11(2)_CR1

Abbreviations

ARDS, acute respiratory distress syndrome; **BP**, blood pressure, **BT**, blood test; **CT**, computed tomography; **GP,** general practitioner; **HR**, heart rate; **PS**, pulmonary surfactant; **RR**, respiratory rate.

Introduction

In 2019, SARS-CoV-2, a new RNA virus of the genus Betacoronavirus of the family Coronaviridae, was discovered. The disease caused by this virus has been designated by the World Health Organization (WHO) as Coronavirus Disease 2019 (COVID-19). The first case was officially registered in Wuhan, China, in December 2019, and on January 30, 2020, the SARS-CoV-2 outbreak was declared an emergency of international concern. Due to the rapid spread and high contagiousness, the WHO labeled COVID-19 a global pandemic on March 11, 2020. According to the WHO, by March 19, 2021, more than 120.9 million cases had been confirmed worldwide, with more than 2.67 million deaths and more than 91 million patients recovered.

Unfortunately, both etiotropic and pathogenetic pharmacotherapies did not prove their efficacy for the treatment of lung damage and other complications of the disease caused by SARS-CoV-2. This is confirmed by frequent, sometimes multidirectional changes in treatment tactics, none of which has received sufficient recognition in accordance with the provisions of evidence-based medicine. It has been found that type II alveolocytes are one of the many targets for the SARS-

***Corresponding author**: Evgeniy S. Ovsyannikov, PhD, ScD. Department of faculty therapy, Voronezh State Medical University named after N.N. Burdenko. Voronezh, Russia. E-mail: ovses@yandex.ru*

CoV-2 virus. Their deaths are accompanied by a pronounced decrease in the PS synthesis.[1] Medical researchers from different countries recognize the PS deficiency as a significant cause of alveolar collapse, followed by microatelectasis and severe disturbances in the ventilation-perfusion relationship. Besides maintaining the surface tension of alveoli, surfactant activates alveolar macrophages. This physiological mechanism prevents the spread of secondary bacterial infection.

The secondary PS deficiency in the pathogenesis of severe pneumonia and ARDS caused by influenza A/H1N1 was the reason for the experimental use of PS in complex therapy.[2] The pathogenetic substantiation of surfactant therapy for ARDS in influenza A/H1N1 was the reason for attempts at clinical use of various PS preparations during the 2009-2010 epidemic. In these small studies, positive results were obtained: the use of PS preparations improved gas exchange even in patients with critical hypoxemia and allowed avoidance of extracorporeal membrane oxygenation.[3] PS preparations can be used in different medicinal forms: an aerosol through an inhaler or intrabronchially by an endoscope. These preparations work as the patient's own surfactant, which is not produced in an appropriate amount due to damage to type II alveolocytes.

The pathophysiological rationale, experimental confirmations, and accumulated clinical experience served as the basis for an attempt to use PS preparations in the treatment of patients with severe COVID-19. During the COVID-19 pandemic, PS preparations were used to treat patients with severe COVID-19 in the Almazov National Medical Research Centre, the Federal Research and Clinical Center of Physical-Chemical Medicine of the Federal Medical Biological Agency, the I.M. Sechenov First Moscow State Medical University Hospital, and the Perinatal Medical Centre in Tyumen.[4] The analysis of 120 cases of the use of PS preparations showed a decrease in mortality from 80% to 14.3% among patients with severe COVID-19.[5]

Voronezh Clinical Emergency Hospital #1 has been working in the context of the COVID-19 pandemic since March 2020. Clinical experience in the diagnosis and treatment of patients with COVID-19 has been accumulated during this period. We present our experience of using a PS preparation in the treatment of a patient with COVID-19.

Case Presentation

A 47-year-old man, on May 25, 2020, felt sudden nasal congestion and a mild sore throat. During the first day, the symptoms were relieved by the use of a vasoconstrictor and herbal lozenges to reduce the sore throat. He did not seek medical attention. However, five days later (May 30), he felt worse: weakness, a rare unproductive cough, and a feeling of heaviness in the chest appeared; the body temperature increased up to 37.8°C (100.04°F).

Anamnesis vitae

The patient has an active lifestyle, being an amateur athlete who regularly trains at least 2 times a week, undergoes an examination by a GP on a yearly basis. Bad habits and chronic diseases were not registered. The patient denies having any allergic, oncological, or other chronic diseases. According to data from the patient's medical record, BP–125/75 mmHg, HR–56-58 bpm, RR–14-16 rpm, SpO_2–99-100%.

On June 1, 2020, the patient visited a GP. He was prescribed outpatient treatment according to a document developed by an interdisciplinary working group of experts based on Russian and foreign clinical experience – temporary guidelines "Prevention, diagnosis, and treatment of new coronavirus infection (COVID-19)," version 6, relevant at the time of seeking medical help. Standard laboratory tests were performed: clinical BT, biochemical BT, PCR tests for SARS-CoV-2. A positive result of the PCR test was obtained on June 6, 2020. According to the recommendations given by the GP, the patient was taking umifenovir 200 mg 4 times a day, josamycin 500 mg twice a day, ambroxol 30 mg 3 times a day, paracetamol 500 mg.

On June 6, 2020, the patient deteriorated. Exertional dyspnea, weakness, fever, and sweating intensified, the duration of attacks of unproductive paroxysmal cough increased, and therefore he called a specialized ambulance team and was delivered to the Voronezh City Clinical Emergency Hospital #1 with a referral diagnosis of "Coronavirus disease verified by PCR test. Severe community-acquired pneumonia."

Clinical Findings and Diagnostic Assessment

The patient's general condition upon admission to the hospital was characterized as severe. He showed signs of inhibited consciousness and his answers to questions were monosyllabic. The body temperature was 37.8°C (100.04°F).

The results of external examination are the following: the patient had moist and pale skin, cyanosis of the lips. No visible changes of the chest. There was a slight soreness of the intercostal muscles on palpation. RR–28 rpm. Vesicular breathing, weakened; no wheezing in the lungs. No visible changes of the heart area. The apical impulse was in the fifth intercostal space, 1.5 cm medially to the left mid-clavicular line. HR–110 bpm, BP–110/70 mmHg. Heart sounds were muffled, rhythmic. The tongue was dry; the abdomen had a normal shape and was soft and painless on palpation. The liver was not enlarged. Respiratory function was reduced. SpO_2 was 92%-93% breathing with atmospheric air. Laboratory study results are presented in Table 1 (June 7, 2020).

On June 6, 2020, a CT of the chest showed polysegmental pneumonia typical for COVID-19 in both lungs parenchyma, multiple zones of ground-glass opacity merging with each other of peribronchial and subpleural locations. There were more than 3 zones with a maximum diameter of over 5 cm. Lung lesion was about 70%.

Treatment

The patient received hydroxychloroquine 400mg twice on the first day, followed by 200 mg twice a day for the next 6 days, azithromycin 500 mg intravenously for 7 days, direct-acting anticoagulants (Enoxaparin 40 mg a day subcutaneously), and oxygen therapy. Over the next 4 days, despite the ongoing therapy, the patient's condition worsened: dyspnea increased and SpO_2 decreased to 88% in spite of the continuous humidified oxygen therapy. Non-invasive

ventilation in prone positioning was initiated in order to relieve respiratory failure. Considering progressive respiratory failure, therapy was amplified by lopinavir+ritonavir (400mg+100mg) twice a day, interferon beta-1b according to the scheme; methylprednisolone 1000mg for 3 days; ampicillin+sulbactam 3.0g twice a day intravenously followed by meropenem 1.0g three times a day; dalteparin sodium 5000 IU subcutaneously; parenteral nutrition based on combinations of dextrose, potassium chloride, calcium chloride, magnesium chloride, sodium chloride, and malic acid; ascorbic acid 10.0g a day intravenously. However, this therapy was not effective. Dyspnea increased, laboratory parameters reflecting the progression of the systemic inflammatory response were getting worse (high levels of C-reactive protein, ferritin, lactate dehydrogenase by July 13, 2020). Considering these facts and the increased risk of ARDS development, it was decided to add tocilizumab 400 mg by a single intravenous drip infusion.

Table 1.

Dynamics of laboratory and instrumental tests

Parameters	06.07.20	07.13.20	07.18.20	09.03.20
Erythrocytes, $\times10^{12}$/l	5.49	4.8	4.6	3.2
Haemoglobin, mg/l	154	139	134	120
Leukocytes, $\times10^{9}$/l	2.8	11.5	8.9	6.8
Band neutrophils, %	7	10	6	2
Segmented neutrophils, %	68	70	68	64
Lymphocytes, %	21	16	19	25
Eosinophils, %	1	0	0	1
Monocytes, %	3	4	7	8
Thrombocytes, $\times10^{9}$/l	162	150	147	280
CRP, mg/l	197	207	35	10
Ferritin, μg/l	755	1308	1100	255
LDH, U/l	310	360	280	200
SpO2, %	92-93	80-82	83-85	95-96

CRP – C-reactive protein, LDH – lactate dehydrogenase, SpO_2 – oxygen saturation

In the following days, a weak positive change in the patient's condition was noted: normalization of body temperature, a slight decrease in levels of CRP and LDH. However, the low level of oxygen saturation remained for a long time, causing the prolongation of non-invasive ventilation for 76 days. A significant improvement in the patient's condition (dyspnea decreased, SpO_2 increased to 95%-96%) was achieved by double endoscopic endobronchial injection of PS preparation (Poractant Alfa 1.5 ml [120 mg]) into both lungs within 2 days.

Subsequently, stable positive clinical and laboratory dynamics were observed (Table 1). Size reduction of the consolidation areas and ground-glass opacity zones was noted after repeating the CT of the chest on August 31, 2020. There were 2 zones with a maximum diameter over 1.5 cm; lung lesion was under 10%. Subpleural areas of pulmonary fibrosis were found in both lungs. The patient was discharged on the 91st day with two negative SARS-CoV-2 PCR test results.

Discussion

At this moment, the preventive prescription of etiotropic and pathogenetic therapy, until the development of a complete symptom complex and life-threatening conditions, is the main approach, which is based on our one-year experience in managing patients with COVID-19. Several medicines are used in the treatment of COVID-19: favipiravir, remdesivir, umifenovir, interferon-alpha. Clinical studies of the efficacy and safety of targeted drugs in patients with severe or critical COVID-19 are also ongoing. Macrophage activation syndrome (MAS), a form of secondary hemophagocytic lymphohistiocytosis, in COVID-19 is a result of massive uncontrolled activation of the immune system provoked by acute viral infection. Considering this fact, patients should be given immunosuppressive therapy along with symptomatic and etiotropic therapy in the majority of cases to suppress the hyperactivation of the immune system.

However, the lack of effective etiotropic and pathogenetic pharmacotherapy of diseases caused by the SARS-CoV-2 virus led the world medical scientific community to search for ways of treatment using medicines that had previously demonstrated their pathogenetic efficiency. Thus, it is known from previous studies that surfactant therapy for ARDS in influenza A/H1N1 improved gas exchange in patients with hypoxemia. In connection with the damage to type II alveolocytes caused by the SARS-CoV-2 virus and a pronounced decrease of PS synthesis, surfactant therapy can be one of the pathogenetically justified ways of treating COVID-19 patients. The administration of PS preparations is likely to reduce the risk of alveolar collapse and disturbances in the ventilation-perfusion relations, and it also prevents the spread of secondary bacterial infection, which decreases the chance of long-course antibiotic therapy.

Conclusion

This clinical case clearly demonstrates that the therapy for patients with COVID-19 is an extremely complex, dynamically changing process. The management of such patients requires constant monitoring, timely laboratory testing, and an adequate response from medical personnel. The surfactant therapy used to treat the patient with severe SARS-CoV-2-virus-induced pneumonia made it possible to stabilize his condition, improve the ventilation-perfusion ratio, and avoid switching to invasive ventilation. Thus, the presence of secondary PS deficiency in the COVID-19 pathogenesis, as well as surfactant therapy for the disease, is an urgent topic for further research.

Competing Interests

The authors declare that they have no competing interests.

References

1. Takano H. Pulmonary surfactant itself must be a strong defender against SARS-CoV-2. Med Hypotheses. 2020 Nov;144:110020. doi: 10.1016/j.mehy.2020.110020.
2. Witczak A, Prystupa A, Kurys-Denis E, Borys M, Czuczwar M, Niemcewicz M, Kocik J, Michalak A, Pietrzak A, Chodorowska G, Krupski W, Mosiewicz J, Tomasiewicz K. Acute respiratory distress syndrome (ARDS) complicating influenza A/H1N1v infection--a clinical approach. Ann Agric Environ Med. 2013;20(4):820-2.
3. Alekseev AM, Yakovlev AA, Shvechkova MV, Seiliev AA, Volchkov VA, Rosenberg OA. Surfactant therapy for pneumonia and ARDS associated with the A/H1N1 virus. Transbaikalian Medical Bulletin. 2011;1:23-27. [Article in Russian].
4. Averyanov AV, Klypa TV, Balionis OI, Bychinin MV, Cherniak AV, Troitskiy AV, Trifonova EV. Inhaled surfactant in patients with COVID-19 who took high-flow oxygen: the results of a retrospective analysis. Meditsinskiy sovet = Medical Council. 2020;(17):75-80. doi: 10.21518/2079-701X-2020-17-75-80. [Article in Russian].
5. Bautin AE, Avdeev SN, Seyliev AA, Shvechkova MV, Merzhoeva ZM, Trushenko NV, Semenov AP, Lapshin KB, Rozenberg OA. Inhalation surfactant therapy in the integrated treatment of severe COVID-19 pneumonia. Tuberculosis and Lung Diseases. 2020;98(9):6-12. doi: 10.21292/2075-1230-2020-98-9-6-12 [Article in Russian].

International Journal of Biomedicine 11(2) (2021) 181-183
http://dx.doi.org/10.21103/Article11(2)_CR2

CASE REPORT

INTERNATIONAL JOURNAL OF BIOMEDICINE

Radiological Clinical Case of Klippel-Feil Syndrome

V. A. Sorokovikov, PhD, ScD; P. V. Seliverstov, PhD, ScD*;
N. A. Pozdeeva, PhD; U. V. Pichugina, PhD; V. A. Safonov

Irkutsk Scientific Center of Surgery and Traumatology
Irkutsk, Russia

Abstract

Klippel-Feil syndrome (KFS) is a genetically determined anomaly of the cervical spine characterized by the abnormal fusion of vertebrae. The clinical signs are a shortness and a restricted mobility of the neck and a low hairline at the back of the head. KFS is typically associated with many other abnormalities of the skeleton and other systems. The clinical case of KFS first diagnosed in an adult is demonstrated in this review.(**International Journal of Biomedicine. 2021;11(2):181-183.**)

Key Words: Klippel-Feil syndrome • vertebrae • cervical spine • spina bifida

For citation: Sorokovikov VA, Seliverstov PV, Pozdeeva NA, Pichugina UV, Safonov VA. Radiological Clinical Case of Klippel-Feil Syndrome. International Journal of Biomedicine. 2021;11(2):181-183. doi:10.21103/Article11(2)_CR2

Introduction

Klippel-Feil syndrome (KFS) is a rare condition: The prevalence is about 1 in 120,000 newborns but there are no precise data due to lack of population studies. KFS was first described in 1912 in France by neurologist Maurice Klippel and radiologist Andre Feil. This pathology is related to hypoplasia or aplasia of vertebrae, disturbance of cervical segmentation, and retarding of their fusion in the first weeks of gestation.[1,2] There are many hypotheses of KFS development: a vascular disorder, an anomaly of the neural tube, a genetic predisposition, and an insufficiency of facet joint segmentation. It is also thought that it could be the result of mother's alcohol abuse or fetal alcohol syndrome, though the precise cause of the pathology is unknown.[2-4]

A. Feil has classified this syndrome into 3 types. Type I (KFS1) presents a reduced number of cervical vertebrae, usually 4-5. Type II (KFS2) is a synostosis of cervical spinal bodies, the fusion of occipital bone and upper thoracic spine. Type III demonstrates a combination of Type I and Type II with the fusion in the lower thoracic and lumbar spine. The accessory ribs and the spina bifida (incomplete closing of the spinal arcus) are often seen in the cervical spine.

The main clinical triad of findings, typical for KFS, are a short neck, a low posterior hairline, and a limited cervical range of motion. The stage of the shortness of neck varies: In the most severe variant the ear lobes could reach the shoulders, the chin could touch the sternum, and swallowing and breathing are difficult. A wide spreading and a shortening of scapulas are characteristic, an elevation of scapula so typical for Sprengel disease could be seen. In some cases, there are the abnormalities of shoulder muscles and wrinkles on the neck, only rarely a radiculopathy arises, caused by compression of the cervical nerve roots. This syndrome has a negative impact on the internal systems, can provoke a development of severe complications and requires a long-term treatment. A conservative therapy for children with KFS includes massage, medical gymnastics, and physiotherapy. Surgery, such as cervicalisation, is also possible. The prognosis is good for individuals without somatic malformations, but these patients have some serious aesthetic and functional problems.

Verification of diagnosis is based on the typical triad of signs after birth, examination findings, family anamnesis, diagnostic imaging, and genetic analyses. It is possible to diagnose KFS with a detailed description of concomitant

***Corresponding author:** Pavel V. Seliverstov, MD, PhD, ScD. Department of Radiology and Minimally Invasive Surgery, Irkutsk Scientific Center of Surgery and Traumatology. Irkutsk, Russia. E-mail: pavv2001@gmail.com*

anomalies only as a result of the collaboration of different specialists: neurologist, orthopedist, geneticist, cardiologist, nephrologist, pulmonologist, ophthalmologist.[5-12]

Case Presentation

A 33-year-old white man presented to the radiological department of Irkutsk Scientific Center of Surgery and Traumatology for a CT and MRI of the cervical spine. This patient lives in the countryside and works as a logger. In January he suffered an industrial injury (a tree fell). He complained of neck pain and periodical numbness in his fingers at night. Before the trauma, during last 2-3 years, he had fatigue in the neck and occipital region. There were no additional complaints. Visually: there was an insignificant shortness of neck (Figure 1) and limited cervical range of motion.

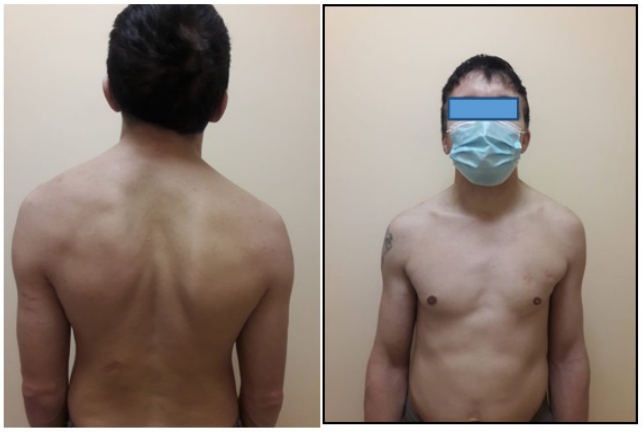

Fig. 1. *The appearance of the KFS patient.*

The cervical and upper thoracic CT (Siemens SOMATOM Scope Power) showed *spina bifida* anterior and posterior at the C1 with diastasis of 0.46-0.47cm; a full concrescense of C2-C3, C5-C6, C7-Th9 vertebrae, an anomaly of C3 as a left-side, hypoplasied, wedge-shaped half-vertebra. A cervical lordosis was transformed into a smooth kyphosis. There was a left-side scoliosis with the top of the curve at the Th3 level with a Cobb angle of 10^0. The intervertebral discs between fused bodies were severely hypoplasied. There was a moderate stenosis of the spinal canal to 1.29 cm at the level of cranial plate of C6. The facet joints between fused vertebrae were consolidated, the joints between the blocks of fused bodies and the uncovertebral joints, also known as the joints of Luschka, had the signs of arthrosis. The posterior parts of the left third and fourth ribs were connected with a wide bone bridge (Figures 2 and 3).

MRI (Siemens MAGNETOM Espree 1.5T MRI System) showed disc herniations at C3-C4 and C5-C6. There were no pathological changes in the spinal cord (Fig.4).

The patient refused to make the genetic analysis, and got the recommendations for physiotherapy and the documents for the disability group.

In conclusion, CT and MRI permit us to visualize the pathologic changes in spine and spinal cord, to evaluate this anomaly. Therefore, it is possible to diagnose KFS, to choose a treatment to provide relief and to improve the quality of life, and to assess the disability group.

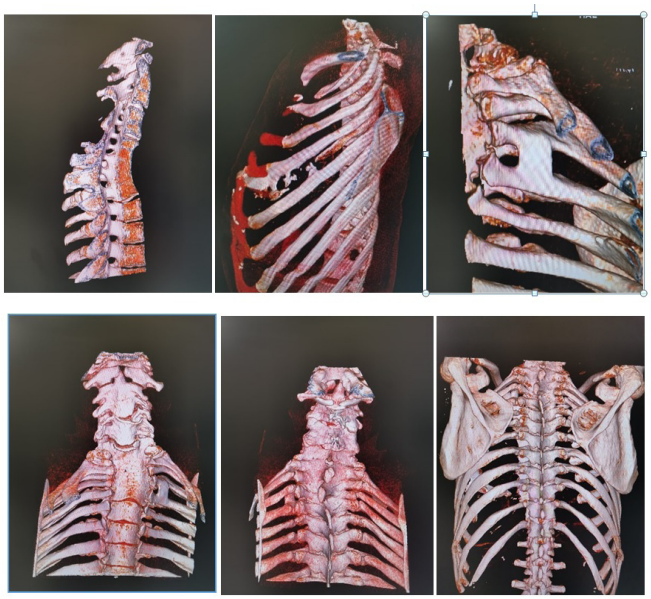

Fig. 2. *Cervical and upper thoracic CT: 3D.*

Fig. 3. *Cervical and upper thoracic CT: MPR.*

Fig. 4. *Cervical and upper thoracic MRI.*

Competing Interests

The authors declare that they have no competing interests.

References

1. Tracy MR, Dormans JP, Kusumi K. Klippel-Feil syndrome: clinical features and current understanding of etiology. Clin Orthop Relat Res. 2004 Jul;(424):183-90.
2. McBride WZ. Klippel-Feil syndrome. Am Fam Physician. 1992 Feb;45(2):633-5.
3. Li Z, Zhao S, Cai S, Zhang Y, Wang L, Niu Y, Li X, Hu J, Chen J, Wang S, Wang H, Liu G, Tian Y, Wu Z, Zhang TJ; DISCO (Deciphering Disorders Involving Scoliosis and COmorbidities) study, Wang Y, Wu N. The mutational burden and oligogenic inheritance in Klippel-Feil syndrome. BMC Musculoskelet Disord. 2020 Apr 11;21(1):220. doi: 10.1186/s12891-020-03229-x.
4. Power BD, Walsh KP, Awan A, Waldron M, O'Grady MJ. Klippel-Feil syndrome as a novel feature of Schimke immunoosseous dysplasia. Am J Med Genet A. 2019 May;179(5):862-863. doi: 10.1002/ajmg.a.61087.
5. Bejiqi R, Retkoceri R, Bejiqi H, Zeka N. Klippel - Feil Syndrome Associated with Congenital Heart Disease. Presentation of Cases and a Review of the Current Literature. Open Access Maced J Med Sci. 2015 Mar 15;3(1):129-34. doi: 10.3889/oamjms.2015.022.
6. Edward JA, Psaltis AJ, Williams RA, Charville GW, Dodd RL, Nayak JV. Endoscopic Resection of Skull Base Teratoma in Klippel-Feil Syndrome through Use of Combined Ultrasonic and Bipolar Diathermy Platforms. Case Rep Otolaryngol. 2017;2017:6384586. doi: 10.1155/2017/6384586.
7. Hitosugi T, Tsukamoto M, Yokoyama T. Anesthetic Management for Twice in a Child with Klippel-Feil Syndrome. Masui. 2017 May;66(5):554-557. [Article in English, Japanese].
8. McLaughlin N, Weil AG, Demers J, Shedid D. Klippel-Feil syndrome associated with a craniocervico-thoracic dermoid cyst. Surg Neurol Int. 2013 Mar 22;4(Suppl 2):S61-6. doi: 10.4103/2152-7806.109440.
9. Ogihara N, Takahashi J, Hirabayashi H, Mukaiyama K, Kato H. Surgical treatment of Klippel-Feil syndrome with basilar invagination. Eur Spine J. 2013 May;22 Suppl 3(Suppl 3):S380-7. doi: 10.1007/s00586-012-2489-3.
10. Pai D, Kamath AT, Kini P, Bhagania M, Kumar S. Concomitant Temporomandibular Joint Ankylosis and Maxillomandibular Fusion in a Child with Klippel- Feil Syndrome: A Case Report. J Clin Pediatr Dent. 2018;42(5):386-390. doi: 10.17796/1053-4625-42.5.11.
11. Stelzer JW, Flores MA, Mohammad W, Esplin N, Mayl JJ, Wasyliw C. Klippel-Feil Syndrome with Sprengel Deformity and Extensive Upper Extremity Deformity: A Case Report and Literature Review. Case Rep Orthop. 2018 Jan 18;2018:5796730. doi: 10.1155/2018/5796730.
12. Tian Y, Fan D, Xu N, Wang S. «Sandwich Deformity» in Klippel-Feil syndrome: A «Full-Spectrum» presentation of associated craniovertebral junction abnormalities. J Clin Neurosci. 2018 Jul;53:247-249. doi: 10.1016/j.jocn.2018.04.047.

International Journal of Biomedicine 11(2) (2021) 184-187
http://dx.doi.org/10.21103/Article11(2)_CR3

CASE REPORT

INTERNATIONAL JOURNAL OF BIOMEDICINE

Endodontic Treatment of Periapical Lesions Using Bioceramic Sealers

Bogdan R. Shumilovich, PhD, ScD; Anna V. Podoprigora, PhD, ScD*; Andrey V. Sushchenko, PhD, ScD; Vladimir V. Rostovtsev, PhD; Irina S. Bishtova, PGS; Iliya V. Stepanov, PhD, ScD

Voronezh State Medical University named after N.N. Burdenko
Voronezh, the Russian Federation

Abstract

This article presents clinical cases of successful endodontic treatment of the main types of combined apical and marginal pathology. Based on the results obtained, the optimal method that ensures a successful treatment result for this pathology in one visit, often without subsequent surgical manipulations, is an adequate endodontic mechanical intervention with subsequent obturation of the root canals with a bioceramic sealer, which is confirmed by the literature data. (**International Journal of Biomedicine. 2021;11(2):184-187.**)

Key Words: cone beam computed tomography • root canal • endodontic treatment

For citation: Shumilovich, BR, Podoprigora AV, Sushchenko AV, Rostovtsev VV, Bishtova IS, Stepanov IV. Endodontic Treatment of Periapical Lesions Using Bioceramic Sealers. International Journal of Biomedicine. 2021;11(2):184-187. doi:10.21103/Article11(2)_CR3

Abbreviations

CBCT, cone beam computed tomography; **MTA**, mineral trioxide aggregate; **MB2**, the second canal of mesiobuccal roots

Introduction

A number of researchers have noted that today in more than 5.7% of the teeth in patients over 40-45 years old with apical periodontal lesions, a comprehensive examination also diagnoses lesions of the marginal periodontium.[1-5] The success of endodontic treatment of such teeth using traditionally used polymer sealers is extremely low.[2,6,7] However, according to the available data, the use of bioceramic sealers that have recently appeared on the market significantly increases the favorable prognosis of endodontic intervention.[6]

Bioceramics inherently are the most biocompatible material and consist of aluminum oxide, zirconium dioxide, bioactive glass, glass ceramics, composite components and coatings, hydroxyapatite and resorbable calcium phosphates. In dentistry, bioceramics based on calcium phosphates are used to restore bone defects, and are based on calcium silicates and bioaggregates (mineral trioxide aggregate, MTA) to ensure the process of apexification and filling of endodontic perforations.[9-11]

Combined apical-marginal lesions develop when the pre-cement is damaged under the influence of bacterial flora from the periodontal sulcus and root canal.[12-14] According to data from studies, the mixed apical-periodontal microflora were found in 21.1% of all patients with this pathology.[10,13] As a rule, there are three types of periodontal lesions: sinusitis (in cases of the upper jaw), lesions in the furcation of the roots, and lesions of the marginal periodontium.[6]

***Corresponding author**: Prof. Anna V. Podoprigora, PhD, ScD. Department of Maxillofacial Surgery, Voronezh State Medical University named after N.N. Burdenko. Voronezh, Russia. E-mail: ovses@yandex.ru*

In addition, the literature indicates a low predictability of the outcome of the treatment of such lesions.[8,11] Classic treatment protocols involve a surgical impact on the content of the bone defect and the removal of granulation tissue with its subsequent restoration and plastics of the soft tissues of the gums.[15,16] This article presents two clinical cases of endodontic treatment of combined apical-marginal periodontal lesions of the molar.

Case Presentation 1

A 49-year-old man presented to the dental clinic for tooth 3.7. In his medical history, somatic diseases were absent. The patient indicated previous endodontic treatment was carried out 6-7 years ago. Percussion of the tooth was painful, thermotest showed a lack of sensitivity, the tooth was filled with composite material, the depth of the periodontal sulcus was within normal limits (<3 mm), except for the distal surface of the tooth. In this area, a periodontal pocket with a depth of 7 mm was determined.

When analyzing the diagnostic CBCT scan, a large area of lightening with indistinct contours was visualized, partially passing over to the vestibular and lingual surfaces of the distal root 3.7 (Figure 1, a-c). The root canals were obturated along the entire length; after creating a direct endodontic access, a paste containing eugenol was found in them (Figure 1, d). After discussing all possible options with the patient, we decided on endodontic intervention for the 3.7 tooth as the first stage of a comprehensive treatment plan, followed by periodontal treatment and orthopedic correction of the occlusion state.

Treatment was performed under magnification using an operating microscope. After local anesthesia, the tooth was isolated and an endodontic access cavity was formed. Next, root canals were disinfected using ProTaper Universal Manual S1 and S2 and abundant irrigation with a 3% sodium hypochlorite solution. Instrumental processing was carried out according to the "long" protocol HyFlex EDM (Coltene, Switzerland) with intermediate active irrigation with a 5% sodium hypochlorite solution with an endoactivator and EDTA 17% solution (Figure 1, e).

Protocol (step by step):

• MB – HyFlex 20/05 EDM, 25/~ EDM, 30/04 CM, 40/04 EDM, 50/03 EDM. MAF – 50/03;

• ML – HyFlex 20/05 EDM, 25/~ EDM, 30/04 CM, 40/04 EDM, 50/03 EDM. MAF – 50/03;

• D – HyFlex 20/05 EDM, 25/~ EDM, 40/04 EDM, 50/03 EDM, 60/02 EDM, H-file 70/02. MAF – 70/02.

Root canal obturation was performed with the GuttaFlow bioseal system (Coltene, Roeko, Germany) containing bioglass, according to the one-pin technique (Figure 1, f). The endodontic access cavity was hermetically closed with a composite. Postoperative CBCT showed complete hermetic root canal filling (Figure 1, g-h). On CBCT after 6 months, the regenerative processes in the bone tissue were clearly defined (Figure 1, i). Subsequent X-ray control was performed 12 months after treatment (Figure 1, j): Bone tissue was almost completely restored, the periodontal pocket was not probed, and there were no complaints.

Case Presentation 2

A 30-year-old woman presented to the dental clinic with a referral from an otolaryngologist. In his medical history, somatic diseases were absent. The causal tooth was 1.6. Local examination: the previous endodontic therapy, the tooth was asymptomatic. CBCT visualized a lightening area with indistinct contours in the periapical region of all roots (Figure 2, a-b). The root canals were obturated along their entire length. When analyzing the diagnostic CBCT, the first cause of the complication was the presence of MB2 (Figure 2, c).

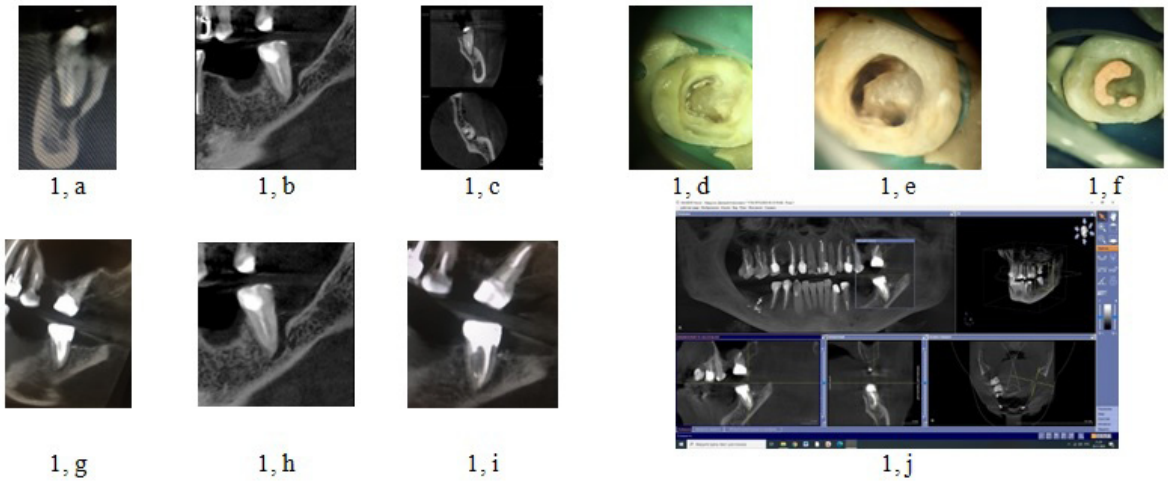

Fig. 1. *a-c) Fragment of CBCT: Initial clinical status (06/26/2019) (tooth 3.7) – the resorption lacuna is visualized as a lightening area with indistinct contours on the distal side of the distal root; d) View of the access cavity, remnants of obturation material; e) View of the cavity after mechanical treatment of root canals; f) View of the cavity after obturation of root canal treatment with GuttaFlow bioseal; g-h) Postoperative CBCT demonstrating complete hermetic root canal filling; i) Fragment of CBCT – 6 months after treatment (01/28/2020). j) Fragment of CBCT – 12 months after treatment (06/23/2020).*

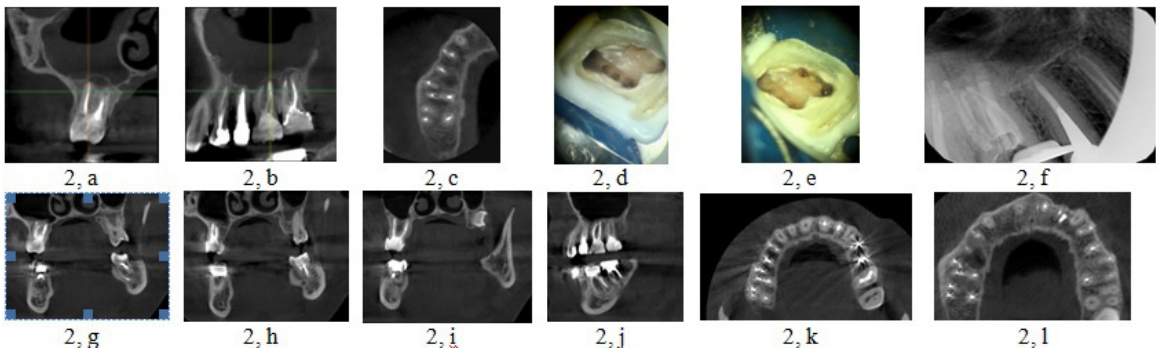

Fig. 2. *a) CBCT (coronal section). The first upper molar on the right (1.6), a "bone" defect and changes in the maxillary sinus are visualized; b) CBCT (lateral section). The first upper molar on the right (1.6), a "bone" defect and changes in the maxillary sinus are visualized; c) CBCT (axial section). The first upper molar on the right (1.6), a "bone" defect is visualized; d-e) Tooth appearance after mechanical treatment of root canals; f) Aiming X-ray of root canal obturation control; g-i) Control CBCT: 11 months after treatment (coronary section); j) Control CBCT: 11 months after treatment (lateral section); k-l) Control CBCT: 11 months after treatment (axial section).*

However, the radiological picture in the region of the buccal distal canal, where the presence of an additional canal was also suggested, alerted us that there might be further problems..

After discussion with the patient, the decision was made in favor of endodontic treatment. Treatment was performed under magnification using an operating microscope. After local anesthesia, the tooth was isolated and an endodontic access cavity was formed. Then the root canals were disinfected with the Remover 30/07 instrument (MicroMega, Coltene, Switzerland). The clinical picture exceeded all expectations and caused us to make serious adjustments to the existing information about the anatomy of the root canals. A total of 7 root canals were identified (Figure 2, d-e). Then the channels were processed according to the following protocol:

• MB1 – HyFlex EDM 20/05, EDM 25/~, CM 30/04, EDM 40/04. MAF – 40/04;

• MB2 – HyFlex EDM Glidepath 10/05, EDM 15/03, EDM 20/05, EDM 25/~, CM 30/04. MAF – 30/04;

• MB3 – HyFlex EDM Glidepath 10/05, EDM 15/03, EDM 20/05, EDM 25/~. MAF – 25/~;

• DB1 – HyFlex EDM 20/05, EDM 25/~, CM 30/04, EDM 40/04, EDM 50/03. MAF – 50/03;

• DB2 – HyFlex EDM Glidepath 10/05, EDM 15/03, EDM 20/05, EDM 25/~, CM 30/04, EDM 40/04. MAF – 40/04;

• DB3 – HyFlex EDM Glidepath 10/05, EDM 15/03, EDM 20/05, EDM 25/~, CM 30/04. MAF – 30/04;

• Palatinal – HyFlex EDM 20/05, EDM 25/~, EDM 40/04, EDM 50/03, EDM 60/02, H-file 80/02. MAF – ≥80/02.

Buccal obturation was performed with GuttaFlow bioseal (Coltene, Roeko, Germany) (Figure 2, f). In the palatal canal, due to significant resorption of the apical part, the apical third of the canal was filled with BioDentin (Dentsply, Switzerland), then GuttaFlow bioseal. On the CBCT fragments after 11 months (Figure 2, g-l), the restoration of bone tissue in the periapical region was verified by the normalization of the X-ray picture in the area of the maxillary sinus, which was confirmed by the otolaryngologist.

Discussion

This article presents clinical cases of successful endodontic treatment of the main types of combined apical and marginal pathology.

The properties of bioglass were described for the first time in the works of L. Hench.[17,18] Preservation of the original anatomy of the root canal during its preparation plays an extremely important role.[6,19] In all demonstrated clinical cases, new HyFlex EDM files (Coltene, Switzerland) were used for instrumentation. The choice of files was dictated by the basic requirements for a rotary instrument in the treatment of such pathologies:

• A minimum lateral load (i.e. high centering properties and inability to cause the transport of the root canal) so with repeated endodontic intervention, the walls of the root canal are already weakened and there is a danger of "tape" perforations.

• An availability of "large" sizes (> 40 ISO) for effective necrotomy.

HyFlex EDM files are fully compliant with these requirements. In addition, they have a controlled shape-memory effect, and at the same time are characterized by a unique combination of the highest flexibility and resistance to breakage.[20] HyFlex EDM NiTi files are manufactured using the EDM method. The working part of the file is processed by the thermal action of pulsed electrical discharges, excited between the electrode-tool and the workpiece, due to which the entire surface of the EDM file is working, and not just the edges as in tools made by the classical milling method.[21] Also, HyFlex EDM files have a changed phase composition and can be deformed due to the reorientation of the formed martensite, which increases their resistance to torsion loads in comparison with other files, including those made using Wire technology.[22]

Also, in such clinical situations, it is necessary to emphasize the importance of CBCT, which provides comprehensive information on the location of the resorption defect in relation to periodontal tissues, tooth tissues and a number of anatomical formations (maxillary sinus, mandibular

canal, etc.).[23,24] It should be noted that, as with any device emitting ionizing radiation, the use of CBCT is justified only if the benefits significantly outweigh the risks. In order to avoid mistakes in diagnosis and harm to the patient, it is important to consider the ALARA principle (As Low As Reasonably Achievable). In accordance with the ALARA concept, the diagnostic effect should certainly be higher than the risk of radiation-induced diseases.[25]

Several studies have also suggested the use of calcium hydroxide paste to treat the comorbidity described above over several visits.[26] However, when choosing such a treatment option, care should be taken when introducing material into the area of the defect due to possible mechanical and chemical irritation of the periodontal tissues, which worsens the prognosis of treatment.[8] Thus, an adequate endodontic mechanical intervention followed by root canal obturation with a bioceramic sealer is the optimal method that ensures a successful treatment of combined apical and marginal lesions of the periodontium in one visit, often without subsequent surgical procedures.[6,8,11]

Competing Interests

The authors declare that they have no competing interests.

References

1. Barros J, Silva MG, Rôças IN, Gonçalves LS, Alves FF, Lopes MA, Pina-Vaz I, Siqueira JF Jr. Antibiofilm effects of endodontic sealers containing quaternary ammonium polyethylenimine nanoparticles. J Endod. 2014 Aug;40(8):1167-71. doi: 10.1016/j.joen.2013.12.021.
2. Tsesis I, Nemcovsky CE, Nissan J, Rosen E. Endodontic-Periodontal Lesions. Evidence-Based Multidisciplinary Clinical Management. Springer; 2019.
3. Amine Kh, El Kholti W, Kissa Ja, Periodontal Root Coverage. An Evidence-Based Guide to Prognosis and Treatment. Springer; 2019.
4. Duncan HF, Cooper PR. Clinical Approaches in Endodontic Regeneration. Current and Emerging Therapeutic Perspectives. Springer; 2019.
5. Peters OA. The Guidebook to Molar Endodontics. Springer; 2017.
6. Jain P. Common Complications in Endodontics. Prevention and Management. Springer; 2018.
7. Hosseinpour S, Walsh LJ, Moharamzadeh K. Regenerative Approaches in Dentistry. An Evidence-Based Perspective, Springer; 2021.
8. Shacham M, Levin A, Shemesh A, Lvovsky A, Ben Itzhak J, Solomonov M. Accuracy and stability of electronic apex locator length measurements in root canals with wide apical foramen: an ex vivo study. BDJ Open. 2020 Nov 17;6(1):22. doi: 10.1038/s41405-020-00052-3.
9. Shumilovich BR, Sushchenko AV, Morozov AN, Kharitonov DU. Comparative clinical and laboratory characteristics of the quality of the filling of root canals using three obturation systems. Dent Oral Craniofac Res. 2015;1(5):160-169.
10. Yilmaz HG, Kalender A, Cengiz E. Use of mineral trioxide aggregate in the treatment of invasive cervical resorption: a case report. J Endod. 2010 Jan;36(1):160-3. doi: 10.1016/j.joen.2009.07.002.
11. Tsesis I, Fuss Z. Diagnosis and treatment of accidental root perforations. Endodontic Topics. 2006;13(1):95-107.
12. Zhou X, Li Yu. Atlas of Oral Microbiology: From Healthy Microflora to Disease. Springer; 2020.
13. Fuss Z, Tsesis I, Lin S. Root resorption--diagnosis, classification and treatment choices based on stimulation factors. Dent Traumatol. 2003 Aug;19(4):175-82. doi: 10.1034/j.1600-9657.2003.00192.x.
14. Tronstad L. Root resorption--etiology, terminology and clinical manifestations. Endod Dent Traumatol. 1988 Dec;4(6):241-52. doi: 10.1111/j.1600-9657.1988.tb00642.x.
15. Heithersay GS. Treatment of invasive cervical resorption: an analysis of results using topical application of trichloracetic acid, curettage, and restoration. Quintessence Int. 1999 Feb;30(2):96-110.
16. Asgary S, Nosrat A. Conservative Management of Class 4 Invasive Cervical Root Resorption Using Calcium-enriched Mixture Cement. J Endod. 2016 Aug;42(8):1291-4. doi: 10.1016/j.joen.2016.05.001.
17. Hench L. Bioceramics. J Amer Ceram Soc. 1998;81(7):1705-1728.
18. Katsamakis S, Slot DE, Van der Sluis LW, Van der Weijden F. Histological responses of the periodontium to MTA: a systematic review. J Clin Periodontol. 2013 Apr;40(4):334-44. doi: 10.1111/jcpe.12058.
19. Wigler R, Koren T, Tsesis I. Evaluation of Root Canal Cleaning and Shaping Efficacy of Three Engine-driven Instruments: SafeSider, ProTaper Universal and Lightspeed LSX. J Contemp Dent Pract. 2015 Nov 1;16(11):910-4. doi: 10.5005/jp-journals-10024-1780.
20. Zupanc J, Vahdat-Pajouh N, Schäfer E. New thermo-mechanically treated NiTi alloys - a review. Int Endod J. 2018 Oct;51(10):1088-1103. doi: 10.1111/iej.12924.
21. Pirani C, Iacono F, Generali L, Sassatelli P, Nucci C, Lusvarghi L, Gandolfi MG, Prati C. HyFlex EDM: superficial features, metallurgical analysis and fatigue resistance of innovative electro discharge machined NiTi rotary instruments. Int Endod J. 2016 May;49(5):483-93. doi: 10.1111/iej.12470.
22. Iacono F, Pirani C, Generali L, Bolelli G, Sassatelli P, Lusvarghi L, Gandolfi MG, Giorgini L, Prati C. Structural analysis of HyFlex EDM instruments. Int Endod J. 2017 Mar;50(3):303-313. doi: 10.1111/iej.12620.
23. European Society of Endodontology position statement: External Cervical Resorption. European Society of Endodontology (ESE) developed by Dummer PMH, Patel S, Lambrechts P, Shemesh H, Mavridou A. Int Endod J. 2018 Dec;51(12):1323-1326. doi: 10.1111/iej.13008.
24. Rosen E, Taschieri S, Del Fabbro M, Beitlitum I, Tsesis I. The Diagnostic Efficacy of Cone-beam Computed Tomography in Endodontics: A Systematic Review and Analysis by a Hierarchical Model of Efficacy. J Endod. 2015 Jul;41(7):1008-14. doi: 10.1016/j.joen.2015.02.021.
25. Rosen E, Tsesis I. [Use of Cone Beam Computed Tomography in endodontics: rational case selection criteria]. Refuat Hapeh Vehashinayim (1993). 2016 Jan;33(1):35-44, 62. [Article in Hebrew).
26. Baratto-Filho F, Limongi O, Araújo Cde J, Neto MD, Maia SM, Santana D. Treatment of invasive cervical resorption with MTA: case report. Aust Endod J. 2005 Aug;31(2):76-80. doi: 10.1111/j.1747-4477.2005.tb00232.x.

Online-Only Articles

International Journal of Biomedicine 11(2) (2021) 188-196
http://dx.doi.org/10.21103/Article11(2)_OA11

ORIGINAL ARTICLE

Obstetrics and Gynecology

INTERNATIONAL JOURNAL OF BIOMEDICINE

The Effect of Vitamin D Metabolic Status and Endometrial Immune Patterns on the Outcomes of ART Programs

Elena G. Chukhnina[1], PGS; Evgeny L. Kazachkov[1], PhD, ScD; Ekaterina E. Voropaeva[1], PhD, ScD; Ella A. Kazachkova[1], PhD, ScD; Miroslava L. Polina[2], PhD; Natalya I. Douglas[3], PhD, ScD

[1]*South Ural State Medical University, Chelyabinsk, Russia*
[2]*Women's Health Medical Center, Moscow, Russia*
[3]*Medical Institute of North-Eastern Federal University named after M.K. Ammosov, Yakutsk, Russia*

Abstract

The objective of this study was to assess the possibility of predicting the outcomes of *in vitro* fertilization (IVF) and IVF/ICSI (intracytoplasmic injection [transfer] of sperm into eggs), protocols based on the serum vitamin D content and endometrial expression of vitamin D receptor (VDR), CD4+T cells, and CD8+T cells.

***Methods and Results*:** The results of IVF and IVF/ICSI programs were analyzed in 147 patients of older reproductive age (36-44 years of age) with tubal-peritoneal factor of infertility. Depending on the outcomes of ART programs, 2 groups were formed. Group 1 included 37 women with the onset of pregnancy; Group 2 included 110 women with negative outcomes of ART programs.

The level of 25(OH)D in the blood serum and follicular fluid (FF) was assessed. The sampling of the material (blood and FF) was carried out on the day of ovarian puncture, the 25(OH)D content – at least three days after the last administration of the drug. Anti-Müllerian hormone (AMH) was determined using AMH reagent (AMH Gen II ELISA) and the Beckman Coulter Access® 2 Immunoassay System (Beckman Coulter, Inc. USA). Morphological examination of the endometrium was performed after biopsy sampling by pipelle biopsy on Day 7 after confirmed ovulation in the cycle preceding ART. The endometrial expression of VDR, CD4+Tcells, and CD8+Tcells was evaluated in 68 women of the sample: 18 – with pregnancy, 50 – with negative outcomes in ART programs.

Vitamin D deficiency (<20 ng/ml) in peripheral blood was detected only in Group 2. Low levels of vitamin D (20-<30ng/ml) in women of this group were four times more frequent (p=0.008) than in Group 1. Women with the onset of clinical pregnancy were more often distinguished by the optimal content of vitamin D in biological fluids – almost twice as much as those with ineffective attempts to treat infertility (*P*=0.009 for peripheral blood). The mean value of the 25(OH)D content in the blood serum in both groups did not differ; in FF it was significantly higher in Group 1 than in Group 2 (*P*=0.003). A strong correlation was revealed between the content of 25(OH)D in the blood serum and FF (r=0.67, *P*=0.003 in both groups), a weak correlation – in cases where it was impossible to sample oocytes and/or embryos (r=0.48, *P*=0.06). The VDR expression in stromal epithelium was higher in Group 2 than in Group 1 (*P*=0,016). It is calculated that a 1% decrease in VDR expression in the stroma increases the chance of a favorable outcome by 1.35 times.The density of labels of CD4+T cells and CD8+T cells in the endometrial stroma did not differ significantly between groups. The expression of CD4+T cells and CD8+T cells in endometrial samples taken from the same infertile women in different phases of the menstrual cycle showed no statistically significant differences.

Conclusion: Morphofunctional peculiarities of the endometrium of infertile women are the basis for predicting the outcomes of ART programs and preparing for pregnancy. **(International Journal of Biomedicine. 2021;11(2):188-196.)**

Key Words: assisted reproductive technology • follicular fluid • 25(OH)D • vitamin D receptor

For citation: Chukhnina EG, Kazachkov EL, Voropaeva EE, Kazachkova EA, Polina ML, Douglas NI. The Effect of Vitamin D Metabolic Status and Endometrial Immune Patterns on the Outcomes of ART Programs. International Journal of Biomedicine. 2021;11(2):188-196. doi:10.21103/Article11(2)_OA11

Abbreviations

ART, assisted reproductive technology; **AMH**, anti-Müllerian hormone; **FF**, follicular fluid; **FSH**, follicle-stimulating hormone; **IVF**, *in vitro* fertilization; **ICSI**, intracytoplasmic sperm injection; **OR**, ovarian reserve; **VDR**, vitamin D receptor.

Introduction

Implantation failures are one of the reasons for the ineffectiveness of ART programs, often due to abnormal molecular transformation of the «implantation window» period.[1] Disturbances in the embryo integration process aroused interest in analyzing the expression of regulatory and structural proteins of the endometrium, prostaglandins, cytokines, growth factors, surface epithelial cells with the presence of mature pinopodia, and steroid hormone receptors during the "implantation window." [2-4]

The involvement of some cell adhesion proteins in the stromal decidualization, necessary for embryo implantation, indicates the prospects of analyzing their expression.[5,6]

Interest in the role of vitamin D in the functional activity of the endometrium is due to its numerous biological functions – regulation of not only calcium-phosphorus metabolism, but also anti-inflammatory and antiproliferative effects.[7] The developed VDR network in the organs of the reproductive system (ovaries, endometrium, fallopian tube epithelium, placenta, decidual cells, hypothalamus and pituitary gland) explains its prognostic potential in the study of infertility causes.[8,9] The role of vitamin D as a cofactor for changes in endometrial activity (proliferation processes, secretory transformations, desquamation) has been studied mainly in experiments on biological models.

The effect of vitamin D on the endometrium is carried out by various mechanisms – the formation of a ligand-dependent transcription factor in the cell nucleus for the regulation of target genes and non-genomic effects due to the connection with cytosolic and membrane receptors.[10,11]

The steroid activity of vitamin D determines the ability to modulate genes encoding proteins involved in the processes of proliferation, differentiation, and apoptosis. An indicator of the body's vitamin D saturation is the circulation of the intermediate active metabolite 25(OH)D in the blood, but the effectiveness of regulation of the signaling pathways is caused by the interaction of vitamin D with VDR in the endometrium.[10,12,13]

VDR expression under the influence of genetic and epigenetic factors leads to change in the metabolism of vitamin D in the endometrium.[14] The effect of the active 1,25-dihydroxyvitamin D3 [1,25(OH)2D3] form on the expression of immune and hormone-mediated reactions determines the role of 1,25(OH)2D3 deficiency in the genesis of gynecological diseases.[7]

Unsatisfactory outcomes of ART programs among women with vitamin D deficiency were noted by Pacis et al.[15] In ART programs, there have been reports of the correlation of serum vitamin D with the quality of oocytes,[16] AMH, the number of antral follicles,[17,18] the number and quality of embryos,[19] and the frequency of clinical pregnancy[20,21] and live birth.[19,22,23]

The relationship of 25(OH)D content in the blood serum and FF with the outcomes of ART programs, in particular the frequency of pregnancy, is denied by many researchers.[23-25] Similar observations were made in women with infertility, polycystic ovary syndrome, and normal OR.[26] The lack of correlation of vitamin D levels with ovarian response to stimulation and embryo quality in IVF/ICSI cycles, especially when using donor oocytes, suggests the influence of vitamin D on the morphofunctional state of the endometrium.[20,21]

The negative results may be explained by the need to analyze the mechanisms of interaction between the active form of vitamin D and the functional VDR activity in the endometrium of women with infertility. Effective interaction between the endometrium and the blastocyst during the implantation window suggests maternal tolerance, determined by the consistency of local immune patterns.[14]

An imbalance in the Th1/Th2 subset of CD4+Tcells with a predominance of the Th1 subset producing proinflammatory cytokines is indicated as a possible cause of miscarriage.[27] Vitamin D regulation of systemic and local immune responses is associated with the ability of Th2 cells to induce cytokines IL-4, IL-5, IL-6, IL-9, IL-10, and IL-13 and to reduce the proliferation of Th1 cells.[6,28]

The search for factors that improve reproductive outcomes, especially in IVF-ICSI cycles, has led to an interest in assessing the content of vitamin D in blood serum and the expression of its receptors and individual immune clusters in the endometrium.

The objective of this study was to assess the possibility of predicting the outcomes of *in vitro* fertilization (IVF) and IVF/ICSI (intracytoplasmic injection [transfer] of sperm into eggs), protocols based on the serum vitamin D content and endometrial expression of VDR, CD4+T cells, and CD8+T cells.

Materials and Methods

The results of IVF and IVF/ICSI programs were analyzed in 147 patients of older reproductive age (36-44 years of age) with tubal-peritoneal factor of infertility in the Center of Obstetrics and Gynecology #1 (Chelyabinsk) and the Medical Center for Women's Health (Moscow), using their own oocytes in "fresh" cycles and cryoprotocols (in delayed embryo transfer, for example, due to preimplantation genetic diagnosis).

Inclusion criteria for the study were tubal factor of infertility, normal or reduced ovarian reserve with a preserved regular ovulatory menstrual cycle, use of the patient's own oocytes, normozoospermia or mild pathozoospermia.

Exclusion criteria were oocyte donation, uterine fibroids more than 3cm, polycystic ovary syndrome, HIV infection, hepatitis B and C.

Depending on the outcomes of ART programs, 2 groups were formed. Group 1 included 37 women with the onset of pregnancy; Group 2 included 110 women with negative outcomes of ART programs. Embryos were obtained in 115 women, and a negative result (absence of oocytes and/or embryos) occurred in 32 women.

We performed 53 programs of IVF and 94 programs of IVF/ICSI. Pregnancy rate was 25.7% per cycle, 32.2% – for the transfer. One hundred and eighteen women used a stimulation protocol with antagonists of gonadotropin-releasing hormones (GnRH), 8 – a long classic protocol, 14 – a modified long protocol with half doses of GnRH agonists, 7 – a short protocol with agonists. The average duration of stimulation was 10.4±1.7 days.

Obtaining oocytes, fertilization, cultivation and transfer of embryos (no more than two), support of the luteal phase with progesterone preparations in the post-transfer period was carried out according to the existing recommendations. Only clinically confirmed pregnancy was taken into account on sonographic imaging of the ovum.

In this sample (n=147), the level of 25(OH)D in the blood serum and FF was assessed. The sampling of the material (blood and FF) was carried out on the day of ovarian puncture, the 25(OH)D content – at least three days after the last administration of the drug.

AMH was determined using AMH reagent (AMH Gen II ELISA) and the Beckman Coulter Access® 2 Immunoassay System (Beckman Coulter, Inc. USA). The studies were carried out on the basis of the central research laboratory of the South Ural State Medical University, the laboratory "Gemotest" (Moscow) using the ELISA system (Personal Lab) and the 25(OH) Vitamin D ELISA kit (Euroimmun AG, Germany).

Ultrasound examination was performed to assess induced folliculogenesis and pregnancy (Voluson E6 system, GE Healthcare, USA).

Morphological examination of the endometrium was performed after biopsy sampling by pipelle biopsy on Day 7 after confirmed ovulation in the cycle preceding ART. Of these, 20 women who underwent hysteroscopy, had additional endometrial sampling during the proliferative phase of the menstrual cycle. The endometrial samples were processed according to the standard technique to obtain paraffin sections with a thickness of 3-5 microns. Morphological studies were performed at the Department of Pathological Anatomy and Forensic Medicine of the South Ural State Medical University (SUSMU). For histological examination, the standard method of fixation in 10% neutral formalin and embedding in paraffin was used. After dewaxing, the sections were stained with hematoxylin and eosin.

The endometrial expression of VDR, CD4+Tcells, and CD8+Tcells was evaluated in 68 women of the sample: 18 – with pregnancy, 50 – with negative outcomes in ART programs. In this sample, 25 IVF programs and 43 IVF/ICSI programs were carried out.

For the immunohistochemical study of endometrial biopsies, the avidin-biotin immunoperoxidase method was used, with standard sets of polyclonal rabbit antibodies against VDR, CD4+T cells, CD8+T cells. The Histophine detection system was used to visualize the primary antibodies.

VDR expression was assessed by counting and percentage of stained stromal cells and endometrial glandulocytes. CD4+ and CD8+ endometrial stromal lymphocytes.

Morphofunctional assessment of the endometrium was performed using licensed software ("Morphology 5.2," Russia). The preparations were examined and photographed using a Primo Star microscope(Carl Zeiss, Germany), with the help of a Pixera Pro 150ES digital camera (Canon, Japan) at an operating magnification of x400.

All patients were informed about the purpose and design of the work and gave their consent to participate in the study and publish its results in the open press. The study was approved by the SUSMU Ethics Committee.

Statistical analysis was performed using the IBM SPSS Statistics for Windows, Version 21.0. Armonk, NY: IBM Corp.). The normality of distribution of continuous variables was tested by the Kolmogorov-Smirnov test with the Lilliefors correction and Shapiro-Wilk test. Continuous variables with normal distribution were presented as mean (standard deviation [SD]); non-normal variables were reported as median (interquartile range [IQR])._Means of 2 continuous normally distributed variables were compared by independent samples Student's t test._Differences of continuous variables departing from the normal distribution, even after transformation, were tested by the Mann-Whitney U-test. The frequencies of categorical variables were compared using Pearson's chi-squared test or Fisher's exact test, when appropriate. Spearman's rank correlation coefficient was calculated to measure the strength and direction of the relationship between two variables. Pearson's Correlation Coefficient (r) was used to determine the strength of the relationship between the two continuous variables. A value of $P<0.05$ was considered significant.

Results and Discussion

The initial characteristics of infertile patients and the results of IVF and IVF-ICSI in the two groups are presented in Table 1. There were no statistically significant differences in the serum content of AMH, FSH, the duration of the menstrual cycle, the results of IVF and IVF-ICSI protocols, as well as the thickness of the endometrium on the day of embryo transfer.

Table 1.
The results of IVF and IVF-ICSI in the two groups

Parameter	Group 1 (n= 18)	Group 2 (n= 50)	*P*-value
Age of women. yrs	38 (37.5;39.5)	40 (38;41)	0.139
Duration of the menstrual cycle	28 (28;28.5)	28 (28;29)	0.771
AMH, ng/ml	2.51 (1.60;3.68)	1.4 (0.74;2.90)	0.170
FSH, мME/ml	7.45 (5.72;7.80)	6.14 (5.14;8.70)	0.337
Duration of stimulation	10 (10;11)	11 (10;11.25)	0.108
Gonadotropin doses	2112.50 (1500;2250)	2025 (1650;2475)	0.480
The number of follicles obtained	8.5 (4.75;14.25)	5.5 (3;10)	0.690
Number of oocytes obtained	6.5 (4;11.5)	4.0 (2;8)	0.058
Number of embryos obtained	5.0 (2;9.25)	3.0 (1;4)	0.003
Transfer day	5 (4;5)	5 (3;5)	0.558
Number of transferred embryos	2 (1.75;2)	1 (1;2)	0.290
Endometrial thickness, mm	10.35 (9;12)	9.6 (8.97;12)	0.316

The number of obtained embryos in the group with favorable outcomes of IVF and IVF-ICSI protocols turned out to be almost one and a half times higher than with negative ones (P=0.003).

Data on the vitamin D content in women's biological fluids, depending on the outcomes of the embryonic stage in IVF programs, are presented in Table 2. There were no differences in the content of 25(OH)D in the peripheral blood in the groups of infertile women; however, the mean vitamin D values in FF were higher, with the highest values in the group with the obtained embryos (P=0.003). The level of vitamin D in biological fluids of women with different AMH did not show any statistically significant differences (60.7±25.6 and 80.3±24.0, respectively).

Table 2.

Average content of 25 (OH)D in blood serum and FF, depending on the production of embryos

Parameter	Group with obtained embryos (n=115)	Group without embryos (n=32)	*P*-value
Blood serum, ng/ml	55.1±14.1	64.7±25.6	0.364
Follicular fluid, ng/ml	92.0±17.5	78.3±27.0	0.003

Table 3.

Content of 25(OH) D (ng/ml) in various biological fluids of women with different ART programs outcomes

Parameter	Group 1 (n=37)	Group 2 (n=110)	*P*-value
in blood serum			
<20	–	5 (4.5%)	-
20-<30	4 (10.8%)	52 (42.3%)	0.008
30–<60	33 (89.2%)	41 (37.3%)	0.009
> more than 60	–	2 (1.8%)	-
in follicular fluid			
<20	–	7 (6.4%)	-
20-<30	–	40 (36.4%)	-
30–<60	37(100%)	68 (61.8%)	0.057
> more than 60	–	2 (1.8%)	-

Table 3 presents the frequency of different levels of the 25(OH)D in the blood serum and FF. Vitamin D deficiency (<20 ng/ml) in peripheral blood was detected only in Group 2. Excessive levels of vitamin D (>60 ng/ml) were observed only in FF, but cases were rare. Low levels of vitamin D (20-<30 ng/ml) in women of this group were four times more frequent (P=0.008) than in Group 1. Women with the onset of clinical pregnancy were more often distinguished by the optimal content of vitamin D in biological fluids – almost twice as much as those with ineffective attempts to treat infertility (P=0.009 for peripheral blood). The frequency of 25(OH)D concentrations from 30ng/ml to 60ng/ml in the FF of infertile women was higher than in the blood serum; for example it was 61.8% vs. 37.3%, in Group 2. The average values of vitamin D in the blood serum and FF are presented in Table 4.

Table 4.

The average content of 25(OH)D in the blood serum and FF of women with different outcomes of IVF and IVF/ICSI programs

Parameter	Group 1 (n=37)	Group 2 (n=110)	*P*-value
Blood serum, ng/ml	48.9±10.4	40.1±19.5	0.550
Follicular fluid, ng/ml	78.0±16.4	61.8±23.7	0.003

The mean value of the 25(OH)D content in the blood serum in both groups did not differ; in FF it was significantly higher in Group 1 than in Group 2 (P=0.003).

A strong correlation was revealed between the content of 25(OH)D in the blood serum and FF (r=0.67, P=0.003 in both groups), a weak correlation – in cases where it was impossible to sample oocytes and/or embryos (r=0.48, P=0.06). Correlation of the 25(OH)D level in the blood serum and FF with the obtained follicles, oocytes and embryos was not detected. The optimal content of 25(OH)D in FF determined a greater probability of pregnancy.

Morphological examination of endometrial biopsies with H&E staining showed the corresponding phase of the menstrual cycle: proliferation (n=20), the middle stage of secretion (n=68) during manipulation on Day 7 after confirmed ovulation. No lymphoid infiltration corresponding to the inflammatory process was detected in the samples.

In endometrial tissue samples, the VDR expression was observed in the nuclei of the stromal cells and glandulocytes of the glands. The VDR protein was also detected in the cytoplasm of endometrial gland cells.

Women of Group 1 were distinguished by a lower density of VDR distribution in the glands and stroma of the endometrium, in comparison to women of Group 2 (Figure 1, a, b; Figure 2 a, b).

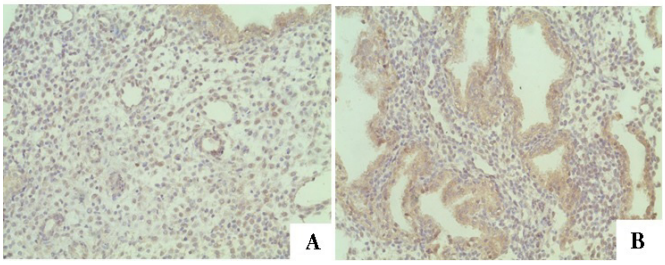

Fig. 1. *VDR expression in the endometrium at the onset of implantation (clinical case). Immunohistochemical method: A ×200, B ×200; A - VDR expression in glands (3.6%); B - VDR expression in stroma (7.0%)*

Timely delivery of a healthy fetus without complications.

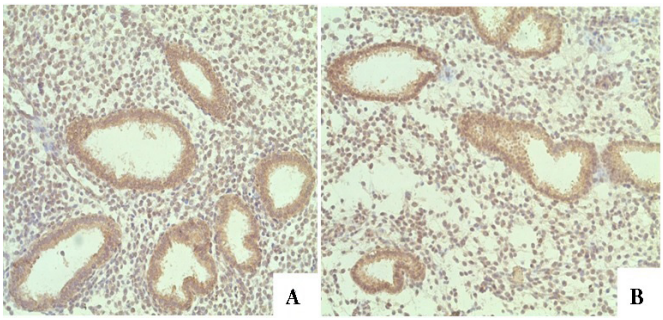

Fig. 2. *VDR expression in the endometrium in the absence of implantation (clinical case). Immunohistochemical method: A ×200, B ×200. A - VDR expression in glands (6.9%) B - VDR expression in stroma(10%)*

The VDR expression in the glands and stroma of the endometrium in the study groups is presented in Table 5. The VDR expression in stromal epithelium was higher in Group 2 than in Group 1 (*P*=0,016).

Table 5.

VDR expression in the glands and stroma of the endometrium in women with different outcomes of IVF and IVF-ICSI protocols (%)

Parameter	Group 1 (n=18)	Group 2 (n=50)	*P*-value
VDR in the stroma	7.0 (4.3;7.1)	8.3 (7.1;8.7)	0.016
VDR in the glands	6.2 (4.5;8.6)	8.8 (7.4;9.2)	0.64

There was a slight increase in the VDR expression in the cells of the stroma and glands in the luteal phase of the menstrual cycle; however, the differences were statistically insignificant, compared to the first phase (Table 6).

Table 6.

VDR expression in the glands and stroma of the endometrium in different phases of the menstrual cycle of infertile women (%)

Parameter	Phase I of the cycle (n=20)	Phase II of the cycle (n=20)	*P*-value
VDR in the stroma	7.7 (3.1;9.1)	8.64 (6.5;9.1)	0.2
VDR in the glands	7.8 (2.9;9.6)	8.76 (6.3;10.2)	0.33

The area under the ROC-curve (AUC), calculated by the ROC-analysis method, allows verification of the prognostic coefficients of clinical pregnancy and the VDR expression in the cells of the stroma and glandulocytes of the endometrial glands. AUC of the VDR expression in the endometrial glands and stroma was 0.672±0.079 (95% CI: 0.52-0.83; *P*=0.03) and 0.74±0.06 (95% CI: 0.62-0.86; *P*=0.003), respectively (Figure 3). The greatest prognostic potential was established for VDR expression in the endometrial stroma.

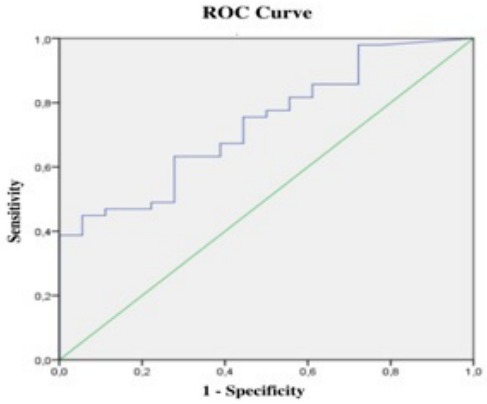

Fig. 3. *ROC analysis of VDR expression in endometrial glands and stromal cells.*

The threshold value of VDR expression in endometrial stroma cells at the cut-off point was 8.7%. At the ROC threshold value of <8.7%, the endometrium was regarded as receptive, favorable for implantation; ≥8.7% – unfavorable. The sensitivity and specificity of the method were 100% and 40%, respectively.

It is calculated that a 1% decrease in VDR expression in the stroma increases the chance of a favorable outcome by 1.35 times.

The expression of CD4+T cells and CD8+T cells (Figure 4, a, b) was identified by the brown staining of the membranes of the corresponding groups of antigen-positive endometrial stroma cells.

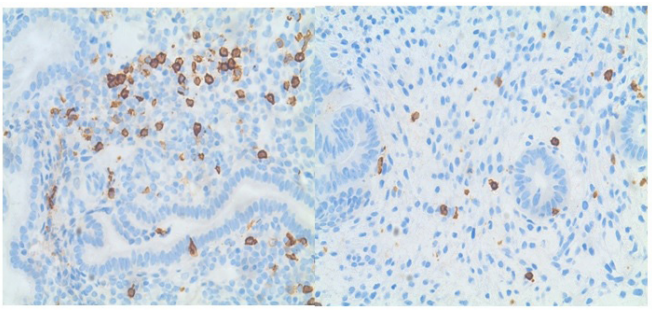

Fig. 4. *CD8+ expression in different outcomes of ART programs.*

a. CD8+ expression in a negative ART outcome (2,203%)
b. CD8+ expression in a positive ART outcome (0.68%)
a, b – Immunohistochemical method, polymer test system
a, b – ×400

The expression of CD8+T cells was weaker in Group 1 than in Group 2 (0.77 and 1.07, respectively). The expression level of labels of CD4+T cells in the groups did not visually differ. The density of labels of CD4+T cells and CD8+T cells in the endometrial stroma did not differ significantly between groups (Table 7).

The expression of CD4+T cells and CD8+T cells in endometrial samples taken from the same infertile women in different phases of the menstrual cycle showed no statistically significant differences (Table 8).

The results of the analysis of correlations between the studied parameters are presented in Table 9. A moderate correlation was found between the expression of CD4+T cells and CD8+T cells in the endometrial stroma (r=0.361, *P*=0.004), as well as VDR in the stroma (r=0.310, *P*=0.013). There was no statistically significant correlation between the expression of CD4+T cells and VDR in glands (r=0.223, *P*=0.079). No correlation was also detected between the expression of CD8+T cells and VDR in the endometrial stroma (r=0.188, *P*=0.14), glands (r=0.040, *P*=0.754).

Table 7.

Expression of endometrial markers depending on the results of ART, %

Marker	Group 1 (n=18)	Group 2 (n=50)	*P*-value
CD4+	0.96 (0.80;1.2)	1.02 (0.92;1.17)	0.12
CD8+	0.77 (0.71;1.18)	1.07 (1.01;1.41)	0.48
CD4/CD8	1.24 (0.94;1.48)	0.95 (0.82; 1.21)	0.08

*Tab**le 8.***

Expression of markers in different phases of the menstrual cycle, %

Marker	Phase I of the cycle (n=20)	Phase II of the cycle (n=20)	*P*-value
CD4+	0.99 (0.68;1.39)	1.02 (0.94;1.16)	0.705
CD8+	0.92 (0.77;1.36)	1.06 (0.68;1.52)	0.588

Table 9.

Correlations between endometrial markers

Marker	VDR in the stroma	VDR in the glands	CD4+	CD8+
VDR in the stroma	-	r=0.656, *P*=0.000	r=0.310, *P*=0.013	r=0.188, *P*=0.14
VDR in the glands	r=0.656, *P*=0.000	-	r=0.223, *P*=0.079	r=0.040, *P*=0.754
CD4+	r=0.310, *P*=0.013	r=0.223, *P*=0.079	-	r=0.361, *P*=0.004
CD8+	r=0.188, *P*=0.14	r=0.040, *P*=0.754	r=0.361, *P*=0.004	-

Discussion

Ineffective IVF attempts on the background of low serum vitamin D levels correspond to the reports of a reduced chance of childbearing in contrast to clinical pregnancy in a meta-analysis of 9 studies (3693 cycles).[30]

There is a high probability of implantation and clinical pregnancy in ART protocols with a sufficient (30–<60 ng/ml) content of vitamin D in the blood serum and FF in comparison to its deficiency (*P*<0.05). The average level of vitamin D in the FF of all infertile women was higher than in the blood serum. Women who received embryos in the ART protocols had higher 25(OH)D values in FF (*P*=0.003). A higher concentration of vitamin D in FF was found in women with clinical pregnancy (*P*=0.003). The data obtained are consistent with the results of Ozkan et al.,[31] who indicated an increase in the probability of clinical pregnancy by 6% with an increase in 25(OH)D per 1ng/ml in FF (*P*=0.03).

Our results show that the level of vitamin 25(OH)D in FF is a significant factor for the outcomes of IVF and IVF/ICSI protocols. The effect of vitamin D on implantation and clinical pregnancy in IVF protocols should be considered from the standpoint of various biological functions: inhibition of cell proliferation, angiogenesis, and antioxidant activity. The revealed correlation between the content of vitamin D in blood serum and FF is consistent with the results obtained by Firouzabadi et al.[32] We believe that the lack and deficiency of vitamin D plays a significant role in predicting unfavorable outcomes of ART programs, in contrast to the conclusions of A. Aleyasin et al.,[16] who did not reveal differences in the content of vitamin D in the FF in women with and without pregnancy in the protocols.

A higher concentration of 25(OH)D in the blood serum is likely to modulate the immunosuppressive effect in the endometrium, which is favorable for the nidation of the blastocyst. Evans et al.[33] link similar biological functions to local vitamin metabolites and the production of 1,25(OH)2D3 in the mucosa in early pregnancy. The metabolic effects of vitamin D in the endometrium should be considered from the perspective of VDR distribution. The expression of the protein in the cytoplasm of the endometrial glands corresponds to the data on the interaction of the active form 1,25(OH)2D with the nuclear receptor and further transport to the nucleus with the realization of the effects of the vitamin D-VDR complex.[34-36] The revealed decrease in VDR expression in the endometrium during the "implantation window," especially in stromal cells, allows us to speculate about the progesterone-like activity of vitamin D, alongside the restriction of local proinflammatory reactions necessary for blastocyst implantation.

We believe that the combination of optimal serum vitamin D levels and low VDR expression in the stroma has a beneficial effect on implantation and outcomes of IVF and IVF/ICSI programs. Similar data were presented by Zelenko et al.,[37] when studying the endometrium of women with endometriosis as opposed to healthy ones. The results of the study performed by Guo et al.[38] were opposite. The authors reported higher VDR expression in the endometrium of women (average age 34.6 years) with the onset of pregnancy. In our study, there were no differences in the VDR expression

in the proliferative and secretory phases of the menstrual cycle, which was consistent with the results of Vienonen et al.,[39] who studied the endometrium of premenopausal women.

The positive effect of a lower expression of CD8+T cells in the endometrium of women before embryo transfer on the outcomes of IVF and IVF/ICSI programs corresponds to the study by Lachapelle et al.[40] in women with recurrent miscarriage. Conclusions about the probability of reproductive losses or implantation failures are logical in cases of high expression of lymphocyte subpopulations in the endometrium, including NK, B-cells, CD4+T cells, and CD8+T cells.[41]

The data obtained suggest that the endometrial susceptibility during implantation is influenced not only by the moderate activity of the D-VDR complex, determined by factors involved in the metabolic transformations of vitamin D, but also by the ratio of immune cell subpopulations. The role of reducing the expression of cytotoxic CD8+T cells is most significant for the invasion of blastocysts containing semi-allogeneic fetal cells. The data obtained make it possible to assume that the prognosis of favorable outcomes of ART programs is based on the activity of signaling molecules in the endometrium, which act as "subtle" mechanisms of fertility regulation.

Conclusion

We determined a great prognostic significance for VDR expression in the endometrial stroma. The absence of differences in VDR expression in the stroma and endometrial glands, as well as CD4+T cells and CD8+T cells in different phases of the menstrual cycle of infertile women characterizes an impaired endometrial functional activity. Favorable outcomes of ART programs are determined by a decrease in the VDR expression in the endometrial stroma: with a reduction by 1%, the chances increase by 1.3 times. A decrease in the level of the endometrial CD8+T cells is significant for ensuring immunological tolerance in the mother-embryo system and predicting favorable outcomes of ART programs. Morphofunctional peculiarities of the endometrium of infertile women are the basis for predicting the outcomes of ART programs and preparing for pregnancy.

Acknowledgments

This research was funded by RFBR and Chelyabinsk Region, Project number 20-415-740014.

Competing Interests

The authors declare that they have no competing interests.

References

1. Herington JL, Guo Y, Reese J, Paria BC. Gene profiling the window of implantation: Microarray analyses from human and rodent models. J Reprod Health Med. 2016 Dec;2(Suppl 2):S19-S25. doi: 10.1016/j.jrhm.2016.11.006.
2. van Mourik MS, Macklon NS, Heijnen CJ. Embryonic implantation: cytokines, adhesion molecules, and immune cells in establishing an implantation environment. J Leukoc Biol. 2009 Jan;85(1):4-19. doi: 10.1189/jlb.0708395.
3. Moffett A, Colucci F. Uterine NK cells: active regulators at the maternal-fetal interface. J Clin Invest. 2014 May;124(5):1872-9. doi: 10.1172/JCI68107.
4. Moffett A, Shreeve N. Reply: First do no harm: continuing the uterine NK cell debate. Hum Reprod. 2016 Jan;31(1):218-9. doi: 10.1093/humrep/dev290.
5. Gellersen B, Brosens JJ. Cyclic decidualization of the human endometrium in reproductive health and failure. Endocr Rev. 2014 Dec;35(6):851-905. doi: 10.1210/er.2014-1045.
6. Adams JS, Hewison M. Unexpected actions of vitamin D: new perspectives on the regulation of innate and adaptive immunity. Nat Clin Pract Endocrinol Metab. 2008 Feb;4(2):80-90. doi: 10.1038/ncpendmet0716.
7. Duda-Wiewiórka M, Pityński K. [Vitamin D in normal and pathologically changed endometrium]. Wiad Lek. 2019;72(3):452-456. [Article in Polish].
8. Lerchbaum E, Obermayer-Pietsch B. Vitamin D and fertility: a systematic review. Eur J Endocrinol. 2012 May;166(5):765-78. doi: 10.1530/EJE-11-0984.
9. Anagnostis P, Karras S, Goulis DG. Vitamin D in human reproduction: a narrative review. Int J Clin Pract. 2013 Mar;67(3):225-35. doi: 10.1111/ijcp.12031.
10. Cermisoni GC, Alteri A, Corti L, Rabellotti E, Papaleo E, Viganò P, Sanchez AM. Vitamin D and Endometrium: A Systematic Review of a Neglected Area of Research. Int J Mol Sci. 2018 Aug 8;19(8):2320. doi: 10.3390/ijms19082320.
11. Hii CS, Ferrante A. The Non-Genomic Actions of Vitamin D. Nutrients. 2016 Mar 2;8(3):135. doi: 10.3390/nu8030135.
12. Viganò P, Lattuada D, Mangioni S, Ermellino L, Vignali M, Caporizzo E, Panina-Bordignon P, Besozzi M, Di Blasio AM. Cycling and early pregnant endometrium as a site of regulated expression of the vitamin D system. J Mol Endocrinol. 2006 Jun;36(3):415-24. doi: 10.1677/jme.1.01946.
13. Grzesiak M, Waszkiewicz E, Wojtas M, Kowalik K, Franczak A. Expression of vitamin D receptor in the porcine uterus and effect of $1,25(OH)_2D_3$ on progesterone and estradiol-17β secretion by uterine tissues in vitro. Theriogenology. 2019 Feb;125:102-108. doi: 10.1016/j.theriogenology.2018.10.026.
14. Saccone D, Asani F, Bornman L. Regulation of the vitamin D receptor gene by environment, genetics and epigenetics. Gene. 2015 May 1;561(2):171-80. doi: 10.1016/j.gene.2015.02.024.
15. Pacis MM, Fortin CN, Zarek SM, Mumford SL, Segars JH. Vitamin D and assisted reproduction: should vitamin D be routinely screened and repleted prior to ART? A systematic review. J Assist Reprod Genet. 2015 Mar;32(3):323-35. doi: 10.1007/s10815-014-0407-9.
16. Aleyasin A, Hosseini MA, Mahdavi A, Safdarian L, Fallahi P, Mohajeri MR, Abbasi M, Esfahani F. Predictive

value of the level of vitamin D in follicular fluid on the outcome of assisted reproductive technology. Eur J Obstet Gynecol Reprod Biol. 2011 Nov;159(1):132-7. doi: 10.1016/j.ejogrb.2011.07.006.
17. Rajaei S, Mirahmadian M, Jeddi-Tehrani M, Tavakoli M, Zonoobi M, Dabbagh A, Zarnani AH. Effect of 1,25(OH)2 vitamin D3 on cytokine production by endometrial cells of women with repeated implantation failure. Gynecol Endocrinol. 2012 Nov;28(11):906-11. doi: 10.3109/09513590.2012.683062.
18. Wojtusik J, Johnson PA. Vitamin D regulates anti-Mullerian hormone expression in granulosa cells of the hen. Biol Reprod. 2012 Mar 30;86(3):91. doi: 10.1095/biolreprod.111.094110.
19. Polyzos NP, Anckaert E, Guzman L, Schiettecatte J, Van Landuyt L, Camus M, Smitz J, Tournaye H. Vitamin D deficiency and pregnancy rates in women undergoing single embryo, blastocyst stage, transfer (SET) for IVF/ICSI. Hum Reprod. 2014 Sep;29(9):2032-40. doi: 10.1093/humrep/deu156.
20. Rudick B, Ingles S, Chung K, Stanczyk F, Paulson R, Bendikson K. Characterizing the influence of vitamin D levels on IVF outcomes. Hum Reprod. 2012 Nov;27(11):3321-7. doi: 10.1093/humrep/des280.
21. Rudick BJ, Ingles SA, Chung K, Stanczyk FZ, Paulson RJ, Bendikson KA. Influence of vitamin D levels on in vitro fertilization outcomes in donor-recipient cycles. Fertil Steril. 2014 Feb;101(2):447-52. doi: 10.1016/j.fertnstert.2013.10.008.
22. Lv SS, Wang JY, Wang XQ, Wang Y, Xu Y. Serum vitamin D status and in vitro fertilization outcomes: a systematic review and meta-analysis. Arch Gynecol Obstet. 2016 Jun;293(6):1339-45. doi: 10.1007/s00404-016-4058-1.
23. Neville G, Martyn F, Kilbane M, O'Riordan M, Wingfield M, McKenna M, McAuliffe FM. Vitamin D status and fertility outcomes during winter among couples undergoing in vitro fertilization/intracytoplasmic sperm injection. Int J Gynaecol Obstet. 2016 Nov;135(2):172-176. doi: 10.1016/j.ijgo.2016.04.018.
24. Franasiak JM, Molinaro TA, Dubell EK, Scott KL, Ruiz AR, Forman EJ, Werner MD, Hong KH, Scott RT Jr. Vitamin D levels do not affect IVF outcomes following the transfer of euploid blastocysts. Am J Obstet Gynecol. 2015 Mar;212(3):315.e1-6. doi: 10.1016/j.ajog.2014.09.029.
25. van de Vijver A, Drakopoulos P, Van Landuyt L, Vaiarelli A, Blockeel C, Santos-Ribeiro S, Tournaye H, Polyzos NP. Vitamin D deficiency and pregnancy rates following frozen-thawed embryo transfer: a prospective cohort study. Hum Reprod. 2016 Aug;31(8):1749-54. doi: 10.1093/humrep/dew107.
26. Cappy H, Giacobini P, Pigny P, Bruyneel A, Leroy-Billiard M, Dewailly D, Catteau-Jonard S. Low vitamin D3 and high anti-Müllerian hormone serum levels in the polycystic ovary syndrome (PCOS): Is there a link? Ann Endocrinol (Paris). 2016 Oct;77(5):593-599. doi: 10.1016/j.ando.2016.02.001.
27. Saito S, Nakashima A, Shima T, Ito M. Th1/Th2/Th17 and regulatory T-cell paradigm in pregnancy. Am J Reprod Immunol. 2010 Jun;63(6):601-10. doi: 10.1111/j.1600-0897.2010.00852.x.
28. Piccinni MP, Scaletti C, Maggi E, Romagnani S. Role of hormone-controlled Th1- and Th2-type cytokines in successful pregnancy. J Neuroimmunol. 2000 Sep 1;109(1):30-3. doi: 10.1016/s0165-5728(00)00299-x.
29. Paramonova NB, Kogan EA, Kolotovkina AV, Burmenskaya OV. Morfologicheskie i molekuliarno-biologicheskie priznaki narusheniia retseptivnosti éndometriia pri besplodii zhenshchin, stradaiushchikh naruzhnym genital'nym éndometriozom [The morphological and molecular biological signs of impaired endometrial receptivity in infertility in women suffering from external genital endometriosis]. Arkh Patol. 2018;80(3):11-18. doi: 10.17116/patol201880311-18. [Article in Russian].
30. Zhao J, Huang X, Xu B, Yan Y, Zhang Q, Li Y. Whether vitamin D was associated with clinical outcome after IVF/ICSI: a systematic review and meta-analysis. Reprod Biol Endocrinol. 2018 Feb 9;16(1):13. doi: 10.1186/s12958-018-0324-3.
31. Ozkan S, Jindal S, Greenseid K, Shu J, Zeitlian G, Hickmon C, Pal L. Replete vitamin D stores predict reproductive success following in vitro fertilization. Fertil Steril. 2010 Sep;94(4):1314-1319. doi: 10.1016/j.fertnstert.2009.05.019.
32. Firouzabadi RD, Rahmani E, Rahsepar M, Firouzabadi MM. Value of follicular fluid vitamin D in predicting the pregnancy rate in an IVF program. Arch Gynecol Obstet. 2014 Jan;289(1):201-6. doi: 10.1007/s00404-013-2959-9.
33. Evans KN, Nguyen L, Chan J, Innes BA, Bulmer JN, Kilby MD, Hewison M. Effects of 25-hydroxyvitamin D3 and 1,25-dihydroxyvitamin D3 on cytokine production by human decidual cells. Biol Reprod. 2006 Dec;75(6):816-22. doi: 10.1095/biolreprod.106.054056.
34. Sayem ASM, Giribabu N, Karim K, Si LK, Muniandy S, Salleh N. Differential expression of the receptors for thyroid hormone, thyroid stimulating hormone, vitamin D and retinoic acid and extracellular signal-regulated kinase in uterus of rats under influence of sex-steroids. Biomed Pharmacother. 2018 Apr;100:132-141. doi: 10.1016/j.biopha.2018.02.008.
35. Emam MA, Abouelroos ME, Gad FA. Expression of calbindin-D9k and vitamin D receptor in the uterus of Egyptian buffalo during follicular and luteal phases. Acta Histochem. 2016 Jun;118(5):471-7. doi: 10.1016/j.acthis.2016.04.009.
36. Jang H, Choi Y, Yoo I, Han J, Hong JS, Kim YY, Ka H. Vitamin D-metabolic enzymes and related molecules: Expression at the maternal-conceptus interface and the role of vitamin D in endometrial gene expression in pigs. PLoS One. 2017 Oct 31;12(10):e0187221. doi: 10.1371/journal.pone.0187221.
37. Zelenko Z, Aghajanova L, Irwin JC, Giudice LC. Nuclear receptor, coregulator signaling, and chromatin remodeling pathways suggest involvement of the epigenome in the steroid hormone response of endometrium and abnormalities

***Corresponding author:** Elena G. Chukhnina, PGS. Department of Pathological Anatomy and Forensic Medicine, South Ural State Medical University, Chelyabinsk, Russia. E-mail: chuhninaeg@yandex.ru*

in endometriosis. Reprod Sci. 2012 Feb;19(2):152-62. doi: 10.1177/1933719111415546.
38. Guo J, Liu S, Wang P, Ren H, Li Y. Characterization of VDR and CYP27B1 expression in the endometrium during the menstrual cycle before embryo transfer: implications for endometrial receptivity. Reprod Biol Endocrinol. 2020 Mar 17;18(1):24. doi: 10.1186/s12958-020-00579-y.
39. Vienonen A, Miettinen S, Bläuer M, Martikainen PM, Tomás E, Heinonen PK, Ylikomi T. Expression of nuclear receptors and cofactors in human endometrium and myometrium. J Soc Gynecol Investig. 2004 Feb;11(2):104-12. doi: 10.1016/j.jsgi.2003.09.003.
40. Lachapelle MH, Miron P, Hemmings R, Roy DC. Endometrial T, B, and NK cells in patients with recurrent spontaneous abortion. Altered profile and pregnancy outcome. J Immunol. 1996 May 15;156(10):4027-34.
41. Marron K, Harrity C. Endometrial lymphocyte concentrations in adverse reproductive outcome populations. J Assist Reprod Genet. 2019 May;36(5):837-846. doi: 10.1007/s10815-019-01427-8.

International Journal of Biomedicine 11(2) (2021) 197-200
http://dx.doi.org/10.21103/Article11(2)_OA12

ORIGINAL ARTICLE

Internal Medicine

INTERNATIONAL JOURNAL OF BIOMEDICINE

Relationship between the Types of Malocclusion and the Localization of Headaches in Adults

Natalya M. Didenko[1], PhD; Arcady Ya. Vyazmin[1], PhD, ScD; Evgeniy V. Mokrenko[1], PhD; Vladimir V. Gazinskiy[1], PhD; Maria I. Suslikova[1], PhD; Marina A. Darenskaya[2*], PhD, ScD; Victoria B. Andreeva[1]; Daniil Aksnes[1]; Marina I. Gubina[1], PhD

[1]*Irkutsk State Medical University*
[2]*Scientific Centre for Family Health and Human Reproduction Problems*
Irkutsk, the Russian Federation

Abstract

The aim of this study was to investigate the manifestations of headaches in adult patients with types of malocclusion and occlusion deformities.

***Methods and Results*:** The study was conducted in 171 adult patients (43 men and 128 women) with malocclusion and occlusion deformities at the age of 18 to 62 years old, who were examined in the orthopedic dentistry clinic. The nature of the dentition closing was studied directly in the patient's oral cavity, and with the help of the "Gnatomat" universal articulator on diagnostic plaster models of the jaws. The occlusal relationships of the teeth were analyzed in the position of the central, anterior, lateral and dynamic occlusions. The biomechanics of the lower jaw movements were studied in 3 mutually perpendicular directions. The detected anomalies and deformities of the occlusion were grouped as sagittal, transversal and vertical. Each group was diagnosed as independent forms of malocclusion, and combined with other anomalies and deformities of the dentoalveolar system. All the subjects were asked to answer the questions of a questionnaire specially developed for our study. The unified questionnaire was developed based on a modified rating questionnaire and the determination of the life disorders index in neck pain. The questionnaire includes blocks of questions aimed at identifying the localization of the headache in the temporal, parietal (in one or both) regions, occipital, frontal regions and in the longitudinal seam region.

We identified complaints of patients with pain in adjacent regions of the head. Of the 171 examined adult patients with malocclusion and occlusion deformities, 99 (57.9%) complained of headaches. The presence of a headache in the parietal region of the head was associated most often with sagittal and transversal malocclusions. The presence of a headache in the temporal part of the head was associated often with vertical malocclusion The results of correlation analysis showed that pain in 2 regions of the head was associated with malocclusion: the temporal region (r_b=0.9892, P=0.0013) and parietal region (r_b=0.9712, P=0.0058). Other regions were not statistically significantly associated with malocclusion.

Conclusion: There is a certain relationship between the types of malocclusion, occlusion deformities and localization of headaches in adults. Headaches in the parietal and temporal regions of the head are associated with malocclusion and occlusion deformities more often. The obtained data can serve as a basis for the development of recommendations for appropriate corrective measures in orthodontic practice. **(International Journal of Biomedicine. 2021;11(2):197-200.)**

Key Words: malocclusion • occlusion deformities • headache

For citation: Didenko NM, Vyazmin AYa, Mokrenko EV, Gazinskiy VV, Suslikova MI, Darenskaya MA, Andreeva VB, Aksnes D, Gubina MI. Relationship between the Types of Malocclusion and the Localization of Headaches in Adults. International Journal of Biomedicine. 2021;11(2):197-200. doi:10.21103/Article11(2)_OA12

Introduction

The relationship between pathological conditions of the dentoalveolar system and disorders in the cranial and facial parts of the head is currently established.[(1)] It has been found that minor changes in the relationship between teeth and jaws, combined with stress factors, lead to painful spasms of the masticatory muscles and, as a result, to headaches and facial pain.[(2-6)] Painful dense formations, in the thickness of which there are regions of hypersensitivity, myofascial trigger points (MTPs), are found in the masticatory muscles of such patients. The term myofascial pain syndrome refers

to sensitive, motor, and vegetative symptoms caused by MTPs.[7] There is evidence that MTPs play a significant role in the pathogenesis of tension headaches.[8] The mechanism by which musculofascial headaches occur is that the trigger point activates and sensitizes the neurons of the spinal cord posterior horns, leading to the reflection of pain in regions distant from the trigger point, according to the segments. The reflected pain is felt as a headache in the frontal, temporal, or parietal regions. These headaches are very common and make up the majority of outpatient visits of patients with complaints of headaches.[9] However, there is still no information on the relationship between the types of malocclusion and the occurrence of headaches.

The aim of this study was to investigate the manifestations of headaches in adult patients with types of malocclusion and occlusion deformities.

Material and Methods

The study was conducted in 171 adult patients (43 men and 128 women) with malocclusion and occlusion deformities at the age of 18 to 62 years old, who were examined in the orthopedic dentistry clinic.

Each patient received sufficient information about the aim, methods, expected benefits, potential risks, and inconveniences that may arise from participation in the study, as well as other significant aspects of the study, before being included in it. Patients had the right to withdraw from the study at any time or withdraw their consent without giving reasons. Voluntary informed consent to participate in the study was issued only after the potential participants had read the information provided to them. After signing the voluntary informed consent, a medical examination was carried out, including an oral examination and a diagnosis provided for in the plan of our study.

The nature of the dentition closing was studied directly in the patient's oral cavity, and with the help of the "Gnatomat" universal articulator on diagnostic plaster models of the jaws. The occlusal relationships of the teeth were analyzed in the position of the central, anterior, lateral and dynamic occlusions. The biomechanics of the lower jaw movements were studied in 3 mutually perpendicular directions. Therefore, the detected anomalies and deformities of the occlusion were grouped as sagittal, transversal and vertical. Each group was diagnosed as independent forms of malocclusion, and combined with other anomalies and deformities of the dentoalveolar system.

All the subjects were asked to answer the questions of a questionnaire specially developed for our study. The unified questionnaire was developed based on a modified rating questionnaire and the determination of the life disorders index in neck pain.[10] The questionnaire includes blocks of questions aimed at identifying the localization of the headache in the temporal, parietal (in one or both) regions, occipital, frontal regions and in the longitudinal seam region.

Statistical analysis was performed using the Statistica 6.0 software package (Stat-Soft Inc., USA). The frequencies of categorical variables were compared using Pearson's chi-squared test or Fisher's exact test, when appropriate. The biserial correlation coefficient (r_b) was calculated to measure the strength and direction of the linear relationship between two variables. A value of $P<0.05$ was considered significant.

Results and Discussion

We identified complaints of patients with pain in adjacent regions of the head. Of the 171 examined adult patients with malocclusion and occlusion deformities, 99 (57.9%) complained of headaches.

There were no differences in the frequency of occurrence of the type of malocclusion or occlusion deformities in patients with headaches (Table 1) At the same time, the presence of a headache in the parietal region of the head was associated most often with sagittal malocclusion in comparison with temporal (P=0.0168), occipital (P=0.0002), and frontal regions ($P<0.0001$). The pain in the parietal region associated with sagittal anomalies was localized more often from 2 sides than from 1 side (P=0.0004). Also, the presence of a headache in the parietal region of the head was associated often with transversal malocclusion, in comparison with occipital ($P<0.0001$), longitudinal seam (P=0.0003) and frontal ($P<0.0001$) regions. The pain in the parietal region associated with transversal anomalies was localized more often from 1 side than from 2 sides (P=0.0004). The presence of a headache in the temporal part of the head was associated often with vertical malocclusion, in comparison with the occipital ($P<0.0001$), longitudinal seam (P=0.0006) and frontal (P=0.0006) regions (Table 1).

Table 1.

The frequency of headaches in patients with malocclusion and occlusion deformities

Head regions	Malocclusion and occlusion deformities n (%)		
	Sagittal 36 (36.4%)	Transversal 37 (37.4%)	Vertical 26 (26.3%)
Temporal region	10 (27.8%)	11 (29.7%)	14 (53.8%)*
Parietal region	20 (55.6%)*	19 (51.4%)*	8 (30.8%)
Occipital region	5 (13.9%)	1 (2.7%)	0
Longitudinal seam	0	4 (10.8%)	2 (7.7%)
Frontal region	1 (2.8%)	2 (5.4%)	2 (7.7%)

** - statistically significant differences with other indicators*

As a result of correlation analysis, we obtained correlation coefficients r_b that characterize the measure of a linear relationship between the dependence of pain in a certain head region on the type of malocclusion or occlusion deformities (Table 2). It was found that pain in 2 regions of the head was associated with malocclusion: the temporal region (r_b=0.9892, P=0.0013) and parietal region (r_b=0.9712, P=0.0058). Other regions were not statistically significantly associated with malocclusion.

Table 2.

Dependence of pain localization in certain head regions on the malocclusion type

Head region	*P*-value	r_b
Temporal region	0.0013 *	0.9892
Parietal region	0.0058 *	0.9712
Occipital region	0.2989	0.5861
Longitudinal seam	0.7985	-0.1589
Frontal region	0.1027	-0.8018

* - *statistically significant correlations*

Tension headache, especially combined with dentoalveolar anomalies, is currently insufficiently studied, and therefore there is still no optimal treatment for it. Headaches of this type belong to comorbid pathologies, negatively affect the patient's quality of life and need a more detailed examination by various specialists.[11-13] In our study, 57.9% of patients with malocclusion and occlusion deformities suffered from headaches. Currently, there are 2 main pathophysiological mechanisms of the mutual influence of headaches and malocclusion and occlusion deformities.[14] This is sensitization of nociceptive structures and a decrease in the activity of antinociceptive systems of the central nervous system.[15] Central sensitization is considered one of the main mechanisms for maintaining chronic pain; if it is present, dependence on peripheral triggering factors is lost, and resistance to therapy develops.[16-18] This assumption is consistent with the data of D. Goncales, which was confirmed by clinical data when examining 300 patients.[19] Impaired antinociceptive functions can also be the cause of the relationship between headaches and malocclusion and occlusion deformities.[13] Soreness and hypertrophy of the masticatory muscles are likely due to central sensitization and impaired pain control. This hypothesis is supported by the data of a number of studies, which showed that patients with malocclusion and occlusion deformities have decreased pain thresholds from pressure contralaterally and ipsilateral with respect to the pain side, not only in the masticatory muscles themselves, but also in distant muscle groups.[20] In this case, even normal proprioceptive impulses from the masticatory muscles are perceived as painful, and the tension in them is a consequence of the activation of the motor cortex during central sensitization.[21]

Currently, there are various tactics of pain syndrome treatment to reduce pain afferentation.[22] We identified a more detailed localization of pain associated with malocclusion and occlusion deformities. These areas were the temporal and parietal areas, which were most often associated with sagittal, transversal and vertical occlusion types of deformities. The identified changes require further research on the relationship between headaches and malocclusion and occlusion deformities. It is also important to identify possible new therapeutic approaches, in particular in the presence of complex cases.

In conclusion, there is a certain relationship between the types of malocclusion, occlusion deformities and localization of headaches in adults. Headaches in the parietal and temporal regions of the head are associated with malocclusion and occlusion deformities more often. The obtained data can serve as a basis for the development of recommendations for appropriate corrective measures in orthodontic practice.

Competing Interests

The authors declare that they have no competing interests.

References

1. Stephanidi AV. [The value of temporomandibular joint muscle dysfunction in the development of cranioalgia syndrome]. Bulletin of the East Siberian Scientific Center of the Siberian Branch of the Russian Academy of Medical Sciences. 2003;5:89-94. [Article in Russian].
2. Bugrovetskaya EA, Gvozdeva SV, Didenko A, Solovykh OG, Bugrovetskaya OG. [Postural balance and occlusion of teeth. The role of occlusion disorders in the occurrence of postural imbalance in neurosomatic diseases]. Manual therapy. 2008;2(30):40-48. [Article in Russian].
3. Darenskaya MA, Grebenkina LA, Mokrenko EV, Shabanov PD, Suslikova MI, Mokrenko ME, Sinyova YuO, Goncharov IS, Gubina MI, Kostritsky IYu, Bulnaeva AF, Proskurnina EV, Kolesnikova LI, Kolesnikov SI. Lipid Peroxidation Activity and Immune Response in Modeling Inflammatory and Degenerative Damage to the Periodontium of Rats. International Journal of Biomedicine. 2019;9(2):159-162. doi: 10.21103/Article9(2)_OA16
4. Darenskaya MA, Kolesnikova LR, Rychkova LV, Pogodina AV, Grebenkina LA, Kolesnikova LI, Kolesnikov SI. Lipid peroxidation-antioxidant defense system functional state in adolescents with arterial hypertension and dental caries comorbidity. Free Radical Biology & Medicine. 2020;159(S1):S88-S89. DOI: 10.1016/j.freeradbiomed.2020.10.229
5. Kolesnikova LR, Darenskaya MA, Kolesnikova LI, Grebenkina LA, Korytov LI, Batoroev YK, Belinskaya EI, Mikhalevich IM, Kolesnikov SI. Morphofunctional State of the Periodontal Tissues in Humans and Rats with Arterial Hypertension. Bull Exp Biol Med. 2020 Oct;169(6):831-835. doi: 10.1007/s10517-020-04990-8.
6. Darenskaya MA, Kolesnikova LR, Rychkova LV, Grebenkina LA, Semenova NV, Kolesnikov SI, Kolesnikova LI. Indicators of Lipid Peroxidation Reactions and State of Structural Tissues of the Dentition System in Wistar Rats under Various Stress Regimes. International Journal of Biomedicine. 2020;10(2):142-147. doi: 10.21103/Article10(2)_OA11
7. Travell JG, Simons DG. Myofascial pain and dysfunction: a guide to trigger points. Moscow: Medicine. 2005. [Book in Russian].
8. Vein AM, Voznesenskaya TG. [Headache]. Clinical Medicine. 1998;11:63-65. [Article in Russian].

***Corresponding author:** Marina A. Darenskaya, PhD, ScD. Scientific Centre for Family Health and Human Reproduction Problems, Irkutsk, the Russian Federation. E-mail: marina_darenskaya@inbox.ru*

9. Fergusson LU, Gervin R. Treatment of myofascial pain: Clinical guidelines. Moscow: MEDpress-inform. 2008. 544. [Book in Russian].
10. Belova AN. Neurorehabilitation: A Guide for Doctors. 2nd ed., Rev. and add. Moscow: Antidor, 2002. 736. [Book in Russian].
11. Shroff B. Malocclusion as a Cause for Temporomandibular Disorders and Orthodontics as a Treatment. Oral Maxillofac Surg Clin North Am. 2018 Aug;30(3):299-302. doi: 10.1016/j.coms.2018.04.006.
12. Kolesnikova LR, Darenskaya MA, Kolesnikova LI, Grebenkina LA, Korytov LI, Batoroev YK, Belinskaya EI, Mikhalevich IM, Kolesnikov SI. Changes in the Periodontium and Pulp in ISIAH Rats Caused by Stress Exposures in Different Modes. Bull Exp Biol Med. 2019 Apr;166(6):722-725. doi: 10.1007/s10517-019-04426-y.
13. Zenkevich AS, Filatova EG, Latysheva NV. [Migraine and temporomandibular joint dysfunction: mechanisms of comorbidity]. Zh Nevrol Psikhiatr Im S S Korsakova. 2015;115(10):33-38. Russian. doi: 10.17116/jnevro201511510133-38.
14. Sonnesen L, Bakke M, Solow B. Malocclusion traits and symptoms and signs of temporomandibular disorders in children with severe malocclusion. Eur J Orthod. 1998 Oct;20(5):543-59. doi: 10.1093/ejo/20.5.543.
15. Al-Moraissi EA, Perez D, Ellis E 3rd. Do patients with malocclusion have a higher prevalence of temporomandibular disorders than controls both before and after orthognathic surgery? A systematic review and meta-analysis. J Craniomaxillofac Surg. 2017 Oct;45(10):1716-1723. doi: 10.1016/j.jcms.2017.07.015.
16. Poștaru C, Postnikov M, Uncuța, D. Evaluation of masticatory muscles function in children with malocclusions associated with tension-type headache. 2020. Available from: http://repository.usmf.md/bitstream/20.500.12710/14895/1/723_ABSTRACT_BOOK_Culegere_de_rezumateABSTRACT_BOOK_Culegere_de_rezumate.pdf
17. Bairova TA, Kolesnikov SI, Kolesnikova LI, Pervushina OA, Darenskaya MA, Grebenkina LA. Lipid peroxidation and mitochondrial superoxide dismutase-2 gene in adolescents with essential hypertension. Bull Exp Biol Med. 2014 Dec;158(2):181-4. doi: 10.1007/s10517-014-2717-4.
18. Kolesnikova LR, Darenskaya MA, Kolesnikova LI, Grebenkina LA, Korytov LI, Batoroev YK, Belinskaya EI, Mikhalevich IM, Kolesnikov SI. Comparative Analysis of the Morphology of Dentition in Normotensive and Hypertensive Rats Exposed to Chronic Stress. Bull Exp Biol Med. 2019 May;167(1):7-10. doi: 10.1007/s10517-019-04449-5.
19. Gonçalves DA, Camparis CM, Speciali JG, Franco AL, Castanharo SM, Bigal ME. Temporomandibular disorders are differentially associated with headache diagnoses: a controlled study. Clin J Pain. 2011 Sep;27(7):611-5. doi: 10.1097/AJP.0b013e31820e12f5.
20. Fernández-de-las-Peñas C, Galán-del-Río F, Fernández-Carnero J, Pesquera J, Arendt-Nielsen L, Svensson P. Bilateral widespread mechanical pain sensitivity in women with myofascial temporomandibular disorder: evidence of impairment in central nociceptive processing. J Pain. 2009 Nov;10(11):1170-8. doi: 10.1016/j.jpain.2009.04.017.
21. Maixner W, Fillingim R, Sigurdsson A, Kincaid S, Silva S. Sensitivity of patients with painful temporomandibular disorders to experimentally evoked pain: evidence for altered temporal summation of pain. Pain. 1998 May;76(1-2):71-81. doi: 10.1016/s0304-3959(98)00028-1.
22. Bianchi J, Pinto ADS, Ignácio J, Obelenis Ryan DP, Gonçalves JR. Effect of temporomandibular joint articular disc repositioning on anterior open-bite malocclusion: An orthodontic-surgical approach. Am J Orthod Dentofacial Orthop. 2017 Dec;152(6):848-858. doi: 10.1016/j.ajodo.2016.09.032.

International Journal of Biomedicine 11(2) (2021) 201-205
http://dx.doi.org/10.21103/Article11(2)_OA13

ORIGINAL ARTICLE

Women's Health

INTERNATIONAL JOURNAL OF BIOMEDICINE

Morphological and Prognostic Characteristics of Breast Cancer in Women Living in the Sakha Republic (Yakutia)

Maria P. Kirillina[1*], PhD; Irina V. Kononova[1], PhD; Sargylana I. Sofronova[1], PhD; Petr M. Ivanov[1], PhD, ScD; Aytalina S. Golderova[2], PhD, ScD

[1]*Yakut Science Centre of Complex Medical Problems, Yakutsk, Russia*
[2]*M. K. Ammosov North-Eastern Federal University, Yakutsk, Russia*

Abstract

Background: This article presents the results of the analysis of the clinical and morphological examination of breast cancer (BC) in women of the Republic of Sakha (Yakutia) (RS(Y)).

Methods and Results: The object of the study was fragments of breast tissue from 294 women who underwent surgical treatment and/or needle biopsy. By ethnicity, there were 118(40.1%) women of indigenous nationalities and 176(59.9%) women of non–indigenous nationalities. The greatest number of cases of BC was registered in the age group of 50-59 (32.6%). The age group of 40-49 was in second place (20.4%). Among the indigenous population, women in the age groups of 40-49 years (23.7%) and 50-59 years (26.3%) predominated. The age groups of 50-59 years (36.9%) and 60-69 years (22.2%) predominated among the non-indigenous women.

Tumors with a size of 2 cm to 5 cm prevailed; they were detected in 185(62.9%) women. Tumors with a spread to the chest wall and skin develop more often in women of non-indigenous nationalities (15.9% of cases), than in women of indigenous nationality (6.8% of cases). Regardless of ethnicity, the most common histological form of BC in women of the RS(Y) was infiltrative ductal cancer (65.3%). Cancer staging according to the TNM staging system showed that in the age group of women under 39 years, Stage IIIB+IIIC (43.2%) was most often registered (P=0.01), while in other age groups, Stage IIA (32.4%) was more often noted.

Conclusion: Our findings suggest that further investigation of the peculiarities of the course of BC in the female population of Yakutia would lead to much improved methods of diagnosis and treatment.**(International Journal of Biomedicine. 2021;11(2):201-205.)**

Key Words: breast cancer • ethnicity • TNM staging system • tumor grade

For citation: Kirillina MP, Kononova IV, Sofronova SI, Ivanov PM, Golderova AS. Morphological and Prognostic Characteristics of Breast Cancer in Women Living in the Sakha Republic (Yakutia). International Journal of Biomedicine. 2021;11(2):201-205. doi:10.21103/Article11(2)_OA13

Introduction

Breast cancer (BC) is an urgent social and medical problem affecting a significant part of the female population. Tumors of this localization occur predominantly among women of active working age. The largest number of women with BC is found in the age group of 40-60 years. There is a period of the most intensive endocrine changes in women, and there is a progressive replacement of epithelial glandular tissue with connective and adipose tissue in the mammary gland.[1,2] Many researchers have found the age peak of the disease is 55-59 years during menopause, when the production of ovarian hormones decreases.[3] After 60 years, the risk for disease is quite high, but the process of tumor growth itself is slower than in young people.[4]

Today in assessing the features of the clinical course, the possible outcome of the disease, and the choice of the most appropriate treatment strategy, such clinical and morphological parameters as age, size of the primary lesion, histologic type of the tumor and the tumor stage, the presence of metastases in axillary lymph nodes, and several other indicators are taken

***Corresponding author:** Maria P. Kirillina, PhD. Yakut Science Centre of Complex Medical Problems, Yakutsk, Russia. E-mail: kirillinamp@mail.ru*

into account.[5-7] There is no doubt that the detection of BC in the early stages contributes to the improvement of long-term treatment results. At the same time, an individual assessment of the prognosis of BC, even at an early process of tumor stage, is considered extremely relevant.

This article presents the results of the analysis of the clinical and morphological examination of BC in women of the Republic of Sakha (Yakutia) (RS(Y)).

Materials and Methods

The object of the study was fragments of breast tissue from 294 women who underwent surgical treatment and/or needle biopsy. Indigenous people were considered Yakuts, Evens, and Evenks and representatives of peoples of the North with low populations. Non-indigenous people were all other nationalities that arrived at various times from the regions of Russia and the CIS countries. By ethnicity, there were 118(40.1%) women of indigenous nationalities and 176(59.9%) women of non–indigenous nationalities.

Tumor grade (G) was determined by the Elston & Ellis grading system,[8] which took into account the preservation of the tubular structure in the tumor, polymorphism, and mitotic activity of cancer cells. This system divided BC into tumors with G1 (low-grade or well-differentiated tumor), G2 (intermediate grade or moderately differentiated tumor), and G3 (high-grade or poorly differentiated tumor).

Morphological method

A macroscopic study of breast tissue was performed with the measurement of tumor size, counting, and measuring of lymph nodes.

Microscopic study

The material was fixed in 10% neutral formalin for 24 hours, followed by pouring into paraffin in the Tissue-Tek 9589. Using the microtome Leica SM 2000R, sections with a thickness of 3–5 microns were made from paraffin blocks; the sections were straightened in a water-bath, and placed on glasses treated with protein. The glasses were left overnight in a dry-air sterilizer at a temperature of 38°C for better fixation and straightening of the sections. The sections were stained with H&E automatically on a Sacura DRS-60 device, according to the following step-by-step program: 1 – toluene 1(10 min); 2 – toluene 2(10 min); 3 – alcohol 1(10 min); 4 – alcohol 2(10 min); 5 – hematoxylin(1 min); 6 – flush in H_2O; 7 – HCL solution(1 min); 8 – H_2O(10 min); 9 – eosin (1 min); 10 – flush in H_2O; 11 – alcohol 3 (5 min); 12 - carbolic acid; 13-toluene. Sections were extracted from the last glass solution and enclosed in polystyrene under cover glasses.

*S*tatistical analysis was performed using statistical software package SPSS version 17.0 (SPSS Inc, Chicago, IL). The frequencies of categorical variables were compared using Pearson's chi-squared test or Fisher's exact test, when appropriate. A value of $P<0.05$ was considered significant.

Results and Discussion

The average age of patients was 54.2±12.1 years. The age groups were as follows: over 50-59 years - 96(32.6%); 60-69 years – 64(21.8%); 40-49 years – 60(20.4%); under 39 years – 37(12.6%); ≥70 years – 37(12.6%) (Table 1).

Table 1.
Distribution of women by age and ethnicity

Age group (yrs)	Indigenous women		Non-indigenous women		Total	
	n (%)	average age	n (%)	average age	n (%).	average age
<39	15 (12.7)	33.7±5.3	22 (12.5)	33.8±3.6	37 (12.6)	33.7±4.3
40–49	28 (23.7)	45.3±2.9	32 (18.2)	45.0±2.8	60 (20.4)	45.1±2.9
50–59	31 (26.3)	54.8±2.7	65 (36.9)	54.1±2.9	96 (32.6)	54.3±2.9
60–69	25 (21.2)	63.4±2.6	39 (22.2)	62.9±3.1	64 (21.8)	63.1±2.9
≥70	19(16.1)	74.2±2.9	18 (10.2)	73.3±3.3	37 (12.6)	73.8±3.2
Total	118 (100)	54.8±12.9	176 (100)	53.8±11.5	294 (100)	54.2±12.1

It should be noted that BC, which was traditionally considered a disease of women over 50 years old, is now noticeably "younger." Cases of 40-year-old, 30-year-old, and even 20-year-old women are not uncommon.[9] This trend can be found in our work. Thus, there were only 2 times more women over age 50 than women under age 50: 197(67%) versus 97(33%). In economically developed countries, postmenopausal women account for approximately 75% of BC cases.[10] The greatest number of cases of BC was registered in the age group of 50-59 (32.6%). The age group of 40-49 was in second place (20.4%). Women under age 39(12.6%) and women over age 70 (12.6%) were also diagnosed with BC.

In this study, there were fewer indigenous women (118 cases) than non-indigenous women (176 cases) (P=0.000). Among the indigenous population, women in the age groups of 40-49 years (23.7%) and 50-59 years (26.3%) predominated. This was followed by the age group of 60-69 years (21.2%). The lowest number of women were in the age groups under 39 years and over 70 years (12.7% and 16.1%, respectively). The age groups of 50-59 years (36.9%) and 60-69 years (22.2%) predominated among the non-indigenous women. This was followed by the age group of 40-49 years (18.2%). In the groups under age 39 and over age 70, the ratio of non-indigenous women was about the same (12. 5% and 10. 2%, respectively).

Thus, non-indigenous women aged 50-59 years provided the most surgical material for BC. There were no statistically significant differences between the groups.

A study of the clinical and morphological features of BC revealed that the majority of women (190/65.0%) were diagnosed with invasive ductal carcinoma. The second most common type of BC was mixed cancer (invasive ductal and lobular) (33/11.2%), and the third most common type was invasive lobular carcinoma (23/7.8%). Neuroendocrine cancer was diagnosed in 15(5.1%) cases, invasive cancer was diagnosed without specifying the form, due to the severity of therapeutic pleomorphism in 7(2.4%) cases, and Paget's cancer was diagnosed in 6(2.0%) cases. Other forms of cancer (medullary, tubular, papillary, etc.) accounted for 6.8% (20 cases).

When studying the occurrence of various forms of BC in age groups, statistically significant differences were found in neuroendocrine cancer between the age groups under 39 years and 50-59 years (P=0.005) , 50-59 years and 60-69 years (P=0.03). There are no statistically significant differences in other forms of BC, which does not contravene similar data from the WHO (2003).

Tumors with a size of 2 cm to 5 cm prevailed; they were detected in 185(62.9%) women; in 41(13.9%) women, there were tumors larger than 5 cm, in 32(10.9%) cases tumors of 1cm to 2cm and in 36(12.2%) cases – tumors with a spread to the chest and skin. Comparison of the data revealed that in women of non-indigenous nationality the tumor spread to the chest wall and skin was in 28(15.9%) cases, while in women of indigenous nationality it was in 8(6.8%) cases ($\chi 2$=5.479, df=1, P=0.019) (Table 2).

Table 2.

Distribution of BC patients (n/%) depending on the tumor size

Age group (yrs)	T categories for BC			
	T1 (<2 cm)	T2 (2-5 cm)	T3 (>5 cm)	T4 (Tumor of any size growing into the chest wall or skin)
<39 n=37	6 (16.2)	19 (51.3)	8 (21.6)	4(10.8)
40-49 n=60	7 (11.7)	32 (53.3)	9 (15)	12 (20)
50-59 n=96	7 (7.3)	67 (69.7)	12 (12.5)	10 (10.4)
60-69 n=64	5 (7.8)	43 (67.2)	8 (12.5)	8 (12.5)
≥70 n=37	7 (18.9)	24 (64.8)	4 (10.8)	2 (5.4)
total n=294	32 (10.9)	185 (62.9)	41 (13.9)	36 (12.2)
By ethnicity				
Indigenous n=118	13 (11.0)	80 (67.8)	17 (14.4)	8 (6.8)
Non-indigenous n=176	19 (10.8)	105 (59.7)	24 (13.6)	28 (15.9)

The relationship between the size of the tumor and the lesion of the lymph nodes was statistically significant (Fig.1). The frequency of lymph node damage showed a statistically significant increase with an increase in the tumor size (from 19% with a tumor size <2 cm to 94% with tumors spreading to the chest wall and skin; P=0.001)).

Cancer staging according to the TNM staging system (Table 3) showed that 26(8.8%) women had Stage I, 122 (41.5%) – Stage IIA, 50(17.0%) – Stage IIB, 20(6.8%) – Stage IIIA, 75(25.5%) – Stage IIIB+IIIC, and 1(0.3%) – Stage IV. In the age group of women under 39 years, Stage IIIB+IIIC (43.2%) was most often registered (P=0.01), while in other age groups, Stage IIA (32.4%) was more often noted. Aggregate indicators in groups of indigenous and non-indigenous women with BC showed that Stage IIA of BC was most common in both ethnic groups. Thus, there was a high rate of detection in late stages (IIIB) in young women (<39 years). This can be explained by low clinical suspicion and the fact that this age group is not included in the breast disease screening program; the Republic of Sakha (Yakutia) screens women 40 years and older.

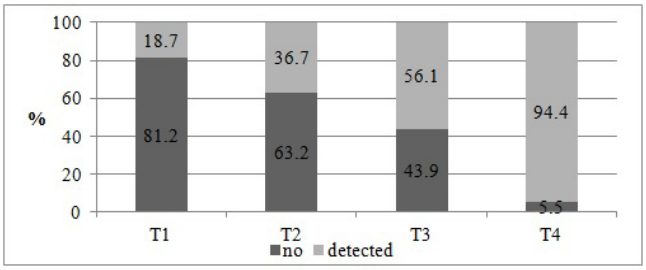

Fig. 1. *The relation between the tumor size and the lesion of the lymph nodes.*

Table 3.

Distribution of BC patients according to the TNM staging system

Age group (yrs)	I*	IIA**	IIB***	IIIA^	IIIB/IIIC^^	IV^^^
<39	4(10.8%)	12(32.4%)	2(5.4%)	2(5.4%)	16(43.2%)	1(2.7%)
40-49	5(8.3%)	19(31.6%)	15(25.0%)	5(8.3%)	16(26.6%)	-
50-59	7(7.3%)	44(45.8%)	19(19.8%)	6(6.2%)	20(20.8%)	-
60-69	5(7.8%)	25(39.1%)	13(20.3%)	5(7.8%)	16(25%)	-
≥70	5(13.5%)	22(59.5%)	1(2.7%)	2(5.4%)	7(19.0%)	-
Total	26(8.8%)	122(41.5%)	50(17.0%)	20(6.8%)	75(25.5%)	1 (0.3%)

*- (T1N0M0), **- (T2N0M0.T0N1M0), ***- (T3N0M0.T2N1M0), ^- (T3N1M0.T0-2N2M0), ^^- (T4N0-2M0.T0-4N3M0), ^^^- (T0-4N0-3M1)

G1 was found in 96 (32.6%), G2 in 146 (49.6%), and G3 in 52 (17.7%) cases (Table 4). When analyzing structural atypia with an assessment of the presence of tubular structures, it was found that 1 point (<75%) was 56(19%) cases, 2 points (10%-75%) – 88(29.9%), and 3 points (less than 10%) - in 150(51%) women.

The analysis of cellular atypia showed that small cells of the same size and shape with a dispersion distribution of chromatin, without nucleoli (1 point) were detected in 44(14.9%) women. A small polymorphism of the nuclei, some cell enlargement (2 points), was found in 168(57.1%) women. Large nuclei of various shapes with one or more nucleoli, coarse chromatin (3 points) were detected in 82(27.9%) cases. The calculation of mitoses showed that 1 point (0–9 mitoses in 10 visual fields) was present in 137 (46.6%) women, 2 points

in (10–19 mitoses) – 91(30.9%) women, and 3 points (20 or more mitoses) in 66 (22.4%) women. Statistically significant dependence of the malignancy degree on the age and ethnicity of the examined women was not found.

Table 4.

Distribution of BC patients depending on the degree of malignancy

	Total n=294	%
Degree of malignancy		
G1	96	32.6
G2	146	49.6
G3	52	17.7
Score (Points)	*Structural atypia*	
1	56	19.0
2	88	29.9
3	150	51.0
Score (Points)	*Cellular atypia*	
1	44	14.9
2	168	57.1
3	82	27.9
Score (Points)	*Mitoses*	
1	137	46.6
2	91	30.9
3	66	22.4

Eighty-six percent of women had an infiltrative form of cancer. Due to the small number of observations of other morphological forms of cancer, it was not possible to establish a relation between the degree of malignancy and the form of cancer.

A statistically significant relationship between the tumor size and the degree of malignancy was found (Figure 2). Thus, the T4 tumor has the degree of histological malignancy G3 (19.2%) significantly more often than G1 (6.2%).

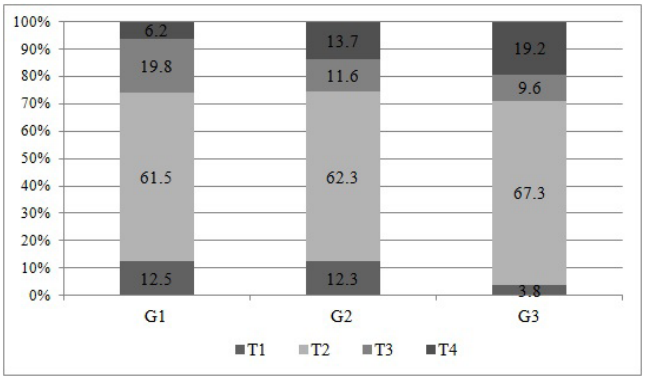

Fig.2. *The degree of malignancy and the size of the tumor.*

Statistically significant dependence by the degree of malignancy of the metastases presence in the lymph nodes was found (Fig.3). Thus, 61.5% of women with G3 had metastases to regional lymph nodes, while with G1- in 40.6% ($\chi2$= 5.1, df=1, $P_{1\text{-}2}$= 0.02), and with G2 – in 41.1% ($\chi2$= 5.6, df=1, $P_{2\text{-}3}$=0.01).

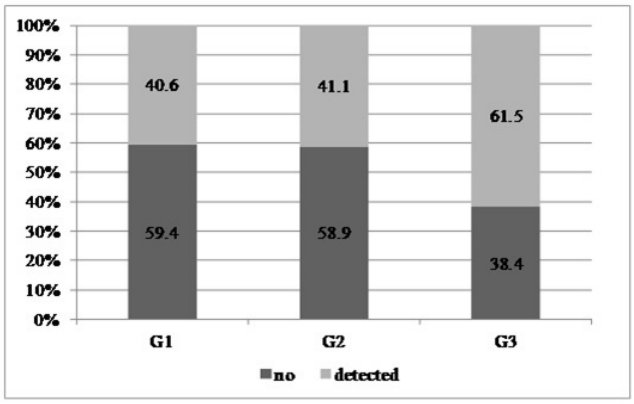

Fig. 3. *The degree of malignancy and damage of the lymph nodes.*

Conclusion

BC is most frequently reported in women of indigenous and non-indigenous nationalities in the age groups of 50-59 years (32.6%) and 60-69 years (21.8%). Tumors with a spread to the chest wall and skin develop more often in women of non-indigenous nationalities (15.9% of cases), than in women of indigenous nationality (6.8% of cases). Regardless of ethnicity, the most common histological form of BC in women of the RS(Y) is infiltrative ductal cancer (65.3%). The TNM staging system showed that the IIA and IIB stages were predominant (58.5% of cases) in the general age group of the examined patients, while in patients under age 39 – IIIB+IIIC stage (43.2%).

We also found a relationship between the size of the primary tumor and the number of lymph nodes affected by metastases (P=0.001), which can be considered as a criterion for the unfavorable clinical course of breast cancer.

Our findings suggest that further investigation of the peculiarities of the course of BC in the female population of Yakutia would lead to much improved methods of diagnosis and treatment.

Competing Interests

The authors declare that they have no competing interests.

References

1. Pisareva LF, Boyarkina AP, Panferova EV et al. The incidence of breast cancer in the female population of the Irkutsk region. Risk factors. Siberian Journal of Oncology. 2012:5(53):12 - 17.
2. Pisareva LF, Odintsova IN, Boyarkina AP. Features of the incidence of breast cancer in the population of the region of Siberia and the Far East, taking into account the factor of migration. Russian Journal of Oncology. 2006; (2):48-50.
3. Kulakov VI, Tokhiyan AA. Problems of malignant neoplasms of the reproductive system in the practice of a gynecologist. Journal of Obstetrics and Women's Diseases. 2001; 30(1):9–12.

4. DePinho RA. The age of cancer. Nature. 2000 Nov 9;408(6809):248-54. doi: 10.1038/35041694.
5. Dulganov KP, Dulganov PK, Dulganov VK. Epidemiology of malignant tumors in the Republic of Buryatia. Ulan-Ude: Buryat Publishing House. State University;, 2001. [In Russiuan].
6. Bozhok AA, Semiglazov VF, Semiglazov VV, et al. Prognostic and predictive factors in breast cancer Problems of Oncology. 2005;51(4):434-443.
7. Pisareva LF, Odintsova IN, Ananina OA, Muranova OYu, Guruina LI.. Epidemiology of breast cancer in the Primorsky Krai. Siberian Journal of Oncology. 2010;1:50-55.
8. Elston CW, Ellis IO. Pathological prognostic factors in breast cancer. I. The value of histological grade in breast cancer: experience from a large study with long-term follow-up. C. W. Elston & I. O. Ellis. Histopathology 1991; 19; 403-410. Histopathology. 2002 Sep;41(3A):151-2, discussion 152-3. PMID: 12405945.
9. Loskutova KS, Argunov VA, Innokentieva AS, Sivtseva TP, Kirillina MP. Immunomorphological characteristics of the hormonal status of primary breast cancer in the Republic of Sakha (Yakutia). Yakut Medical Journal. 2009;(1):46-49.
10. Anderson WF, Chatterjee N, Ershler WB, Brawley OW. Estrogen receptor breast cancer phenotypes in the Surveillance, Epidemiology, and End Results database. Breast Cancer Res Treat. 2002 Nov;76(1):27-36. doi: 10.1023/a:1020299707510.

International Journal of Biomedicine 11(2) (2021) 206-211
http://dx.doi.org/10.21103/Article11(2)_OA14

ORIGINAL ARTICLE

Radiology

INTERNATIONAL JOURNAL OF BIOMEDICINE

Normal Diaphragm Measurements in the Saudi Population Using Posteroanterior Chest Radiograph

S. Alghamdi[1*], PhD; L. Bushara[1], PhD; D. Bilal[1], PhD; Hind Alghamdi[2], MD; Ikhlas Abdulaziz[1], PhD; R. Aljondi[1], PhD; S. Aldahery[1], PhD; A Tajaldeen[3], PhD

[1]*Department of Applied Radiologic Technology, College of Applied Medical Sciences, University of Jeddah, Jeddah, Saudi Arabia*
[2]*Radiology Department, King Fahad General Hospital, Jeddah, Saudi Arabia*
[3]*Radiological Science Department, College of Applied Medical Science, Imam Abdulrahman Bin Faisal University, Dammam, Saudi Arabia*

Abstract

The aim of this study was to establish normal measurements of the hemidiaphragm widths and heights in the Saudi population by a posteroanterior (PA) chest X-ray in the Mecca Region.

Methods and Results: The data were collected prospectively at King Abdulaziz Hospital in Saudi Arabia, Jeddah, between March and April 2021, using a computed radiography imaging unit. A total of 45 patients (51.1% men and 48.9% women; the age range between 15 and 79 years) were included in the study. Measurements were obtained on an ideal PA chest radiograph by measuring the distance from the highest points of the right hemidiaphragm and left hemidiaphragm. The width from the right and left costophrenic angle was also measured as an ended point. The total diaphragm width (DW) was 278.32±24.83 mm, the total right diaphragmatic dome height (RDDH) -51.30±10.58 mm, and left diaphragmatic dome height (LDDH) - 38.40±9.21 mm.

The DW was greater in men than in women: 291.74±20.4 mm and 264.28±21.2 mm, respectively. RDDH and LDDH were also greater in men than in women: 55.4±6.77 mm and 47.005±12.19 mm, and 43.29±6.65 mm and 33.28±8.83 mm, respectively

Conclusion: Computed radiography was useful in measuring the diaphragm because measurement points can be identified accurately and easily due to the availability of the processing system functions such as the ability to manipulate the image resolution, image contrast, and magnification.**(International Journal of Biomedicine. 2021;11(2):206-211.)**

Key Words: diaphragm • posteroanterior chest X-ray • Saudi population

For citation: Alghamdi S, Bushara L, Bilal D, Alghamdi H, Abdulaziz I, Aljondi R, Aldahery S, Tajaldeen A. Normal Diaphragm Measurements in the Saudi Population Using Posteroanterior Chest Radiograph. International Journal of Biomedicine. 2021;11(2):206-211. doi:10.21103/Article11(2)_OA14

Abbreviations

CT, computed tomography; **DW**, diaphragm width; **LDDH**, left diaphragmatic dome height; **LHD**, left hemidiaphragm; **PA**, posteroanterior; **RDDH**, right diaphragmatic dome height; **RHD**, right hemidiaphragm.

Introduction

The diaphragm is a thin layer of muscle that has the main function of controling the process of normal breathing, also acting as a physical barrier separating the thorax from the abdomen.[1,2] Often, it can be a cause of dyspnea due to dysfunction, which can be either intrinsic or extrinsic.[3] It has several links to the thoracic wall that can be seen with radiological imaging, such as CT, which is an important point of reference for image interpretation.[4] Evaluation of chest X-rays may seem simple, but it is actually a complex task and requires observation of the diaphragm's location and shape, which are commonly used to determine whether the lungs are underinflated or hyperinflated.[5] Therefore, an understanding of the normal anatomy of the chest is essential for an accurate diagnosis of the diaphragm.[6]

The crus of the diaphragm extends to the lumbar vertebral bodies and disks beneath the diaphragm, attaches the diaphragm to the lumbar vertebral bodies and disks, and is joined by *the median arcuate ligament.*[1]) *The median arcuate ligament* extends as fibrous bands between the first and second lumbar vertebral bodies and the first lumbar transverse process over *the anterior psoas muscle* as fibrous bands,[7] while *the lateral arcuate ligament* consists of fascial bands covering *the quadratus lumborum muscle* and extending from the twelfth thoracic transverse process to the middle portion of the twelfth thoracic ribs.[1] These ligaments are better depicted with CT imaging.[8] While the use of CT has increased considerably in recent decades, a chest X-ray is the most commonly performed imaging test.[9]

During inhalation, the diaphragm contracts and moves in the inferior direction, thereby increasing the thoracic cavity volume by drawing air into the lungs.[2] The RHD appears to be marginally higher than the LHD. Additionally, the diaphragm's anterior and medial portions are regularly higher than the posterior and lateral portions.[1] This finding is relatively common; therefore, during interpretation, radiologists should be familiar with variants of the diaphragm to avoid unnecessary concern and further evaluation. Accordingly, an elevated hemidiaphragm on a chest X-ray can occur for a number of reasons. It can be from diminished lung volume, phrenic nerve paralysis, eventration of the diaphragm, subphrenic abscess, hepatomegaly, or splenomegaly.[10]

An elevated diaphragm might be difficult for clinicians to identify due to their relative rareness.[11] As the elevated diaphragm is usually undiagnosed during clinical examination, it should not be neglected, since this can adversely affect the quality of life, and can also be a predictor of the seriousness of pathology.[12] A chest X-ray is the most frequent radiologic examination used to evaluate the diaphragm because it is very simple and accessible.[5]

Knowledge of the normal height of RHD and LHD can be helpful in diagnosing some chest diseases and some sub-diaphragmatic organ diseases,[13] as knowledge of the normal height of the diaphragm could help the radiologists to indicate other radiologic examinations, such as abdominal ultrasound, CT chest or cervical MRI (if it was found that there is diaphragmatic elevation), in order to find the cause of this disorder.[14] Since the literature includes very little data on determining the normal variation in diaphragm position and shape,[15] the aim of this study was to establish normal measurements of the hemidiaphragm widths and heights in the Saudi population by a PA chest X-ray in the Mecca Region.

Materials and Methods

The data were collected prospectively at King Abdulaziz Hospital in Saudi Arabia, Jeddah, between mid-March and April 2021, using a computed radiography imaging unit. A total of 45 patients (51.1% men and 48.9% women; the age range between 15 and 79 years) were included in the study. PA chest X-ray was performed by using an X-ray machine (Shimadzu, Japan. Focal spot: Small (0.6) mm / Large (1.2) mm; Maximum kV: 150 kVp; Maximum mA: 500mA; Year of Installation: 2011.3-1-3). Images were processed with a Fuji FCR CAPSULA XLII Computed Radiography System.

All participants were diagnosed with a normal chest X-ray. Excluded were patients with severe pathological conditions, such as pleural effusion, collagen vascular disease, pulmonary hypertension, cardiomegaly, ascites, liver cirrhosis, hepatomegaly, or splenomegaly.

Image acquisition

Measurements were obtained on an ideal PA chest radiograph by measuring the distance from the highest points of the RHD and LHD. The width from the right and left costophrenic angle was also measured as an ended point. The *PA view* is a standard view for a chest X-ray. For all adults. patients were in an upright position facing the cassette with the patient's chin resting at the middle of the top of the Bucky. The feet were placed slightly apart to keep the patient steady. The median sagittal plane was adjusted to the middle of the cassette. The shoulders were rotated forward and in contact with the cassette by placing the dorsal aspect of the hands behind and below the hips, with the elbows brought forward or allowing the arms to encircle the Bucky (Figure 1).

***Fig. 1**. A PA Chest X-ray. Recommended patient position.*[19]

For an ideal PA chest X-ray, patients were asked to take a deep breath and hold it, and the image was acquired at inspiration. The exposure factor was 110kVp and 8mAs. A PA chest X-ray image of a middle-aged female is presented in Figure 2. The detail of signs of a good quality PA image and anatomy is included in the quality of the image and the radiological anatomy part.

Fig. 2. PA CXR image showing a good quality image, with equidistant clavicles at the level of the T4 thoracic vertebra, all the necessary areas of the chest included. The anterior 7 ribs and the posterior 10 ribs are visible above the diaphragm showing good inspiration. There is a subtle abnormal finding – RT upper.

Image analysis

Two certified technologists, bachelor's degree (BSc) in diagnostic imaging and PhD in cross sectional imaging, independently reviewed the chest X-ray images for diaphragm measurement for all patients on two separate days (at least two weeks apart).. Images were initially reviewed to be excluded for the absence of severe pathology. During a separate subsequent session, images were measured as the following (Figure 3):

- A vertical line was drawn at the maximum height of each hemidiaphragm.
- A straight parallel line was drawn at the maximum height of each hemidiaphragm, to measure the distance between both lines.
- A straight line was drawn between two costophrenic angles to measure the width.

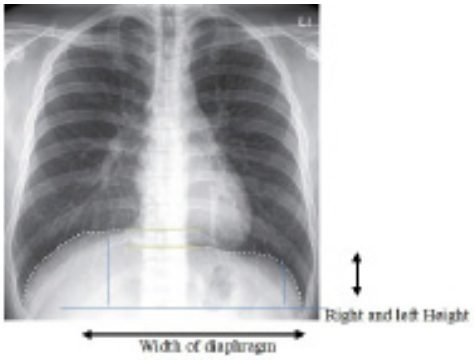

Fig. 3. *Diaphragm measurement of the RHD and LHD (Study Protocol).*

Statistical analysis was performed using the IBM SPSS Statistics for Windows, Version 22.0. Armonk, NY: IBM Corp.). The normality of distribution of continuous variables was tested by the Kolmogorov-Smirnov test with the Lilliefors correction and Shapiro-Wilk test. Baseline characteristics were summarized as frequencies and percentages for categorical variables and as mean±standard deviation (SD) for continuous variables. Means of 2 continuous normally distributed variables were compared by independent samples Student's t test. Differences of continuous variables departing from the normal distribution, even after transformation, were tested by the Mann-Whitney U-test. The frequencies of categorical variables were compared using Pearson's chi-squared test or Fisher's exact test, when appropriate.A probability value of $P<0.05$ was considered statistically significant.

Results

The following figures and tables presented the data obtained from 45 normal subjects after measuring the width and height of the RHD and LHD. The other variables taken were age and gender. Correlations were applied by presenting a trend line and resultant equations in the graphs; this was done for males (51.1% of the sample) and the females (48.9% of the sample), as well as the total sample values.

Figure 4 presents the frequency distribution of age/years for the age groups (15-25), (26-36), (37-47), (48-58), (59-69), (70-79) by the valid percentage 28.9%, 26.7%, 26.7%, 8.9%, 6.7%, 2.2%, respectively. Figure 5 presents the frequency distribution of gender by the valid percentage of 51.1% for males and 48.9% for females.

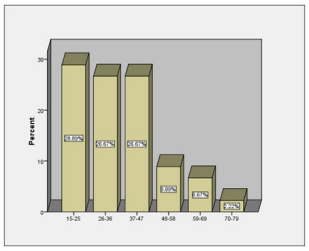

Fig. 4. *The frequency distribution of age/years for the age groups.*

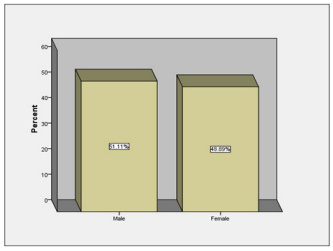

Fig. 5. *The frequency distribution of gender*

Table 1 presents the total sample means and standard deviations of the variables. The sample age was 36.29±15.18 years. The total DW was 278.32±24.83mm, the total RDDH -51.30±10.58mm, and LDDH - 38.40±9.21mm. Table 2 compares the values of DW, LDDH, and RDDH in different age groups. The DW and RDDH were greater in age group 70-79 years, and LDDH was greater in age group 26-36 years.

Table 1.

Descriptive statistics for age, DW, RDDH and LDDH

Variable	N	Minimum	Maximum	Mean	SD
Age	45	15	79	36.29	15.18
DW	45	212.0	338.5	278.32	24.83
RDDH	45	29.0	69.0	51.30	10.58
LDDH	45	20.0	56.6	38.40	9.21

Table 2.

The values of DW, LDDH, and RDDH in different age groups

Age\years		DW	RDDH	LDDH
15-25	Mean	275.85	50.52	39.62
	Std. Deviation	22.53	10.57	8.01
26-36	Mean	275.50	53.20	40.88
	Std. Deviation	28.36	8.70	10.63
37-47	Mean	274.66	50.16	38.61
	Std. Deviation	22.60	11.19	8.62
48-58	Mean	302.80	51.32	34.00
	Std. Deviation	28.15	16.29	10.58
59-69	Mean	273.83	47.23	29.90
	Std. Deviation	19.50	12.12	8.75
70-79	Mean	303.60	64.20	33.20
Total	Mean	278.32	51.30	38.40
	Std. Deviation	24.83	10.58	9.21
P-value		0.361	0.79	0.445

Table 3 showed a significant correlation between DW and RDDH, LDDH in different ages. The DW was greater in men than in women: 291.74±20.4mm and 264.28±21.2mm, respectively (Table 4). RDDH and LDDH were also greater in men than in women: 55.4±6.77mm and 47.005±12.19mm, and 43.29±6.65mm and 33.28±8.83, respectively (Table 4).

Table 3.

Correlations between DW and RDDH, LDDH in different ages.

		Age	DW	RDDH	LDDH
Age	Pearson Correlation	1	.160	-.007-	-.278-
	Sig. (2-tailed)		.295	.961	.065
	N	45	45	45	45
DW	Pearson Correlation	.160	1	.528**	.377*
	Sig. (2-tailed)	.295		.000	.011
	N	45	45	45	45
RDDH	Pearson Correlation	-.007-	.528**	1	.393**
	Sig. (2-tailed)	.961	.000		.007
	N	45	45	45	45
LDDH	Pearson Correlation	-.278-	.377*	.393**	1
	Sig. (2-tailed)	.065	.011	.007	
	N	45	45	45	45
**. Correlation is significant at the 0.01 level (2-tailed).					
*. Correlation is significant at the 0.05 level (2-tailed).					

Table 4.

Independent t test to compare DW, RDDH and LDDH in different gender

	Gender	N	Mean	Std. Deviation	Std. Error Mean
DW	Male	23	291.74	20.4029	4.2543
	Female	22	264.28	21.2577	4.5322
RDDH	Male	23	55.400	6.7725	1.4122
	Female	22	47.005	12.1929	2.5995
LDDH	Male	23	43.291	6.6465	1.3859
	Female	22	33.286	8.8324	1.8831
Age	Male	23	33.87	15.212	3.172
	Female	22	38.82	15.067	3.212

Figure 6 showed the relationship between age and RDDH/LDDH. Figure 7 showed the relationship between age and diaphragm width.

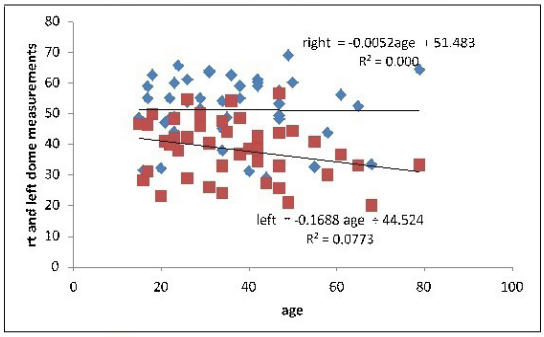

Fig. 6. *Scatter plot. The relationship between age and RDDH, LDDH*

$RDDH = -0.0052age + 51.483 \quad R^2 = 0.000$

$LDDH = -0.1688\ age + 44.524 \quad R^2 = 0.0773$

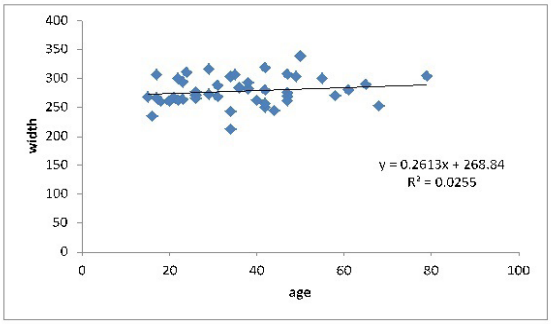

Fig. 7. *Scatter plot. The relationship between age and DW.*

$Y = 0.2613x + 268.84\ ,\ R^2 = 0.0255$

Discussion

On chest X-rays, the position and shape of the diaphragm are commonly used as indicators of normal or abnormal lung volume.[15] However, there is a lack of research that evaluates the normal diaphragm position and shape on an X-ray, based on the measurements and documentation of pulmonary function, without taking into account the observed variability, which includes measurements performed on an ideal PA chest X-ray, and measurement points clearly identified.[10,15,16] This study showed that measurements of the RHD and LHD based on the height and width are slightly sensitive, even when excluding patients with severe clinical pathology.

It has been documented that the use of a chest X-ray as an imaging test is beneficial for chest diagnosis, and in most cases, the diagnosis of hemidiaphragm paralysis can be diagnosed radiologically.[16] Nason et al.[1] identified that the RHD is normally slightly higher than the LHD. Some previous studies published similar findings. H.A.A. Salih [13] obtained 100 cases to measure the height difference between RHD and LHD on PA chest digital radiographs obtained from Sudanese patients with normal chest and abdomen. The authors found

that the RHD is normally higher than LHD in 98% of patients in the range of 1–3 cm with the age ranging from 16–42 years. In addition, Suwatanapongched et al.[15] have prospectively determined and compared the spectrum of diaphragm position and shape on chest X-rays between non-obese and obese patients by using three methods. The first measurement was by relating each hemidiaphragm dome to the vertebral level of the thoracic spine. Secondly, a horizontal line was drawn through the midpoint of the intersecting shadows of the anterior sixth and posterior tenth ribs, on each side. The height of both right and left lungs was used as a third indicator of diaphragm position, measured from the inferior margin of the second rib to the hemidiaphragm dome. The shape of the diaphragm was also determined but only on the right side by using the radius of curvature of the RHD as an indicator.[15] This study also found that the RHD is higher than the LHD in 93% of cases by 03–0.9 cm, with the age ranging from 18–86 years.

These findings support that the radiological evaluation of the diaphragm might pose a potential pitfall, as the normal height of the hemidiaphragm may considerably vary and a wide range of normal or abnormal circumstances based on easily recognized anatomic landmarks used, and analysis of factors that might contribute to this variation, such as age and weight, can provide a more reliable basis for such evaluation. To improve the diagnostic sensitivity of chest radiographs of elevated diaphragm pathologies, the CT is sometimes suggested as a complementary test.[17] However, it must be taken into consideration that the radiation dose associated with a chest CT is much higher than a routine chest X-ray.[18]

This study found a result that is conformable with previous studies, but on the Saudi population. Although the findings showed that the RHD is higher than the LHD, we found that the RHD in the Saudi population is higher than in other populations, such as the Sudanese.[13] It was also found that the RHD is higher in males than in females.

To the best of the researchers' knowledge, this is the first study that evaluated the height and width of hemidiaphragm on chest X-rays among the Saudi population.

The limitation of this study is that the clinical indication of the study population contains chest symptoms that were not generally considered normal. However, all patients had a normal chest X-ray and no radiographic abnormalities predicted to impact the diaphragm height and width. The Saudi population reflects patients routinely seen in a hospital-based practice. The results might not be similar in an asymptomatic, non-referred, unselected population. This study can be repeated on a larger sample in order to provide a more rigorous definition of the normal height and width of the diaphragm and identify factors that influence the variation.

Conclusion

The height of RHD and LHD, as well as DW was higher in men than in women. There is a significant correlation between hemidiaphragm height, DW and age, as they increase during the age increasing.

Competing Interests

The authors declare that they have no competing interests.

References

1. Nason LK, Walker CM, McNeeley MF, Burivong W, Fligner CL, Godwin JD. Imaging of the diaphragm: anatomy and function. Radiographics. 2012 Mar-Apr;32(2):E51-70. doi: 10.1148/rg.322115127.
2. Kocjan J, Adamek M, Gzik-Zroska B, Czyżewski D, Rydel M. Network of breathing. Multifunctional role of the diaphragm: a review. Adv Respir Med. 2017;85(4):224-232. doi: 10.5603/ARM.2017.0037.
3. Onders RP, Elmo M, Kaplan C, Katirji B, Schilz R. Extended use of diaphragm pacing in patients with unilateral or bilateral diaphragm dysfunction: a new therapeutic option. Surgery. 2014 Oct;156(4):776-84. doi: 10.1016/j.surg.2014.07.021.
4. Iochum S, Ludig T, Walter F, Sebbag H, Grosdidier G, Blum AG. Imaging of diaphragmatic injury: a diagnostic challenge? Radiographics. 2002 Oct;22 Spec No:S103-16; discussion S116-8. doi: 10.1148/radiographics.22.suppl_1.g02oc14s103.
5. Puddy E, Hill C. Interpretation of the chest radiograph. Anaesth Crit Care Pa 2007;7:71-75.
6. Sheard S. The Chest X-ray: a Survival Guide. Clin Radiol 2009;64:1246-1247.
7. Candelaria I, Oliveira C, Donato H, et al. The diaphragm: revision of the normal anatomy, function and iconographic review of frequent pathology with CT. Eur Radiol 2014.
8. Gmachowska A, Pacho R, Anysz-Grodzicka A, Bakoń L, Gorycka M, Jakuczun W, Patkowski W. The Role of Computed Tomography in the Diagnostics of Diaphragmatic Injury After Blunt Thoraco-Abdominal Trauma. Pol J Radiol. 2016 Nov 4;81:522-528. doi: 10.12659/PJR.897866.
9. Smith-Bindman R, Lipson J, Marcus R, Kim KP, Mahesh M, Gould R, Berrington de González A, Miglioretti DL. Radiation dose associated with common computed tomography examinations and the associated lifetime attributable risk of cancer. Arch Intern Med. 2009 Dec 14;169(22):2078-86. doi: 10.1001/archinternmed.2009.427.
10. Dubé BP, Dres M. Diaphragm Dysfunction: Diagnostic Approaches and Management Strategies. J Clin Med. 2016 Dec 5;5(12):113. doi: 10.3390/jcm5120113.
11. Kansal AP, Chopra V, Chahal AS, Grover CS, Singh H, Kansal S. Right-sided diaphragmatic eventration: A rare entity. Lung India. 2009 Apr;26(2):48-50. doi: 10.4103/0970-2113.48898.
12. Kokatnur L, Rudrappa M. Diaphragmatic Palsy. Diseases. 2018 Feb 13;6(1):16. doi: 10.3390/diseases6010016.
13. SALIH HAA. Measurement of the height difference between right and left hemi diaphragm in normal Sudanese

***Corresponding author**: Dr. S Alghamdi, PhD. Department of Applied Radiologic Technology, College of Applied Medical Sciences, University of Jeddah, Jeddah, Saudi Arabia. E-mail: ssalghamdi85@gmail.com*

adult using posteroanterior chest radiograph. Sudan University of Science and Ttechnology; 2013.
14. Klein JS, Rosado-de-Christenson ML. A Systematic Approach to Chest Radiographic Analysis. 2019 Feb 20. In: Hodler J, Kubik-Huch RA, von Schulthess GK, editors. Diseases of the Chest, Breast, Heart and Vessels 2019-2022: Diagnostic and Interventional Imaging [Internet]. Cham (CH): Springer; 2019. Chapter 1. PMID: 32096946.
15. Suwatanapongched T, Gierada DS, Slone RM, Pilgram TK, Tuteur PG. Variation in diaphragm position and shape in adults with normal pulmonary function. Chest. 2003 Jun;123(6):2019-27. doi: 10.1378/chest.123.6.2019.
16. Brant WE, Helms CA. Diagnostic imaging methods. Fundamentals of Diagnostic Radiology. 2nd ed Philadelphia (PA). Lippincott Williams and Wilkins; 1999.
17. Chetta A, Rehman AK, Moxham J, Carr DH, Polkey MI. Chest radiography cannot predict diaphragm function. Respir Med. 2005 Jan;99(1):39-44. doi: 10.1016/j.rmed.2004.04.016.
18. Kazerooni EA. High-resolution CT of the lungs. AJR Am J Roentgenol. 2001 Sep;177(3):501-19. doi: 10.2214/ajr.177.3.1770501.
19. Kalra MK, Maher MM, Rizzo S, Kanarek D, Shepard JA. Radiation exposure from chest CT: issues and strategies. J Korean Med Sci. 2004 Apr;19(2):159-66. doi: 10.3346/jkms.2004.19.2.159. Erratum in: J Korean Med Sci. 2004 Jun;19(3):487. Shephard JA [corrected to Shepard JA].

International Journal of Biomedicine 11(2) (2021) 212-215
http://dx.doi.org/10.21103/Article11(2)_OA15

ORIGINAL ARTICLE

Experimental Biology

INTERNATIONAL JOURNAL OF BIOMEDICINE

Morphological Features of Foreign Body Giant Cells in Experimental Conditions

Mariya A. Zatolokina[1*]; Ekaterina S. Mishina[1]; Alexander A. Sozykin[2]; Marina V. Gorbunova[3]; Alexander G. Alekseev[3]

[1]*Kursk State Medical University, Kursk, Russia*
[2]*Rostov State Medical University, Rostov-on-Don, Russia*
[3]*Medical Institute, Orel State University named after I.S. Turgenev, Orel, Russia*

Abstract

Background: The purpose of our work was determined by the accumulation of a significant amount of experimental material under the conditions of implantation of a foreign body, a mesh implant, into the region of the anterior abdominal wall in order to obtain experimental inflammation, in which foreign body giant cells (FBGCs) were constantly visualized as reactive formations. This research aimed to study the dynamics of morphological changes in FBGCs under conditions of experimental implantation of a foreign body, a mesh implant, and the possible mechanism of their formation

Methods and Results: This study was carried out on male Wistar rats, in which a foreign body was implanted—a mesh endoprosthesis made of polypropylene—in the region of the anterior abdominal wall under the aponeurosis of the rectus abdominis muscles. A section of the anterior abdominal wall with the implanted endoprosthesis was excised on Days 10, 21, 30, and 60 after surgery, fixed in 10% buffered formalin solution. The obtained samples were embedded in paraffin according to standard prescriptions; histological sections with a thickness of 5-7μm were made and stained with H&E, according to the methods of Van Gieson and Mallory, and an immunohistochemical study was performed using the marker of cell proliferation (Ki-67). The revealed structural features of multinucleated cells were recorded by microphotography using a photo attachment and a Levenhuk video camera (USA).

During the study, it was revealed that the amount, functional activity and morphological diversity of FBGCs gradually increased, reaching a maximum by Day 30 of the experiment. At a later date, some of them died, while the remaining part was differentiated, splitting into small multinucleated cells and mononuclear elements, morphologically identical to macrophages and fibroblasts. The formation of FBGCs continued as long as the mesh implant was in the body.

Conclusion: FBGCs are reactive formations that arise in response to various endo- and exogenous irritation.(**International Journal of Biomedicine. 2021;11(2):212-215.**)

Key Words: foreign body giant cells • multinucleated giant cells • endoprosthetics • reactivity • phagocytosis

For citation: Zatolokina MA, Mishina ES, Sozykin AA, Gorbunova MV, Alekseev AG. Morphological Features of Foreign Body Giant Cells in Experimental Conditions. International Journal of Biomedicine. 2021;11(2):212-215. doi:10.21103/Article11(2)_OA15

Introduction

Multinucleated elements include striated muscle fibers, mesenchymal tissue at a certain stage of its development, and multinucleated cells that appear as reactive formations in reticular, connective, and epithelial tissues. The non-nomenclature designation of multinucleated cells is extremely diverse, in particular, osteoclasts (multinucleated cells of bone tissue), as well as foreign body giant cells (FBGCs) and Langhans cells, which can be found in connective tissue in inflammation.[1-3] I.I. Mechnikov first noticed the role of the FBGCs: In 1883, I.I. Mechnikov experimentally confirmed the phagocytic function of FBGCs, and also believed that FBGCs appear as reactive formations in inflammation of various etiologies.[4]

***Corresponding author**: Prof. Mariya A. Zatolokina, PhD, ScD. Department of Histology, Embryology, and Cytology. Kursk State Medical University. Kursk, Russia. E-mail: marika1212@mail.ru*

Currently, the majority of domestic and foreign authors are of the opinion that FBGCs are physiological elements of the connective tissue system, and their number, size, and degree of phagocytic activity serve as criteria for determining the degree of connective tissue reactivity.

At the beginning of the last century, A. Nemilov (1937) wrote that the morphogenesis of FBGCs has a special biological significance, manifested by the general ability of a multicellular organism to respond to changes in environmental conditions by changing the degree of dissection of the multinucleated giant cells (MNGCs). Considering the fact that FBGCs occur in some organs with certain functional rearrangements, under conditions of various experimental influences during regenerative processes and are reactive formations with the function of phagocytosis, it seems appropriate to dwell in more detail on the methods of their formation described in the available literature.[5,6]

There are two theories that claim to explain the genesis of FBGCs: the proliferative theory and the syncytial theory. The adherents of the first theory believe that multinucleation occurs as a result of direct or indirect division of the nucleus of one cell. Supporters of the second theory are of the opinion that FBGCs arise from the fusion of several mononuclear cells. At the same time, there is also a third opinion, the authors of which consider both ways of their occurrence equally possible.

There are also several points of view regarding the further fate of FBGCs. Most researchers claim that after fulfilling their phagocytic and resorbing functions, FBGCs die. A smaller group of researchers believe that multinucleated cells are stable viable formations capable of long-term differentiation, up to splitting into mononuclear cells, and only a few authors note that multinucleated cells are an accumulation of degenerating cells fused with each other.[7]

The purpose of our work was determined by the accumulation of a significant amount of experimental material under the conditions of implantation of a foreign body, a mesh implant, into the region of the anterior abdominal wall in order to obtain experimental inflammation, in which FBGCs were constantly visualized as reactive formations.

This research aimed to study the dynamics of morphological changes in FBGCs under conditions of experimental implantation of a foreign body, a mesh implant, and the possible mechanism of their formation and their state under experimental conditions.

Materials and Methods

This study was carried out on male Wistar rats, in which a foreign body was implanted—a mesh endoprosthesis made of polypropylene—in the region of the anterior abdominal wall under the aponeurosis of the rectus abdominis muscles.

In vivo experiments were carried out in accordance with the legislation of the Russian Federation, in strict compliance with the European Convention for the protection of animals used for experimental and other purposes (Strasbourg, France, 1986), the provisions of Directive 210/63/EU of the European Parliament and the Council of the European Union of 22 September 2010 on the protection of animals used for scientific purposes (Article 27).

Biomaterial. A section of the anterior abdominal wall with the implanted endoprosthesis was excised on Days 10, 21, 30 and 60 after surgery, fixed in 10% buffered formalin solution. The obtained samples were embedded in paraffin according to standard prescriptions; histological sections with a thickness of 5-7 μm were made and stained with H&E, according to the methods of Van Gieson and Mallory, and an immunohistochemical study was performed using the marker of cell proliferation (Ki-67).

The revealed structural features of multinucleated cells were recorded by microphotography using a photo attachment and a Levenhuk video camera (USA). The morphometry of multinucleated cells (determination of the FBGC area (S), the numerical density of FBGCs in 1mm^2, the number of nuclei and their diameter (d)) was carried out using an open-source program, Imago J, for image analysis and processing.

Statistical analysis was performed using the Statistica 10.0 software package (Stat-Soft Inc., USA).

Results and Discussion

During the study, it was revealed that on Day 10 of the experiment, multinucleated cells of relatively small size (S = 1730 [1092;3799] μm^2) were seen between the threads of the endoprosthesis and in the immediate vicinity of them, containing about a dozen nuclei in different locations (Fig. 1 [A,B]; Fig. 2 [A, C]). In some cells, large normochromic nuclei with a well-defined, eccentrically located nucleolus and chromatin clumps were seen along the cell periphery (Fig. 2B), leaving the central part of the cytoplasm free; in other cells, large nuclei were in the center and crowded; in the third, the nuclei were displaced to the periphery, to one of the poles of the cell; fourth, they were evenly dispersed throughout the cytoplasm. Also, these nuclei were not the same size: along with very large (d = 5 [4;14] μm), we saw very small nuclei (d = 2.5 [1;5] μm) (Fig.1B).

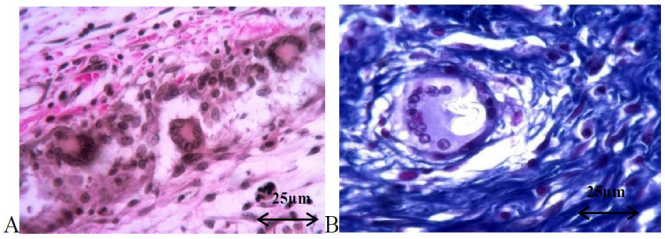

Fig. 1. *Micrograph of FBGC on Day 10 after the experiment. A - ×200, B - ×400. Van Gieson staining (A) and Mallory staining (B).*

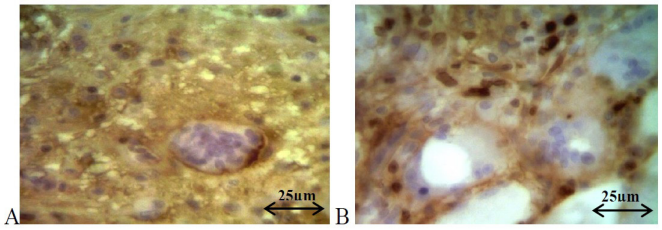

Fig. 2. *Micrograph of FBGC on Day 21 after the experiment. Immunohistochemical detection of Ki-67, ×400*

Most of the nuclei were dense, basophilic, and some were light. Chromatin in the nuclei was dispersed; one or two nucleoli were clearly visible. The cytoplasm of FBGCs was heteromorphic: In some it was oxyphilic; in others it was basophilic and dense; and in a third type, which underwent lysis, the cytoplasm was barely noticeable and weakly colored, and the dark basophilic nuclei of these cells were scattered over the surface of a foreign body (Fig.1B). MNGCs had active phagocytic properties, as evidenced by the presence in their cytoplasm of various captured particles of dead cells.

Three weeks after the beginning of the experiment, around the foreign body (mesh implant threads) the amount of FBGCs increased 1.7 times, against the background of the absence of a significant increase in their dimensional characteristics. The cell cytoplasm was weakly basophilic, often heterogeneous. The darker endoplasm passed to the periphery into a lighter, thinner ectoplasm. The sizes of the nuclei were slightly increased, their diameters varied from 4 [2;7] μm up to 17 [9;40] μm. The color of the cytoplasm was pale; in some cells, the nuclei were sharply basophilic and rich in chromatin. Many FBGCs have been involved in phagocytosis.

It should be noted that during the immunohistochemical study, none of FBGCs was found to give a positive expression of Ki-67, which may indirectly testify in favor of the syncytial theory of their origin (Fig.2 [A,B]).

On Day 30 of the experiment, the number of multinucleated cells (both small and giant), in comparison with Day 10, significantly increased by 2.1 times, against the background of their constant localization on the threads of the Endoprosthesis (Fig.3 [A,B]). The formation of multinucleated cells continued, as evidenced by the lacing cytoplasm and the splitting of multinucleated cells (Fig.3 [C,D]).

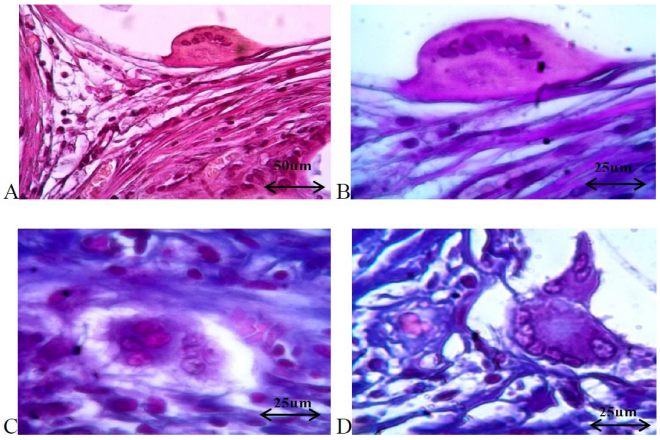

***Fig. 3**. Micrograph of FBGC on Day 30 after the experiment (×400). Van Gieson staining (A, B) and Mallory staining (C, D).*

In the cytoplasm of FBGCs, light gaps appeared, which, as it were, separated from the cell areas containing 2-4 nuclei (Fig.3B), which then separated into individual cells. In some areas, we also saw non-viable multinucleated cells subjected to cytolysis.

Two months after the beginning of the experiment, the density and number of FBGCs were increased, in comparison with the previous period, by 1.5 times, and in comparison with Day 10 of the experiment by 2.5 times. Small multinucleated cells (S = 2167.5 [895.7;3268.2] μm^2) were located mainly near the threads of the endoprosthesis and their nuclei were small, dark, and located throughout the territory of homogeneously stained cytoplasm (Fig.5A). These cells had a high functional activity, as evidenced by phagocytosed particles visualized in the cytoplasm. At the same time, the process of the FBGC cleavage into smaller multinucleated cells was observed (Fig.4 [A,B]), as evidenced by the presence of light gaps in the cytoplasm, allocating zones containing several nuclei (from 10 to 15 nuclei per cell) (Fig.4B). The splitting of multinucleated cells was also evidenced by the configuration of their bodies, in which grooves corresponding to the outlines of the evolved cells were found (Fig.4A).

Along with their differentiation, multinucleated cells died—lysis and disintegration of the cytoplasm and nuclei were noted. Such disintegrating multinucleated cells were localized at some distance from the threads of the endoprosthesis. In most FBGCs, the *enlightened* cytoplasm was observed, followed by resorption of the cytoplasm, mainly in its central part (Fig.4 [C,D]). Heterochromic nuclei, pushed to the periphery, underwent lysis and decay.

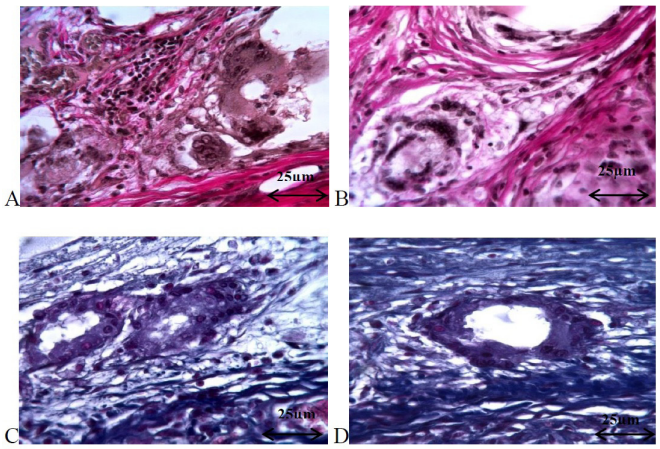

***Fig. 4.** Micrograph of FBGC on Day 60 after the experiment. ×200 (A), ×400 (B,C,D). Van Gieson staining (A) and Mallory staining (B,C,D).*

Summarizing all of the above, the amount, functional activity and morphological diversity of FBGCs gradually increased, reaching a maximum by Day 30 of the experiment. At a later date, some of them died, while the remaining part was differentiated, splitting into small multinucleated cells and mononuclear elements, morphologically identical to macrophages and fibroblasts. The formation of FBGCs continued as long as the mesh implant was in the body.

Conclusion

Thus, the results of this study and the literature data allow us to draw the following conclusions:

1. The origin of FBGCs can be explained by the syncytial theory, according to which giant multinucleated cells are formed by the fusion of several mononuclear cells.[8,9]

2. FBGCs are found in a multicellular organism in normal conditions, in the experiment, and in pathology (inflammation).

3. FBGCs are reactive formations that arise in response to various endo- and exogenous irritation.

4. Literary data regarding the potency and further fate of FBGCs indicate two directions: In the first case, FBGCs turn into degenerative formations and die; in the second case, the phenomena of differentiation occur in multinucleated elements, leading to their splitting into mononuclear cells.

Competing Interests

The authors declare that they have no competing interests.

References

1. Dolzhikov AA, Kolpakov AYa, Yarosh AL, Molchanova AS, Dolzhikova IN. [Giant foreign body cells and tissue reactions on on the surface of implants]. Kursk scientific and practical bulletin "Man and His health." 2017;(3):86-94. [Article in Russian].
2. Zatolokina MA, Kuznetsov SL, Mutova TV, Mishina ES, Zatolokina ES. [Morphology of multinucleated giant cells in different types of stimulation to reparative regeneration in hernioplasty]. Pathogenesis. 2018;16(4):19-27. doi: 10.25557/2310-0435.2018.04.19-27. [Article in Russian].
3. Brodbeck WG, Macewan M, Colton E, Meyerson H, Anderson JM. Lymphocytes and the foreign body response: lymphocyte enhancement of macrophage adhesion and fusion. J Biomed Mater Res A. 2005 Aug 1;74(2):222-9. doi: 10.1002/jbm.a.30313.
4. Brodbeck WG, Anderson JM. Giant cell formation and function. Curr Opin Hematol. 2009 Jan;16(1):53-7. doi: 10.1097/MOH.0b013e32831ac52e.
5. Elchaninov AV, Fatkhudinov TKh., Usman NY, Kananykhina EY, Arutyunyan IV, Makarov AV, Lokhonina AV, Eremina IZ, Surovtsev VV, Goldshtein DV, Bolshakova GB, Glinkina VV, Sukhikh GT. [Dynamics of macrophage populations of the liver after subtotal hepatectomy in rats]. BMC Immunology. 2018;19(1):23. [Article in Russian].
6. Kastellorizios M, Tipnis N, Burgess DJ. Foreign Body Reaction to Subcutaneous Implants. Adv Exp Med Biol. 2015;865:93-108. doi: 10.1007/978-3-319-18603-0_6.
7. Kirk JT, McNally AK, Anderson JM. Polymorphonuclear leukocyte inhibition of monocytes/macrophages in the foreign body reaction. J Biomed Mater Res A. 2010 Sep 1;94(3):683-7. doi: 10.1002/jbm.a.32682.
8. Perdiguero EG, Geissmann F. The development and maintenance of resident macrophages. Nat Immunol. 2016 Jan;17(1):2-8. doi: 10.1038/ni.3341.
9. You Q, Holt M, Yin H, Li G, Hu CJ, Ju C. Role of hepatic resident and infiltrating macrophages in liver repair after acute injury. Biochem Pharmacol. 2013 Sep 15;86(6):836-43. doi: 10.1016/j.bcp.2013.07.006.

International Journal of Biomedicine 11(2) (2021) 216-219
http://dx.doi.org/10.21103/Article11(2)_OA16

ORIGINAL ARTICLE

Microscopy Research and Technique

INTERNATIONAL JOURNAL OF BIOMEDICINE

Comprehensive Study of the Structural Components of the Skin: From Routine Methods to Modern Microscopy Methods

Ekaterina S. Mishina[1*]; Mariya A. Zatolokina[1]; Marina V. Gorbunova[2]; Alexander G. Alekseev[2]; Elena S. Chernomortseva;

[1]*Kursk State Medical University, Kursk, Russia*
[2]*Medical Institute, Orel State University named after I.S. Turgenev, Orel, Russia*

Abstract

Background: Modern methods of microscopy expand our capabilities to detail objects and move to the study of native tissue. The varieties of laser microscopy, which are becoming more and more popular, have broad prospects in the study of morphological properties, combining high resolution and minimal exposure to aggressive media during sample preparation. However, in the scientific literature, the aspects of the structure of individual structural components of the skin or morphofunctional changes in various pathological conditions are not well covered. In this regard, the purpose of our study was a multilevel analysis of structural components using both classical and modern morphological methods.

Methods and Results: The material for this study was skin fragments obtained from laboratory male Wistar rats. The study of the structural components was carried out by the methods of light microscopy, scanning electron microscopy, and laser scanning microscopy. The results of our study indicate that the most effective way to obtain complete information is an integrated approach to the study of tissue morphology, where the researcher requires deep knowledge and the use of not only modern methods, but also the possibility of combining them with existing classical methods.(**International Journal of Biomedicine. 2021;11(2):216-219.**)

Key Words: skin • light microscopy • scanning electron microscopy • laser scanning microscopy

For citation: Mishina ES, Zatolokina MA, Gorbunova MV, Alekseev AG, Chernomortseva ES. Comprehensive Study of the Structural Components of the Skin: From Routine Methods to Modern Microscopy Methods. International Journal of Biomedicine. 2021;11(2):216-219. doi:10.21103/Article11(2)_OA16

Abbreviations

MPM, multiphoton microscopy; **LM**, light microscopy; **SEM**, scanning electron microscopy; **LSM**, laser scanning microscopy; **H&E**, hematoxylin and eosin; **TEM**, transmission electron microscopy.

Introduction

Over the long history of microscopic research, a large amount of information has been accumulated about the microstructure of tissues and organs, which we can obtain from scientific journals, monographs, and educational literature. At this stage, modern morphology seeks to obtain information about the structure of living tissues of organs. The main components that determine the quality of the "research - result" sequence are sample preparation and technical characteristics of the optical device. In this regard, each of these stages undergoes its perfection—the quality of optics, increase in resolution and in sample preparation, reduction in destructive effects.

At present, morphologists have in their arsenal a fairly large set of microscopic methods, any of which can be used depending on the task at hand. However, there is no complex data in the available literature that allows one to compare the data obtained using different methods. In this regard, the

***Corresponding author**: Ekaterina S. Mishina, PhD. Department of Histology, Embryology, and Cytology. Kursk State Medical University. Kursk, Russia. E-mail: katusha100390@list.ru*

purpose of our study was a multilevel analysis of structural components using both classical and modern morphological methods.

Material and Methods

The material for this study was skin fragments obtained from laboratory male Wistar rats. The study of the structural components was carried out by the methods of light microscopy (LM), scanning electron microscopy (SEM), and laser scanning microscopy (LSM).

Results

Among the routine methods of microscopy, the main one is still LM with H&E staining,[1,2] the result of which is staining of nuclei in colors from purple to blue (the shade depends on the type of hematoxylin and the duration of staining), and of cytoplasm and extracellular matrix in colors from pink to red (the shade depends on the pH of the eosin and the duration of the staining) (Figure 1A). This technique is intended rather for an overview, histological or pathological examination and further morphometric processing. The next stage for the study of tissue is the use of histochemistry, as a method of histology, which makes it possible to isolate individual structures due to the specific chemical interaction of tissue components with a dye or mixture of dyes. The most popular methods for studying the fibrous components of the skin are staining according to Van Gieson (Figure 1B) and Mallory. Due to the non-absolute specificity of the methods, it is not always possible to determine the biochemical nature of tissues. In order to selectively stain fibers, it is necessary to carry out careful differentiation.[3-6]

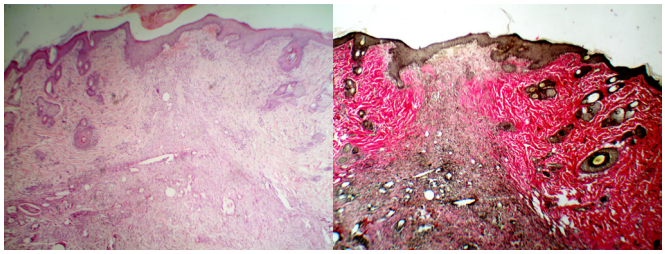

Fig. 1. *Micrograph of the skin: a section of the connective tissue scar. A - H&E staining (Magnification ×40). B - Van Gieson staining (Magnification ×40)*

Of course, light-optical methods are applicable for microscopy at low magnification. The use of electronic techniques allows "depth of penetration" and expands knowledge of the ultra-microstructure of an object. But each method has its own target priorities. For SEM, this is primarily the acquisition of information about the shape and surface of the structure, whereas TEM adds knowledge about the intracellular, more detailed (at higher magnification) structure.[7,8] All of the above methods give an idea of the morphological picture, taking into account the errors caused by numerous stages of sample preparation—the action of formaldehyde, alcohols, xylenes, etc.

The beginning of the study of the morphology of living tissue was the study of samples isolated from cultured cells of tissues by the phase-contrast method. Improvements on this method—Hoffman modulation contrast and Nomarski interference contrast—make it possible to study the cultured cells, as well as the structure of living cells, at the maximum resolution (×1000) of the light microscope.[9,10] The use of an inverted microscope with a cell incubator and time-lapse imaging makes it possible to study the structural dynamics of cultured cells from the moment of their seeding to the formation of a confluent monolayer, and changes in the shape of cells in a wide range from spherical to elongated and flattened, which confirms their high plasticity (Figure 2A). The process of cell division, the interaction of cells with each other, and adaptation to new cultural conditions have been studied in detail, all of which can be regarded as cells' acquisition of a peculiar cultural phenotype (Figure 2B).

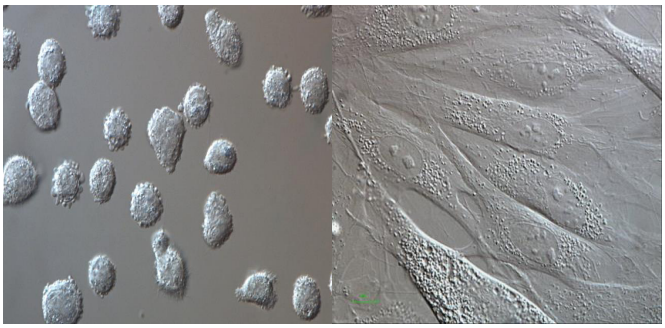

Fig. 2. *Micrograph of the culture of isolated fibroblasts. A - at the attachment stage. 3 hours after reseeding. B - at the monolayer stage. Nomarski interference contrast (Magnification ×600).*

Another method for the study of cultured fibroblasts (the method of intravital microscopy) is the study of cultures by direct, confocal, scanning multiphoton microscopy. Cell structures containing fluorophores will fluoresce in the green or yellow range, depending on the wavelength of infrared radiation.[11-13] Confocal microscopy expands the range of our capabilities for a detailed study of other cellular structures, as well as their chemical composition, and allows the addition of immunocytochemical methods, in particular the use of fluorescent proteins.[14] It is applicable to both the study of fixed preparations and intravital study.

Concerning the morphology of living tissue, various types of laser microscopy are used, and one of the most promising methods is MPM, which is based on the ability of some tissues to autofluorescence.[15-18] The main advantage of MPM over electron microscopy is the identification of cellular and fibrous components with absolutely preserved architectonics and dimensional data of the object under study (Figure 3A). With MPM of the dermis, the cells in it fluoresce in the green and yellow spectral channels. A sufficiently pronounced signal comes from the fibrous elements of the extracellular matrix surrounding the cells (Figure 3 B).

A similar glow caused by infrared photons will be generated by the fibrous structures of the connective

tissue—elastic and collagen fibers. The latter, in addition to multiphoton autoluminescence, generates radiation called the second optical harmonic. In this case, some of the infrared photons are not absorbed by electrons, but are reflected from the electron shells of collagen atoms and scattered as radiation with half of the wavelengths of infrared photons. This radiation generated by the reflection of infrared photons will be differentiated by special filters in the form of a blue-blue glow. Elastic fibers with autoluminescence properties will give a green or yellow glow.

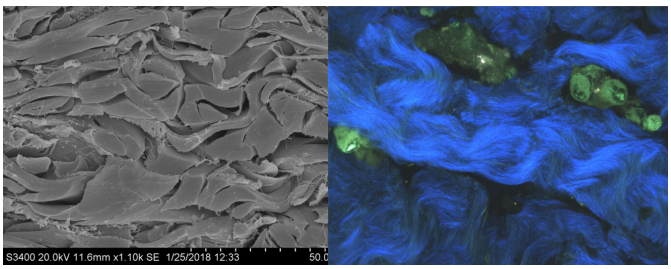

Fig. 3. *Micrograph of the dermis of the skin. A – SEM (×1100). B - Two-photon laser scanning confocal microscopy (×400)*

The nature of the second harmonic is associated with the anisotropic structural organization of collagen fibers. Thus, we can identify the biochemical nature of the fibrous structures. Considering the ability of an enhanced generation of infrared radiation at a greater depth, with MFM we have the possibility of layer-by-layer scanning of the examined skin (Figure 4).

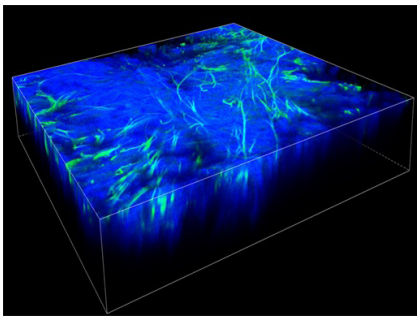

Fig. 4. *Micrograph of the dermis of the skin. Two-photon laser scanning confocal microscopy (3D reconstruction), × 400*

Discussion

Nonlinear optical microscopy is a convenient tool for biomedical imaging due to the physical principles underlying the creation of contrast between individual objects. One of its main advantages is the ability to reconstruct a volumetric image, which, in particular, makes it possible to perform morphological studies ex vivo (on biopsy samples) and in vivo. And in the future, the results of such studies will become important diagnostic criteria in clinical practice. As a result of the above, we can conclude that modern methodological capabilities are gradually bringing us closer to the visualization of living tissues without the use of sample preparation. The knowledge accumulated by classical histology will help us in interpreting the data obtained using new methods, which can take a key place in the integration of cell biology, biochemistry, physiology, molecular genetics, and proteomics in solving fundamental problems and applied problems of biomedical research. A fairly wide variety of such methods allows one to choose the optimal technique for specific needs, taking into account the advantages and disadvantages of specific methods, and important diagnostic criteria in clinical practice, as well as existing methodological limitations.

Competing Interests

The authors declare that they have no competing interests.

References

1. Borodin VO, Sabirov DKh, Tsybina AN, Zvada EA. [Microscopic methods and their role in modern biological sciences]. Scientific Review. Pedagogical Sciences. 2019;5 (2):36-40. [Article in Russian].
2. Korzhevsky DE. [Application of hematoxylin in histological technique]. Morphology. 2007;132(6):77-81. [Article in Russian].
3. Atyakshin DA, Gerasimova OA, Meshkova VYu, Samodurova NYu, Samoilenko TV, Shishkina VV. [A new histochemical approach for evaluating tryptase expression in mast cell populations]. Journal of Anatomy and Histopathology. 2020;9(3):94-101. [Article in Russian]. doi: 10.18499 / 2225-7357-2020-9-3-94-101
4. Nadezhdin SV, Fedorova MZ, Burzhinskaya VA. Theoretical foundations of modern microscopy methods. Belgorod: BelGU; 2008. [in Russian].
5. Omelyanenko NP, Slutskiy LI. Connective tissue (Histophysiology and Biochemistry). Edited by Mironov SP. M.: Izvestia; 2009 (Vol. 1). [In Russian].
6. Senturk GE, Canillioglu YE. Which histochemical staining technique should I choose for biological specimens Microscopy: advances in scientific research and education. Formatex Research Center. 2014:769-72.
7. Morphological research and electron microscopy: a guide. Edited by Korzhevsky DE. SPb.: SpetsLit; 2013. [In Russian].
8. Shapovalova YeYu, Boyko TA,. Baranovskiy YuG, Morozova MN, Barsukov NP, Ilchenko FN, Baranovskiy AG. Effects of fibroblast transplantation on the content of macrophages and the morphology of regenerating ischemic cutaneous wounds. International Journal of Biomedicine. 2017;7(4):302-306. doi: 10.21103/Article7(4)_OA6
9. Potaturkina-Nesterova NI, Nemova IS, Artamonova MN, Gorelnikova EA, Kuyarov AA, Potekhina LP, Radaeva OA, Samyshkina NE. [Modern methods of microscopy in the study of biological objects]. Modern Problems of Science and Education. 2012;(6). [Article in Russian].
10. Chen F, Tillberg PW, Boyden ES. Optical imaging. Expansion microscopy. Science. 2015 Jan 30;347(6221):543-8. doi: 10.1126/science.1260088
11. Korzhevsky DE, Kirik OV, Sukhorukova EG. Molecular morphology. Methods of fluorescence and confocal laser

microscopy. SPb.: SpetsLit; 2014. [In Russian].
12. Snegireva LV. [Optical research methods in biology and medicine]. International Journal of Experimental Education 2017;2:51–52. [Article in Russian].
13. Feofanov AV. [Spectral laser scanning confocal microscopy in biological research]. Advances in Biological Chemistry. 2007;47:371–410. [Article in Russian].
14. Bewersdorf J, Egner A, Hell SW. Microscopy. In: Handbook of biological confocal microscopy. Boston, MA, Springer US 2006; 561–570.
15. Bancelin S, Decencière E, Machairas V, Albert C, Coradin T, Schanne-Klein MC, Aimé C. Fibrillogenesis from nanosurfaces: multiphoton imaging and stereological analysis of collagen 3D self-assembly dynamics. Soft Matter. 2014 Sep 21;10(35):6651-7. doi: 10.1039/c4sm00819g.
16. Betzig E, Patterson GH, Sougrat R, Lindwasser OW, Olenych S, Bonifacino JS, Davidson MW, Lippincott-Schwartz J, Hess HF. Imaging intracellular fluorescent proteins at nanometer resolution. Science. 2006 Sep 15;313(5793):1642-5. doi: 10.1126/science.1127344.
17. Springer Protocols. Fibrosis: Methods and Protocols (Methods in Molecular Biology, 1627). Edited by Laure Rittié. Human Press; 2017.
18. Wu K, Li G. Investigation of the Lag Phase of Collagen Fibrillogenesis Using Fluorescence Anisotropy. Appl Spectrosc. 2015 Oct;69(10):1121-8. doi: 10.1366/14-07780.

International Journal of Biomedicine 11(2) (2021) 220-223
http://dx.doi.org/10.21103/Article11(2)_CR4

CASE REPORT

INTERNATIONAL JOURNAL OF BIOMEDICINE

Vitamin D Deficiency Manifested by Premature Ventricular Complexes from RVOT: A Report on Two Twins

Gabriel Cismaru*, Cecilia Lazea, Daniela Iacob, Simona Cainap

"Iuliu Haţieganu" University of Medicine and Pharmacy
Cluj-Napoca, Romania

Abstract

Vitamin D receptor is present in almost every cell of the body. Although some studies have suggested that values >30ng/ml would be sufficient, there is no consensus on the optimal values of serum vitamin D. Vitamin D deficiency can lead to "benign" manifestations, such as back pain, joint pain, fatigue, and heavy sweating. Premature ventricular contractions (PVCs) originating from the right ventricular outflow tract (RVOT) are considered "benign," as they occur in patients without structural heart disease and their exact cause remains unknown. We describe the case of a 10-year-old boy with frequent PVCs and vitamin D deficiency that was corrected after vitamin D supplementation. On the contrary, his twin brother had normal serum vitamin D and no PVCs. The disappearance of PVCs occurred after treatment with vitamin D 2000 IU/day.(**International Journal of Biomedicine. 2021;11(2):220-223.**)

Key Words: right ventricular outflow tract • twins • vitamin D • premature ventricular contractions • 24-hour Holter ECG

For citation: Cismaru G, Lazea C, Iacob D, Cainap S. Vitamin D Deficiency Manifested by Premature Ventricular Complexes from RVOT: A Report on Two Twins. International Journal of Biomedicine. 2021;11(2):220-223. doi:10.21103/Article11(2)_CR4

Introduction

A vitamin D receptor is present in almost every cell in the body, including cardiomyocytes. Although some studies have suggested that values >30 ng/ml would be sufficient, there is no consensus on the optimal values of serum vitamin D. Recommendations for normal vitamin D levels are based on research on bone metabolism. According to different studies, the normal value varies between 30 ng/ml, 40 ng/ml, and 50 ng/ml. To date, there is no study that recommends values based on the effects of vitamin D on other systems, such as the heart, or the body's defense against viral infections or cancer.

Vitamin D deficiency can be responsible for manifestations that are considered "benign," such as back pain, joint pain, fatigue, and heavy sweating, or major symptoms such as bone deformities, fractures, slow growth, or seizures. Premature ventricular contractions (PVCs) originating from the right ventricular outflow tract (RVOT) are considered "benign," as they occur in patients without structural heart disease and their exact cause remains unknown. In patients with chronic kidney disease and low 25-OH vitamin D, beta-blockers+vitamin D supplementation was better than beta-blockers alone in lowering the number of PVCs on 24-hour Holter ECG.[1]

Studies on twins provide a solid basis for analysis of environmental influences on a given condition that occurs in one of the children. Our report aims to highlight the changes that occurred in one child with vitamin D deficiency and RVOT PVCs and his twin brother with normal vitamin D and no PVC.

Case Presentation

We present the clinical case of 2 twins who presented together for a cardiological consultation. Both were 10 years old, one (P.A.) weighing 26 kg and the second (P.B.) 38 kg. Frequent PVCs were detected in P.A. during a preoperative anesthetic consultation for phimosis. The morphology of the PVCs suggested RVOT origin (Figure 1), with left branch block morphology, low inferior axis, and precordial transition in V4. His twin brother, P.B., had no PVCs on the ECG.

***Corresponding author**: Dr. Gabriel Cismaru, PhD. "Iuliu Hatieganu" University of Medicine and Pharmacy Cluj-Napoca, Romania. E-mail: gabi_cismaru@yahoo.com*

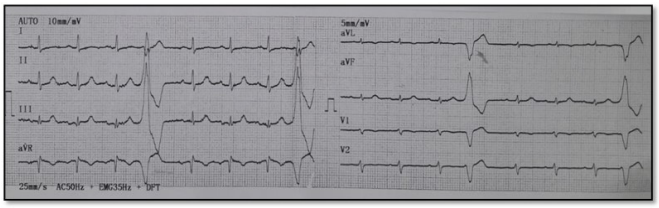

Fig. 1. *A 12-lead ECG.*
Frequent PVCs with a LBBB morphology and inferior axis.

Cardiac ultrasound was performed on both, and was normal, with right and left cavities of normal size, normal systolic function, ejection fraction of 60%, and no valvulopathies were noted. The next examination was a 24-hour Holter ECG, which showed high burden of PVCs in P.A.: 47.640, evenly distributed during the 24 hours, both during the day and night (Figure 2). During physical exertion, PVCs disappeared. All these characteristics were suggestive of "benign" PVC and were associated with a serum vitamin D value of 24.7 ng/ml. Propranolol 2x10mg had no effect in lowering the PVC burden. On the other hand, P.B. had no PVCs in the 24-hour Holter ECG, and serum 15-OH vitamin D had a value of 30.5 ng/ml.

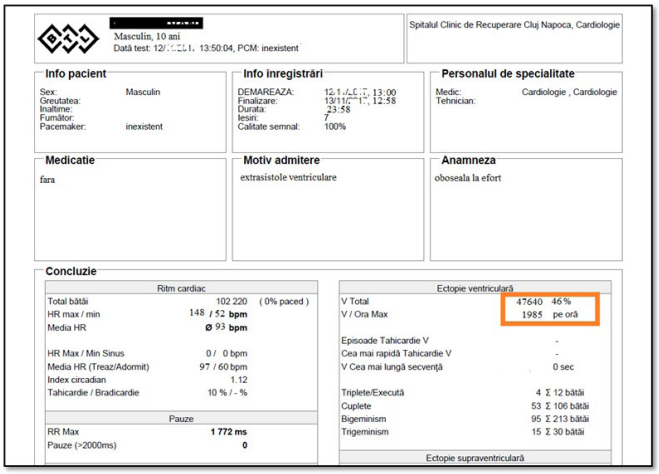

Fig. 2. *A 24-hour Holter ECG.*
A high burden of PVCs (47.640).

Given the low value of serum vitamin D in P.A. and the fact that PVCs were "benign," it was decided not to administer antiarrhythmic medication but to supplement the intake of vitamin D. Thus, we began with 2000 UI daily, and after 4 months the value of 25OH-vitamin D increased to 35.5ng/ml and the number PVCs decreased to 11.728 per 24 hours. The same dose of 2000 IU/24 hours was continued and after 3 months it reached a value of 41 ng/ml and 3800 PVCs per 24 hours. After another 3 months 25-OH vitamin D was 47.3 ng/ml and 1400 PVCs per 24 hours were present in the Holter ECG (Figure 3). On the contrary, P.B. had serum 25-OH vitamin D values of 30.5 ng/ml and no PVC was present in 24-hour Holter ECG.

The father of the twins gave informed consent for the publication of the case report, except images with their face that could reveal their identity. Publication of the report was approved by the Ethics Committee of the Rehabilitation Hospital.

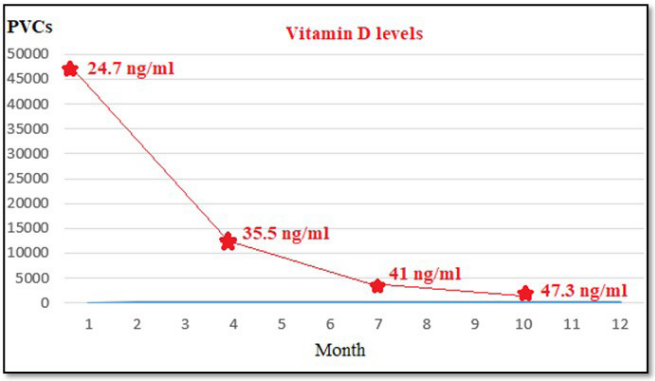

Fig. 3. *Association between serum 25-OH vitamin D level and PVC number on 24-hour Holter ECG.*

Discussion

We presented the case of two twins: one with vitamin D deficiency and frequent PVCs and the other with normal serum vitamin D level and absence of PVCs. The supplementation of vitamin D 2000 IU/day in the first child led to normalization of the serum value in about 10 months with a significant decrease in the number of PVCs, so that no antiarrhythmic drug treatment or catheter ablation was needed.

Our patient did not use other medicines during treatment with vitamin D, and the number of PVCs decreased significantly. Even if there are seasonal variations [2] in serum levels of 25-OH vitamin D, they can not explain the dramatic decrease in the number of PVCs from 47,360 to 1400 per 24 hours.

As this was the first dosage of vitamin D in the twins, it is not possible to specify whether the deficiency was present at birth or was acquired along the way. It is known that children born from twin pregnancies suffer more often from vitamin D deficiency because the need is higher than in single children.[3,4] To supplement vitamin D deficiency, different therapeutic regimens and doses have been tried: 1000 IU/day for 12 months,[5] 2000 IU/day for 3-6 months,[6,7] 2500 IU/day for 4-6 months,[8,9] 5000 IU/day for 3 months.[10] We used 2000 IU/day in a 26 kg child and it took about 10 months to reach a value close to 50 ng/ml.

When the PVC burden is high, catheter ablation is generally indicated for >24% per 24 hours.[11] This can be done by inserting a catheter in the right ventricle and searching for the focus responsible for PVCs. Usually, for this morphology of PVCs, the focus is located in the RVOT, and it can be destroyed with 30-50W energy applications of radiofrequency current.[12] But ablation is an invasive technique and most patients prefer the less invasive alternative (ie antiarrhythmics) or no drug. It is known that PVCs are induced by excess calcium through an increased level of cAMP in cardiomyocytes, which in turn leads to increased intracellular calcium inflow.[13] There are several causes of this phenomenon, and vitamin D deficiency can lead to increased cAMP concentration and thus increased intracellular calcium inflow. Therefore, it is important to detect a deficiency of serum vitamin D because it would be possible to act directly on the cause that determined the occurrence of PVCs.

Cardiomyocyte beta1-adrenergic receptor can activate guanosine nucleotide-binding protein, and lead to increased cAMP, hence the beneficial effect of beta-blockers in the treatment of PVCs. Unfortunately, our patient's treatment with propranolol failed to reduce the number of PVCs; therefore, vitamin D supplementation seemed the most reasonable action. One explanation for the failure of beta-blockers to control PVCs might be given by Weishaar et al.,[14] who found no difference in serum catecholamine levels between 1) vitamin D sufficient; 2)vitamin D deficient with hypocalcemia and c)vitamin D deficient with normocalcemia rats.

Furthermore, vitamin D deficiency is associated with increased parathormone PTH levels, which decreases cellular calcium intake and reduces calcium reuptake to the sarcoplasmic reticulum, and therefore increases intracellular calcium levels; this might be the mechanism related to the development of PVCs from RVOT.[15] Therefore, we believe that beta-blockers have a mild effect on PVC burden in patients with a high number PVCs and vitamin D deficiency, which was also confirmed by the study of Kiuchi et al.[1] Furthermore, in a recent report[16] vitamin D supplementation associated with cardiac rehabilitation decreased the PVC burden in Holter ECG more than cardiac rehabilitation alone.

Although some studies have suggested that values >30 ng/ml would be sufficient, there is no consensus on the optimal values of serum vitamin D. The Endocrine Society has set the lower threshold for normal vitamin D plasmatic concentration to 30 ng/ml or 75 nmol/l. These levels were demonstrated to maintain bone health but there is no data for optimal levels that protect against viral infections, cancers, atherosclerosis, or other health problems.[17] Garland et al.[18] suggested that increasing 25(OH)D to a range of 40 to 60 ng/ml from the current US average could reduce the risk of breast cancer by 25% and colon cancer by 27%.

We believe that for cardiac health, especially in patients with PVCs, the optimal level of serum 25-OH vitamin D should be >50 ng/ml. Studies should be conducted to determine the optimal level of vitamin D in this category of patients.

It is important to note that P.A. had frequent PVCs in the context of a level of vitamin D-25 of 24.7 ng/ml. So what should be the optimal level of serum vitamin D? Is the value of 30ng/ml as it appears in bone health studies sufficient? It seems that this value would be insufficient because the PVCs of P.A. decreased significantly at a level of 47.3 ng/ml. However, even this value of vitamin D did not lead to the total disappearance of PVCs, which remained at 1400 per 24 hours. It is not known what value of 25-OH vitamin D is needed to obtain the total resolution of PVCs. Or should another calcium or magnesium supplement be added to help the resolution of PVCs? Further studies should resolve these questions.

Conclusion

We presented the case of two twins: one with vitamin D deficiency and frequent PVCs and the other with normal serum vitamin D level and absence of PVCs. The supplementation of vitamin D 2000 IU/day in the first child led to normalization of the serum value in about 10 months with a significant decrease in the number of PVCs, so that no antiarrhythmic drug treatment or catheter ablation was needed.

Competing Interests

The authors declare that they have no competing interests.

References

1. Kiuchi MG, e Silva GR, Paz LMR, Chen Sh, Hoye NA, Souto GLL. Influence of vitamin D levels on the treatment of premature ventricular complexes in patients with chronic kidney disease. IJC Metabolic & Endocrine. 2017;14:53-58.
2. Snellman G, Melhus H, Gedeborg R, Olofsson S, Wolk A, Pedersen NL, Michaëlsson K. Seasonal genetic influence on serum 25-hydroxyvitamin D levels: a twin study. PLoS One. 2009 Nov 13;4(11):e7747. doi: 10.1371/journal.pone.0007747. Erratum in: PLoS One. 2010;5(9) doi: 10.1371/annotation/e85fe043-b072-422d-acd5-9d27f02390b3.
3. Frasca D, Morganti G, Cherubini S. Un caso di rachitismo carenziale in una coppia di gemelli [Nutritional rickets in twins: a case report]. Pediatr Med Chir. 2013 May-Jun;35(3):130-3. doi: 10.4081/pmc.2013.46. [Article in Italian].
4. Goswami D, Rani R, Saxena A, Arora MS, Batra S, Sreenivas V. Maternal and neonatal vitamin-D status in twin versus singleton pregnancies. J Obstet Gynaecol Res. 2016 Oct;42(10):1250-1257. doi: 10.1111/jog.13060.
5. Breslavsky A, Frand J, Matas Z, Boaz M, Barnea Z, Shargorodsky M. Effect of high doses of vitamin D on arterial properties, adiponectin, leptin and glucose homeostasis in type 2 diabetic patients. Clin Nutr. 2013 Dec;32(6):970-5. doi: 10.1016/j.clnu.2013.01.020.
6. Moghassemi S, Marjani A. The effect of short-term vitamin D supplementation on lipid profile and blood pressure in post-menopausal women: A randomized controlled trial. Iran J Nurs Midwifery Res. 2014 Sep;19(5):517-21.
7. Ryu OH, Chung W, Lee S, Hong KS, Choi MG, Yoo HJ. The effect of high-dose vitamin D supplementation on insulin resistance and arterial stiffness in patients with type 2 diabetes. Korean J Intern Med. 2014 Sep;29(5):620-9. doi: 10.3904/kjim.2014.29.5.620.
8. Gepner AD, Ramamurthy R, Krueger DC, Korcarz CE, Binkley N, Stein JH. A prospective randomized controlled trial of the effects of vitamin D supplementation on cardiovascular disease risk. PLoS One. 2012;7(5):e36617. doi: 10.1371/journal.pone.0036617.
9. Gepner AD, Haller IV, Krueger DC, Korcarz CE, Binkley N, Stein JH. A randomized controlled trial of the effects of vitamin D supplementation on arterial stiffness and aortic blood pressure in Native American women. Atherosclerosis. 2015 Jun;240(2):526-8. doi: 10.1016/j.atherosclerosis.2015.04.795.
10. Yiu YF, Yiu KH, Siu CW, Chan YH, Li SW, Wong LY, Lee SW, Tam S, Wong EW, Lau CP, Cheung BM, Tse HF. Randomized controlled trial of vitamin D supplement on endothelial function in patients with type 2 diabetes. Atherosclerosis. 2013 Mar;227(1):140-6. doi: 10.1016/j.atherosclerosis.2012.12.013.
11. Muresan L, Cismaru G, Martins RP, Bataglia A, Rosu R, Puiu M, Gusetu G, Mada RO, Muresan C, Ispas DR, Le Bouar R, Diene LL, Rugina E, Levy J, Klein C, Sellal JM, Poull IM,

Laurent G, de Chillou C. Recommendations for the use of electrophysiological study: Update 2018. Hellenic J Cardiol. 2019 Mar-Apr;60(2):82-100. doi: 10.1016/j.hjc.2018.09.002.
12. Cismaru G, Mester P, Muresan L, Rosu R, Gusetu G, Puiu M, Pop D, Mircea PA, Zdrenghea D. Idiopathic ventricular premature contractions originating from the postero-lateral tricuspid annulus leading to left ventricular disfunction. Int J Clin Exp Med. 2015 Mar 15;8(3):4690-3.
13. Nelson DL, Lehninger AL, Cox MM. Lehninger Principles of Biochemistry (5th ed.). New York: W.H. Freeman; 2008
14. Weishaar RE, Kim SN, Saunders DE, Simpson RU. Involvement of vitamin D3 with cardiovascular function. III. Effects on physical and morphological properties. Am J Physiol. 1990 Jan;258(1 Pt 1):E134-42. doi: 10.1152/ajpendo.1990.258.1.E134.
15. Rostand SG, Drüeke TB. Parathyroid hormone, vitamin D, and cardiovascular disease in chronic renal failure. Kidney Int. 1999 Aug;56(2):383-92. doi: 10.1046/j.1523-1755.1999.00575.x.
16. Cismaru G, Gurzau D, Fringu F, Martis A. Vitmamin D supplementation with Cardiac Rehabilitation reduces the number of RVOT Premature Ventricular Contractions. Balneo Research Journal. 2020;11(4):566-568
17. Holick MF, Binkley NC, Bischoff-Ferrari HA, Gordon CM, Hanley DA, Heaney RP, Murad MH, Weaver CM; Endocrine Society. Evaluation, treatment, and prevention of vitamin D deficiency: an Endocrine Society clinical practice guideline. J Clin Endocrinol Metab. 2011 Jul;96(7):1911-30. doi: 10.1210/jc.2011-0385. Epub 2011 Jun 6. Erratum in: J Clin Endocrinol Metab. 2011 Dec;96(12):3908.
18. Garland CF, Gorham ED, Mohr SB, Garland FC. Vitamin D for cancer prevention: global perspective. Ann Epidemiol. 2009 Jul;19(7):468-83. doi: 10.1016/j.annepidem.2009.03.021.

International Journal of Biomedicine 11(2) (2021) 224-227
http://dx.doi.org/10.21103/Article11(2)_CR5

CASE REPORT

INTERNATIONAL JOURNAL OF BIOMEDICINE

A Case of Successful Prolonged Resuscitation of a Patient with General Hypothermia

Albina A. Ivanova[1], PhD, ScD; Alexander F. Potapov[1], PhD, ScD; Dmitriy V. Bosikov[2], PhD; Ivan I. Protodiakonov[2]; Tatiana A. Androsova[2]; Elena M. Klimova[2]

[1]M. K. Ammosov North-Eastern Federal University
[2]Center for Emergency Medical Care of Yakutsk
Yakutsk, the Republic of Sakha (Yakutia), Russia

Abstract

This article presents a case of a successful prolonged cardiopulmonary resuscitation (CPR) performed by the emergency medical services on a patient with general hypothermia (GH) and frostbite in the extremities. The resuscitation activities continued for more than 3.5 hours and resulted in a successful restoration of spontaneous BC. An extended CPR was performed while the patient was being warmed up (wrapping in a blanket and insulating pads, infusion of warmed fluids, gastric lavage and urinary bladder lavage with water heated to +45°C). After the restoration of BC, the patient was hospitalized and subsequently discharged without any neurological deficit.(**International Journal of Biomedicine. 2021;11(2):224-227.**)

Key Words: general hypothermia • clinical death • cardiopulmonary resuscitation

For citation: Ivanova AA, Potapov AF, Bosikov DV, Protodiakonov II, Androsova TA, Klimova EM. A Case of Successful Prolonged Resuscitation of a Patient with General Hypothermia. International Journal of Biomedicine. 2021;11(2):224-227. doi:10.21103/Article11(2)_CR5

Abbreviations

AV, artificial ventilation; **BC**, blood circulation; **CPR**, cardiopulmonary resuscitation; **ECM**, external cardiac massage; **GH**, general hypothermia; **HR**, heart rate; **PEA**, pulseless electrical activity; **RR**, respiratory rate; **VF**, ventricular fibrillation.

Introduction

The injuries caused by the effect of cold natural temperatures on the human body are one of the serious challenges for emergency medicine. This problem is particularly urgent in northern latitudes and characterized by low and ultra-low natural temperatures.

Along with a severe clinical course and frequently developed complications in the respiratory and excretory systems, a distinctive feature of cold injury is a high mortality rate and disability of the patients due to amputations of various segments of extremities. The outcomes of treatment are determined both by the degree of hypothermia and the depth of local tissue damage, as well as by the tactics of treating the patients, especially the adequacy of resuscitation activities during the pre-thaw phase (from the onset of injury to the start of tissue rewarming and restoration of circulation) and the early post-thaw phase (from the start of tissue warming and restoration of circulation to the end of Day 1).

The complex of resuscitation activities in the event of death from hypothermia has certain peculiarities, taking into account the need for warming the patients. In an event of death from hypothermia, a number of countries apply the "no one is dead until warm and dead" approach, which was recommended by the European Resuscitation Council.[1]

***Corresponding author:** Prof. Albina A. Ivanova, PhD, ScD. M.K. Ammosov North-Eastern Federal University, Yakutsk, the Republic of Sakha (Yakutia), Russia. E-mail: iaa_60@mail.ru*

To this end, modern high-tech treatment methods are used, including extracorporeal core warming and irrigation of body cavities with warmed fluids.[2]

The primary tasks of intensive care in hypothermia include ensuring adequate oxygenation of the body, maintaining hemodynamics and preventing fatal heart rhythm disorders along with achieving the general warming of the patient.[3] At present, the basic approach to treating patients with frostbite of extremities is to ensure slow and gradual rewarming of the damaged tissues through internal heat production, which helps to prevent tissue necrosis, or reduce its area.[3,4]

The aim of our research was to present a clinical case of a successful, prolonged resuscitation of a patient having experienced clinical death due to GH.

Case Presentation

An anesthesiology-intensive care team arrived at the site where a man was found in the street 14 minutes after the call had been received. According to the official data of the Meteorological Office, on the day of the accident, the air temperature in the area where the patient was found was -41°C. At the initial examination, the patient was in extremely grave condition. He was unconscious, with the Glasgow Coma Scale score of 6. The pupils were wide, with no photoreaction. One could smell alcohol from his mouth. There were traces of vomit on the skin. The skin was pale cyanotic and cold. There were signs of frostbite in the lumbar area of the hands, shins, and feet up to degree 3. He could breathe, with RR of 20 per minute. The heart sounds were muffled, with HR of 69 bpm, blood pressure could not be measured. The glucometer reading was 7.1 mmol/L. It was impossible to determine the blood oxygen level due to the absence of peripheral pulsation. Continuous cardiac monitoring was started. The cardiac monitor showed an irregular idioventricular rhythm with a frequency of 53 per minute, with the ventricular complex deformed due to the Osborne wave.

During the examination, the BC stopped, the monitor showed VF. Electrical defibrillation was performed with a biphasic rectangular pulse with the energy of 150J, which led to the restoration of sinus rhythm and return of the pulse in the carotid artery. The oral cavity was sanitized, and the infusion of warmed saline started. Then, premedication with Atropine solution (1 mg), induction with Ketamine solution (100 mg), and muscle relaxation with Rocuronium bromide solution (50 mg) were followed by trachea intubation, and artificial ventilation was started. At the same time, the team used a special warming blanket and insulating pads on the limbs.

In 5 minutes, the monitor recorded a recurrence of VF, which was stopped by a double electrical shock of 150-200J with an interval of 2 minutes. Between the shocks, continuous external cardiac massage and artificial ventilation with an Ambu bag were performed. After the resuscitation, the patient was connected to a mechanical ventilator.

For 35 minutes, spontaneous circulation was maintained, respiration was provided by mechanical ventilation, HR was 50 bpm, blood pressure – 70/40 mmHg, saturation – 94%. The team doctor made a decision to start medical evacuation of the patient to the Republican Hospital #2 - Center for Emergency Medical Aid (RH No.2–CEMA). On the way there, the monitor registered VF again. A double electrical shock of 200J with an interval of 2 minutes in combination with continuous external cardiac massage, mechanical ventilation, and intravenous administration of an Adrenaline solution (2.0) did not restore the HR. The doctor decided to use the AutoPulse Zoll automatic compression device and began intensive warming of the patient during continuing automated compressions.

It should be noted that gastric lavage and urinary bladder lavage are mandatory in the resuscitation of patients with GH. However, ambulance teams usually have to provide their services to patients with cold injuries outdoors, where it is not possible to perform the lavage with warmed water. Meeting this condition is something to work out during the pre-hospital stage, since it prolongs the time of transporting patients to the hospital.

Further, the resuscitation activities continued for 3 hours 5 minutes from the last circulatory arrest and included chest compressions with the AutoPulse device, mechanical ventilation with an Ambu bag, continuous infusion of warmed saline, gastric lavage and urinary bladder lavage with water heated to 45°C. The patient's body was warmed to a temperature of 35.5°C in the armpit. During that period, the type of circulatory arrest underwent a transformation from VF into the pulseless electrical activity and back; the resuscitation tactics of applying electrical shocks changed accordingly. As a result of the activities applied, spontaneous BC was restored. When the CPR was complete, the patient's HR and pulse were 49 per minute, blood pressure – 30/00 mmHg, saturation – 74%, core temperature – 35.8°C, and the monitor showed sinus bradycardia. The further diagnosis was as follows: General hypothermia, severe. Frostbite in both hands, lumbar area, both shins and feet. Clinical death was declared at 08:10. CPR. Resuscitation at 08:12. Recurrence of clinical death at 08:17. CPR. Resuscitation at 08:21. Recurrence of clinical death at 08:54. CPR. Resuscitation at 11:50. The patient reached the RH No.2-CEMA in the early post-resuscitation period.

Table 1 presents the course of the resuscitation activities that were carried out.

The long-term outcome of treatment is favorable: the patient came out of a coma without any neurological deficit, the frostbitten limbs were preserved, amputation avoided.

In conclusion, the presented case signals the urgency of the problem with cold injury in the region. The injury is characterized by severe frostbite of extremities with tissue necrosis combined with hypothermia, which significantly complicates the treatment of the injury. It should be emphasized that today there are no national standards or clinical guidelines for the treatment of patients with hypothermia, including the use of active warming methods, a unified technique for reliable diagnosis of the severity of tissue damage and a degree of hypothermia, without which timely and adequate treatment of patients is impossible. Given these circumstances, the institution previously developed an algorithm for CPR in patients with hypothermia and implemented it in the activities of ambulance teams. Following the algorithm resulted in a successful rescue of the patient in the case described.

Table 1.
The sequence of the extended cardiopulmonary resuscitation

Time	Data from the cardiac monitor, hemodynamics, core temperature	Activities
08:03	Irregular idioventricular rhythm with a frequency of 53 per minute, the ventricular complex deformed due to the Osborne wave	Preliminary examination; infusion of warmed NaCl; insulating pads
08:10	VF	150 J shock
08:10-08:12		ECM, AV with an Ambu bag
08:12	Organized rhythm, pulse over the carotid arteries	Infusion of warmed NaCl, oral cavity sanitation, trachea intubation, AV
08:17	Recurrence of VF	Adrenalin 1.0 IV, 150 J electrical shock
08:17-08:19		ECM, AV with an Ambu bag, infusion of warmed NaCl
08:19	VF	Adrenalin 1.0 IV, 200 J electrical shock
08:19-08:21		ECM, AV with an Ambu bag, infusion of warmed NaCl
08:21	Organized rhythm, pulse over the carotid arteries	Mechanical ventilation
08:21-08:54	Organized rhythm on the monitor. Spontaneous blood circulation, breathing – mechanical ventilation, HR – 50 per minute, pulse – 50 per minute, blood pressure – 70/40 mm/Hg, saturation – 94%.	Continued infusion of warmed NaCl
08:54 -08:58	VF	Double 200 J electrical shock with 2-minute interval, Adrenalin 1.0 IV as per scheme, ECM, AV with an Ambu bag between the shocks, infusion of warmed NaCl
08:58 – 10:01	VF Core temperature < 35.0°C	Automatic compressor Autopulse Zoll applied; AV with an Ambu bag, continued infusion of warmed NaCl; gastric lavage and urinary bladder lavage with water heated to 45°C; Adrenalin 1.0 IV with 10-minute interval, 200 J defibrillation with 2-minute interval
10:01 – 10:03	PEA of the heart	Automatic compressor Autopulse Zoll; AV with an Ambu bag, infusion of warmed NaCl; gastric lavage and urinary bladder lavage with water heated to 45°C
10:03	VF	Adrenalin 1.0 IV; 200 J electrical shock
10:03-10:05		Automatic compressor Autopulse Zoll; AV with an Ambu bag, infusion of warmed NaCl; gastric lavage and urinary bladder lavage with water heated to 45°C
10:05	VF	Automatic compressor Autopulse Zoll; AV with an Ambu bag, infusion of warmed NaCl; gastric lavage and urinary bladder lavage with water heated to 45°C
10:05-10:19	VF	Automatic compressor Autopulse Zoll; AV with an Ambu bag, infusion of warmed NaCl; gastric lavage and urinary bladder lavage with water heated to 45°C; Adrenalin 1,0 IV with 10-minute interval
10:19	VF	200 J electrical shock
10:19-10:21	VF	Automatic compressor Autopulse Zoll; AV with an Ambu bag, infusion of warmed NaCl; gastric lavage and urinary bladder lavage with water heated to 45°C
10:21-10:39	VF	Automatic compressor Autopulse Zoll; AV with an Ambu bag, infusion of warmed NaCl; gastric lavage and urinary bladder lavage with water heated to 45°C; Adrenalin 1,0 IV with 10-minute interval
10:39	VF, core temperature 35.5°C	200 J electrical shock
10:39-10:57	VF	Automatic compressor Autopulse Zoll; infusion of warmed NaCl; AV with an Ambu bag, gastric lavage and urinary bladder lavage with water heated to 45°C; Adrenalin 1,0 IV with 10-minute interval, 200 J defibrillation
10:57 – 11:50	PEA of the heart	Automatic compressor Autopulse Zoll; AV with an Ambu bag, infusion of warmed NaCl; gastric lavage and urinary bladder lavage with water heated to 45°C; Adrenalin 1.0 IV with 10-minute interval

Table 1 (continued).

The sequence of the extended cardiopulmonary resuscitation

Time	Data from the cardiac monitor, hemodynamics, core temperature	Activities
11:50	Organized rhythm, sinus bradycardia; pulse over the carotid artery	Mechanical ventilation, saline infusion
11:50-12:26	Organized rhythm, sinus bradycardia; pulse over the carotid artery. Blood pressure – 30/00 mmHg, HR – 49 per minute, core temperature – 35.8°C, saturation – 71%	Mechanical ventilation, saline infusion; Dopamine infusion at rate 15 mcg/kg/min

Competing Interests

The authors declare that they have no competing interests.

References

1. European Resuscitation Council Guidelines for Resuscitation 2015 Section 9 Rite Aid. Available from: https://www.resuscitationjournal.com/article/S0300-9572(15)00343-3/fulltext

2. Monika BM, Martin D, Balthasar E, Stefan L, Roland D, Lars E, Luca M, Markus N, Mario S, Eva RK, et al. The Bernese Hypothermia Algorithm: a consensus paper on in-hospital decision-making and treatment of patients in hypothermic cardiac arrest at an alpine level 1 trauma centre. Injury. 2011 May;42(5):539-43. doi: 10.1016/j.injury.2010.11.037.

3. Mails WJ, Cold injuries guidelines, State Alaska, 2014 Available from: http://dhss.alaska.gov/dph/emergency/documents/ems/documents/alaska%20dhss%20ems%20cold%20injuries%20guidelines%20june%202014.pdf

4. Diagnostics and treatment of frostbite. Clinical Guidelines, 2017 (In Russian). Available from: http://combustiolog.ru/wp-content/uploads/2013/07/Diagnostika-i-lechenie-otmorozhenij-2017.pdf

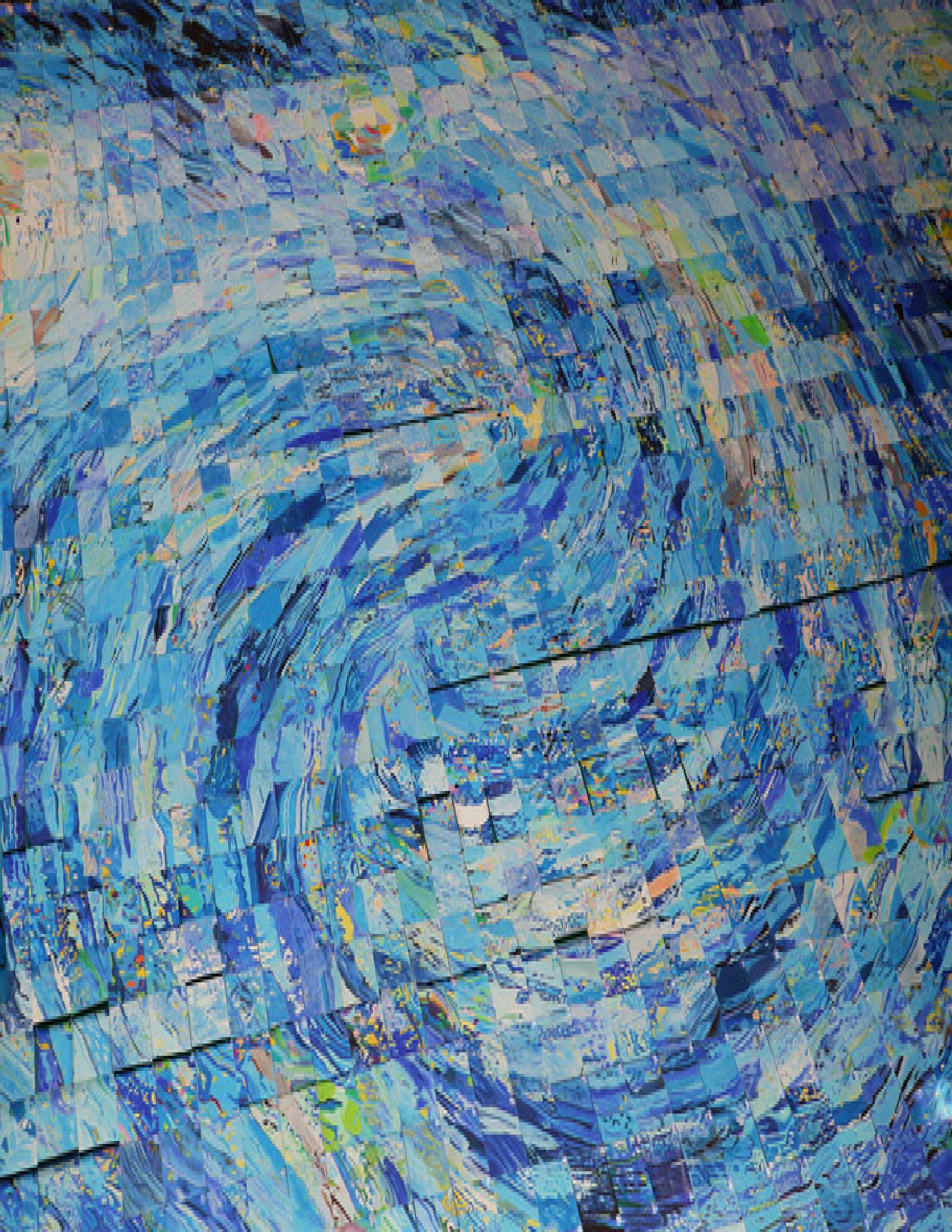

IJBM

INTERNATIONAL JOURNAL OF BIOMEDICINE

Instructions for Authors

International Journal of Biomedicine (IJBM) publishes peer-reviewed articles on the topics of basic, applied, and translational research on biology and medicine. International Journal of Biomedicine welcomes submissions of the following types of paper: Original articles, Reviews, Perspectives, Viewpoints, and Case Reports.

All research studies involving animals must have been conducted following animal welfare guidelines such as *the National Institutes of Health (NIH) Guide for the Care and Use of Laboratory Animals*, or equivalent documents. Studies involving human subjects or tissues must adhere to the *Declaration of Helsinki and Title 45, US Code of Federal Regulations, Part 46, Protection of Human Subjects*, and must have received approval of the appropriate institutional committee charged with oversight of human studies. Informed consent must be obtained.

Pre-submissions

Authors are welcome to send an abstract or draft manuscript to obtain a view from the Editor about the suitability of their paper. Our Editors will do a quick review of your paper and advise if they believe it is appropriate for submission to our journal. It will not be a full review of your manuscript.

Manuscript Submission

Manuscript submissions should conform to the guidelines set forth in the Recommendations for the Conduct, Reporting, Editing and Publication of Scholarly Work in Medical Journals (ICMJE Recommendations), available from www.ICMJE.org.

Original works will be accepted with the understanding that they are contributed solely to the Journal, are not under review by another publication, and have not previously been published except in abstract form.

All manuscripts must be submitted through the International Journal of Biomedicine`s online submission system (www.ijbm.org/submission.php). Manuscripts must be typed, double-spaced using a 14-point font, including references, figure legends, and tables. Leave 1-inch margins on all sides. Assemble the manuscript in this order: Title Page, Abstract, Key Words, Text (Introduction, Methods, Results, and Discussion), Acknowledgments, Sources of Funding, Disclosures, References, Tables, Figures, and Figure Legends. References, figures, and tables should be cited in numerical order according to first mention in the text.

The preferred order for uploading files is as follows: Cover letter, Full Manuscript PDF (PDF containing all parts of the manuscript including references, legends, figures and tables), Manuscript Text File (MS Word), Figures (each figure and its corresponding legend should be presented together), and Tables. Files should be labeled with appropriate and descriptive file names (e.g., SmithText.doc, Fig1.eps, Table3.doc). Text, Tables, and Figures should be uploaded as separate files. (Multiple figure files can be compressed into a Zip file and uploaded in one step; the system will then unpack the files and prompt the naming of each figure. See www.WinZip.com for a free trial.)

Authors who are unable to provide an electronic version or have other circumstances that prevent online submission must contact the Editorial Office prior to submission to discuss alternate options (editor@ijbm.org).

Cover Letter

The cover letter should be saved as a separate file for upload. In it, the authors should (1) state that the manuscript, or parts of it, have not been and will not be submitted elsewhere for publication; (2) state that all authors have read and approved the manuscript; and (3) disclose any financial or other relations that could lead to a conflict of interest. If a potential conflict exists, its nature should be stated for each author. When there is a stated potential conflict of interest a footnote will be added indicating the author's equity interest in or other affiliation with the identified commercial firms.

The corresponding author should be specified in the cover letter. All editorial communications will be sent to this author. A short paragraph telling the editors why the authors think their paper merits publication priority may be included in the cover letter.

Types of articles

Original articles

Original articles present the results of original research. These manuscripts should present well-rounded studies reporting innovative advances that further knowledge about a topic of importance to the fields of biology or medicine. These can be submitted as either a full-length article (no more than 6,000 words, 4 figures, 4 tables) or a Short Communication (no more than 2,500 words, 2 figures, 2 tables). An original

article may be Randomized Control Trial, Controlled Clinical Trial, Experiment, Survey, and Case-control or Cohort study.

Case Reports

Case reports describe an unusual disease presentation, a new treatment, a new diagnostic method, or a difficult diagnosis. The author must make it clear what the case adds to the field of medicine and include an up-to-date review of all previous cases in the field. These articles should be no more than 5,000 words with no more than 6 figures and 3 tables. Case Reports should consist of the following headings: Abstract (no more than 100 words), Introduction, Case Presentation (clinical presentation, observations, test results, and accompanying figures), Discussion, and Conclusions.

Reviews

Reviews analyze the current state of understanding on a particular subject of research in biology or medicine, the limitations of current knowledge, future directions to be pursued in research, and the overall importance of the topic. Reviews could be non-systematic (narrative) or systematic. Reviews can be submitted as a Mini-Review (no more than 2,500 words, 3 figures, and 1 table) or a long review (no more than 6,000 words, 6 figures, and 3 tables). Reviews should contain four sections: Abstract, Introduction, Topics (with headings and subheadings, and Conclusions and Outlook.

Perspectives

Perspectives are brief, evidenced-based and formally structured essays covering a wide variety of timely topics of relevance to biomedicine. Perspective articles are limited to 2,500 words and usually include ≤10 references, one figure or table. Perspectives contain four sections: Abstract, Introduction, Topics (with headings and subheadings), Conclusions and Outlook.

Viewpoints

Viewpoint articles include academic papers, which address any important topic in biomedicine from a personal perspective than standard academic writing. Maximum length is 1,200 words, ≤70 references, and 1 small table or figure.

Manuscript Preparation

Title Page

The first page of the manuscript (title page) should include (1) a full title of the article, (2) a short title of less than 60 characters with spaces, (3) the authors' names, academic degrees, and affiliations, (4) the total word count of the manuscript (including Abstract, Text, References, Tables, Figure Legends), (5) the number of figures and tables, and (6) the name, email address, and complete address of corresponding author.

Disclaimers. An example of a disclaimer is an author's statement that the views expressed in the submitted article are his or her own and not an official position of the institution or funder.

Abstract

The article should include a brief abstract of no more than 200 words. Limit use of acronyms and abbreviations. Define at first use with acronym or abbreviation in parentheses. The abstract should be structured with the following headings: Background, Methods and Results, and Conclusions. The Background section should describe the rationale for the study. Methods and Results should briefly describe the methods and present the significant results. Conclusions should succinctly state the interpretation of the data. Authors should supply a list of up to four key words not appearing in the title, which will be used for indexing. The key words should be listed immediately after the Abstract. Use terms from the Medical Subject Headings (MeSH) list of Index Medicus when possible.

Main text in the IMRaD format

Introduction should describe the purpose of the study and its relation to previous work in the field; it should not include an extensive literature review.

Methods should be concise but sufficiently detailed to permit repetition by other investigators. Previously published methods and modifications should be cited by reference. A subsection on statistics should be included in the Methods section.

Results should present positive and relevant negative findings of the study, supported when necessary by reference to Tables and Figures.

Discussion should interpret the results of the study, with emphasis on their relation to the original hypotheses and to previous studies. The importance of the study and its limitations should also be discussed.

The IMRaD format does not include a separate Conclusion section. The conclusion is built into the Discussion. More information on the structure and content of these sections can be found in the Recommendations for the Conduct, Reporting, Editing and Publication of Scholarly Work in Medical Journals (ICMJE Recommendations), available from www.ICMJE.org.

Acknowledgments, Sources of Funding, and Disclosures

Acknowledgments : All contributors who do not meet the criteria for authorship should be listed in an acknowledgments section. Examples of those who might be acknowledged include a person who provided purely technical help, writing assistance, or a department chairperson who provided only general support. Authors should declare whether they had assistance with study design, data collection, data analysis, or manuscript preparation. If such assistance was available, the authors should disclose the identity of the individuals who provided this assistance and the entity that supported it in the published article.

Sources of Funding: All sources of financial support for the study should be cited on the title page, including federal or state agencies, nonprofit organizations, and pharmaceutical or other commercial sources.

Disclosure and conflicts of interest: All authors must disclose any financial or other relations that could lead to a conflict of interest. If a potential conflict exists, its nature should be stated for each author. All sources of financial support for the study should be cited, including federal or state agencies, nonprofit organizations, and pharmaceutical or other commercial sources. Please use ICMJE Form for Disclosure of Potential Conflicts of Interest (http://www.icmje.org/conflicts-of-interest/).

References

References should follow the standards summarized in the NLM's International Committee of Medical Journal Editors (ICMJE) Recommendations for the Conduct, Reporting,

Editing and Publication of Scholarly Work in Medical Journals: Sample References webpage (www.nlm.nih.gov/bsd/uniform_requirements.html) and detailed in the NLM's Citing Medicine, available from www.ncbi.nlm.nih.gov/books/NBK7256/. MEDLINE abbreviations for journal titles (www.ncbi.nlm.nih.gov/nlmcatalog/journals) should be used. The first six authors should be listed in each reference citation (if there are more than six authors, "et al" should be used following the sixth). Periods are not used in authors' initials or journal abbreviations. Examples of journal reference style:

Journal Article: Serruys PW, Ormiston J, van Geuns RJ, de Bruyne B, Dudek D, Christiansen E, et al. A Polylactide Bioresorbable Scaffold Eluting Everolimus for Treatment of Coronary Stenosis: 5-Year Follow-Up. J Am Coll Cardiol. 2016;67(7):766-76. doi: 10.1016/j.jacc.2015.11.060.

Book: Murray PR, Rosenthal KS, Kobayashi GS, Pfaller MA. Medical Microbiology. 4th ed. St. Louis: Mosby; 2002.

Chapter in Edited Book: Meltzer PS, Kallioniemi A, Trent JM. Chromosome alterations in human solid tumors. In: Vogelstein B, Kinzler KW, editors. The Genetic Basis of Human Cancer. New York: McGraw-Hill; 2002:93–113.

References should be numbered consecutively in the order in which they are first mentioned in the text. Identify references in text, tables, and legends by Arabic numerals in parentheses and listed at the end of the article in citation order.

Tables

Tables should be comprehensible without reference to the text and should not be repetitive of descriptions in the text. Every table should consist of two or more columns; tables with only one column will be treated as lists and incorporated into the text. All tables must be cited in the text and numbered in order of appearance. Tables should include a short title. Place explanatory matter in footnotes, not in the heading. Explain all nonstandard abbreviations in footnotes, and use symbols to explain information if needed. Each table submitted should be double-spaced, each on its own page. Each table should be saved as its own file as a Word Document. Explanatory matter and source notations for borrowed tables should be placed in the table footnote.

Figures and Legends

All illustrations (line drawings and photographs) are classified as figures. All figures should be cited in the text and numbered in order of appearance. Figures should be provided in .tiff, .jpeg or .eps formats. Color images must be at least 300 dpi. Gray scale images should be at least 300 dpi. Line art (black and white or color) and combinations of gray scale images and line art should be at least 1,000 dpi. The optimal size of lettering is 12 points. Symbols should be of a similar size. Figures should be sized to fit within the column (86 mm) or the full text width (180 mm). Line figures must be sharp, black and white graphs or diagrams, drawn professionally or with a computer graphics package. Legends should be supplied for each figure and should be brief and not repetitive of the text. Any source notation for borrowed figures should appear at the end of the legend. Figures should be uploaded as individual files.

Units of Measurement

Measurements of length, height, weight, and volume should be reported in metric units (meter, kilogram, or liter) or their decimal multiples. Temperatures should be in degrees Celsius. Blood pressures should be in millimeters of mercury. All measurements must be given in SI or SI-derived units. Drug concentrations may be reported in either SI or mass units, but the alternative should be provided in parentheses where appropriate.

Style and Language

The journal accepts manuscripts written in English. Spelling should be US English only. The language of the manuscript must meet the requirements of academic publishing. Reviewers may advise rejection of a manuscript compromised by grammatical errors. Non-native speakers of English may choose to use a copyediting service.

Abbreviations and Symbols

Use only standard abbreviations; use of nonstandard abbreviations can be confusing to readers. Avoid abbreviations in the title of the manuscript. The spelled-out abbreviation followed by the abbreviation in parenthesis should be used on first mention unless the abbreviation is a standard unit of measurement.

Drugs should be referred to by their generic names. If proprietary drugs have been used in the study, refer to these by their generic name, mentioning the proprietary name, and the name and location of the manufacturer, in parentheses.

Permissions

To use tables or figures borrowed from another source, permission must be obtained from the copyright holder, usually the publisher. Authors are responsible for applying for permission for both print and electronic rights for all borrowed materials and are responsible for paying any fees related to the applications of these permissions. This is necessary even if you are an author of the borrowed material. It is essential to begin the process of obtaining permission early, as a delay may require removing the copyrighted material from the article. The source of a borrowed table should be noted in a footnote and of a borrowed figure in the legend. It is essential to use the exact wording required by the copyright holder. A copy of the letter granting permission, identified by table or figure number, should be sent along with the manuscript. A permission request form is provided for the authors use in requesting permission from copyright holders.

Open Access Policy

All articles published by International Journal of Biomedicine are made freely and permanently accessible online immediately upon publication, without subscription charges or registration barriers. Articles published under an IMRDC user license are protected by copyright and may be used for non-commercial purposes. A copy of the full text of each Open Access article is archived in an online repository separate from the journal. The International Journal of Biomedicine's articles are archived in Scientific Electronic Library (Russian Science Citation Index). The authors can also self-archive the final publisher's version/PDF on personal website, departmental website, institutional repository with a link to publisher version.

Users may access, download, copy, translate, text and data mine (but may not redistribute, display or adapt) the articles for non-commercial purposes provided that users cite the article using an appropriate bibliographic citation (i.e. author(s), journal, article title, volume, issue, page numbers, DOI and the link to the definitive published PDF version on www.ijbm.org).

Article Processing Charges

When a paper is accepted for publication, the author is issued an invoice for payment of Article Processing Charge (APC). APC can be paid by the author or on their behalf, for example, by their institution or funding body.

APC helps IMRDC recover the costs of publication—including peer review management, production of the journal printed version, and online hosting and archiving, as well as inclusion in citation databases, enabling electronic citation in other journals that are available electronically. IJBM publishes all content Open Access and makes the content freely available online for researchers and readers.

IJBM charges a processing fee of $100 per printed black and white journal page and $200 per printed page of color illustrations. IJBM charges a processing fee of $85 per page in the case of online-only publications. For online-only publications, all illustrations submitted in color will be published in color online, at no cost to the author.

Under IJBM's existing policy, certain categories of authors are eligible for a discount. The amount of discount depends on factors such as country of origin, position of the author in the institute and quality and originality of the work. Young researchers and first time authors may also qualify for a discount. To apply for a discount, please contact our office using the 'Contact Us' page or send email to the Publisher (editor@ijbm.org) with the following information:

- Your name and institution with full address details
- Reason for applying for a waiver
- Title of your paper
- Country of residence of any co-authors.

Page Proofs

Page proofs are sent from the Publisher electronically and must be returned within 72 hours to avoid delay of publication. Generally, peer review is completed within 3-4 weeks and the editor's decision within 7-10 days of this. It is therefore very rare to have to wait more than 6 weeks for a final decision.

IMRDC Author Services

If you need help preparing a manuscript for submission, our publisher, IMRDC, offers a range of editorial services for a fee, including Advanced Editing and Translation with Editing. Please note that use of IMRDC Author Services does not guarantee acceptance of your manuscript.

It is important to note that when citing an article from IJBM, the correct citation format is **International Journal of Biomedicine.**